UNIVERSIDAD COMPLUTENSE DE MADRID

FACULTAD DE FARMACIA

UNIVERSIDAD
COMPLUTENSE
MADRID

TESIS DOCTORAL

Temperate phages (prophages) and phage tail-like bacteriocins in the genomes of *Pseudomonas aeruginosa* isolates from nosocomial environments

Fagos atemperados (profagos) y bacteriocinas similares a colas de fago en los genomas de aislados de *Pseudomonas aeruginosa* de ambientes nosocomiales

MEMORIA PARA OPTAR AL GRADO DE DOCTOR PRESENTADA POR

MANUEL GONZÁLEZ DE ALEDO FERRÁNDEZ

DIRECTORES

RAFAEL MARÍA CANTÓN MORENO

MARÍA DEL MAR TOMÁS CARMONA

UNIVERSIDAD COMPLUTENSE DE MADRID

FACULTAD DE FARMACIA

Programa de Doctorado en Microbiología y Parasitología

UNIVERSIDAD
COMPLUTENSE
MADRID

TESIS DOCTORAL

Temperate phages (prophages) and phage tail-like bacteriocins in the genomes of *Pseudomonas aeruginosa* isolates from nosocomial environments

Fagos atemperados (profagos) y bacteriocinas similares a colas de fago en los genomas de aislados de *Pseudomonas aeruginosa* de ambientes nosocomiales

MEMORIA PARA OPTAR AL GRADO DE DOCTOR PRESENTADA POR

MANUEL GONZÁLEZ DE ALEDO FERRÁNDEZ

DIRECTORES

RAFAEL MARÍA CANTÓN MORENO

MARÍA DEL MAR TOMÁS CARMONA

El **Dr. Rafael María Cantón Moreno**, jefe del Servicio de Microbiología y Parasitología del Hospital Universitario Ramón y Cajal de Madrid y responsable del Área 2 de Microbiología, Inmunología e Infección del Instituto Ramón y Cajal de Investigación Sanitaria (IRYCIS).

La **Dra. María del Mar Tomás Carmona**, facultativo del Servicio de Microbiología y Parasitología del Complejo Hospitalario Universitario A Coruña e investigadora del Instituto de Investigación Biomédica de A Coruña.

CERTIFICAN QUE:

MANUEL GONZÁLEZ DE ALEDO FERRÁNDEZ, ha realizado en el Servicio de Microbiología y Parasitología del Hospital Universitario Ramón y Cajal de Madrid, bajo su dirección, el trabajo que presenta para optar al grado de Doctor a través del programa de Doctorado en Microbiología y Parasitología de la Facultad de Farmacia de la Universidad Complutense de Madrid, con el título:

"Temperate phages (prophages) and phage tail-like bacteriocins in the genomes of *Pseudomonas aeruginosa* isolates from nosocomial environments"

"Fagos atemperados (profagos) y bacteriocinas similares a colas de fago en los genomas de aislados de *Pseudomonas aeruginosa* de ambientes nosocomiales"

Y para que así conste, firmamos la presente certificación en Madrid a 17 de julio de 2025:

DR. RAFAEL MARÍA CANTÓN MORENO

DRA. MARÍA DEL MAR TOMÁS CARMONA

TABLE OF CONTENTS

LIST OF ABBREVIATIONS:

A

Abi: Abortive infection

Acr: Anti-CRISPR

AHL: N-acyl homoserine lactone

B

Bp: base pair

C

cAMP: cyclic adenosine-monophosphate

c-di-GMP: cyclic di-guanosine-monophosphate

CF: Cystic fibrosis

CRISPR-Cas: Clustered regularly interspaced short palindromic repeats and CRISPR-associated proteins)

D

DPA: Dipicolinic acid

dsDNA: double-stranded deoxyribonucleic acid

DSF: Diffusible-like factors

DTR: Difficult-to-treat resistance

E

ECDC: European Center for Disease Prevention and Control

eDNA: Extracellular DNA

EDTA: ethylenediaminetetraacetic acid

H

HGT: horizontal gene transfer

I

ICU: Intensive care unit

i.e.: *id est*

L

LPS: Lipopolysaccharide

M

MALDI-TOF: matrix-assisted laser desorption/ionization time of flight mass spectrometry

MDR: multidrug-resistant

MGE: mobile genetic element

MLST: multilocus sequence typing

P

PDR: pandrug-resistant

ppGpp: guanosine tetraphosphate

pppGpp: guanosine pentaphosphate

PQS: *Pseudomonas* quinolone signal

PTLB: Phage tail-like bacteriocin

Q

QQ: Quorum quenching

QS: Quorum sensing

R

RBP: Receptor binding protein

R-M: Restriction-modification

ROS: Reactive oxygen species

S

SCV: Small colony variant

ST: Sequence type

T

T/A: Toxin/antitoxin

TIVP: Type IV pilus/pili

T1SS: Type I Secretion System

T2SS: Type II Secretion System

T3SS: Type III Secretion System

T4SS: Type IV Secretion System

T6SS: Type VI Secretion System

X

XDR: Extensively drug-resistant

LIST OF FIGURES:

LIST OF TABLES:

RATIONALE:

In 1973, inspired by Lewis Carroll's novel "Alice in Wonderland", the evolutionary biologist Leigh Van Valen proposed the Reed Queen hypothesis to explain the biological competition that drives natural selection. In this tale, Alice runs next to the Red Queen, but gets frustrated realizing how she seemed not to be moving, likely because the landscape was running along with her. The Red Queen explains then that "*in Wonderland it takes all the running you can do to stay in place*" having to run twice as fast to observe any movement.

Applied to the Red Queen hypothesis, predators and preys must be continuously evolving just not to be extinct and remain in balance. This hypothesis has been selected as the common thread of the thesis as it could be applied not only to the bacteria versus phage arms race, but also to the continuously occurring bacteria versus scientific community fight. This includes the development of new antimicrobials, screening and diagnostics strategies, as well as the optimization of antimicrobial treatments. Moreover, this hypothesis could also be extended to the bacteria versus bacteria population dynamics driven by the production of phage tail-like bacteriocins.

FUNDAMENTO:

En 1973, inspirado por la novela "Alicia en el País de las Maravillas" de Lewis Carroll, el biólogo evolutivo Leigh Van Valen propuso la hipótesis de la Reina Roja con el fin de explicar cómo la selección natural está dominada por eventos de competición biológica. En el cuento, Alicia corre junto a la Reina Roja, frustrada al ver que no se está desplazando, probablemente porque el entorno se mueve junto a ella. La Reina Roja le explica entonces que "*en el País de las Maravillas, necesitas correr todo lo que puedas para mantenerte en el mismo lugar*", teniendo que correr el doble de rápido para realmente desplazarse a algún sitio.

Aplicando la hipótesis de la Reina Roja, presas y depredadores deben estar en continua evolución simplemente para no extinguirse y mantenerse en equilibrio. Esta hipótesis ha sido seleccionada como el hilo conductor de la tesis ya que resulta aplicable no sólo a la carrera armamentista entre fagos y bacterias, sino también a lucha permanente entre la comunidad científica y las bacterias. Esto incluye el desarrollo de nuevos antimicrobianos, estrategias de cribado y diagnóstico, así como la optimización de tratamientos antibióticos frente a la aparición continua de resistencias antimicrobianas. Asimismo, dicha hipótesis también podría extenderse a las dinámicas poblacionales bacteria-bacteria mediadas por la producción de bacteriocinas similares a las colas de fago.

ABSTRACT

Pseudomonas aeruginosa is a ubiquitous pathogen responsible for a number of infections, often from **nosocomial origin**. The unique combination of antibiotic resistance genes and virulence factors has flagged this bacterium as one of the biggest threats to global health. Among the approximately 6.2 million base pairs that conform its genome, temperate phages -namely prophages- contribute the most to **genomic diversity** in *P. aeruginosa*.

In this thesis, the genomes of different *P. aeruginosa* strains from hospitals in Portugal, The Netherlands, Ukraine, and Spain have been sequenced and analyzed through various bioinformatic approaches. With this information, the presence, abundance, and composition of **prophages** and **phage tail-like bacteriocins** (PTLBs) were studied.

In **Chapter 1**, the genomes of 53 *P. aeruginosa* isolates from Portuguese and Spanish Intensive Care Units were analyzed. A total of 113 prophages were identified within the collection, being 13 of them integral and present in more than one strain simultaneously. All prophages had a length ranging from 20,199 to 63,401 bp and a GC% between 56.2% and 63.6%. The number of open reading frames (ORFs) oscillated between 32 and 88, and in 3/13 prophages, more than 50% of the ORFs had an unknown function. A number of proteins in relation to viral defense and to prophage interference into their host's quorum sensing system and regulatory cascades were found, supporting the idea that prophages have an influence in bacterial pathogenesis and anti-phage defense.

In **Chapter 2**, we studied 9 *P. aeruginosa* strains recovered from Ukrainian patients evacuated to two Spanish and five Dutch hospitals between March and December 2022. The strains, all of them belonging to the ST773 clone, produced an NDM-1 carbapenemase, constituting its first detection in Western Europe. All 9 strains shared the same core genome, PTLB cluster, and resistome, irrespective of their country of isolation, finding the greatest differences in prophage distribution and carrying each strain up to 9 temperate phages. These results highlight the importance of genomic surveillance and of the understanding of the resistance dynamics in multidrug-resistant bacteria.

Finally, in **Chapter 3**, the genomes of 32 *P. aeruginosa* isolates from critical care patients in Portugal and Spain were analyzed in search for PTLB clusters. These pyocins were all localized within the tryptophan operon, and were classified into 4 groups attending to their tail fiber protein sequence. PTLBs were produced in liquid culture and purified to perform killing spectrum assays, showing variable range of activity (0-37.5%). With these results, we explored exploring the potential use of PTLBs as an alternative to traditional antimicrobials and as novel typing tools.

RESUMEN

Pseudomonas aeruginosa es un patógeno ubicuo causante de una gran variedad de infecciones, a menudo de **origen nosocomial**. La combinación peculiar de genes de virulencia y de resistencia antimicrobiana ha posicionado a esta bacteria como una de las mayores amenazas a la salud global. De entre los aproximadamente 6,2 millones de pares de bases de su genoma, los fagos atemperados -o profagos- contribuyen en su mayoría a la **diversidad genómica** de *P. aeruginosa*.

En esta tesis, los genomas de diferentes cepas de *P. aeruginosa* procedentes de hospitales en Portugal, Países Bajos, Ucrania y España fueron secuenciados y analizados a través de diferentes herramientas bioinformáticas. Con esta información se estudió la presencia, abundancia y composición de los **profagos** y **bacteriocinas similares a las colas de fago** (PTLBs).

En el **Capítulo 1** se estudiaron los genomas de 53 cepas de *P. aeruginosa* aislados de pacientes críticos de Portugal y España. Un total de 113 profagos fueron identificados en la colección, 13 de ellos íntegros y presentes en más de una cepa simultáneamente. Todos los profagos tenían una longitud entre 20.199 a 63.401 pares de bases y un contenido en GC entre 56,2% y 63,6%. El número de marcos de lectura abiertos variaba entre 32 y 88, y en 3/13 profagos más del 50% de ellos tenían función desconocida. También se describieron proteínas de defensa viral e interferencia con el sistema de *quorum sensing* y cascadas regulatorias, apoyando la idea de que los profagos pueden influenciar en la patogénesis bacteriana y en la defensa anti-fago.

En el **Capítulo 2** estudiamos 9 cepas de *P. aeruginosa* aisladas de pacientes ucranianos evacuados a dos hospitales españoles y 5 neerlandeses entre marzo y diciembre de 2022. Los aislados, todos de ellos pertenecientes al clon ST773, producían una carbapenemasa tipo NDM-1, siendo esta su primera detección en Europa occidental. Las 9 cepas compartían el mismo genoma núcleo, agrupación de PTLBs y resistoma, independientemente de su país de origen, encontrando las mayores diferencias en la distribución de los profagos y portando cada cepa hasta 9 profagos. Estos resultados resaltan la importancia de la vigilancia epidemiológica y el conocimiento de las dinámicas de resistencia en las bacterias multirresistentes.

Finalmente, en el **Capítulo 3** analizamos los genomas de 32 aislados de *P. aeruginosa* de pacientes críticos en Portugal y España en busca de PTLBs. Estas se localizaron todas en el operón triptófano, y fueron clasificadas en 4 grupos atendiendo a la secuencia las fibras de la cola. Las PTLBs fueron producidas en cultivos líquidos y purificadas para llevar a cabo ensayos de rango de letalidad, mostrando una actividad variable (0-37,5%). Con estos resultados pudimos explorar el potencial uso de las PTLBs como una alternativa a los antimicrobianos tradicionales y como nuevas herramientas de tipado bacteriano.

1. INTRODUCTION

1.1 *Pseudomonas aeruginosa*

The genus *Pseudomonas*, included within the class *Gammaproteobacteria*, encompasses 342 species and 18 subspecies, being ***P. aeruginosa*** the most clinically relevant both by its pathogenicity and antimicrobial resistance (AMR) profiles (1, 2).

P. aeruginosa was first described in 1894 by the Polish-German botanist and mycologist Walter Migula at the Karlsruhe Institute of Technology (Karlsruhe, Germany). While it is widely believed to be derived from the Greek words *ψευδο* (*pseudo*, false) and *μονάς* (*monas*, unit), some scientists suggest that its name originated from its resemblance to a group of eukaryotic and prokaryotic nanoflagellates known as "Monas" at that time. Initially named "*Pseudomonas pyocyanea*" for the blueish pus that characterized its infections, it was later on renamed "*Pseudomonas aeruginosa*" to reflect its **production of green pigment**, being "*aeruginosa*" the Latin word for copper rust (3, 4).

P. aeruginosa is a **motile** Gram-negative rod commonly found in environmental soil and water, as well as within plants and animals (5–7). It typically measures approximately 0.5 to 0.8 µm in width and 1.5 to 3.0 µm in length (8). This **ubiquitous** pathogen is not believed to belong to the normal microbiota of healthy individuals, being infections often from **nosocomial origin** in patients at risk: patients admitted to Intensive Care Units (ICU), with mechanical ventilation, catheters, neutropenia, burns, or cystic fibrosis (CF), among others. **Community-acquired** infections have also been described following contact with contaminated waters -such as recreational waters, contact lenses or humidifiers- and generally resulting in conjunctivitis, otitis externa or auto-limited skin and soft tissue infections (9).

The clinical significance of this species has granted it a preferential position in the **ESKAPE group**, a list of microorganisms of concern in nosocomial environments for their pathogenesis, transmission and AMR (10). Moreover, the World Health Organization has recently classified carbapenem-resistant *P. aeruginosa* among the high priority bacterial pathogens due to the global threat it represents, especially in health-care settings. This initiative seeks to address the need for research and development in new antibacterial drugs as well as to promote the implementation of the recent advances in surveillance platforms (11).

1.1.1. Metabolism

P. aeruginosa shows a remarkable **metabolic adaptability**, governed by a complex network of transcription factors and enabling rapid changes in its metabolism to survive in a wide variety of environments (12, 13). This bacterium uses oxygen as the main terminal electron acceptor, generally rendering a strict **aerobic metabolism**, but can also use nitrate (NO^{3-}), nitrite (NO^{2-}), and nitrous oxide (N_2O) -in a process known as denitrification- to grow anaerobically in oxygen-depleted environments, such as in the CF airway or the inner layers of a biofilm (14). *P. aeruginosa* also shows both **catalase and oxidase activities** (15–18).

Regarding carbohydrate metabolism, the genus *Pseudomonas* lacks essential glycolysis -or Embden-Meyerhof-Parnas pathway- enzymes, resulting in glucose being metabolized through the **Entner-Doudoroff** pathway with 6-phosphogluconate as an intermediate metabolite (19, 20). Hence, organic acids and amino acids stand as their preferred carbon source (21). Despite

not being able to ferment glucose- and thus being considered as a **nonfermenting bacterium**-, *Pseudomonas* can in fact ferment the amino acid L-arginine and pyruvate, the latter through a NADH-dependent lactate dehydrogenase (22, 23).

1.1.2. Genomic characteristics

In 2000, the *P. aeruginosa* **PAO1 strain** was the fourth bacterial genome to be completed (24). The sequenced strain, a spontaneous mutant from an Australian isolate recovered from a wound infection, has been used as the archetypical reference strain since (25). Its genome is comprised of 6,264,404 base pairs (bp) and has a 66.6% content in guanine and cytosine, making a total of 5,707 genes of which 5,586 are predicted open reading frames (ORFs). Of them, as many as 558 still have an unknown function (26).

The *P. aeruginosa* pangenome results of a combination of both the core genome -common to almost all *P. aeruginosa* strains- and the strain-specific accessory genome. The **core genome** makes up the major segments of the *P. aeruginosa* genome, about 90% of its entirety. These regions exhibit minimal genetic variation (0.5-0.7%), and primarily contain housekeeping genes. In contrast, the **accessory genome** comprises non-conserved DNA segments of variable lengths, typically found in extrachromosomal elements or as blocks of inserted DNA at specific sites. Rather than being randomly dispersed, these DNA segments tend to cluster at particular sites within the core genome, commonly referred to as genomic islands, with a length of >10 kb (27). Other **Mobile Genetic Elements** (MGE) such as phages, plasmids and transposons account for this accessory genome, contributing to enriching strain variability. These MGE usually encode virulence factors and AMR genes. Altogether, genomic islands and prophages contribute the most to genomic variability in *P. aeruginosa* (28).

1.1.3. Virulence factors

P. aeruginosa can produce a myriad of **virulence factors**, both displayed on the bacterial surface or secreted, to help in host invasion, pathogenesis development, and the evasion of the host's immune system (29). Prominent examples of this virulome are summarized in TABLE 1 and are described below:

1.1.3.1. Flagella and pili

P. aeruginosa possesses a **single, polar flagellum** with crucial roles in motility, adhesion and biofilm formation. This structure is constituted by flagellin monomers, encoded in the *fliC* gene (30). Regarding pili, five different *pilA* alleles have been identified in *P. aeruginosa* -classes I to V-, being type IV pili (TIVP) the most deeply characterized in *P. aeruginosa*. TIVP is involved in cell adhesion and twitching motility -in contrast to the swimming motility- in a flagellum-independent manner. It can also serve as a bacteriophage receptor and contribute to biofilm formation during the first steps of colonization (31). Although pili in *P. aeruginosa* can successfully bind DNA, this pathogen has traditionally been considered incapable of undergoing natural transformation, and DNA binding has been thought to be related to biofilm formation (32). However, recent evidence is starting to call in question this dogma (33).

1.1.3.2. Secretion systems

Secretion systems are molecular machineries in Gram-negative bacteria responsible for delivering enzymes to the extracellular space or to other cell's cytoplasm. They are used to metabolize complex carbon sources, to chelate metals or as defenses against competing bacteria and the host's immune system. They differ in the number of steps they take to secrete toxins and on the processing of secreted toxins (34, 35).

-**Types I and II**. Whereas type I secretion system (T1SS) directly **secretes toxins** -such as the alkaline protease- to the extracellular space, the type II (T2SS) secretes them in a two-step manner, with precursors transiting through the periplasmic space and being activated to be functional. Examples of toxins secreted by the T2SS are phospholipase C, protease IV, elastase or the exotoxin A (36, 37).

-**Type III.** This system is **cell-contact dependent** and involves a protein complex that directly injects toxins into the host cell's cytoplasm. It is composed by 42 genes -clustered in several operons- that encode proteins forming the needle complex, a translocation system, transcriptional regulators, chaperones and the effector proteins. Among the latter are included ExoS and ExoT, toxins with adenosine diphosphate (ADP)-ribosyltransferase and guanosine triphosphatase (GTPase)-activating functions; ExoU, a phospholipase responsible for phagocyte and parenchymal cell death whose activity is enhanced by the presence of superoxide dismutase, such as in the alveolar epithelium; and ExoY, an adenylyl cyclase. The presence of these toxins among *P. aeruginosa*'s isolates is highly variable and influences their virulence, being considered its **major virulence factor** (38).

-**Type V**. This secretion system is characterized for its simplicity, with secreted molecules **catalyzing their own transport**. These molecules are usually comprised of a single aminoacidic chain with a C-terminal domain that forms a pore in the membrane and an N-terminal catalytic domain or two different peptides with the homologous functions. Examples of proteins secreted this way are LepA/LepB (involved in eukaryotic cell attachment), CdrA/CdrB (adhesin) and other lytic enzymes (serin proteases, metallopeptidases and lipases) (39).

-**Type VI**. Similarly to the T3SS, T6SS is formed by a protein complex with resemblance to a T4 bacteriophage tail, with protein Hcp1 polymerizing to form a tube and VgrG1a as a spike. To date, the function of the secreted proteins remains unknown. However, they can target both bacterial and eukaryotic cells, **delivering toxic effector proteins** to the cytosol (40, 41).

1.1.3.3. Lipopolysaccharide (LPS)

The LPS, also known as **endotoxin**, is one of the main constituents of the outermost layer of the cell wall in Gram-negative bacteria (42). This structure plays a fundamental role in bacterial **structural integrity** and in triggering the host's **inflammatory response** as well as in evading the host's immune system. The LPS is an amphipathic molecule -both hydrophobic and hydrophilic- composed of the lipid A, an oligosaccharide core, and a long-chain polysaccharide (O-antigen) (FIGURE 1).

-The **lipid A** is constituted by a di-phosphorylated disaccharide linked to several fatty acids, which serve as a hydrophobic anchoring into the phospholipid bilayer. It is highly **conserved** among Gram-negative bacteria and it is responsible for its **toxicity**. When exposed

during cell division, cell death or shedding of outer membrane vesicles, the lipid A triggers the dimerization of two Toll-like receptor 4 (TLR4)-MD2 complexes in macrophages and the release of pro-inflammatory molecules such as TNF-α, IL-6 and IL1β. These cytokines play an important physiological role in the activation of the host's immune system, but an uncontrolled secretion can lead to **septic shock** -hypotension, disseminated intravascular coagulation and multiple organ failure- and eventually to death. Although lipid A in *Pseudomonas* presents less endotoxic activity than in i.e. *Escherichia coli* or *Salmonella* spp, LPS modifications such as the increase in lipid A acylation are associated with augmented inflammatory responses in the late stages of CF (43, 44).

-The **oligosaccharide core** is comprised of both an inner and an outer core. The inner core in *P. aeruginosa* is a highly phosphorylated tetrasaccharide -two residues of keto-deoxyoctulosonate (KdoI and KdoII) and two residues of L-glycero-D-manno-heptose (HepI and HepII)- linked to one of the glucosamine molecules of the lipid A. The outer core, however, consists of a pentasaccharide: one D-galactosamine (D-GalN), one L-rhamnose (L-Rha), and three molecules of D-glucose (GlcI, GlcII and GlcIII). The core is **highly conserved** among *P. aeruginosa* isolates, being the variability concentrated in the outer core (45).

-The **O-antigen** constitutes the most external and **most variable** fraction of the LPS, and it is responsible for the **evasion of the host's immune system**. As the most exposed molecule within the bacterial surface, it is the main target of host antibodies. The O-antigen consists of a repetition of between one and eight glycosidic residues, and its incomplete synthesis results in different glycosidic chains within the same strain. Different sugar and linkages combinations determine the 20 different *Pseudomonas* serotypes based on the International Antigenic Typing Scheme (IATS) classification. Finally, the O-antigen can be absent in **rough** -as opposed to **smooth**- *P. aeruginosa* strains producing uncapped core oligosaccharides. Even in smooth strains, up to 80% of the outer membrane LPS can lack the O-antigen, with its highest manifestation in isolates from a chronic infection origin (44).

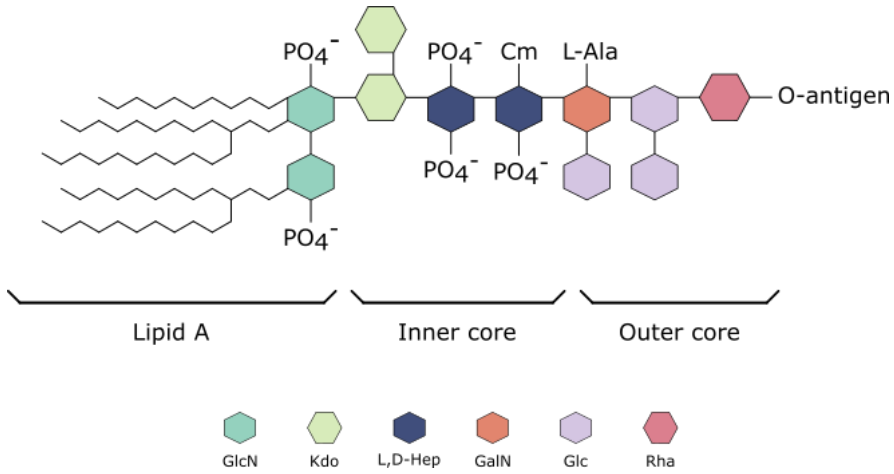

Figure 1. Schematic representation of the LPS structure, divided into lipid A, inner core, outer core, and O-antigen. Cm: 7-O-carbamoylation. GalN: galactosamine. Glc: glucose. GlcN: glucosamine. Kdo: 3-deoxy-D-*manno*-oct-2-ulosonic acid. L,D-Hep: L-*glycero*-D-*manno*-heptose. $PO4^-$: phosphate group. Rha: rhamnose. Source: Created by the author with Inkscape v1.1, adapted from (46).

1.1.3.4. Biofilm and biofilm-associated exopolysaccharides

Biofilms constitute one of the main virulence factors in *Pseudomonas*, serving as a scaffold for its growth, retaining water and nutrients, and protecting the bacterial communities against antimicrobials and the host's immune system. Biofilm formation usually involves four steps: **surface attachment** of planktonic bacteria, **microcolony formation**, biofilm **maturation**, and biofilm **shedding**, contributing to its dispersion in order to colonize new locations and to re-start the cycle (FIGURE 2). This process is sustained by different changes in *Pseudomonas* gene expression involving QS, exopolysaccharide secretion and twitching motility. The switch from a motile and more virulent phenotype to a static, mucoid and hypersecreting one evidences once again this pathogen's versatility and adaptability (47).

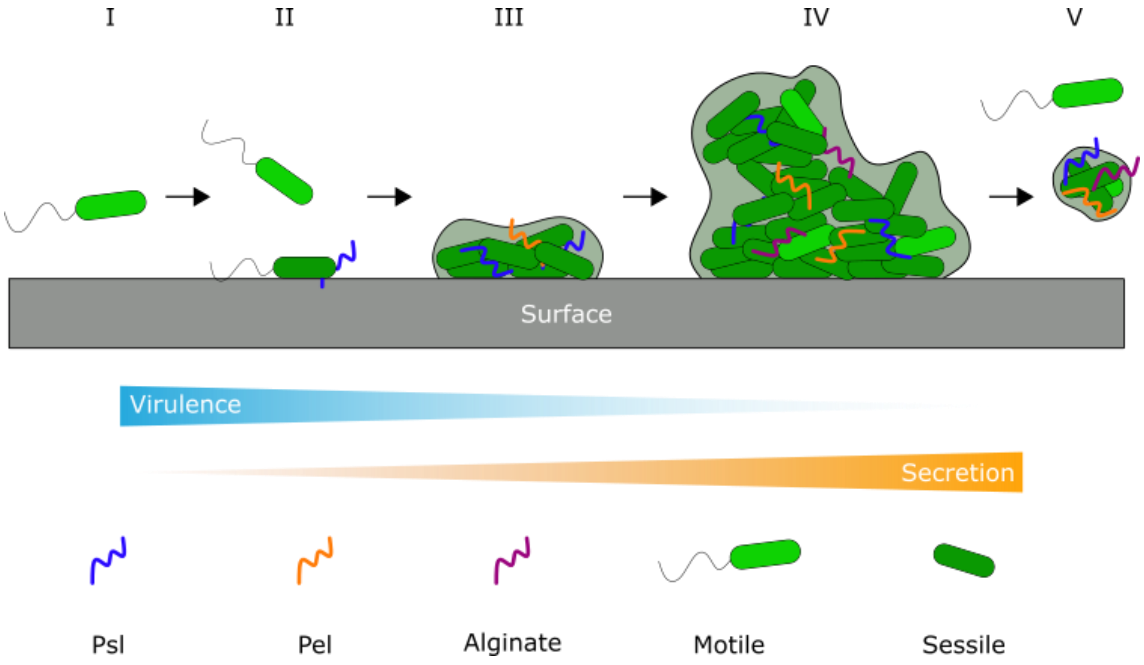

Figure 2. Biofilm formation steps. I: Planktonic cells. II: Attachment. III: Microcolony formation. IV: Biofilm maturation. V: Dispersion. Source: Created by the author with Inkscape v1.1, adapted from (47).

P. aeruginosa is known to produce three different **exopolysaccharides** -alginate, Psl, and Pel- which, together with proteins, lipids, extracellular DNA (eDNA), cell debris, and water, form **biofilms**, among others, in indwelling medical devices and in the respiratory tract of CF patients.

-**Alginate** is a linear and negatively charged polymer composed of different β-D-mannuronate and its C-5 epimer α-L-guluronate subunits linked by β-1,4 glycosidic bonds. Although it can be produced by other microbial species, its overproduction in *P. aeruginosa* leads to a **mucoid phenotype**, with special relevance in colonization and persistence in the **CF airways**. (48). This can be achieved by the accumulation of inactivating mutations in *mucA*, an anti-sigma factor that sequesters the alginate activator AlgT (47).

-**Psl** is a branched, pentameric, and uncharged polymer consisting of a single residue of L-rhamnose, a residue of D-glucose, and three residues of D-mannose linked by glycosidic bonds. Despite not being essential for biofilm formation, it has an important role in both the first and latter steps of this process. As Psl-producing planktonic *P. aeruginosa* swims for **surface**

exploration, a track of this pentasaccharide is left behind and can be sensed and followed by other bacteria of the same species, enhancing cell attachment and the formation of microcolonies via secondary messengers (cyclic di-guanosine-monophosphate or c-di-GMP). In addition, in the final stages of biofilm formation Psl is able to bind extracellular adhesins and eDNA, contributing to **structural stability** (48, 49).

-**Pel** is a cationic polymer comprised of galactosamine and its N-acetylated form linked by partially de-N-acetylated α-1,4 glycosidic bonds. Its cationic nature provides tolerance to positively-charged antimicrobials and enables **binding to eDNA** enhancing biofilm stability. Pel has been shown to be crucial in cell-to-cell attachment and in pellicle development at the air-liquid interface -harnessing the higher oxygen concentrations-, thus its name. Together with Psl, they constitute the main *Pseudomonas*-specific exopolysaccharides and play an important role in non-mucoid biofilms (47).

1.1.3.5. Rhamnolipids

Rhamnolipids are rhamnose-bound glycolipids with an amphipathic nature, acting as surfactants- i.e. detergents- in nature (50). They are produced as mono- and di-rhamnolipids in the late log and stationary phases of the bacterial growth curve, by both clinical and environmental strains (51). These molecules are known to inhibit biofilm formation and to promote swarming motility in *P. aeruginosa*, enabling the **exploration** of new niches (52). Other roles in *P. aeruginosa* infections are the **solubilization of quorum sensing (QS)** mediators such as the Pseudomonas Quinolone Signal (PQS, in detail below)(53), **antibacterial activity** against Gram-positive –and some Gram-negative– bacteria, intra-species cooperation to avoid the social cheater-mediated collapse of the bacterial population by *lasR* mutants (54), and, less likely, the solubilization of hydrophobic carbon sources such as alkanes for bacterial uptake (55). The host's respiratory tract can also be affected by these surfactants via the stimulation of upper airway epithelial cells for **cytokine secretion** (56) and high-viscoelasticity **mucous secretion** (57), and the **inhibition of the ciliary movement** (58). In this regard, Kohler and colleagues demonstrated in a multicenter study analyzing tracheal aspirates in intubated patients that the development of ventilation-associated pneumonia was associated with the production of rhamnolipids in *P. aeruginosa* isolates (59).

1.1.3.6. Metallophores

Metallophores are molecules secreted by bacteria and some fungi to bind extracellular **metal ions**, which are otherwise insoluble in most environments, in order to facilitate its **uptake** by active transport via specific surface receptors. To date, three main metallophores have been described for *P. aeruginosa*: **pyoverdine**, **pyochelin** and **pseudopaline** (60). The first two are responsible for ferric ion (Fe^{3+}) sequestering, whereas the last one binds cobalt -for vitamin B12 or cobalamin biosynthesis (61)-, nickel -as a cofactor for the urease enzyme (62)-, and zinc -essential for the correct function of metallo-β-lactamases in β-lactam resistance (63)-. Their production is sequential, being pyochelin the first one to be secreted. Upon iron starvation, pyoverdine is produced as it has a higher affinity for this metal (64). Metallophores have been associated with **virulence**, with pyoverdine-defective strains having limited pathogenicity in *in vivo* models (65). This is thought to be not only due to iron scavenging but also because of pyoverdine acting as a metabolic signal stimulating the production of other virulence factors,

such as exotoxin A and endoprotease PrpL (66). However, in chronic infections such as the lower respiratory tract pathogenic colonization in CF patients, pyoverdine synthesis is reduced (67), possibly due to the ability of *P. aeruginosa* to scavenge iron through the uptake of the host's heme molecules, more abundant in inflammatory conditions (66).

1.1.3.7. Other pigments (pyocyanin, pyomelanin and pyorubin)

Pyocyanin is a major redox blue pigment in *P. aeruginosa*, and its expression is regulated through QS by both AHL and PQS (68). It has been shown to promote **cell-to-cell aggregation** and **biofilm synthesis** by inducing the release of DNA through oxidative stress- via reactive oxygen species such as superoxide and hydrogen peroxide (69)-, by binding the eDNA (70, 71), and by reducing Fe^{3+} into Fe^{2+}, increasing its bioavailability (72). On the other hand, **pyomelanin** is a brown pigment associated with resistance to pyocins (73), resistance to oxidative stress (74) and iron reduction (75). Finally, **pyorubin** is a reddish-brown pigment with a role in protecting against oxidative stress and antibacterial properties (76).

Table 1. Main virulence factors in *P. aeruginosa* and their role in pathogenesis.

Virulence factor	Role in pathogenesis	References
Flagellum	Swimming motility Adhesion Biofilm formation	(30)
Pili	Twitching motility Adhesion Biofilm formation	(31–33)
Secretion system I	Alkaline protease secretion	(36)
Secretion system II	Phospholipase C, protease IV, pyocyanin, elastase and exotoxin A secretion	(37)
Secretion system III	Injection of ExoS, ExoT, ExoU, and ExoY toxins into target cells	(38)
Secretion system V	LepA/LepB, CdrA/CdrB and lytic enzyme secretion	(39)
Secretion system VI	Unknown	(40, 41)
LPS	Structural integrity Pro-inflammatory effect Evasion of host's immune response	(42–45)
Alginate	Biofilm formation	(47, 48)
Psl		(48, 49)
Pel		(47)
Rhamnolipids	Swarming motility Biofilm disruption Intra- and inter-species growth inhibition Host's respiratory tract alteration	(50, 51)

Pyoverdine	Fe^{2+}, Co^{2+}, Zn^{2+} and Ni^{2+} scavenging	(60)
Pyochelin		
Pseudopaline		
Pyocyanin	Oxidative stress, biofilm formation, iron reduction	(68)
Pyomelanin	Resistance to oxidative stress Resistance to pyocins	(73)
Pyorubin	Resistance to oxidative stress Antibacterial	(76)

1.1.4. Quorum sensing and other bacterial signaling systems

Quorum sensing (QS) was first reported for *Vibrio fischeri* as a mean of bacterial communication to produce bioluminescence in a coordinated manner when a certain population density was achieved (77). It generally consists of a diffusible signal molecule- termed **autoinducer**-, its synthase, and its cognate receptor. The autoinducer is constitutively produced, but remains unable to trigger any response at low concentrations. However, when the adequate bacterial density is achieved, the autoinducer concentration surpasses a given **threshold** and the bacterial population **acts in unison**. These intercellular interactions have been observed in a number of Gram-negative and Gram-positive bacteria, coordinating their virulence through changes in gene expression, being *P. aeruginosa* one of the most prominent examples (78).

Approximately **10% of the genes** in *P. aeruginosa* are under QS regulation (79). The bacterial functions controlled by this cell-to-cell communication include extracellular protease synthesis (80), swarming motility activation (81), biofilm production (82), pyoverdine and pyochelin expression (83, 84), rhamnolipid production (50, 51) and even the development of AMR through modifications in efflux-pump expression (85, 86).

Up to date, two main QS systems can be found in *P. aeruginosa* (87)(FIGURE 3):

-**N-acyl homoserine lactones (AHLs)**, which derive from S-adenosylmethionine (SAM) and an acyl chain linked through an amide bond. They are produced by two homologous AHL synthases in *Pseudomonas*, LasI and RhlI. Whereas LasI synthesizes the long chain N-(3-oxooctanoyl)-homoserine lactones (3-oxo-C8-HSL), N-(3-oxodecanoyl)-homoserine lactones (3-oxo-C10-HSL), N-(3-oxododecanoyl)-homoserine lactones (3-oxo-C12-HSL) and N-(3-oxotetradecanoyl)-homoserine lactones (3-oxo-C14-HSL); RhlI produces the short chain AHLs N-butanoyl-homoserine lactones (C4-HSL) and N-hexanoyl-homoserine lactones (C6-HSL) (78). When the AHLs bind their respective receptors, LasR and RhlR, they **dimerize** in a more stable and soluble complex which recognizes and binds specific DNA sequences at the promoters and **inducing gene transcription** (88)(FIGURE 4).

-***Pseudomonas* quinolone signal (PQS)**. This system relies on 4-quinolones as autoinducers, a family of more than 50 compounds with 2-heptyl-3-hydroxy-4-quinolone as the most representative one (89). Their synthesis is regulated by the *pqsABCDE* operon, and its role in **bacterial fitness** is thought to be both pro- and anti-oxidant, eradicating damaged cells and promoting the survival of the fittest. This selective killing can further contribute to biofilm stability by the release of eDNA by targeted cells. Besides, the PQS system is able to auto-regulate

itself, inducing its own synthesis and packaging into extracellular vesicles. There is a considerable hierarchy in the three QS systems of *P. aeruginosa*, with the *las* system upregulating the other two, *rhl* and PQS (90).

Besides QS systems, other signaling systems can be found in *P. aeruginosa* (FIGURE 3):

-**Diketopiperazines (DKPs)** are cyclic peptides believed to bind and trigger LuxR receptors in *P. aeruginosa* (91). However, the high DKP concentrations required for this interaction in the original studies and the fact that more recent researchers could not demonstrate any activity -neither agonistic or antagonistic- of these peptides over LuxR puts their role in QS into question (92).

-**Nucleotidic molecules** (cAMP, c-di-GMP, alarmones). In *P. aeruginosa*, cyclic adenosine-monophosphate (**cAMP**) is synthetized by adenylate cyclase enzymes, primarily CyaB, with some contribution from CyaA (93, 94). The previously described exoenzyme ExoY, injected by the T3SS, can also act as an adenylate cyclase producing cAMP and contributing to pathogenicity. This second messenger is responsible for **binding transcription factors** from the CRP family (cAMP regulator proteins) such as the Virulence factor Regulator, which activates the Las QS cascades and upregulates the expression of a variety of virulence factors (T3SS, ExoA, TIVP) while inhibiting the flagellum synthesis (95, 96).

On the other hand, cyclic di-guanine monophosphate (**c-di-GMP**) is synthetized and degraded by diguanylate cyclases and phosphodiesterases, respectively, and it controls biofilm production and metabolic activity (97, 98), motility and aggregation (99), and the production of virulence factors (100, 101). Moreover, high levels of di-c-GMP have been associated with the development of a **small colony variant (SCV) morphotype**, a trait related with persistence and the establishment of chronic infections (102).

Finally, **alarmones** are modified nucleotides -ppGpp and pppGpp- involved in the **stringent response**, a bacterial adaptation to environmental changes such as **nutrient starvation**, elevated osmolarity and highly acidic or alkaline pH levels (103). It has been suggested that (p)ppGpp are involved in T3SS activation, synthesis of virulence factors (elastase, pyocyanin, pyoverdine and alginate), tolerance to H_2O_2, and activation of swarming motility and biofilm formation (104, 105)

-The **Global activator of Antibiotic and Cyanide synthesis** system is responsible for the transition from acute to **chronic infections** by producing a set of RNA binding proteins (RsmA and RsmF), which target and sequester mRNA to modulate protein production (106). This two-component system is comprised by a membrane-bound sensor kinase (GacS), which undergoes autophosphorylation upon the detection of environmental changes- mainly carbon scarcity-, and a cytoplasmic response regulator (GacA), to which a phosphate group is transferred by the activated sensor kinase to acquire an active conformation and enable *rsm* gene expression (107).

-**Diffusible signal factors (DSF)**. There is scarce information on DSF, which comprise a range of fatty acids able to cross the bacterial membrane by passive diffusion in order to regulate gene expression in different bacterial species such as *Xanthomonas campestris*, *Stenotrophomonas maltophilia*, *Xylella fastidiosa* and the *Burkholderia cepacia* complex (108–110). In *P. aeruginosa*, the DSF-like molecule *cis*-2-decenoic acid is believed to be synthetized

and perceived by a 5-gene cluster (PA4978 -PA4983), inducing biofilm disruption, virulence factor production, increased metabolic activity and enhanced motility (111).

It should be noted that these systems are not watertight and independent. In fact, **interactions** between them have been documented. For instance, c-di-GMP signaling can inhibit the cAMP cascades (112), the stringent response can lead to a 3-oxo-C12-HSL premature production (113) and the c-di-GMP and GAC/Rsm systems can coordinate to regulate iron uptake (114).

The **QS communication** can overcome the intra-species level and operate in an **inter-species** manner, with *P. aeruginosa* controlling growth and virulence of other microorganisms. QS in Gram-positive bacteria relies in peptides instead of AHLs, however, is has been reported that long chain AHLs produced by *P. aeruginosa* can inhibit *Staphylococcus aureus* growth and modulate its virulence (83). The *Pseudomonas* produced 3-oxo-C12-HSL reduced the expression of exotoxins and cell wall fibronectin-binding proteins while increasing protein A production by antagonizing the *S. aureus* QS systems *agr* and *sar*. This has been proposed as a possible explanation for the colonization dynamics in patients with CF, who are initially colonized by *S. aureus* until *P. aeruginosa* eventually takes over (115).

QS communication in *P. aeruginosa* can even transgress the kingdom and domain levels, having **effects in eukaryotic cells** such as yeasts. Hyphal development in *Candida albicans* is orchestrated by the fungal QS autoinducer farnesol, a sesquiterpene with a backbone of C12 analogous to that of 3-oxo-C12-HSL (116). AHLs produced by *P. aeruginosa* can thus activate fungal QS cascades through cAMP synthesis inhibition, hindering the formation of germinal tube. These inter-kingdom communications have an important role in shaping biofilm composition and in polymicrobial infections (117).

Furthermore, QS in Pseudomonas can have an effect not only on competing species but also on their **host** (78, 79). The LasR/LasI autoinducer 3-oxo-C12-HSL has been proved to **stimulate macrophages** to promote the release of anti-inflammatory cytokines (IL-10) while inhibiting the production of the pro-inflammatory ones (TNF-α) (118, 119). This same molecule is known to **induce apoptosis** of hematopoietic cells, airway epithelial cells, endothelial cells and fibroblasts (120–122), as well as to disrupt the cell junction proteins in the intestinal epithelium (123, 124).

Finally, **quorum quenching (QQ)** consists on the silencing of the QS communication. This can be achieved by: a) autoinducer synthesis inhibition; b) autoinducer degradation or inactivation; c) efflux pump inhibition to decrease extracellular autoinducer concentration; d) QS receptor inhibition by autoinducer antagonists; and e) interference with downstream biochemical cascades triggered by the autoinducer (125). In light of quorum sensing's regulatory role in bacterial pathogenicity, strategies for quorum quenching have been proposed as alternative treatments to classical antimicrobials (126)(FIGURE 5).

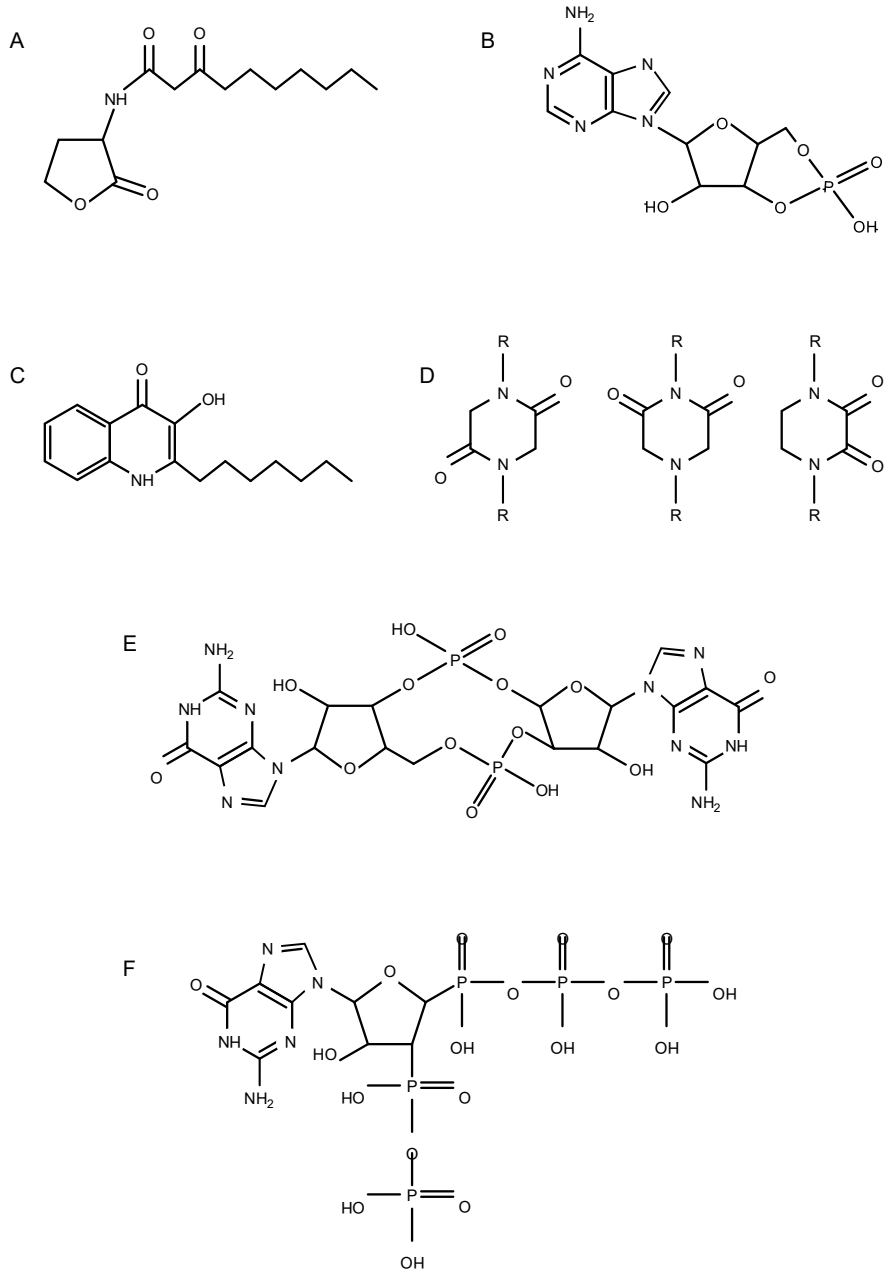

Figure 3. Molecular structure of common *P. aeruginosa* autoinducers in QS. A: N-(3-oxodecanoyl)-homoserine lactone. B: cAMP. C: 2-heptyl-3-hydroxy-4-quinolone. D: diketopiperazines. E: c-di-GMP. F: pppGpp alarmone. Source: Created by the author with Inkscape v1.1.

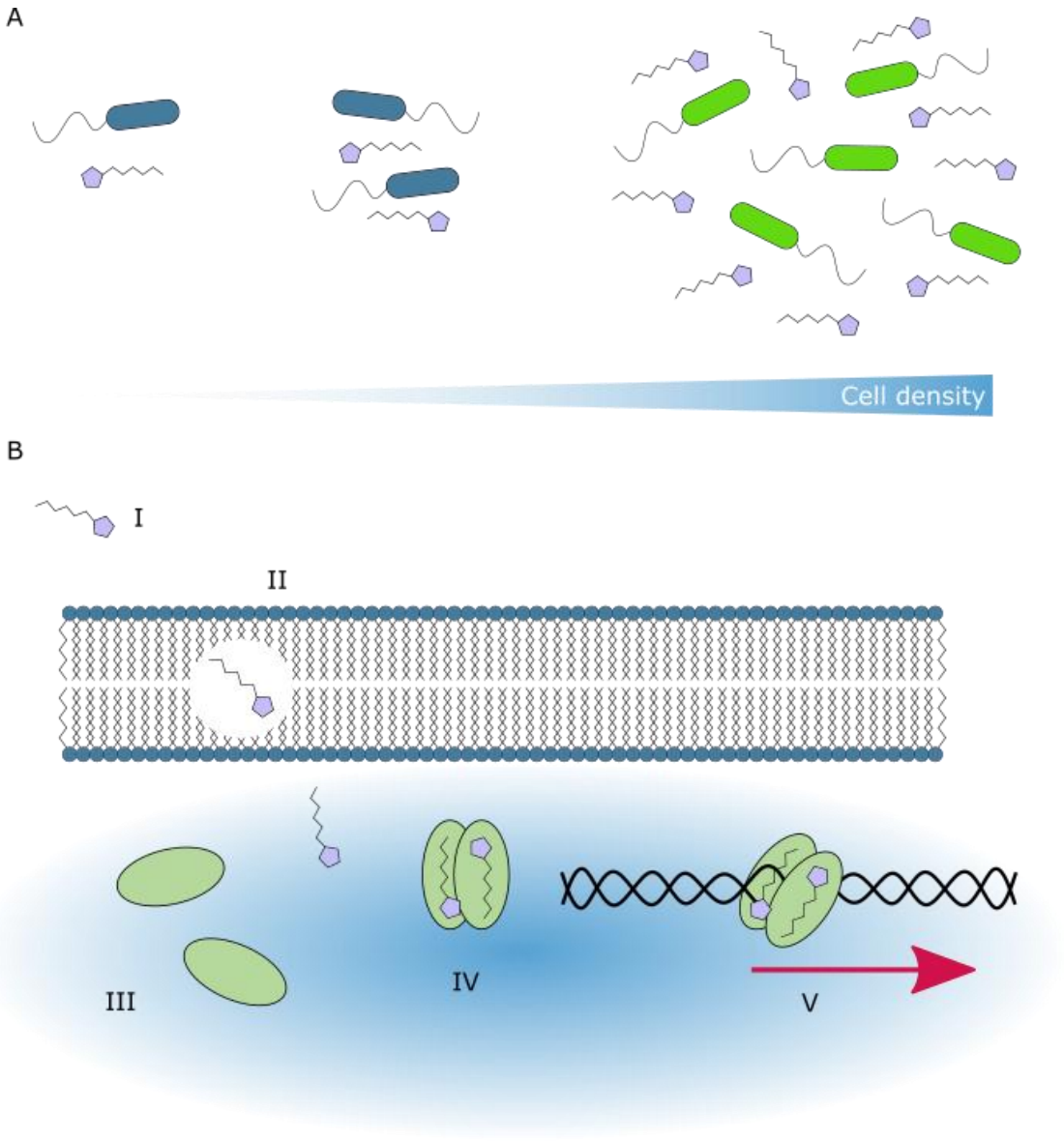

Figure 4. A: Coordinated activation of the bacterial population upon achieving a given threshold. B: Gene transcription activation mediated by AHLs autoinducers. I) Autoinducer; II) Autoinducer diffusion through the bacterial plasma membrane; III) autoinducer receptor; IV) receptor dimerization; V) transcription activation of QS-regulated genes. Source: Created by the author with Inkscape v1.1.

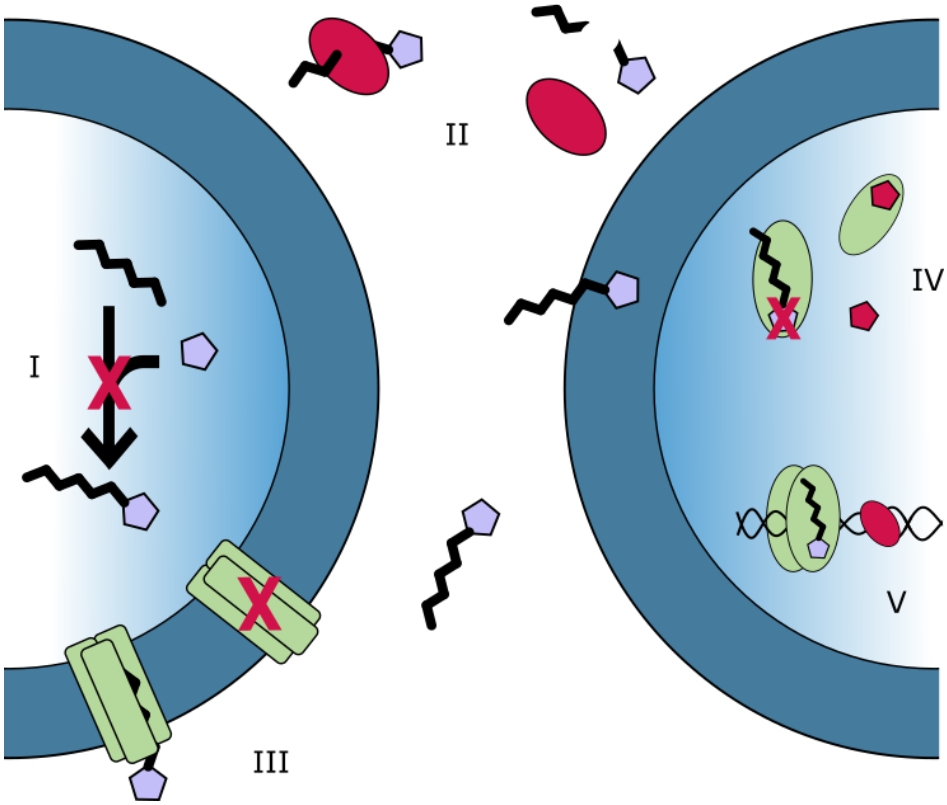

Figure 5. Quorum quenching strategies. I) Inhibition of autoinducer synthetases; II) Autoinducer cleavage; III) Decrease in autoinducer efflux pumps; IV) blockage of receptor dimerization through antagonist binding; V) inhibition of downstream biochemical cascades. Source: Created by the author with Inkscape v1.1.

1.1.5. Antimicrobial resistance (AMR)

In addition to its virulence factor production, *P. aeruginosa* infections present a considerable challenge due to the increased levels of **antibiotic resistance** within this species. In 2012, a joint initiative between the European Centre for Disease Prevention and Control (ECDC) and the Centers for Disease Control and Prevention (CDC) established a standardized terminology to classify important nosocomial pathogens in accordance to their patterns of acquired AMR. In this vein, antimicrobials were sorted into families and isolates were categorized as **multidrug-resistant (MDR)**, **extensively drug-resistant (XDR)** and **pandrug-resistant (PDR)**. In *P. aeruginosa*, MDR occurs when there is non-susceptibility to at least one agent in three or more antimicrobial families, XDR when there is non-susceptibility to at least one agent in all but two or less antimicrobial families, and PDR when there is resistance to all listed agents (127). The antimicrobial families and agents relevant to this pathogen are listed in TABLE 2.

Furthermore, another category has been set to help clinical microbiologists and infectious diseases physicians in their daily clinical practice: the **difficult-to-treat (DTR)** resistance phenotype (128). This classification assesses non-susceptibility to all first-line agents such as carbapenems, cephalosporins, penicillin/inhibitor combinations, monobactams, and fluoroquinolones. By excluding antimicrobials with high toxicity and lower efficacy, it affords a comprehensive perspective on the clinical use of antimicrobials (129). New β-lactam/inhibitor

combinations -*i.e.* ceftolozane/tazobactam, imipenem/relebactam, meropenem/vaborbactam, ceftazidime/avibactam, and aztreonam/avibactam- as well as cefiderocol were not included in these definitions.

Table 2. Antimicrobial families and antimicrobial agents to be considered for MDR, XDR and PDR classification. Adapted from (127).

Family	Agent
Aminoglycosides	Amikacin
	Gentamicin
	Netilmicin
	Tobramycin
Antipseudomonal carbapenems	Doripenem
	Imipenem
	Meropenem
Antipseudomonal cephalosporins	Cefepime
	Ceftazidime
Antipseudomonal fluoroquinolones	Ciprofloxacin
	Levofloxacin
Antipseudomonal penicillins / β-lactamase inhibitors	Piperacillin / tazobactam
	Ticarcillin / clavulanic acid
Monobactams	Aztreonam
Phosphonic acids	Fosfomycin
Polymyxins	Colistin
	Polymyxin B

1.1.5.1. Intrinsic AMR

Antimicrobial intrinsic resistance in *P. aeruginosa* does not rely on a single mechanism, but is rather achieved by a **combination** of low permeability of the outer membrane, active antibiotic expulsion by efflux pumps and antibiotic modifications (130):

-Reduced outer membrane permeability. The nature and composition of the outer membrane in *P. aeruginosa* restricts the types of molecules that can pass through, being 100 to 400-fold **less permeable** to substrates such as glucose-6-phosphate than that in *E. coli* (131). **Porins** are channels in the outer membrane characterized by an aminoacidic β-barrel structure. The cell wall in *P. aeruginosa* is characterized by the presence of narrow porins through which antibiotic diffusion -mainly β-lactams and quinolones- is hindered, and only a fraction of them is opened at any given time (132, 133). They can be classified into four different classes: **non-specific porins**, which facilitate the gradual diffusion of various small hydrophilic molecules (OprF); **specific porins**, equipped with sites tailored to allow traffic of particular molecules (OprB, OprD, OprE, OprO, OprP); **gated porins**, serving as outer membrane proteins regulated by ions,

facilitating the intake of ion complexes (OprC, OprH); and **efflux porins**, essential for the efflux pumps' functionality (OprM, OprN, OprJ) (134).

-Efflux pumps: They are complex structures which **extrude** different toxic molecules -such as reactive oxygen species (ROS), metabolites or antimicrobials- out of the bacterial cell, contributing to their clearance (135). **Six families** of efflux pumps have been described for *P. aeruginosa*: the ATP-binding cassette superfamily (ABC) (136), the multidrug and toxic compound extrusion family (137), the major facilitator superfamily (MFS) (138), the proteobacterial antimicrobial compound efflux family (PACE) (139), the resistance/nodulation/cell division family (RND) (140), and the small multidrug resistance family (SMR) (141). Among them, RND efflux pumps play a key role in AMR, with four main **multidrug efflux pump (Mex)-porin complexes** being described for *P. aeruginosa*: MexAB-OprM for the expulsion of β-lactams and quinolones; MexXY-OprM for aminoglycosides; MexCD-OprJ for β-lactams; and MexEF-OprN for quinolones (130). These protein complexes are formed by the combination of three different proteins: the abovementioned efflux porins (OprJ/M/N), an adaptor protein located at the periplasm (MexA/C/E/X); and an RND transporter (MexB/D/F/Y) (142).

-Antibiotic modifications: It can be achieved by antibiotic modification, having special relevance for **β-lactams**.

This pathogen carries an inducible chromosomal *ampC* gene encoding a **group 1 class C β-lactamase**, with hydrolytic activity for penicillins and cephalosporins, but not for carbapenems. In a **basal state**, the physiologic cell wall synthesis and degradation leads to the liberation of muropeptides, which are transported into the cell through an AmpG permease. Then, the NagZ N-acetylglucosaminidase and the AmpD amidase modify these cell wall debris yielding anhydromuramic acid, N-acetylglucosamine and tripeptides, being the latter processed into UDP-pentapeptides and transported into the periplasmic space for its recycling (143). The intracellular UDP-pentapeptide surplus binds to AmpR, maintaining it in a conformation that **hampers efficient transcription** from the *ampC* promoter, possibly by preventing the RNA polymerase recognition of this region (144). This results in a low basal level of *ampC* expression (FIGURE 6A).

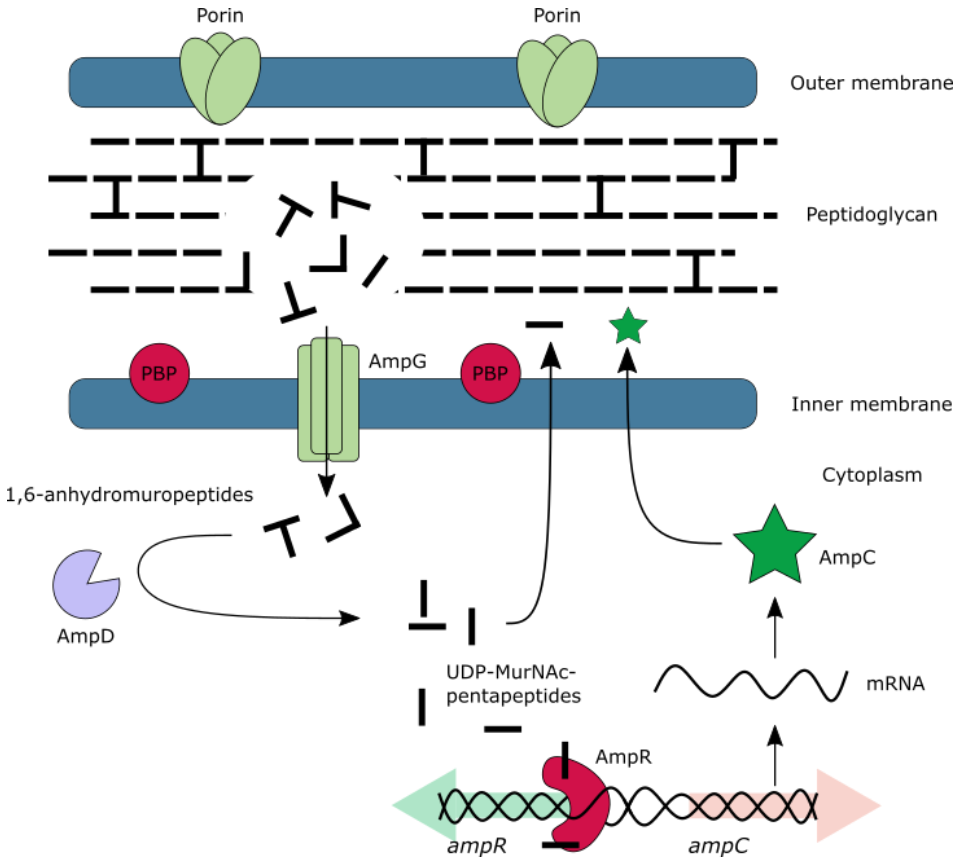

Figure 6A. AmpC β-lactamase basal production in *P. aeruginosa*. PBP: Penicillin binding protein. Source: Created by the author with Inkscape v1.1.

1.1.5.2. Adaptive AMR

The presence of antimicrobials or other environmental stressors- such as biocides, pH changes, oxygen concentration or carbon sources- can lead to an adaptive AMR pattern, based on the differential expression of *Pseudomonas* genes rather than the acquisition of new ones. Owing to the high proportion of regulatory genes in this species (up to 10%), the expression of these genes can also be modulated by the biofilm or swarming states of the bacterial cells (145).

The most prominent example is the *ampC* gene induction, triggered by certain β-lactam compounds such as cefoxitin, imipenem, and clavulanic acid, which are able to inhibit low-molecular-mass penicillin-binding proteins, such as the PBP4. This leads to an increase in the levels of intracellular muropeptides, which saturate AmpD and accumulate intracellularly, eventually replacing the repressing UDP-pentapeptides bound to AmpR. This drives a **conformational change** that facilitates the recognition of the *ampC* promoter by the RNA polymerase and leads to an **increased expression** of this gene. Interestingly, this state can be reverted by removing the inducing antibiotic (146)(FIGURE 6B).

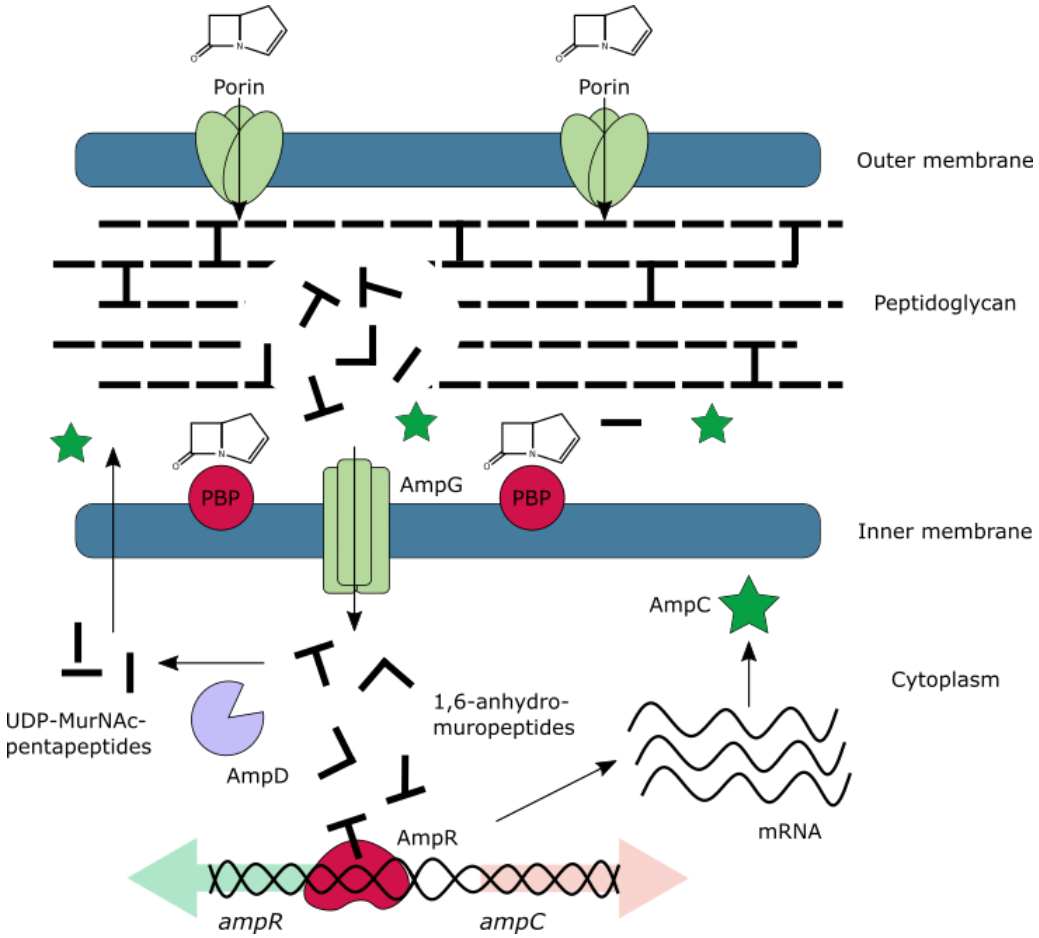

Figure 6B. Induction of AmpC production by cefoxitin, imipenem or clavulanic acid. PBP: Penicillin binding protein. Source: Created by the author with Inkscape v1.1.

On the other hand, **polycationic antimicrobials** such as aminoglycosides and polymyxins enter the cell upon interactions with the negatively charged **LPS** rather than through porins. Thus, resistance to these molecules can be achieved by the **modification** of these negative charges, hampering the ionic interactions. Resistance to colistin and aminoglycosides has been reported in the presence of subinhibitory concentrations of these antibiotics, in a regulatory process involving the two-component regulators ParR-ParS and the LPS-modification operon (*arnBCADTEF*) (147).

Another mechanism triggered by the exposure to subtherapeutic concentrations of antimicrobials is the **overexpression** of genes that encode **efflux pumps**. It is the case of transporter MexY, which is overproduced by *P. aeruginosa* after aminoglycoside exposure, leading to an increased efflux of these antimicrobials (148).

This adaptive AMR patterns might explain why, in some cases, *in vitro* antibiotic susceptibility has difficulties to predict the *in vivo* outcomes (149).

1.1.5.2. Acquired AMR

Finally, AMR can be achieved by the **acquisition** of exogenous genetic material or the **accumulation of mutations** in regulatory and other core genome genes.

-**AmpC derepression**. In an analogous process as in AmpC induction, it appears when muropeptide concentration in the cytosol increases. This situation generally occurs upon the accumulation of mutations that **inactivate the AmpD amidase**, the AmpR transcriptional regulator or the *ampR-ampC* intergenic region (150). It has been proposed that mutations in PBP4 trigger the activation of a two-component regulator (CreBC-BlrAB) that also leads to β-lactam resistance (151). Unlike in induction, derepression constitutes an irreversible process (FIGURE 6C).

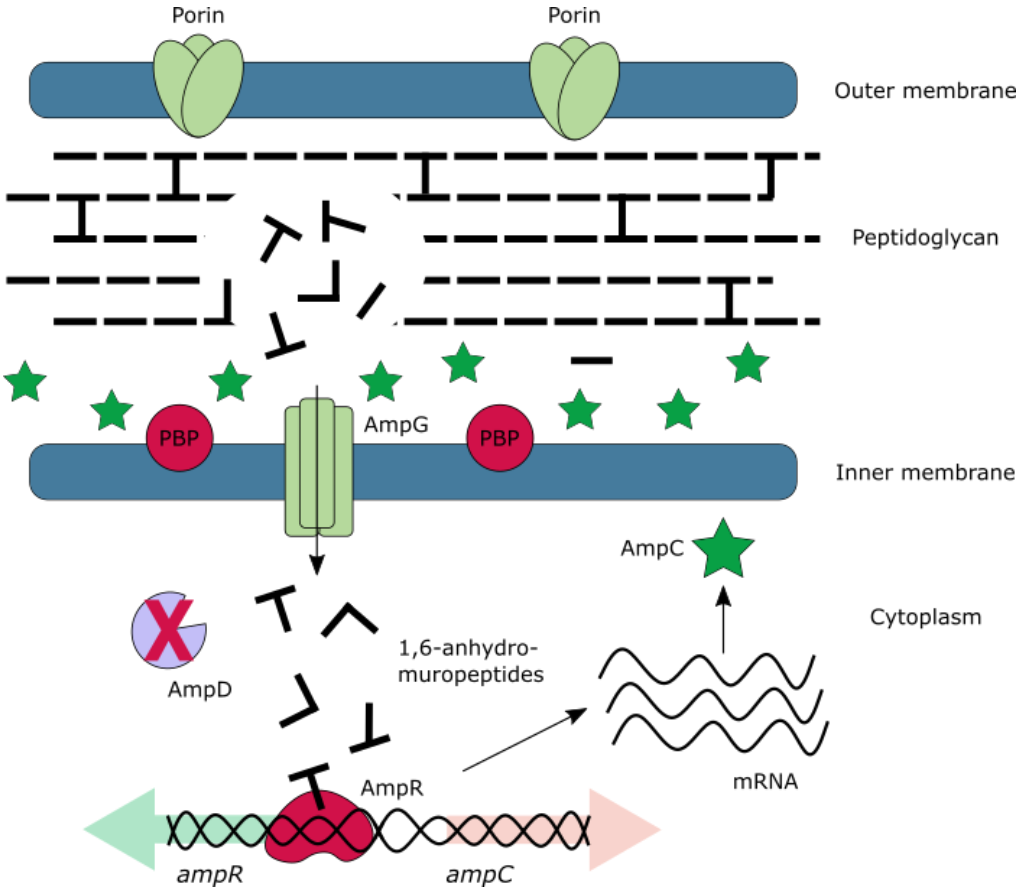

Figure 6C. Derepression of the *ampC* gene by the accumulation of mutations in the amidase AmpD, which leads to an increase in 1,6-anhydromuropeptides that maintain the AmpR regulator in an inactivated state. PBP: Penicillin binding protein. Source: Created by the author with Inkscape v1.1.

-Mutations in efflux pump regulatory genes. Loss of function of given regulators, such as mexR or mexZ, result in the constitutive overexpression of the efflux pumps MexAB-OprM and MexXY-OprM, resulting in resistance to aminoglycoside, fluoroquinolones and the fourth-generation cephalosporin cefepime and meropenem -but not imipenem- by antibiotic clearance. As for the MexCD-OprJ efflux pump, the same outcome has been described upon the inactivation of the NfxB repressor (145).

-Mutations in porins. The accumulation of mutations in porins such as OprD give rise to non-functional channels, hampering imipenem -but not meropenem- uptake and conferring the bacterium resistance to this antibiotic (152, 153).

-Mutations in target enzymes: Additionally, other AMR strategy involves the accumulation of mutations within bacterial genes encoding enzymes targeted by antimicrobials. Notably, mutations in *gyrA* and *gyrB*, as well as *parC* and *parE* -genes coding for DNA gyrase and topoisomerase IV, respectively- result in **diminished binding affinity to fluoroquinolones** (145).

In addition to the abovementioned AMR mechanisms, *P. aeruginosa* can **acquire exogenous genetic material** through **horizontal gene transfer**, contributing to survival in the presence of antimicrobials. There are three main ways for the DNA incorporation into its genome: by the direct exchange of DNA between two bacterial cells through physical contact or **conjugation** (154); when infecting bacteriophages transfer DNA from one bacterium to another or **transduction** (155); and when bacteria integrate free DNA fragments from the environment or **transformation** (33). The newly acquired genetic information usually comprises antimicrobial modifications.

In this regard, **carbapenemases** represent an emerging challenge and one of the most significant threats in pseudomonal AMR, due to their ability to confer the harboring bacteria **resistance** to all classic β-lactam antibiotics -including the broad-spectrum carbapenems-, as well as to the newest β-lactam/**β-lactamase inhibitor combinations**: ceftolozane/tazobactam, imipenem/relebactam and ceftazidime/avibactam. These genes are usually encoded by mobile genetic elements, like integrons or plasmids, contributing to its worldwide dissemination (156).

β-lactamases can be classified into **four Ambler classes (A-D)** depending on their amino acidic sequence and active site structure, with carbapenemases in *P. aeruginosa* belonging fundamentally to class B, and to a lower stent to classes A and D (157). **Class B** are **metalloenzymes** that rely on zinc at their active site for their catalytic activity, whereas classes A and D enzymes are serin-proteases (158). **Class A** carbapenemases are able to hydrolyze penicillins, cephalosporins and carbapenems, and their action can be blocked by **β-lactamase inhibitors** such as clavulanic acid, tazobactam, avibactam, vaborbactam or relebactam. On the contrary, class B carbapenemases remain unaffected by β-lactamase inhibitors, and confer resistance to all β-lactams but aztreonam. They can be inhibited *in vitro* by chelating agents like ethylenediaminetetraacetic acid (EDTA) and dipicolinic acid (DPA) or recently developed β-lactam inhibitors, such as taniborbactam and xeruborbactam. Finally, **class D** carbapenemases hydrolyze penicillins as well as first and second generation cephalosporins, having a **weaker activity** against third and fourth generation cephalosporins as well as against carbapenems. They are resistant to most of β-lactamase inhibitors, but can be phenotypically detected by a strong temocillin hydrolysis (159). The most frequent carbapenemases in *P. aeruginosa* are summarized in TABLE 3. It can be noted that the most diverse and abundant carbapenemases in *P. aeruginosa* belong to the Ambler class B.

Table 3. Characteristics of the main carbapenemases found in *P. aeruginosa*. CA: Clavulanic acid; TZ: tazobactam; AV: avibactam; VB: vaborbactam; RB: relebactam; TB: taniborbactam EDTA: ethylenediaminetetraacetic acid, DPA: dipicolinic acid. Adapted from (160).

Ambler Class	Carbapenemase name	Abbreviation	β-lactam Spectrum	Inhibition
A	Guiana extended spectrum	GES	Penicillins; 1st, 2nd, 3rd and 4th generation cephalosporins; carbapenems; monobactams	CA, TZ, AV, VB, RB
	Klebsiella pneumoniae carbapenemase	KPC		
B	Central Alberta metallo-β-lactamase	CAM	Penicillins; combinations with β-lactamase inhibitors; 1st, 2nd, 3rd and 4th generation cephalosporins; carbapenems	EDTA, DPA, TB
	Dutch imipenemase	DIM		
	Florence imipenemase	FIM		
	German imipenemase	GIM		
	Hamburg metallo-β-lactamase	HMB		
	Imipenemase metallo-β-lactamase	IMP		
	New Delhi metallo-β-lactamase	NDM		
	Sao Paulo metallo-β-lactamase	SPM		
	Seoul imipenemase	SIM		
	Verona integron-encoded metallo-β-lactamase	VIM		
D	Oxacillinase	OXA	Penicillins; combinations with β-lactamase inhibitors; 1st and 2nd generation cephalosporins. Weak activity against 3rd and 4th generation cephalosporins, carbapenems and monobactams	TB

The **epidemiology** of carbapenemase-producing *P. aeruginosa* is highly variable around the globe, with notable differences observed among regions. In a recently published prospective study that included 44 hospitals worldwide, carbapenem-resistant *P. aeruginosa* isolated from December 2018 to December 2019 were analyzed. In the **USA**, a 98% of the isolates did not carry a known carbapenemase gene, with the remaining 2% being VIM and KPC enzymes (1% each). However, in **Central and South America** the majority of the isolates produced KPC (32%),

followed by no carbapenemase (31%), VIM (18%), two or more simultaneous carbapenemases (18%) and other carbapenemases (1%). Regarding **Australia and Singapore**, 43% of the isolates carried no carbapenemase, followed by NDM and IMP (21% each), VIM (7%), GES (5%), and two or more simultaneous carbapenemases (2%). On the other hand, isolates from the **Middle East** did not carry a carbapenemase in 70% of the cases, while an 18% carried VIM enzymes, 8% GES and 4% IMP. Finally, a majority of the carbapenem-resistant isolates in **China** did not carry a carbapenemase (68%), followed by the KPC carbapenemase (23%), VIM (4%), IMP (2%), and lastly GES enzymes, two or more carbapenemases, and other carbapenemases (1% each). Interestingly, 30-day mortality was higher in patient with carbapenemase-producing *P. aeruginosa* infections when compared to the non-carbapenemase ones (22% vs 12%), highlighting the importance of detecting and adequately treating this kind of infections (161).

Regarding **Europe**, a prospective study collected more than 9,000 *P. aeruginosa* isolates between 2013 and 2017 from different geographic regions. A 27.4% of them (2556/9330) were considered as meropenem non-susceptible, with a 18.5% harboring a carbapenemase (473/2556) and the remaining 81.5% having a different resistance mechanism. Among carbapenemases, the **most frequent** were the **VIM** enzymes (75.1%, 355/473), followed by GES (16.1%, 76/473), IMP (8.3%, 39/473), and NDM (0.6%, 3/473). Although VIM-harboring isolates were collected in almost all surveyed subregions, some differences between countries could be observed: GES-type carbapenemases predominated in Portugal, IMP enzymes were mainly found in Czechia and surrounding countries, NDM enzymes were only found in Germany and Italy, and no KPC-producing *P. aeruginosa* was isolated in Europe during the course of the study (162).

Moreover, certain strains of *P. aeruginosa* might harbor **extended-spectrum-β-lactamases (ESBLs)**, such as PER-1 or certain GES enzymes, granting them a significant level of resistance against most β-lactams, like penicillins, cephalosporins, and aztreonam. In this regard, β-lactam inhibitors such as tazobactam and avibactam efficiently inhibit ESBL activity (163).

On the other hand, **aminoglycoside resistance** by exogenous genetic material acquisition takes place through two different approaches:

-**Antibiotic modification**, which can be achieved via three different bacterial enzymes: aminoglycoside phosphotransferase, which inactivates kanamycin, neomycin, and streptomycin; aminoglycoside acetyltransferase, which targets gentamicin, tobramycin, netilmicin, kanamycin, and amikacin; and aminoglycoside nucleotidyltransferase, which affects gentamicin, amikacin, and tobramycin (164).

-**Target enzyme modification**, which concerns the methylation of the 16S ribosomal RNA, thus reducing the affinity of these antimicrobials to the bacterial ribosome during mRNA translation and protein synthesis. For *P. aeruginosa,* a 16S methyltransferase codified by the *rmtA* gene, typically associated with MGEs, has been described to confer aminoglycoside panresistance (165).

Finally, for antimicrobials that enter the cell by binding the LPS –*i.e.* polymyxins and aminoglycosides, as explained above-, the acquisition of **modifying enzymes** that alter this **receptor**'s composition can hamper antibiotic intake (166, 167). All of these resistance mechanisms found in *P. aeruginosa* are summarized in FIGURE 7.

To sum up, the concerning issue of AMR in *P. aeruginosa*, even to last-resort antimicrobials, highlights the need for developing **new antimicrobial strategies**, such as virulent bacteriophages, bacteriophage endolysins, CRISPR-Cas, pyocins, and QS modulators, which will be discussed in greater detail later in the text.

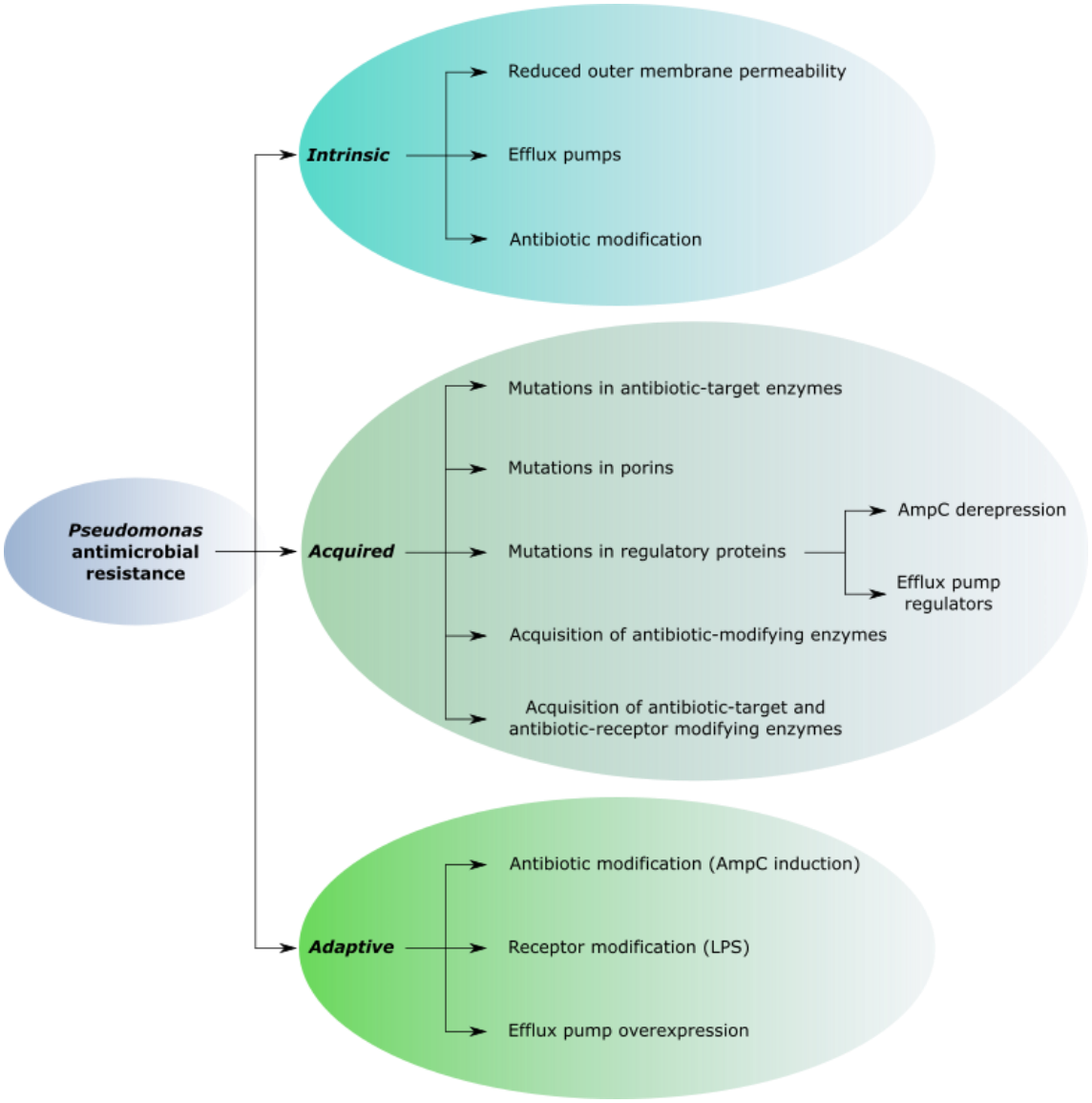

Figure 7. Schematic representation of the different AMR patterns in *P. aeruginosa* attending to their nature: intrinsic, adaptive, or acquired. Source: Created by the author with Inkscape v1.1.

1.1.6. *P. aeruginosa* typing and high-risk clones

As discussed in 1.1.2., there can be **great genomic differences** between two isolates belonging to the same species attending to their accessory genome, with an impact in both pathogenicity and AMR. This makes it fundamental to **classify bacteria** at a deeper level, with the aim of understanding and predicting bacterial virulence, assess drug resistance occurrence and spread, and study bacterial epidemiology (168).

Typing methods can be phenotypic- or genotypic-based (169). **Phenotypic** methods include LPS **serotyping**, using 17 different antisera to determine differences in the O-antigen (170); **biotyping**, which consists of analyzing bacterial metabolism through biochemical reactions, protein fingerprint through Matrix-Assisted Laser Desorption/Ionization Time of Flight Mass Spectrometry (MALDI-TOF), or the Fourier transform infrared spectroscopy (171–173); **antibiotyping**, based on antibiotic resistance patterns (174); **phage typing**, harnessing the phage's narrow spectrum to classify bacteria attending to their phage susceptibility (175); and **pyocin typing**, which can have an analogous basis as phage typing, studying pyocin susceptibility, or on the contrary by studying pyocin production (176, 177). Further phenotypic methods could include the analysis of colony morphology, pigmentation, and bacterial motility. While these phenotypic methods have been proven to be useful in epidemic situations for acute infections, their conveniency for chronic infections is argued. Upon chronification -such as in CF colonization- *P. aeruginosa* often experiences phenotypic changes without altering its genetic background. An illustrative example involves the transition from a smooth O-antigen capped LPS to a less toxigenic, rough and uncapped LPS rendering serotyping unpractical, with polyagglutinable strains and unagglutinable ones (178). Phage and antimicrobial sensitivity, as well as colony morphology and biochemical profiles, can also evolve as a consequence of the pathogen's adaptation to the host's environment.

On the other hand, **genotypic methods** allow for a deeper discrimination between clones while circumventing the phenotypic plasticity of *P. aeruginosa*. The first- and second-generation genotyping methods included the restriction and subsequent agarose electrophoresis analysis of plasmids and complete genomes, respectively. This approach was revolutionized upon the development of pulsed-field gel electrophoresis, in which the periodic reorientation of electrophoretic fields allowed for a better band separation and thus increased resolution (179). In modern times, with the increased availability of sequencing technology, **multilocus sequence typing (MLST)** has become the gold standard technique for bacterial typing, with higher rates of discrimination and reproducibility. With this method, fragments from seven loci coding for housekeeping genes in *P. aeruginosa* are amplified and sequenced (TABLE 4), and combinations of different alleles account for different **sequence types (STs)** (180).

Table 4. Housekeeping genes and their function used for MLST typing in *P. aeruginosa*. Adapted from (180)

Locus	Gene function
acsA	Acetyl coenzyme A synthetase
aroE	Shikimate dehydrogenase
guaA	GMP synthase
mutL	DNA mismatch repair protein
nuoD	NADH dehydrogenase I chain C, D

ppsA	Phosphoenolpyruvate synthase
trpE	Anthralite synthetase component I

P. aeruginosa is considered to conform a **nonclonal** and **epidemic** population. It is composed of a vast array of infrequent and genetically unrelated genotypes undergoing frequent recombination events at high rates, especially for antimicrobial-susceptible and CF isolates, in which the majority of the strains **represent their own single ST** (181, 182). To date, up to 4,916 different STs have been deposited in the PubMLST database for *P. aeruginosa* (183). Often, antimicrobial pressure selects for **epidemic clones** due to their MDR/XDR profiles and their ability to acquire MGE and to spread in healthcare settings. These are often referred to as **high-risk clones** (184).

Globally, the most disseminated and prevalent *P. aeruginosa* high-risk clone is **ST235**, characterized by a great genomic plasticity and ability to acquire MGE encoding AMR genes such as β-lactamases, possibly due to a non-functional CRISPR-Cas system and a DNA methylase (DprA) involved in homologous recombination (185). This clone's high virulence can be explained by the production of the T3SS toxin ExoU, and infections originated by strains belonging to this ST are associated with worse outcomes. Besides, the O11 serotype has been associated -although not exclusively- with this ST (186, 187). This clone has also been described as the most prevalent *P. aeruginosa* clone in Portuguese healthcare settings to date, usually associated with the production of GES-type carbapenemases (188, 189).

In Spain, *P. aeruginosa* **ST175** is currently considered to be the most prevalent high-risk clone (190). Although acquisition of carbapenemases through MGE has been described in this ST, antimicrobial resistance is usually achieved by a combination of AmpC derepression and hyperexpression (mutations in OprD and AmpR, respectively), MexXY overexpression (mutations in MexZ) and several quinolone resistance-associated mutations (GyrA and ParC). Finally, its reduced virulence can be accounted for by the presence of the ExoS toxin production and absence of the ExoU one (186, 187).

Finally, the **ST773** constitutes an emerging clone usually associated with the production of the NDM-type carbapenemase. This clonal spread has been reported in the Republic of Korea -challenging the predominance of the ST235 high-risk clone (191)-, Turkey (192), South Africa (193) or India (194). The presence of this ST was first reported in Western Europe upon the arrival of patients transferred as a consequence of the war in Ukraine. Since 2022, the same clone has been isolated in Germany, The Netherlands and Spain from this profile of patients (195–197). As a result, the European Center for Disease Prevention and Control (ECDC) issued in March 2022 a technical report with considerations for the prevention of infectious diseases in the context of the war in Ukraine. In this document, the ECDC urges healthcare providers to pre-emptively isolate and to screen for carriage of MDR microorganisms in patients transferred from hospitals in Ukraine or with a history of hospital admission in Ukraine in the previous 12 months (198).

1.2. Bacteriophages

Bacteriophages -phages for short- are viruses that infect bacteria, and they constitute the **main bacterial predator** in nature. Phages are estimated to be the **most abundant** component of the biosphere, with an estimated of 10 phages for every bacterium on Earth, adding a total of $>10^{31}$ phages worldwide (199–201). Phage presence has been confirmed in every environment where bacteria thrive, from deep ocean waters to barren deserts (202, 203). In the human gastrointestinal tract, bacterial abundance (10^9 bacteria/g feces) is comparable to the viral one in a 1:1 ratio, being phages accountable for the majority of the virus-like particles (204–207).

Phages play crucial ecological roles by **shaping bacterial populations**: they control bacterial levels in nature by lysing target bacteria while recycling their components (lytic phages) and are able to drive evolution by transferring genetic material along different isolates through a process termed transduction (lysogenic phages)(208).

Although single- and double-stranded RNA and DNA phages have been described, the vast majority of them -about 95%- possess a **double-stranded DNA (dsDNA)** genome encapsulated within an icosahedral protein capsid from which a protein tail spans (209). These phages belong to the class *Caudoviricetes*, which comprises 4 orders and 47 families. Among these families, 33 have not yet been assigned to an order (210).

1.2.1. Bacteriophage life cycles

Phages, as other viruses, are **obligate parasites** that require to infect a host -*i.e*. a bacterium- to reproduce by harnessing the cellular molecular machinery for RNA synthesis and DNA replication (211). The life cycle of a tailed phage unfolds through a series of sequential steps (FIGURE 8):

1. **Adsorption**. The first step in the phage infection cycle involves the interaction of the viral tail proteins -namely receptor-binding proteins or RBP- with various protein structures or carbohydrate moieties exposed on the bacterial surface, which serve as receptors. These receptors are usually cell wall moieties, flagellar proteins (FliC, FljB, Flik), pili (type F pilus, TIVP, the mating pair formation complex), LPS or capsular sugars (212). Adsorption begins with a **reversible interaction** between the phage and the bacterium, allowing the phage to wander around the bacterial surface in search of its receptor. Once located, **irreversible attachment** occurs, triggering a **conformational change** in the phage that leads to the injection of its DNA. In some cases, the RBPs and receptors involved in the reversible interaction differ from those involved in the irreversible attachment, with the reversible ones being more abundant and exposed, facilitating the encounter with the irreversible ones (213).
2. **DNA ejection**. Conformational changes following irreversible binding of the RBP to the receptor lead to the ejection of **viral DNA and associated proteins** into the bacterial cytoplasm, while the emptied protein capsid remains attached at the bacterial surface. This ejection -not to be confused with injection, as the capsid does not reduce its volume- introduces first the last end of the DNA to be packed into the capsid, which is conveniently located near the aperture, with the exception of phage T4. Various hypotheses have been proposed regarding the driving forces for this DNA ejection: when the tail tube is wider than the DNA double strand, it allows for the diffusion of K^+ ions out of the cell, thereby attracting water to flow in the opposite

direction dragging the viral DNA to the cytoplasm. On the contrary, when the tail tube is so narrow that it only allows the dsDNA to pass through, assisting enzymes pull one of the ends to the cytoplasm until it is recruited by an RNA polymerase, which further draws it out of the capsid (214).

3. **Behavior decision**. After ejection, the phage has to "decide" whether to follow a lytic or lysogenic cycle.

    A. **Lytic cycle**. In the first case, the phage highjacks the bacterial transcription machinery to synthetize regulatory and structural proteins to form new capsids, as well as the replication machinery to **copy its DNA** while degrading the host's chromosome. Once the capsids are formed and the dsDNA is packed inside, **lytic proteins** -*i.e.* holins for the cytoplasmic membrane, endolysins for the peptidoglycan, and spanins in Gram-negatives to fuse the cytoplasmic and outer membranes (215)- **burst** the infected bacterium from the inside and the phage progeny is released. Strictly lytic phages are phages without the ability to develop a lysogenic cycle, due to the lack of integrases and/or lysogeny regulatory proteins. These viruses, known as **virulent phages**, have been employed for more than a hundred years for treating bacterial infections as an alternative to classic antibiotics in a procedure known as **phage therapy** (216, 217).

    B. **Lysogenic cycle**. Conversely, if the phage opts for a lysogenic cycle, the ejected genetic material **integrates** into the host's chromosome -becoming a **prophage or temperate phage**- and reproduces in a passive way, being copied along with bacterial reproduction and passed onto the offspring cells (218). When the parasitized bacteria, known as the lysogen, encounters a **stressor** -such as toxic molecules, changes in temperature and pH or nutrient starvation (219)-, **prophage induction** starts a new lytic cycle: genes encoding the structural and lytic proteins cease to be repressed, the prophage is excised from the chromosome and new virions are assembled, resulting in the final lysis from the inside of the lysogen. The released phage progeny is then able to infect new hosts and develop a following lytic or lysogenic cycle.

    Although this decision process has been demonstrated to be **stochastic**, there are several **external signals** that can tilt the balance in favor of one of the two cycles. This manner of influencing lysogeny over lysis can have an explanation in survival, since if a phage lyses the bacteria in a faster pace than they reproduce, eventually it will not have a host to prey on and the phage would extinguish as well. Hence, when bacterial populations diminish, one survival strategy for phages could be to cease bacterial lysis and to integrate into the bacterial chromosome, reproducing passively along with bacteria. One example is the **arbitrium system** found in *Bacillus sp* phages belonging to the SPBeta group, where phages synthesize a small peptide -comprised of 6 amino acids- with

every effective infection, being released to the environment. After several lytic infection cycles, peptide concentration rises and the SPBeta phages turn more prone to a lysogenic infection (220). In turn, the same systems that promote lysogeny can control prophage induction too (221). The discovery of these means of communication between phages and their environment have led researchers to consider the possible **roles of QS in phages**, and so far some QS genes have been found within their genomes (222).

In addition, recent publications emphasize that lysis and lysogeny are not a dichotomy, and that phage nature defined by their biological cycles might be more complex (223). In this regard, a **phage classification** into four different groups has been proposed: (I) **lytic and non-temperate**, for strictly lytic phages that do not overgo lysogenic cycles and that culminate infection with the bacterial lysis from the inside; (II) **chronic and non-temperate**, for phages that do not overgo lysogenic cycles but neither lyse the parasitized bacterium, being rather chronically released; (III) **lytic and temperate**, for lytic phages that can also overgo lysogenic cycles and (IV) **chronic and temperate**, for phages that instead of lysing the bacterium are chronically released but can also overgo lysogenic cycles. Furthermore, the term **pseudolysogeny** refers to the phenomenon where phages -both virulent and temperate- remain in host cell's cytoplasm as inactive circular episomes, pausing their cycle in response to the host's nutrient deficiency until conditions improve (224).

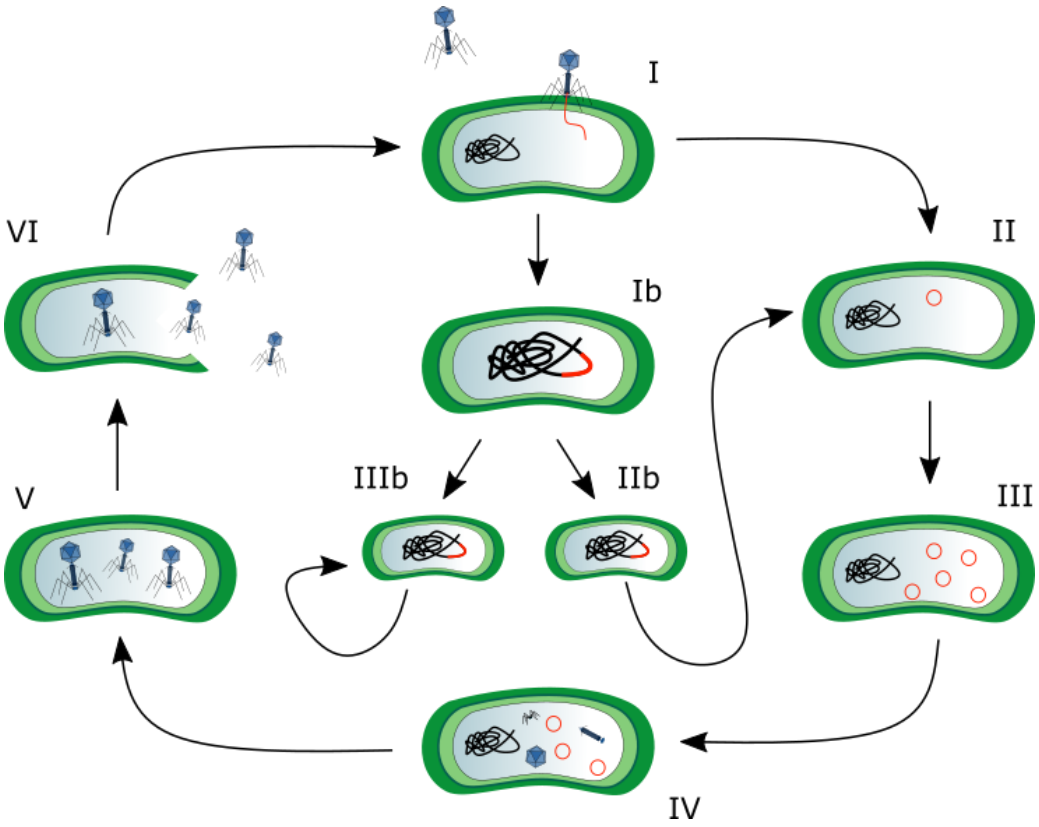

Figure 8. Steps involved in phage biological cycles. I: Attachment and DNA ejection. II: dsDNA circularization. III: dsDNA replication. IV: phage protein synthesis. V: virion assembly. VI: host cell lysis from within. Ib: dsDNA integration. IIb: prophage activation and initiation of the lytic cycle. IIIb: lysogen multiplication and indefinitely prophage passing into progeny. Source: Created by the author with Inkscape v1.1.

This thesis will focus on phages with the ability to develop a lysogenic cycle, that is **temperate pages or prophages**, which encompasses categories III and IV.

1.2.2. Temperate phages (prophages)

As previously explained, **prophages** are **temperate phages** that can display a lysogenic cycle and lyse the parasitized bacterium to free the progeny or rather be chronically released while maintaining the bacterial cell wall's integrity (223). Due to their ability to **integrate indefinitely into the host's chromosome**, their use in phage therapy has been dismissed and research interest has been mainly focused in their strictly lytic counterparts. However, there are intriguing aspects about prophages that make them worthy of study, from the previously described interactions between phages and bacterial QS systems to the ecological advantages they provide to their hosts.

Prophages **reproduce passively**, being copied along with the rest of the bacterial chromosome and being transmitted to the daughter cells. In order not to be curated through time, prophages can give a number of **evolutionary advantages** to the lysogen, which in turn allow bacteria to thrive in hostile environments and ensure the phage's survival. For that purpose, despite having the majority of their genes repressed, some prophages have genes unrequired for the phage cycle actively expressing while in their temperate state. These genes are referred to as **morons** (225) and their products are involved in:

1. **Toxin production**. Classic infectious diseases such as botulism, diphtheria, or cholera have in common that they are all bacterial infections aggravated by the production of toxins. These toxins are not encoded by the bacteria themselves but by a prophage inserted into their chromosome, being infections caused by non-lisogenized bacteria generally less severe. These toxins and their roles are summarized in TABLE 5.
2. **Antimicrobial resistance**. Various antibiotic resistance genes have been described in prophage genomes, allowing the selection of lysogenized bacteria in the presence of certain antimicrobials. **Aminoglycoside-modifying enzymes** and **β-lactamases** have been described within prophages infecting Gram-positive (*S. aureus*, *Enterococcus faecium*) and Gram-negative bacteria (*P. aeruginosa*, *E. coli*, *Enterobacter cloacae*, *Klebsiella pneumoniae* and *Acinetobacter baumannii*)(226). In other studies, AMR genes such as bla_{TEM}, *sul1* and *tetW*, conferring resistance to β-lactams, sulfonamides and tetracycline respectively, were found in phage particles isolated from different kinds of food (227). Additionally, in a study analyzing prophages in *A. baumannii*, nine different AMR gene families were found, with an overrepresentation of the small multidrug resistance efflux pump AbeS as well as the OXA-23-like and OXA-51-like oxacillinases (228).
3. **Biofilm formation**. Prophages have been shown to promote biofilm formation through different ways. One example is the **liberation of eDNA** upon prophage induction in *E. coli*, which contributed to the development of the extracellular matrix. Furthermore, fimbriae and adhesin expression were reduced in prophage-defective mutants when compared to the lysogen wild types, suggesting a role of

prophages the regulation of these genes (229). On the contrary, prophages can **also mediate cell lysis and dispersal in biofilms** in *P. aeruginosa*, allowing to the colonization of new niches (Webb et al., 2003).

4. **Bacterial population fitness and tissue colonization**. Since increasing the survival of the host cell also rises the probability of survival of the prophage, prophages often carry genes that are beneficial for host fitness. In *P. aeruginosa*, prophages have been shown to increase adherence to epithelial cells, resistance to phagocytosis, transmissibility, and competitiveness in murine lung infection models (230–232).

Table 5. Diseases caused by prophage-encoded toxins, bacteria responsible for the infection and toxin role in pathogenesis.

Disease	Bacteria	Gene	Action	Reference
Botulism	*Clostridium botulinum*	*bont*	Cleavage of proteins involved in fusion of neurotransmitter-containing vesicles, blocking the release of acetylcholine from the pre-synaptic neurons at neuromuscular junctions	(233, 234)
Cholera	*Vibrio cholerae*	*ctxA*	ADP-ribosylation of Gsα leading to increased intracellular concentrations of cyclic AMP and opening of Cl^- channels, producing secretory diarrhea	(235)
Diphtheria	*Corynebacterium diphteriae*	*tox*	NAD^+-dependent ADP-ribosylation of elongation factor 2, protein synthesis inhibition and cell death by apoptosis	(236)
Hemolytic uremic syndrome	*E. coli*	*stx*	Adenine cleavage in the 28S rRNA, protein synthesis inhibition and cell death by apoptosis	(237)
Scarlet fever	*Streptococcus pyogenes*	*speA*	Superantigen. Polyclonal T-cell activation. Massive cytokine release	(238, 239)
Toxic shock syndrome	*S. aureus*	*tst*	Superantigen. Polyclonal T-cell activation. Massive cytokine release	(240)

1.2.3. Bacteria versus phage arms race

1.2.3.1. Bacterial defense mechanisms against bacteriophages

In 1973, inspired by Lewis Carrol's novel "Alice in Wonderland", Leigh Van Valen proposed the **Red Queen hypothesis** to explain the dominance of biological competition over abiotic factors in driving natural selection. Applied to bacteria and phages, this hypothesis remarks that co-evolving antagonistic organisms must continuously adapt to environmental pressures to survive through sequential cycles of **adaptation and counter-adaptation** (241–243).

To overcome phage infection, bacteria have developed a series of mechanisms that interfere with every step of the usual biological cycle in phages (TABLE 6):

-**Adsorption**. Blocking the first step in phage infection can involve the accumulation of mutations in phage receptors that make phages unable to recognize them, or directly the deletion of the receptor. Bacteria can also increase exopolysaccharide production, hindering the access of phages to their receptors, or bud outer membrane extracellular vesicles loaded with membrane receptors to sequester phages in the medium. Finally, some bacteria are able to produce ligands that competitively bind to their receptors impeding their recognition by phage RBPs (244).

-**Ejection**. The entrance of the phage DNA into the target bacterial cell can be eluded by superinfection exclusion and abortive infection. **Superinfection exclusion** happens when a prophage protects the parasitized bacterium against other lytic phage's infection, by for example reducing the formation of TIVP or O-antigen, as described for *P. aeruginosa* (245). This defense can be homotypic, when it provides defense against phages closely related to the responsible prophage, or heterotypic, when it impedes infection by a non-related phage. In contrast, **abortive infection (Abi)** represents a bacterial strategy in which the phage-infected bacterium detects the infection and commits suicide before phages complete their cycle, ensuring protection for the rest of the bacterial population. It is a last-resort defense mechanism which activates only if the first-line ones -*i.e.* CRISPR-Cas and R/M enzymes- have failed (246). There are different Abi systems, which can act by: 1) degrading or depolarizing the inner membrane (247, 248); 2) random excision of both phage and host DNA (249); 3) unselective cleavage of both phage and host mRNAs (250); 4) tRNA degradation (251); 5) translational machinery proteolytic inactivation (252).

Among these Abi systems, two different mechanisms could be remarked: the **cyclic oligonucleotide-based antiphage signaling system** and the **toxin/antitoxin** modules **(T/A)**. It consists of small and cyclic secondary messengers that are produced when the bacterium senses a phage infection and that elicit the activation of the Abi system effector proteins (253). T/A modules, on the contrary, are pairs of constitutively synthetized toxins and their cognate antitoxins. In type II, the most frequent, both the toxin and the antitoxin are proteins, being the antitoxin more unstable and prone to lysis. When phage infection occurs and cell growth is arrested, toxin concentration surpasses the antitoxin one, resulting in cell death. The role of T/A modules in phage defense, despite being originally questioned, is gaining more evidence with time (254).

-**Phage replication**. **Restriction-modification (R-M) systems** are bacterial defenses present in almost every genus. On the one hand, modification enzymes methylate the bacterial DNA to tag it as self, having more specificity for hemimethylated DNA -DNA with modifications in only one of the strains- and thus prioritizing recently copied bacterial DNA. On the other hand, restriction enzymes work by recognizing specific unmethylated nucleotide sequences or patterns and cleaving them. Whenever foreign -and thus generally unmethylated- DNA enters the cell, restriction enzymes will break it down to protect the host from phages and other MGE (255). In contrast, **CRISPR-Cas** (clustered regularly interspaced short palindromic repeats and CRISPR-associated proteins) constitute an **adaptive immune system** in both bacteria and archaea. The CRISPR-Cas system is composed of a series of exogenous DNA sequences called spacers, which are surrounded by similarly sized direct and inverted repeats known as palindromic repeats, along with upstream *cas* genes. These spacers originate from foreign phages or plasmids that enter the bacterial cell, and their sequential integration into the CRISPR array supposes the acquisition of a "memory fragment" of these invaders. If the foreign DNA re-enters the cell in a future, the bacterium identifies the matching DNA sequences to its spacers and cuts them using the nuclease activity of Cas proteins, acting as a specific defense mechanism against these sequences (256).

1.2.3.2. Bacteriophage counterdefense mechanisms

As part of the arms race, bacteriophages are subjected to selective pressure caused by bacterial anti-phage mechanisms, favoring **evolutionary adaptations** to overcome these obstacles (TABLE 6). The bacterial defense mechanisms of accumulating mutations in phage receptors and masking them with a polysaccharide capsule can be surpassed by phages through the acquisition of pertinent **mutations in RBPs** and the production of polysaccharide **depolymerases** (244).

In addition, there are different **anti-Abi systems** that can be employed by infecting phages to arrest abortive infection and to continue their biological cycle. One of them is the production of proteins RIIA and RIIB in phage T4, which override the Rex Abi system in *E. coli* (257). Another possibility is the re-ligation of $tRNA^{LYS}$, cleaved through the PrrC Abi system (258); the production of toxins and antitoxins to interfere with the bacterial T/A modules (254); and the production of phage methyltransferases to disguise viral DNA as from bacterial origin (259).

Finally, regarding **anti-CRISPR** strategies, phages can accumulate mutations in spacer-homologue sequences to evade recognition by Cas proteins; build protein barriers to protect the viral genome from the action of the CRISPR-Cas systems (260); or utilize anti-CRISPR (Acr) proteins, small peptides -usually around 50-150 amino acids- that bind to CRISPR machinery elements to avoid viral DNA identification or inhibit the activity of Cas proteins (261).

Table 6. Mechanisms developed by bacteria to overcome phage infections and the phage counterdefense responses. RBP: Receptor binding protein. CRISPR-Cas: clustered regularly interspaced short palindromic repeats and CRISPR-associated proteins. ACR: Anti-CRISPR.

Affected process	Bacterial anti-phage mechanism	Phage counterdefense mechanism
Phage adsorption	Loss or structural change in receptors	Mutations in RBP
	Exopolysaccharide production to mask receptors	Exopolysaccharide degradation
	Production of outer membrane vesicles to sequester phages	-
	Receptor masking by production of blocking proteins	-
Phage ejection	Superinfection exclusion	-
	Abortive infection	Anti-Abi defenses
Phage replication	Restriction-modification systems	Phage DNA-methyltransferases
	CRISPR-Cas	Anti-CRISPR proteins (ACR)
	Abortive infection	Anti-Abi defenses

1.2.4. Prophages in *P. aeruginosa*

In the recent years, research on temperate phages infecting *P. aeruginosa* strains has been mainly focused on filamentous phages. These are lysogenic phages that display chronic infections without lysing the host bacterium to release their progeny, but rather extruding them through a protein machinery assembled within the bacterial cell wall. These entities have important implications in *P. aeruginosa* chronic infections -such as those in CF patients-, since their accumulation in the extracellular matrix can lead to their arrangement into liquid crystals that promote biofilm formation and hamper antibiotic penetration (262–265).

However, when it comes to tailed temperate phages -currently re-located into the class Caudoviricetes- most studies are limited to reporting only the number of prophages carried by the *P. aeruginosa* strains, usually detected by automated bioinformatic tools, without exploring their sequence, ORF function or insertion sites in detail (266–269).

Among the few studies that dissect the molecular characteristics of prophages within the genomes of *P. aeruginosa* strains, Kyrkou and colleagues analyzed 197 isolates from 12 CF patients. They identified 14 unique prophages that were inducible by mitomycin C, ciprofloxacin, or spontaneously, and described their wide ranges of length (36,566 – 51,941 bp), GC content (66.0 – 57.3%), and the presence of phage morons influencing bacterial virulence and invasion. Interestingly, they were also able to trace the bacterial isolates over a period of 4 years and observed that the prophages maintained high genomic conservation. The authors concluded that, given the fact that these phages could have been induced yet were not lost, they might be positively selected by their host, suggesting a role in bacterial fitness and persistence (270).

1.3. Bacteriocins

To date, there is controversy with the concept, definitions and classification of bacteriocins. Whereas in some literature bacteriocins are ribosomally synthesized **toxic peptides with antimicrobial activity** (271), others also consider as so protein complexes such as phage tail-like bacteriocins (PTLBs) or tailocins, the secreted proteins by the type VI secretion system (T6SS), or the contact dependent inhibition proteins (272). However, the term "bacteriocin" is being broadened to encompass a wider range of microbiome-derived antimicrobial molecules, including peptides produced by non-ribosomal peptide synthetases. Together, these metabolic byproducts contribute to shape microbiomes driving intra- and inter-species competition by targeting selected strains of a given species (273). Bacteriocins can promote **niche invasion** in already stablished bacterial communities constituted by sensitive bacteria to the bacteriocin produced by the invading strain; they can **protect** a producing strain **from invading** sensitive **strains** aiming to colonize the community; or the can **spatially shape microbial communities** by differential compartmentalization based on bacteriocin sensitivity and resistance (FIGURE 9)(274).

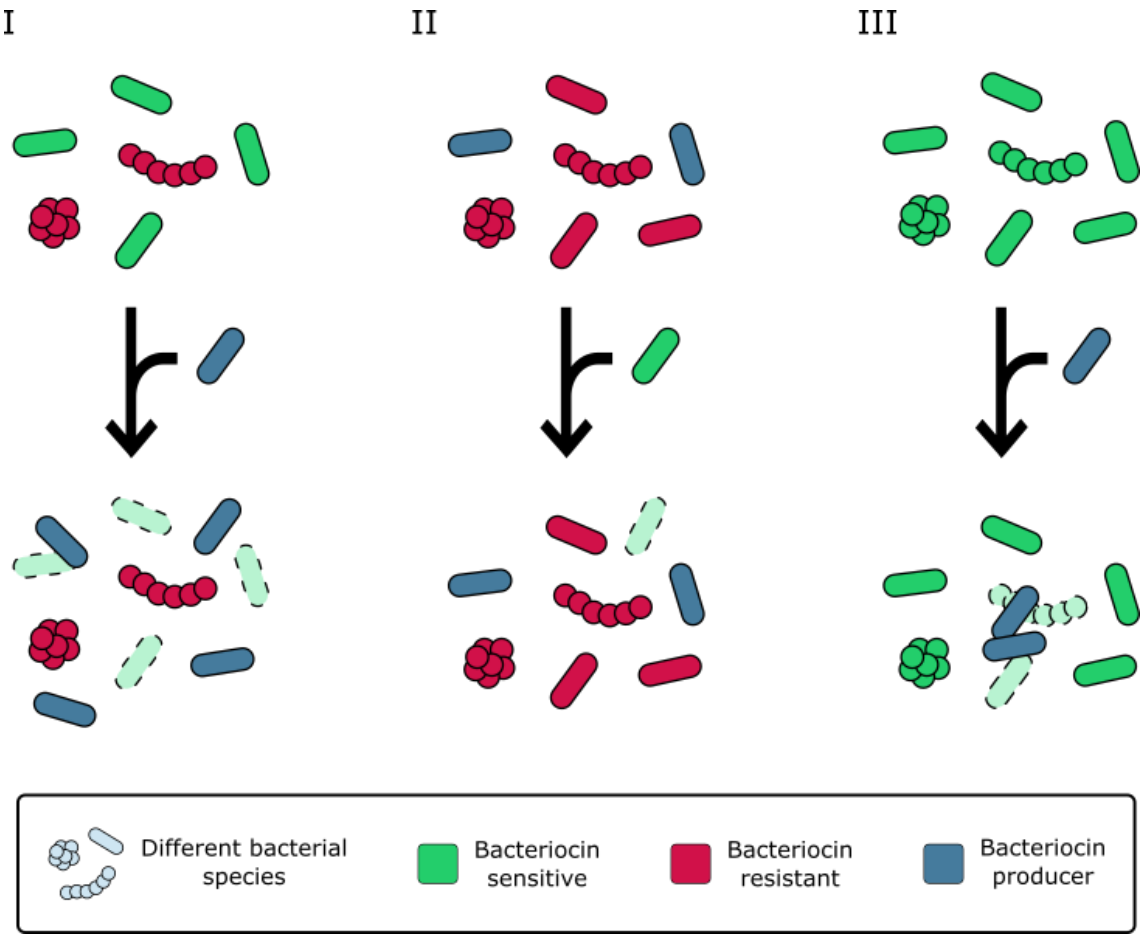

Figure 9. Bacteriocins shaping microbiomes. I) Niche invasion; II) Protection from invading species; III) Spatial distribution of bacteria. Bacteria with dotted lines and faint colors bacteriocin-killed cells. Source: Created by the author with Inkscape v1.1, adapted from (274).

Bacteriocins can be named differently depending on the producing strain. Those from *E. coli* are termed colicins, diffocins is used for the ones produced by *Clostridioides difficile*, lacticins by *Lactococcus lactis*, and **pyocins** by *P. aeruginosa* -formerly *P. pyocianea*-. On a more general basis, microcins are produced by Enterobacterales, enterocins by enterococci and staphylococcins by staphylococci.

Bacteriocins can be classified into small antimicrobial peptides (less than 8kDa, grouped as class I when they undergo post-transcriptional modifications and class II for the unmodified ones (271, 275, 276)) or as high molecular-weight bacteriocins (S-type (277) and phage tail-like bacteriocins or PTLBs). This thesis will focus on PTLBs.

P. aeruginosa is able to produce protease-resistant pyocins that resemble phage tails, having an analogous structure and ejection machinery to the tails of myovirus and siphovirus. These are commonly named as **PTLBs** or **tailocins**:

-**R-type** (rigid) PTLBs show a rod-like structure conformed by a protein tube covered with a sheath, which in turn ends in a baseplate from which protein fibers protrude. Protein fibers are able to specifically recognize its receptor, generally the carbohydrate moieties of the bacterial LPS, leading to conformational changes in the PTLB that eventually cause the contraction of the **sheath** and the penetration of the core through the outer plasma membrane. This puncture

causes the depolarization of the membrane and the release of the cell content into the environment, leading to the target bacterium's death (277).

-**F-type** (flexible) PTLBs. Unlike R-type pyocins, the F-type are characterized by a single hollow rod -without a sheath- characterized by its flexibility. Another difference between them would be the absence of a baseplate in F-type pyocins, being the protein fibers attached to the distal part of the PTLB and commonly presenting with globular structures.

Table 7. PTLBs produced by *P. aeruginosa*.

Pyocin type	Structure	Characteristics	Other
F-type	Phage tail-like structure	Flexible Non-contractile Protease resistant	Analogous to λ-phage (siphovirus)
R-type	Phage tail-like structure	Rigid Contractile Protease resistant	Analogous to T-even phage (myovirus)

Due to the structural similarities between PTLBs and phage tails, some authors hypothesize that PTLBs are in fact defective prophages that have lost their capsids, leaving only their tails intact (278). However, evidence rather points out to a **common ancestor** that resulted in the origin of PTLBs, phages and T6SS, developed by **independent evolutionary pathways** (272)(FIGURE 10).

PTLBs share a **common regulatory pathway** in *P. aeruginosa*. Their transcription is activated by PrtN, whose expression is in turn repressed by the PrtR regulator under basal conditions. However, in the presence of a stressor causing DNA damage the protein RecA activates and promotes PrtR degradation, ending the transcription inhibition of the *prtN* gene and activating pyocin synthesis. Interestingly, PrtR shares structural similarities with other regulators such as the archetypical cI prophage repressor (279). Regarding **gene location**, pyocins are usually located in the bacterial chromosome in a conserved structure. R- and F-type pyocins can be found in the genome of PAO1 between the *trpE* and *trpG* genes, arranged in a **pyocin cluster** with the regulator genes *prtR* and *prtN* upstream and a lytic cassette between the two tailocins (272).

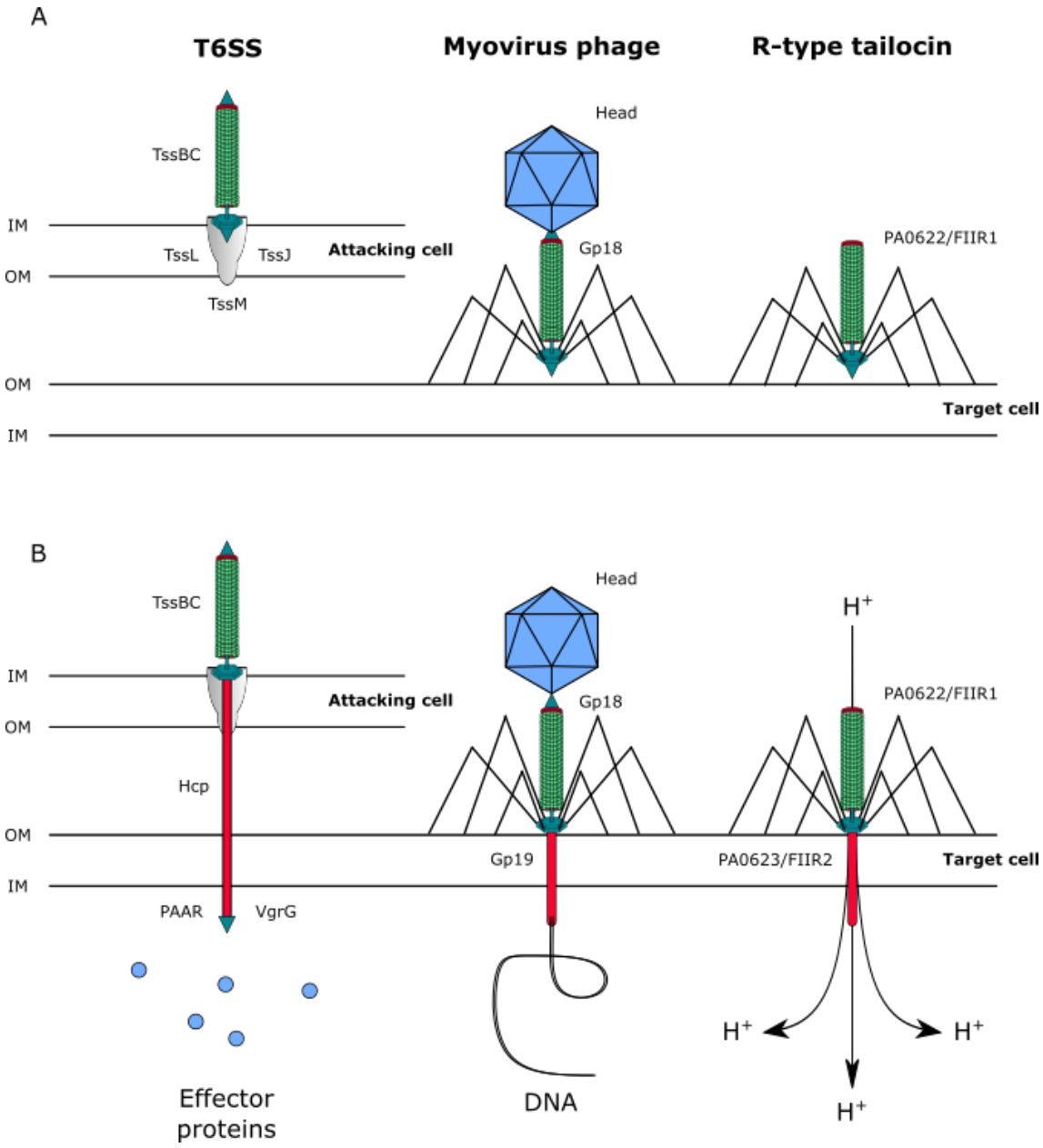

Figure 10. Schematic representation of the structural similarities between T6SS, a phage of the myovirus tail morphology group and an R-type tailocin. A) The three entities before contraction. B) After contraction, the T6SS injects effector proteins into the target cell, the myovirus tail morphology group phage ejects its DNA and the R-type tailocin creates a pore through which protons and the bacterial content escape, depolarizing the bacterial cell wall. IM: Inner membrane. OM: Outer membrane. Source: Created by the author with Inkscape v1.1, adapted from (280).

2. JUSTIFICATION OF THE STUDY AND OBJECTIVES

Pseudomonas aeruginosa is a ubiquitous and opportunistic pathogen accountable for a variety of infections, many of them of nosocomial origin. The key to its pathogenicity lies on a combination of both AMR and virulence factor production. Lysogenic phages or prophages infect their target bacteria and integrate into their chromosome to be passively copied by its replication machinery. These phages are known to influence both AMR and bacterial virulence, conferring the parasitized bacteria evolutionary advantages that prevents their clearance. On the other hand, tailocins are phage tail-like bacteriocins (PTLBs) produced by bacteria such as *P. aeruginosa* and harnessed to eliminate competing microorganisms. Both entities, prophages and PTLBs, have a similar structure and are believed to derive from a common ancestor together with the type VI secretion system (T6SS). This thesis focuses on the genomic analysis of MDR *P. aeruginosa* isolates from nosocomial origin, with special attention to the abundance, characteristics and possible role in pathogenesis of both prophages and PTLBs. This is achieved through the following objectives:

OBJECTIVE 1: To characterize prophages within *P. aeruginosa* clinical strains isolated in patients admitted to Intensive Care Units in Portugal and Spain.

1.1. Analysis of prophage prevalence in clinical strains, its distribution within clonal complexes, and its correlation with the geographical origin of the strain.

1.2. Annotation of prophage genomes and characterization of their tail morphology.

1.3. Analysis of the insertion sites of prophages within bacterial genomes.

1.4. Examination of the prophage-encoded anti-phage defense mechanisms.

OBJECTIVE 2: To describe the emergence and spread of NDM-1-producing *P. aeruginosa* ST773 clone simultaneously in Spain and in The Netherlands following the war in Ukraine, and to characterize both prophages and PTLBs from their genomes.

2.1. Phenotypic characterization of the antimicrobial susceptibility patterns of the isolates.

2.2. Molecular characterization and resistome analysis.

2.3. Identification and analysis of mobile genetic elements.

2.4. Identification and characterization of prophages and PTLBs.

OBJECTIVE 3: To characterize PTLBs within *P. aeruginosa* clinical strains isolated in patients admitted to Intensive Care Units in Portugal and Spain.

3.1. Identification of PTLB clusters. Classification and analysis of phylogenetic relationship.

3.2. Bacteriocin morphological characterization.

3.3. Analysis of PTLB range and influence of LPS and bacterial serotype.

3. SCIENTIFIC WORK

Study 1: **González de Aledo, Manuel** et al. "Prophage identification and molecular analysis in the genomes of *Pseudomonas aeruginosa* strains isolated from critical care patients." mSphere vol. 8,4 (2023): e0012823. doi:10.1128/msphere.00128-23

SUMMARY: Prophages are bacteriophages integrated into the bacterial host's chromosome. This research aims to analyze and characterize the existing prophages within a collection of 53 *Pseudomonas aeruginosa* strains recovered from infected patients admitted to intensive care units (ICUs) in Portugal and Spain. A total of 113 prophages were localized in this collection, with 18 of them being present in more than one strain simultaneously. After annotation, five of them were discarded as incomplete, and the 13 remaining prophages were characterized. Of 13, 10 belonged to the siphovirus tail morphology group, 2 to the podovirus tail morphology group, and 1 to the myovirus tail morphology group. All prophages had a length ranging from 20,199 to 63,401 bp and a GC% between 56.2% and 63.6%. The number of open reading frames (ORFs) oscillated between 32 and 88, and in 3/13 prophages, more than 50% of the ORFs had an unknown function. With our findings, we show that prophages are present in the majority of the *P. aeruginosa* strain collection isolated from Portuguese and Spanish critically ill patients, many of them found in more than one circulating strain at the same time and following a similar clonal distribution pattern. Although a great sum of ORFs had an unknown function, number of proteins in relation to viral defense (anti-CRISPR proteins, toxin/antitoxin modules, proteins against restriction-modification systems) as well as to prophage interference into their host's quorum sensing system and regulatory cascades were found. This supports the idea that prophages have an influence in bacterial pathogenesis and anti-phage defense.

IMPORTANCE: Despite being known for decades, prophages remain understudied when compared to the lytic phages employed in phage therapy. This research aims to shed some light into the nature, composition, and role of prophages found within a set of circulating strains of *Pseudomonas aeruginosa*, with special attention to high-risk clones. Given the fact that prophages can effectively influence bacterial pathogenesis, prophage basic research constitutes a topic of growing interest. Furthermore, the abundance of viral defense and regulatory proteins within prophage genomes detected in this study evidences the importance of characterizing the most frequent prophages in circulating clinical strains and in high-risk clones if phage therapy is to be used.

AMERICAN SOCIETY FOR MICROBIOLOGY | mSphere

Check for updates

| Bacteriophages | Research Article

Prophage identification and molecular analysis in the genomes of *Pseudomonas aeruginosa* strains isolated from critical care patients

Manuel González de Aledo,[1] Lucia Blasco,[2] Maria Lopez,[2] Concha Ortiz-Cartagena,[2] Inés Bleriot,[2] Olga Pacios,[2] Marta Hernández-García,[1] Rafael Cantón,[1,3] Maria Tomas[2,3]

AUTHOR AFFILIATIONS See affiliation list on p. 18.

ABSTRACT Prophages are bacteriophages integrated into the bacterial host's chromosome. This research aims to analyze and characterize the existing prophages within a collection of 53 *Pseudomonas aeruginosa* strains from intensive care units (ICUs) in Portugal and Spain. A total of 113 prophages were localized in the collection, with 18 of them being present in more than one strain simultaneously. After annotation, five of them were discarded as incomplete, and the 13 remaining prophages were characterized. Of 13, 10 belonged to the siphovirus tail morphology group, 2 to the podovirus tail morphology group, and 1 to the myovirus tail morphology group. All prophages had a length ranging from 20,199 to 63,401 bp and a GC% between 56.2% and 63.6%. The number of open reading frames (ORFs) oscillated between 32 and 88, and in 3/13 prophages, more than 50% of the ORFs had an unknown function. With our findings, we show that prophages are present in the majority of the *P. aeruginosa* strains isolated from Portuguese and Spanish critically ill patients, many of them found in more than one circulating strain at the same time and following a similar clonal distribution pattern. Although a great sum of ORFs had an unknown function, number of proteins in relation to viral defense (anti-CRISPR proteins, toxin/antitoxin modules, proteins against restriction-modification systems) as well as to prophage interference into their host's quorum sensing system and regulatory cascades were found. This supports the idea that prophages have an influence in bacterial pathogenesis and anti-phage defense.

IMPORTANCE Despite being known for decades, prophages remain understudied when compared to the lytic phages employed in phage therapy. This research aims to shed some light into the nature, composition, and role of prophages found within a set of circulating strains of *Pseudomas aeruginosa*, with special attention to high-risk clones. Given the fact that prophages can effectively influence bacterial pathogenesis, prophage basic research constitutes a topic of growing interest. Furthermore, the abundance of viral defense and regulatory proteins within prophage genomes detected in this study evidences the importance of characterizing the most frequent prophages in circulating clinical strains and in high-risk clones if phage therapy is to be used.

KEYWORDS antiviral defense, prophage, CRISPR-Cas, quorum sensing, *Pseudomonas aeruginosa*

Pseudomonas aeruginosa is a ubiquitous opportunistic pathogen associated with numerous nosocomial infections, often related with medical devices and procedures (e.g., endovascular catheters, mechanical ventilation or surgical wound, and burn infections) as well as chronic respiratory diseases, such as those present in cystic fibrosis and bronchiectasis patients and those with chronic obstructive pulmonary disease

Editor Michael J. Imperiale, University of Michigan, Ann Arbor, Michigan, USA

Address correspondence to Maria Tomas, MA.del.Mar.Tomas.Carmona@sergas.es.

Manuel González de Aledo and Lucia Blasco contributed equally to this article. Author order was determined by research developed.

Rafael Cantón and Maria Tomas contributed equally to this article. Author order was determined by research developed.

The authors declare no conflict of interest.

See the funding table on p. 18.

Received 12 March 2023
Accepted 11 May 2023
Published 27 June 2023

(COPD) (1). These non-fermentative Gram-negative rods are of special concern due to their increasing drug-resistance rates, mainly achieved through a combination of a decreased permeability of the outer membrane, active drug expulsion from the bacterial cell, and the acquisition of mobile genetic elements encoding antibiotic-resistance genes (2). *P. aeruginosa* has also been included into the ESKAPE group, a classification of six bacteria to which special attention has to be paid due to their increased antimicrobial-resistance rates (3). Besides, its ability to produce a wide range of virulence factors such as biofilms, exotoxins, siderophores, or secretion systems makes this pathogen a serious threat able to adapt to a continuously changing environment (4).

On the other hand, bacteriophages or phages are viral particles infecting bacteria and archaea. In recent years, special consideration has been drawn to lytic phages due to their ability to target and eradicate specific clones of a given bacteria, outstanding as promising narrow-spectrum antimicrobial weapons (5). Nevertheless, the importance of prophages—phages integrated into the bacterial host's chromosome—is still starting to be recognized. These viruses have been considered for years as "dormant" as the majority of their genes are generally repressed. However, they have now been shown to interact with the bacterial cell's regulatory cascade to interfere with the host's immune system as well as to encode toxins, lytic proteins, and antimicrobial-related genes (6). However, in spite of being known for decades, it is still a lot what remains unexplored.

Over time, bacteria have evolved and acquired numerous mechanisms for their defense against bacteriophages including restriction-modification (RM) systems, the clustered regularly interspaced short palindromic repeats (CRISPR) and CRISPR-associated (*cas*) genes, the abortive infection (Abi) systems as well as the accumulation of a variety of mutations in surface receptor proteins (7, 8). Interestingly, in the midst of this evolutionary race between bacteria and the viruses that prey on them, toxin/antitoxin (T/A) systems have also been proposed as an anti-phage defense. These modules, consisting of a toxin that arrests cell growth and a cognate antitoxin that neutralizes the toxin, are known to maintain plasmid stability and to confer a persister state of the bacterial host cells, allowing antibiotic tolerance. However, there is growing evidence that some T/A systems may act as anti-phage bacterial defenses (9, 10).

Moreover, new anti-viral mechanisms have been recently described such as the use of cyclic nucleotides as signaling molecules [CBASS (11), Pycsar (12), adenine deamination—RADAR (13)] and NAD+ depletion as a widespread response to viral infection (14, 15).

Besides, in the environment bacteria live in complex, spatially structured, and multispecies communities (16), which highlights the need to consider antiphage strategies at the community level. The mechanisms involved are quorum sensing network (17–19), the release of extracellular vesicles (20, 21) or the formation of biofilm structures (16, 22).

Finally, chemical inhibition of phages through small molecules secreted in the extracellular space represents another effective multicellular strategy against phage infection, which, unlike most defense systems described until now, does not rely on proteins or RNA. Among them, we could highlight anthracycline, aminoglycosides, and viperin molecules (23).

On the other hand, bacteriophages have developed counterdefense mechanisms such as anti-CRISPR (Acr) proteins and viral DNA methyltransferases. Acr proteins, firstly discovered in prophages infecting *P. aeruginosa* strains (24), are small peptides (typically between 50 and 150 amino acids) known to inhibit CRISPR-Cas activity by binding the different elements that form the CRISPR machinery, and thus preventing DNA recognition, or by inhibiting Cas proteins' activity once the protein complex has been assembled around the target DNA (25). Moreover, bacteriophages have been shown to encode DNA methyltransferases while lacking their cognate restriction endonuclease. These enzymes, known as orphan DNA methyltransferases, mimic those of the restriction-modification systems, making the bacterial restriction endonucleases unable to recognize viral DNA as exogenous and impeding its cleavage (26).

The goal of the current work is to broaden knowledge into the nature, composition, and role of the prophages found within a set of a *P. aeruginosa* strain collection recovered from critically ill patients from both Portuguese and Spanish hospitals and to analyze the genes they harbor to overcome bacterial defenses.

MATERIALS AND METHODS

Isolate collection and genome sequencing

For the present study, 53 *P. aeruginosa* strains were studied. They were recovered from urinary tract, low respiratory tract, and intra-abdominal infections in patients admitted to ICU in both Portuguese (n = 40) and Spanish (n = 13) hospitals as part of the STEP and SUPERIOR studies (27–29). The whole genome extraction and sequencing methods are described elsewhere, and genomes were deposited in GenBank under the Bioproject PRJNA629475 and accession numbers JABDTR000000000-JABDVT000000000. Nucleotide sequence data reported are available in the Third Party Annotation (TPA) Section of the DDBJ/ENA/GenBank databases under the accession numbers TPA: BK061475-BK061480 and BK061585-BK061591.

Genome assembly and prophage identification

The 150 bp paired-end sequence reads were *de novo* assembled using SPAdes v3.13.0 (https://cab.spbu.ru/software/spades/) with the following settings: minimum contig length 300 bp, minimum contig coverage five, and no read trimming (30).

Assembled genomes of *P. aeruginosa* isolates were analyzed with the Phaster (PHAge Search Tool Enhanced Release) software (https://phaster.ca/) and only those identified as intact (score >90) were included into the study (31). Prophages within the different strains were compared through Nucleotide BLAST v2.13.0 (Basic Local Alignment Search Tool, https://blast.ncbi.nlm.nih.gov/Blast.cgi) and those with a coverage >80% and identity >90% were considered to be the same prophage.

Viral genome annotation

Prophages found in more than one strain simultaneously were selected for further analysis. Viral genomes were annotated using RAST software v2.0 (Rapid Annotation Using Subsystem Technology, https://rast.nmpdr.org/rast.cgi). In addition, all ORFs were manually annotated with HMMER v3.3.2 (http://hmmer.org/) and HHpred v57c8707149031cc9f8edceba362c71a3762bdbf8 [https://toolkit.tuebingen.mpg.de/tools/hhpred (32)]. For HMMER, annotations were considered valid for E-values below 0.01 and for HHpred for E-values ≤ 10^{-5} (i.e., probability >98%). Whenever discordance between annotations was found, RAST was prioritized to HMMER and HMMER to HHpred.

To establish the tail morphology group, the closest bacteriophage candidate given by Phaster was searched into the Virus-Host database (33). These results were subsequently confirmed by a BLAST search against the NCBI database using the terminase large subunit.

A phylogenetic tree was constructed using the terminase large subunit nucleotide sequence as a reference. Sequences were aligned using MAFFT v7.407 (34) default options, and phylogenetic analysis was performed in RaxmlHPC-PTHREADS-AVX2 v8.2.12 (35) under the GTRGAMMA model and 100 bootstrap replicates. FigTree (http://tree.bio.ed.ac.uk/software/figtree/) was used to visualize the phylogenetic tree.

Furthermore, antibiotic resistance genes were searched in the viral genomes through RGI v5.2.1 (Resistance Gene Identifier, https://card.mcmaster.ca/analyze/rgi) and ResFinder v4.1 (https://cge.cbs.dtu.dk/services/ResFinder/). Anti-CRISPR proteins were also investigated through several tools: CRISPRCasFinder v1.1.2 (https://crisprcas.i2bc.paris-saclay.fr/CrisprCasFinder/Index), AcrFinder (https://bcb.unl.edu/AcrFinder/

index.php), PaCRISPR (https://pacrispr.erc.monash.edu/server.jsp), and anti-CRISPRdb (http://guolab.whu.edu.cn/anti-CRISPRdb/search.php).

Prophage integration sites were identified analyzing their flanking genes and locating them in a reference strain (PAO1). When possible, this was confirmed by BLAST analysis using the *attL* and *attR* sequences provided by Phaster for each prophage.

In addition, protein three-dimensional structure was predicted using Phyre2 (Protein Homology/analogY Recognition Engine, v2.0, http://www.sbg.bio.ic.ac.uk/phyre2/html/page.cgi?id=index) from the aminoacidic sequence. This software compares the obtained hidden Markov model with a set of models generated from known protein structures to detect high confidence similarities. Besides, protein three-dimensional structure was also predicted using the Expasy Swiss-Model tool (36).

Prophage activation, bacteriophage isolation, and transmission electron microscopy

Prophage activation was induced with mitomycin C as described by López et al. (37). For that purpose, *P. aeruginosa* strains were incubated overnight at 37°C with shaking (180 rpm) and were afterward used to inoculate 15 mL of Luria-Bertani (LB) broth. Optical density was measured at a wavelength of 600 nm (OD_{600}) until cultures reached 0.5. Then, mitomycin C was added at a concentration of 10 µg/mL and cultures were incubated with the same conditions until they became clear, meaning that lysis had occurred (approximately 1–3 h). Cell debris was then precipitated by centrifugation at 3,500 rpm for 10 min and the supernatant was filtered through a 0.22 µm filter (Millipore Express PES membrane, Merck, Darmstadt, Germany). After addition of NaCl to a final concentration of 0.5 M, suspensions were mixed and left on ice for 1 h. Subsequently, the suspensions were centrifuged at 3,500 rpm for 40 min at 4°C and the supernatants were collected into sterile tubes, to which PEG 6000 (10% wt/vol) was added and dissolved by rocking the tubes at room temperature for 1 h. After an overnight incubation at 4°C, bacteriophages were precipitated at 3,500 rpm for 40 min at 4°C and resuspended in SM buffer (0.1 M NaCl, 1 mM $MgSO_4$, 0.2 M Tris-HCl, pH 7.5). Finally, samples were stored at 4°C until preparation for TEM with a JEM-1011 (JEOL, Akishima, Japan) electron microscope.

RESULTS AND DISCUSSION

Genome assembly and prophage search

Genomes belonging to the 53 *P. aeruginosa* isolates were *de novo* assembled. The number of contigs of the obtained bacterial genomes ranged from 206 to 3,252 (mean 1,633). The number of intact bacteriophages found in each genome ranged from 0 to 5, with a median of 2, adding a total of 113 prophages (Table 1). Among them, 18 prophages were found to be present in more than one strain simultaneously by BLAST analysis. In 7/53 (13.2%) strains, no intact prophages were found.

Prophage analysis and annotation

The resulting 18 prophages were manually annotated by RAST, HMMER, and HHpred. After annotation, five of them were discarded upon realization that they were uncomplete, lacking essential viral proteins.

Among the remaining 13 prophages, phages vB_PaeM-D14A, vB_PaeS-D14B, vB_PaeS-D14C, and vB_PaeS-D14F were present in more than 10/53 *P. aeruginosa* isolates. All prophages belonged to the class *Caudoviricetes*, and according to the Virus-Host database, the majority of them (10/13) belonged to the siphovirus tail morphology group. Prophages vB_PaeP-D14I and vB_PaeP-D14S were classified as members of the podovirus tail morphology group, whereas prophage vB_PaeM-D14A was classified as a member of the myovirus tail morphology group. A BLAST search against the NCBI database confirmed these results, showing homology of their terminase large subunit with other viruses from the same group (query cover values of 100.0% and

TABLE 1 Information on the analyzed *P. aeruginosa* strains and number of intact prophages found by Phaster[a]

Strain	Contigs (*n*°)	Clonal complex	Region (country)	Source[b]	Intact phages (*n*°)
1–13	365	235	Aveiro (Portugal)	IAI	3
2–10	2,393	499–1LV	Lisbon (Portugal)	LRTI	3
2–21	2,178	309–1LV	Lisbon (Portugal)	IAI	1
2–29	645	235	Lisbon (Portugal)	UTI	3
3–5	1,871	348–1LV	Lisbon (Portugal)	UTI	1
3–38	533	348	Lisbon (Portugal)	LRTI	2
3–41	1,084	348–1LV	Lisbon (Portugal)	LRTI	1
3–49	709	235	Lisbon (Portugal)	IAI	4
3–58	514	348	Lisbon (Portugal)	IAI	1
3–69	2,676	554–1LV	Lisbon (Portugal)	LRTI	0
4–14	1,846	313–1LV	Coimbra (Portugal)	LRTI	4
4–17	493	235	Coimbra (Portugal)	UTI	4
4–29	2,595	179–1LV	Coimbra (Portugal)	LRTI	1
4–71	346	235	Coimbra (Portugal)	IAI	4
4–79	206	235	Coimbra (Portugal)	UTI	4
4–86	265	235	Coimbra (Portugal)	IAI	4
4–92	387	235	Coimbra (Portugal)	UTI	4
4–93	567	235	Coimbra (Portugal)	UTI	4
4–94	814	235	Coimbra (Portugal)	IAI	4
4–120	247	235	Coimbra (Portugal)	UTI	4
4–121	1,216	235–1LV	Coimbra (Portugal)	UTI	3
4–125	1,807	253–1LV	Coimbra (Portugal)	IAI	0
5–15	936	235	Porto (Portugal)	IAI	1
5–23	449	244	Porto (Portugal)	LRTI	3
6–25	2,029	244–1LV	Porto (Portugal)	LRTI	3
6–38	316	253	Porto (Portugal)	IAI	2
6–59	1,402	179	Porto (Portugal)	UTI	0
6–102	2,552	446–1LV	Porto (Portugal)	LRTI	1
7–41	2,487	3292–1LV	Lisbon (Portugal)	LRTI	1
8–1	2,824	348–1LV	Lisbon (Portugal)	LRTI	0
8–12	2,922	253–1LV	Lisbon (Portugal)	LRTI	0
8–24	876	244–1LV	Lisbon (Portugal)	UTI	4
8–36	798	244	Lisbon (Portugal)	UTI	5
8–58	1,669	244–1LV	Lisbon (Portugal)	IAI	0
9–25	1,248	244–1LV	Lisbon (Portugal)	UTI	3
9–35	3,182	308–1LV	Lisbon (Portugal)	LRTI	0
9–41	1,804	235–1LV	Lisbon (Portugal)	LRTI	1
9–86	331	554	Lisbon (Portugal)	IAI	2
10–58	369	244	Porto (Portugal)	LRTI	4
10–99	2,212	1233–1LV	Porto (Portugal)	IAI	1
C11	1,942	175	Barcelona (Spain)	UTI	3
C58	2,635	175–2LV	Barcelona (Spain)	UTI	2
D4	2,903	27–1LV	Seville (Spain)	IAI	2
E16	2,438	175–1LV	Santander (Spain)	UTI	1
E17	2,525	175–1LV	Santander (Spain)	IAI	1
F43	2,892	175–2LV	A Coruña (Spain)	IAI	1
G6	3,019	175–1LV	Valencia (Spain)	IAI	2
G7	3,252	175–2LV	Valencia (Spain)	IAI	1
G26	2,826	175–1LV	Valencia (Spain)	IAI	2
G31	2,698	175–1LV	Valencia (Spain)	IAI	2
H18	2,573	175–2LV	Majorca (Spain)	UTI	2

(*Continued on next page*)

TABLE 1 Information on the analyzed *P. aeruginosa* strains and number of intact prophages found by Phaster (*Continued*)

Strain	Contigs (*n*°)	Clonal complex	Region (country)	Source[b]	Intact phages (*n*°)
H19	2,606	309–2LV	Majorca (Spain)	IAI	2
H52	424	309	Majorca (Spain)	UTI	2
				Total	113

[a]Adapted from Hernández-García et al. (27)
[b]IAI, intraabdominal infection; LRTI, lower respiratory tract infection; UTI, urinary tract infection.

identity values above 90.0%). The only exception was prophage vB_PaeS-D14E, in which those values were 62.0% and 74.6%.

A phylogenetic tree of the 13 prophages was built with the terminase large subunit as a reference (Fig. 1A). It can be noted the close proximity between prophages belonging to the podovirus group and their separation from the rest of the prophage collection. Regarding geographical distribution of the prophages, prophages vB_PaeS-D14O, vB_PaeS-D14P, and vB_PaeS-D14Q were found to be circumscribed to Spanish regions, being the remaining 10 prophages found mainly in Portuguese isolates. Interestingly, despite the geographical proximity to Portugal, prophages found at the A Coruña region resembled more similar to other Spanish regions (Fig. 1B).

Regarding their genome size, all prophages had a length ranging from 20,199 to 63,401 bp, being phage vB_PaeS-D14Q the shortest (20,199–24,677 bp) and phage vB_PaeP-D14I the largest (63,401 bp). Their GC content was found to be between 56.2% and 63.6%, considerably lower than their host's GC content, which is 65–67% for *P. aeruginosa* (38). The differences in the GC content constitute a sign of an exogenous origin of the prophage regions and usually indicate a recent acquisition (39). The more adapted a prophage is to a species, the more similar its GC content is to their host's. However, we did not see that prophages with the highest GC content were the most frequent (phages vB_PaeP-D14S and vB_PaeP-D14I were present only in 2/53 strains despite having 63.2–63.8% GC) and neither prophages with the lowest GC content

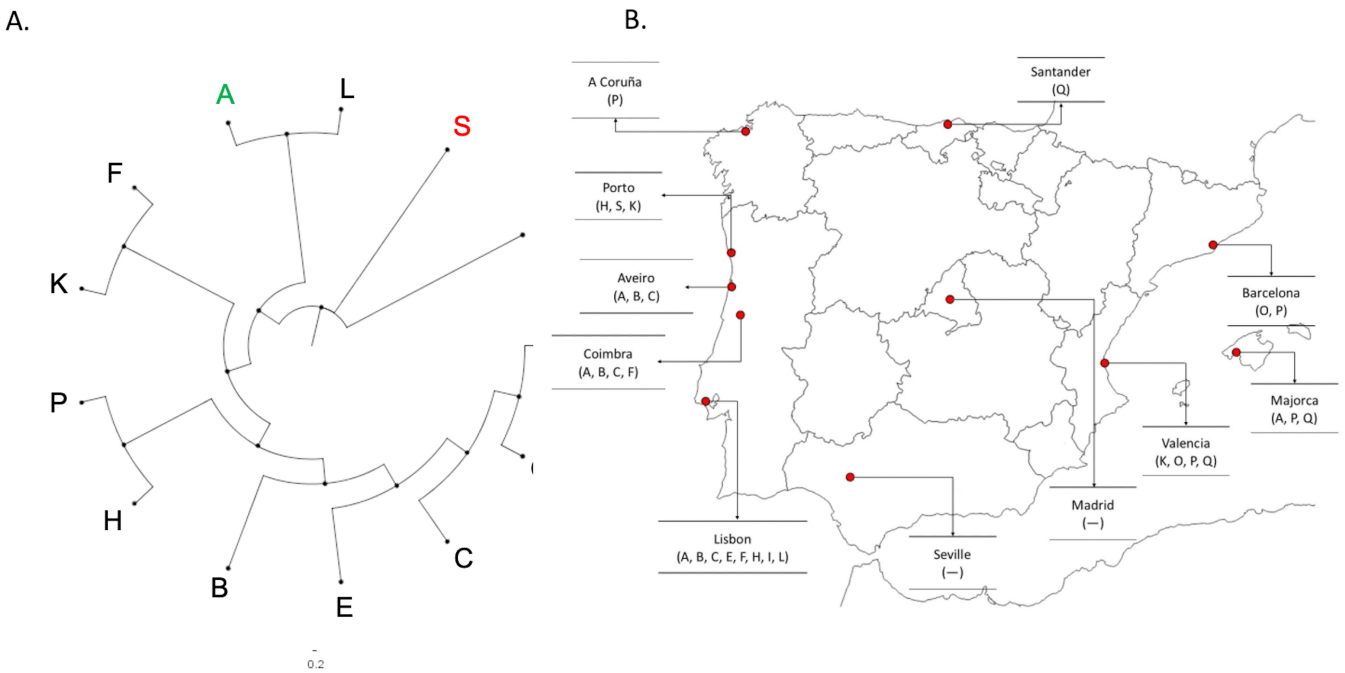

FIG 1 (**A**) Maximum likelihood phylogenetic tree of the 13 prophages studied. Prophages of the siphovirus tail morphology group are represented in black, myovirus in green, and podovirus in red. (**B**) Geographical localization of the prophages in the Iberian Peninsula. A: vB_PaeM-D14A, B: vB_PaeS-D14B, C: vB_PaeS-D14C, E: vB_PaeS-D14E, F: vB_PaeS-D14F, H: vB_PaeS-D14H, I: vB_PaeP-D14I, K: vB_PaeS-D14K, L: vB_PaeS-D14L, O: vB_PaeS-D14O, P: vB_PaeS-D14P, Q: vB_PaeS-D14Q, S: vB_PaeP-D14S. The blank map from the Iberian Peninsula was obtained from https://d-maps.com/carte.php?num_car=2209.

TABLE 2 Information on the 13 prophages identified in more than one bacterial strain

Prophage	Strains harbouring the prophage (nº)	Tail morfology	Length (bp)	GC content (%)	ORFs (nº)	Annotated ORFs (%)	Accession number	Link accession Genbank
vB_PaeM-D14A	15 (+1*)	Myovirus	36,399–37,203	62.2–63.6	50–52	74.0	BK061475	https://www.ncbi.nlm.nih.gov/nuccore/BK061475
vB_PaeS-D14B	12	Siphovirus	41,283–41,609	61.1	64–65	49.2	BK061476	https://www.ncbi.nlm.nih.gov/nuccore/BK061476
vB_PaeS-D14C	13	Siphovirus	38,595	58.6	60	56.7	BK061477	https://www.ncbi.nlm.nih.gov/nuccore/BK061477
vB_PaeS-D14E	2	Siphovirus	40,769	61.9	62	56.5	BK061478	https://www.ncbi.nlm.nih.gov/nuccore/BK061478
vB_PaeS-D14F	9 (+3*)	Siphovirus	39,504	63.2	57	59.7	BK061479	https://www.ncbi.nlm.nih.gov/nuccore/BK061479
vB_PaeS-D14H	1 (+2*)	Siphovirus	63,196	60.7	81	51.9	BK061480	https://www.ncbi.nlm.nih.gov/nuccore/BK061480
vB_PaeP-D14I	2	Podovirus	63,401	63.8	65	50.8	BK061585	https://www.ncbi.nlm.nih.gov/nuccore/BK061585
vB_PaeS-D14K	2	Siphovirus	35,464–39,623	62.5–62.6	53–56	60.7	BK061586	https://www.ncbi.nlm.nih.gov/nuccore/BK061586
vB_PaeS-D14L	2	Siphovirus	40,814–40,999	61.7	66	48.5	BK061587	https://www.ncbi.nlm.nih.gov/nuccore/BK061587
vB_PaeS-D14O	3	Siphovirus	48,888	56.2	88	46.6	BK061588	https://www.ncbi.nlm.nih.gov/nuccore/BK061588

(*Continued on next page*)

TABLE 2 Information on the 13 prophages identified in more than one bacterial strain (*Continued*)

Prophage	Strains harbouring the prophage (nº)	Tail morfology	Length (bp)	GC content (%)	ORFs (nº)	Annotated ORFs (%)	Accession number	Link accession Genbank
vB_PaeS-D14P	5 (+3*)	Siphovirus	35,019–39,280	61.1–61.6	48–55	58.2	BK061589	https://www.ncbi.nlm.nih.gov/nuccore/BK061589
vB_PaeS-D14Q	3 (+3*)	Siphovirus	20,199–24,677	58.6–58.9	32–39	71.8	BK061590	https://www.ncbi.nlm.nih.gov/nuccore/BK061590
vB_PaeP-D14S	2	Podovirus	50,727	63.2–63.3	46	50.0	BK061591	https://www.ncbi.nlm.nih.gov/nuccore/BK061591

[a]ORF, open reading frame.
[b]Prophages found fragmented within several contigs.

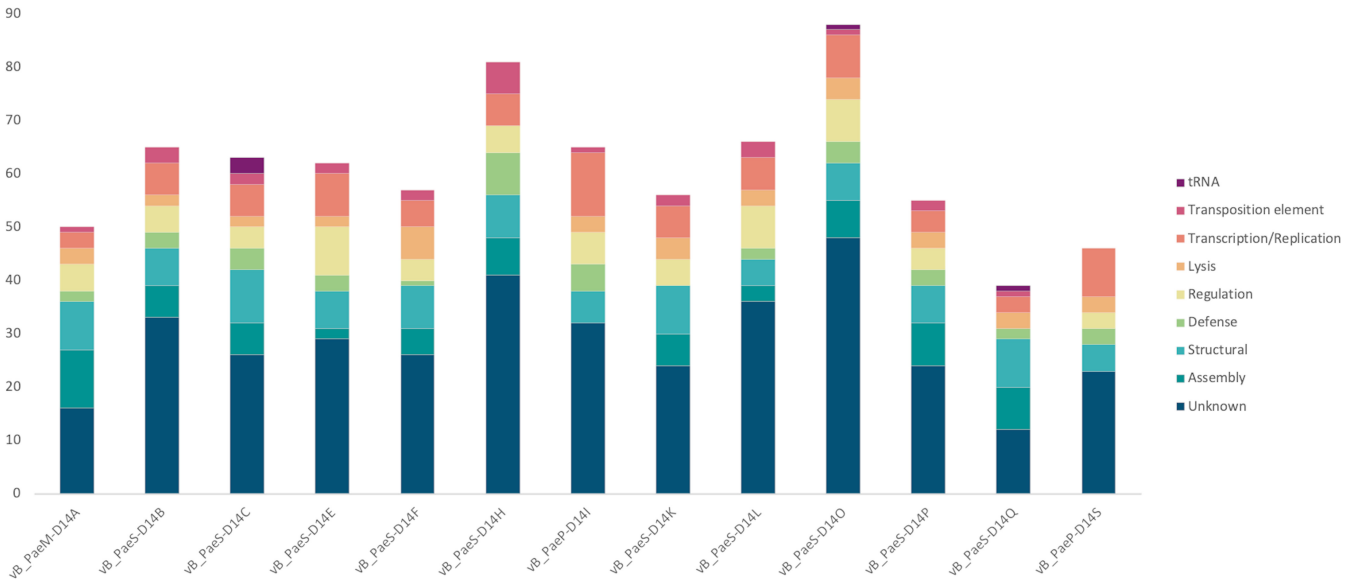

FIG 2 ORF classification in the different analyzed prophages. Y-axis represents the number of ORFs.

were the least abundant (prophage vB_PaeS-D14C had a GC content of 58.6% and was present in 13/53 strains). In addition, the number of ORFs oscillated between 32 in phage vB_PaeS-D14Q and 88 in phage vB_PaeS-D14O. Finally, regarding ORF annotation, in 3/13 prophages more than 50% of the ORF had an unknown function (Table 2). This is consistent with previous studies (40), highlighting the need to deepen in prophage basic research in order to unravel the different viral mechanisms unknown to date.

When ORF function was classified into different categories, it could be noted that the majority of the genes coded for structural and assembly proteins, viral transcription/replication enzymes, or that they had an unknown function (Fig. 2). However, a number of proteins with special attributes were found in relation to viral defense (anti-CRISPR proteins, toxin/antitoxin modules), prophage interference into their host's quorum sensing (QS) system, and regulatory proteins.

TABLE 3 Viral defense and regulatory proteins found in each prophage

	Viral defense proteins						Regulatory proteins	
Prophage	Acr[a]	Glycosyltransferases and acetylases	Defense against restriction/modification systems	TA systems	DNA scission proteins	QS	Latency promoting repressors	Other proteins
vB_PaeM-D14A	1 (7)	ND[b]	DNA-cytosine methyltransferase	ND	ND	TraR homolog	CII Cro/cI	ND
vB_PaeS-D14B	1 (6)	ND	ND	Putative toxin, BrnT family Putative antitoxin, CopG family	ND	LuxR family protein	Cro CI	ND
vB_PaeS-D14C	1 (2)	Glycosyltransferase family 9	S-adenosyl-L-methionine-dependent methyltransferase	Toxin YafO	ND	TraR homolog	Cro CI CII	ND
vB_PaeS-D14E	0 (4)	ND	DNA-cytosine methyltransferase (EC 2.1.1.37)	Toxin BrnT	ND	LuxR family protein	Cro CI	ND
vB_PaeS-D14F	1 (9)	ND	ND	ND	ND	ND	CII	ND
vB_PaeS-D14H	0 (5)	ND	DNA-cytosine methyltransferase	YefM antitoxin YoeB toxin	Holliday junction resolvase YqaJ-like exonuclease Restriction alleviation protein	ND	Cro CI CII	BCI PrtN
vB_PaeP-D14I	0 (6)	ND	DNA methyltransferase C-5 cytosine-specific DNA methylase	AbiEi antitoxin	Restriction alleviation protein	ND	CI LexA	BCI
vB_PaeS-D14K	0 (9)	ND	ND	ND	ND	ND	Cro/cI CII	ND
vB_PaeS-D14L	1 (4)	ND	ND	YafO family toxin	ND	LuxR family protein	Cro CI	ND
vB_PaeS-D14O	1 (17)	O-antigen acetylase Glycosyltransferase family 9	S-adenosyl-L-methionine-dependent methyltransferase	ND	ND	TraR homolog	Cro CI CII	ND
vB_PaeS-D14P	0 (8)	ND	ND	ND	Holliday junction resolvase	ND	Cro CI CII	BCI
vB_PaeS-D14Q	0 (3)	Glycosyltransferase family 9	S-adenosyl-L-methionine-dependent methyltransferase	ND	ND	ND	ND	ND
vB_PaeP-D14S	1 (6)	ND	Site-specific DNA-methyltransferase	AbiEi antitoxin	ND	ND	CI	BCI

[a]Acr: proven anti-CRISPR proteins. Numbers in brackets refer to putative Acr.
[b]ND, not detected; QS, quorum sensing; TA, toxin/antitoxin.

Viral defense proteins

Anti-CRISPR proteins

Among the 13 analyzed prophages, 11 were found by guilt-by-association to carry putative Acrs through AcrFinder, ranging from one putative Acr in prophage vB_PaeS-D14E to 10 putative Acrs in prophages vB_PaeS-D14F and vB_PaeS-D14O. These proteins were mainly grouped in a single cluster, but in some prophages more than one cluster could be found (two clusters in prophages vB_PaeM-D14A, vB_PaeP-D14I, vB_PaeS-D14K, and vB_PaeP-D14S, and three clusters in prophages vB_PaeS-D14F and vB_PaeS-D14O) (Table 3; Table S1). It should be noted that some predicted Acrs were already annotated with another function (i.e., terminase small subunit, tail structural proteins or holins). However, previous studies propose that some prophage proteins, such as head-tail adaptors or decoration proteins, could simultaneously act as Acr proteins, suggesting that Acr proteins might have evolved from viral structural components (41, 42).

Besides, the PaCRISPR tool was also used to detect putative Acr proteins (43). All prophages except for one (vB_PaeP-D14S) were found to carry at least one putative Acr, being prophages vB_PaeS-D14O and vB_PaeS-D14P the ones with the greater sum (nine and six, respectively). Unlike the proteins found with the previous tool, putative Acr detected by PaCRISPR did not have a previously known function, being the majority of them (29/36, 80.6%) annotated as hypothetical or unknown phage proteins. Five ORFs were predicted to be a putative Acr simultaneously by AcrFinder and PaCRISPR, and were considered as proven Acr (Table 3).

Finally, two additional Acr proteins were found using anti-CRISPRdb, in prophages vB_PaeS-D14C and vB_PaeP-D14S, both of them showing homology with members of the AcrIIA7 family, with E-values of $3.73e^{-30}$ and 0.002, respectively. This family of Acr, which has already been characterized in the genomes of tailed bacteriophages, is believed to interfere with the type II-A CRISPR-Cas system by inhibiting Cas9 (44). Given the fact that these ORFs did not have any other assigned function by RAST, HMMER, or HHpred and the considerably high homology scores with known viral defense proteins, Acr could be assigned as their function with high confidence.

Defense against restriction-modification systems

Eight out of the 13 prophages coded for DNA methyltransferases, used by the prophage to methylate its own DNA in order to protect it from the host cell's restriction-modification system, to regulate viral gene expression and to facilitate DNA packaging into the preformed capsids (45, 46). Besides, restriction alleviation proteins were found in prophages vB_PaeS-D14H and vB_PaeP-D14I, known to protect them from the host cell's restriction-modification system (47, 48) (Table 3).

Glycosyltransferases and acetylases

Among the prophages harboring DNA methyltransferases, three of them (vB_PaeS-D14C, vB_PaeS-D14O, and vB_PaeS-D14Q) were found to carry an adjacent glycosyltransferase (Table 3). Bacteriophages are known to encode them to glycosylate their DNA in order to protect it from restriction-modification systems and to modify the O-antigen present in the lipopolysaccharide (LPS) (49). Prophages harness these modifications to avoid the host cell's superinfection and to prevent the progeny to be retained on the bacterial surface if the lytic cycle is to be initiated. One of these prophages was also found to code for an O-antigen acetylase (vB_PaeS-D14O).

Toxin/antitoxin systems

Prophage vB_PaeS-D14B was found to code for a complete toxin/cognate antitoxin module belonging to the type II system with homology to BrnT toxin and a CopG family antitoxin (50). On the other hand, prophage vB_PaeS-D14H coded for the

complete type II TA system YoeB/YefM (51). In this same prophage, although two contiguous ORF were firstly annotated as type II TA system YdaT/YdaS homologs, a deep search into literature showed that these proteins were actually the prophage regulatory proteins CII and Cro (52). The type II toxin YafO was also found in prophages vB_PaeS-D14C and vB_PaeS-D14L (53), as well as a type IV antitoxin AbiEi in prophages vB_PaeP-D14I and vB_PaeP-D14S (54) (Table 3). TA systems have been proposed to protect bacteria from phages, together with CRISPR and restriction-modification systems. In this context, it is not surprising to find prophages carrying antitoxins alone, to counteract bacterial defenses, or even toxins alone to compete against external phages preying on their host (9).

DNA scission proteins

Prophages coded for junction-resolving enzymes, such as Holliday junction resolvases (in prophages vB_PaeS-D14H and vB_PaeS-D14P) and a YqaJ-like exonuclease (phage vB_PaeS-D14H) (Table 3). These enzymes have been previously described in bacteriophages in the degradation of host's DNA and in self DNA maturation and cleaving prior to packaging (55).

DNA gyrase inhibitor

Prophage vB_PaeP-D14I was found to code for a DNA gyrase inhibitor with homology with YacG in *Escherichia coli* (56), as shown by HHpred (>97% probability). This peptide is comprised of 76 amino acids, with a molecular weight of 8.75 kDA and an estimated pI of 8.3. Phyre2 analysis of the aminoacidic sequence yielded a protein model with homology to the above mentioned YacG protein with a confidence of 52.5. Another protein model was predicted by the Swiss-Model tool by Expasy (Fig. 3). This peptide was named as *Pseudomonas* YacG-like DNA gyrase inhibitor. Recently, a peptide with similar anti-DNA gyrase properties has been described for the *P. aeruginosa* bacteriophage LUZ24 (57).

Quorum Sensing

Proteins belonging to the LuxR family were identified in prophages vB_PaeS-D14B, vB_PaeS-D14E, and vB_PaeS-D14L. They were present in a single copy in each prophage and did not share any significant similarity with the *P. aeruginosa* QS receptors lasR and rhlR. However, they showed homology with other transcriptional regulators belonging to the LuxR family by both BLAST (>80% query cover and >99% identity) and HMMER (E-value $< 1 \times 10^{-26}$). These receptors constitute one of the first and most studied QS systems essential for intercellular communication and gene regulation triggering when a population threshold is reached. Although the archetypical QS tandems consist of a receptor (i.e., LuxR) and its cognate autoinducer synthase (i.e., LuxI), the presence of LuxR "solos" responsible for intraspecies and interspecies communication has also been described for proteobacteria in general and for *Pseudomonas* in particular (58–60). The presence of these receptors in prophage genomes has been linked to a potential role in phages to sense bacterial population density, and therefore to adapt viral infection to it (61) (Table 3). Finally, in prophages vB_PaeM-D14A, vB_PaeS-D14C, and vB_PaeS-D14O, a single copy of a TraR family transcriptional regulator was found in each prophage, all of them conserving a previously described DXXDXA motif in the N-terminal helix. Although they did not share any significant similarity with lasR and rhlR, they showed homology with a *P. aeruginosa* TraR/DksA family transcriptional regulator by BLAST (>85% query cover and >98% identity), HMMER (E-value $< 1 \times 10^{-10}$) and HHpred (probability >99%). TraR is a QS receptor, and their homologs have been recently suggested to play a role in redirecting the host's transcriptional machinery to viral promoters (62, 63).

Regulatory proteins

Lytic/lysogenic cycle switches

In 12 out of the 13 prophages, regulatory proteins in charge of maintaining the lysogenic cycle (CI, CII, and Cro) were found (Table 3). This regulatory network has been characterized in depth for bacteriophage λ, one of the most representative siphovirus. Briefly, the CI repressor is responsible for maintaining a stable lysogenic state by preventing lytic genes' expression, and for its own synthesis. This synthesis is also stimulated by the CII transcriptional regulator. On the contrary, Cro negatively regulates CII transcription, indirectly reducing CI levels, and thus promoting the lytic cycle. Upon DNA damage, SOS response is triggered and the CI regulator cleaved, consequently initiating the lytic cycle. This process, alongside with the functions of all other regulators (CIII, antitermination protein N and proteins O, P, and Q, among others), have been thoroughly reviewed by Oppenheim and colleagues (64). The fact that no regulatory proteins were found in relation with the lysogenic cycle in prophage vB_PaeS-D14Q responds to a poor annotation of this prophage rather than its absence, given its essential role in prophage homeostasis.

Other regulatory proteins

Prophage vB_PaeS-D14H was found to code for the pyocin activating protein PrtN, involved in upregulating pyocin synthesis, a bacteriocin produced by most *Pseudomonas* strains (65, 66). Additionally, the Bacteriophage Control Infection (*bci*) gene, responsible for increasing the host's infectivity by regulating biofilm production, motility, and virulence factor synthesis in *P. aeruginosa* (67), was found in 4/13 prophages (Table 3).

Prophage integration sites

Successful localization of the prophages' integration site within the *P. aeruginosa* bacterial chromosome was possible in 7/13 cases (Fig. 4). Prophages vB_PaeM-D14A, vB_PaeP-D14I, and vB_PaeS-D14L were inserted before, between or after host tRNA coding sequences. All tRNA genes were found to be intact, meaning that the prophage insertion did not affect the integrity of the sequence. This is of particular interest in the

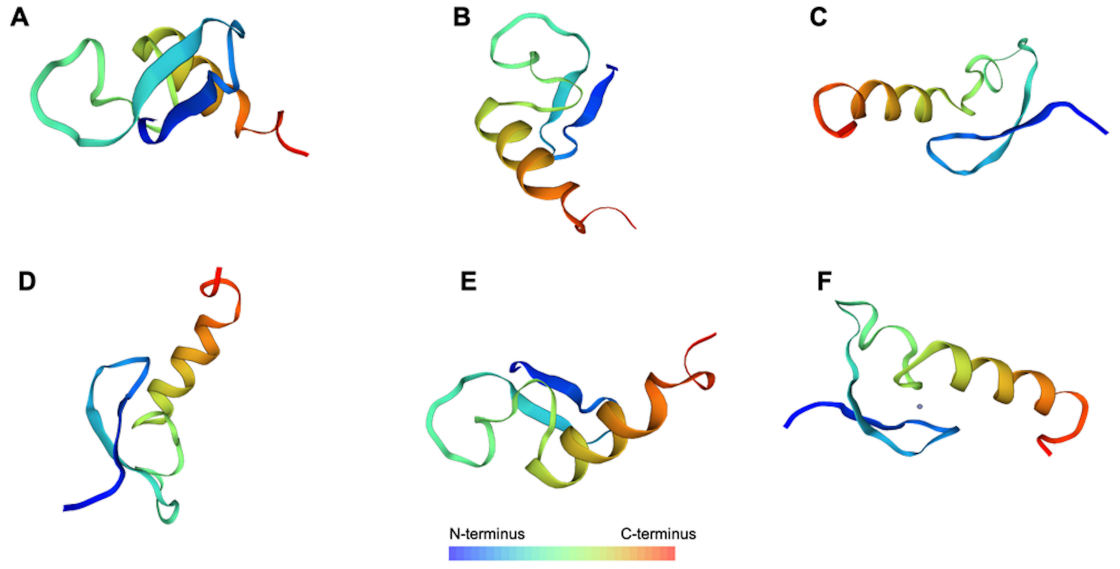

FIG 3 Putative DNA gyrase inhibitor representation as predicted by the Swiss-Model tool by Expasy and its corresponding amino acid sequence. (A through F): different positions of the predicted three-dimensional model. F: purple circle represents an atom of Zn^{2+} as a ligand.

case of prophage vB_PaeM-D14A, in which the *attR/L* sequence was found to be in the middle of the tRNA-Thr-TGT gene, suggesting that the prophage carried a copy of the same gene so its integration would replace the truncated gene, which is consistent with previous studies (68).

Interestingly, prophage vB_PaeS-D14B was found to be inserted prior to a HigA antitoxin, which was confirmed to be integral by BLAST analysis, meaning that prophage insertion did not disrupt the antitoxin gene. However, the cognate toxin, known to be arranged upstream the antitoxin gene (69), could not be localized within the bacterial genome. On the other hand, prophage vB_PaeS-D14E was localized between a hypothetical protein and an Ornithine carbamoyltransferase (EC 2.1.3.3), both of them conserved and adjacent in PAO1.

Finally, prophage vB_PaeS-D14F was localized integrated into the glyoxylate carboligase (EC 4.1.1.47) gene, disrupting it. This enzyme is responsible for the metabolism of glyoxylate, allowing bacterial growth on glycolate or oxalate. It is also remarkable the finding that this prophage carried a copy of the IclR family transcriptional regulator, involved in the repression of a shortcut in the metabolic pathway of glyoxylate known as the glyoxylate shunt (70). Although the significances of these findings remain unknown, the accumulation of metabolites such as glyoxylate in *P. aeruginosa* has been shown to influence bacterial tolerance and protect cells against antibiotics such as tobramycin through a blockage of the TCA cycle and a reduction in antibiotic uptake (71).

The remaining 5/13 prophages could not be localized within the bacterial genome because the extension of the prophage comprised the whole contig, not being able to identify any flanking ORF in common with the PAO1 or the clonal complexes CC235 and CC175—i.e., the most prevalent in the collection—reference genomes.

Clonal distribution

Correlation between the *P. aeruginosa* clone and prophage harboring was studied. In the collection of 53 *P. aeruginosa* strains, CC235 was found to be the most prevalent ($n = 14$), followed by CC175 ($n = 10$) and CC244 ($n = 7$).

In CC235, prophages vB_PaeM-D14A and vB_PaeS-D14C were found in 13/14, prophage vB_PaeS-D14B in 12/14 and prophage vB_PaeS-D14F in 10/14. The only four pandrug-resistant strains out of the 53, all of them belonging to the CC235, were found to simultaneously harbor phages vB_PaeM-D14A, vB_PaeS-D14B, and vB_PaeS-D14C. Interestingly, the only single strain of the CC235 which did not harbor any of these prophages was also the only CC235 strain which did not carry the GES-13 β-lactamase. This isolate also presented point mutations in genes associated with antimicrobial resistance, such as the membrane porine oprD and the efflux pumps mexY and muxC that the rest of the strains in the clonal complex did not have. Efflux pumps and porines constitute phage receptors, and mutations on these proteins could explain the differential carriage of prophages. However, the number of isolates is not big enough to develop association analyses.

In the strains belonging to the CC175 ($n = 10$); however, more diversity in prophage arrangement was found. Although all of the 10 strains coded for at least one of the prophages under study, the distribution of the phages (vB_PaeS-D14K, vB_PaeS-D14O, vB_PaeS-D14P, and vB_PaeS-D14Q) was uneven. The same appears to happen with CC244, in which prophages vB_PaeS-D14H, vB_PaeP-D14I, vB_PaeS-D14L, and vB_PaeP-D14S were found to be distributed without a clear association (Table 4).

Prophage isolation and TEM

Finally, prophages detected by *in silico* analysis were proven to be intact and able to initiate the lytic cycle. A representative member of each tail morphology group (myovirus, siphovirus, and podovirus) was chosen to be isolated and imaged by TEM. For the myovirus representative (vB_PaeM-D14A), the *P. aeruginosa* strain 1–13 was selected (Fig. 4A); for the podovirus representative (vB_PaeP-D14I), the *P. aeruginosa* strain 8–24 was

TABLE 4 Prophage distribution among the three more frequent sequence types (STs) of the *P. aeruginosa* collection[a]

					Antibiotic susceptibility													
Strain	Clonal complex	O-antigen serogroup	Prophages	β-lactamase	P/T[b]	C/T	CAZ	FEP	ATM	IMI	MER	CIP	GM	NN	AK	COL	FOS	TGC
1–13	CC235	O11	A, B, C	GES-13	R	R	R	R	R	R	R	R	R	R	R	S	R	R
2–29	CC235	O11	A, B, C	GES-13	R	R	R	R	R	R	R	R	R	R	R	R	R	R
3–49	CC235	O11	A, B, C, F	GES-13	R	R	R	R	R	R	R	R	R	R	R	S	R	R
4–17	CC235	O11	A, B, C, F	GES-13	R	R	R	R	R	R	R	R	R	R	R	S	R	R
4–71	CC235	O11	A, B, C, F	GES-13	R	R	R	R	R	R	R	R	R	R	R	S	R	R
4–79	CC235	O11	A, B, C, F	GES-13	R	R	R	R	R	R	R	R	R	R	R	R	R	R
4–86	CC235	O11	A, B, C, F	GES-13	R	R	R	R	R	R	R	R	R	R	R	S	R	R
4–92	CC235	O11	A, B, C, F	GES-13	R	R	R	R	R	R	R	R	R	R	R	S	R	R
4–93	CC235	O11	A, B, C, F	GES-13	R	R	R	R	R	R	R	R	R	R	R	R	R	R
4–94	CC235	O11	A, B, C, F	GES-13	R	R	R	R	R	R	R	R	R	R	R	S	R	R
4–120	CC235	O11	A, B, C, F	GES-13	R	R	R	R	R	R	R	R	R	R	R	R	R	R
4–121	CC235	O11	A, B, C	GES-13	R	R	R	R	R	R	R	R	R	R	R	S	R	R
5–15	CC235	O11	-	OXA-2	S	S	R	R	R	R	R	R	R	R	I	S	R	R
9–41	CC235	O11	A, C, F	GES-13	R	R	R	R	R	R	R	R	R	R	R	S	R	R
C11	CC175	O4	O, P	-	R	S	R	R	I	R	I	R	R	R	S	S	R	R
C58	CC175	O4/O11	O, P	VIM-2	R	R	R	R	I	R	R	S	R	R	S	S	R	R
E16	CC175	O4	Q	VIM-36	R	S	R	R	I	R	R	R	R	R	S	S	R	R
E17	CC175	O4	Q	-	R	R	R	R	R	R	R	R	R	R	S	S	R	R
F43	CC175	O4/O6	P	-	R	S	R	R	R	R	S	R	R	R	S	S	R	S
G6	CC175	O4	K, P, Q	VIM-20 OXA-2	S	R	R	S	I	R	R	R	R	R	I	S	R	S
G7	CC175	O4	P, Q	VIM-20 OXA-2	S	R	R	R	I	R	R	R	R	R	R	R	R	S
G26	CC175	O4	O, P	-	R	S	R	R	I	R	I	R	R	R	S	S	R	R
G31	CC175	O4	P, Q	VIM-20 OXA-2	S	R	R	R	I	R	R	R	R	R	R	S	R	R
H18	CC175	O4	P, Q	-	R	S	R	R	R	R	R	R	R	R	S	S	R	R
5–23	CC244	O5	H	-	R	S	R	R	R	R	R	R	S	S	S	R	R	R
6–25	CC244	O12	S	-	R	S	R	R	R	R	R	R	R	S	I	R	R	R
8–24	CC244	O5	H, I, L	VIM-2	R	R	R	R	I	R	R	S	R	R	R	S	R	R
8–36	CC244	O5	H, I, L	VIM-2	R	R	R	R	I	R	R	S	R	R	R	S	R	R
8–58	CC244	O5	-	-	S	S	R	R	I	R	R	S	S	S	S	S	R	R
9–25	CC244	O12	S	-	R	S	R	R	R	R	R	R	S	S	I	S	R	R
10–58	CC244	O12	-	-	R	S	R	R	R	R	R	R	S	S	S	S	R	R
3–5	CC348	O12	-	OXA-1	R	S	R	R	R	R	R	R	R	R	R	S	R	R
3–38	CC348	O12	E	OXA-1	R	R	R	R	R	R	R	R	R	R	R	S	R	R

(*Continued on next page*)

TABLE 4 Prophage distribution among the three more frequent sequence types (STs) of the *P. aeruginosa* collection (*Continued*)

					Antibiotic susceptibility													
3–41	CC348	O12	E	OXA-1	R	R	R	R	R	R	R	R	R	R	R	S	R	R
3–58	CC348	O12	-	OXA-1	R	R	R	R	R	R	R	R	R	R	R	S	R	R
8–1	CC348	O12	-	-	R	S	R	R	R	R	R	R	R	S	I	S	R	R

[a]A: vB_PaeM-D14A, B: vB_PaeS-D14B, C: vB_PaeS-D14C, E: vB_PaeS-D14E, F: vB_PaeS-D14F, H: vB_PaeS-D14H, I: vB_PaeP-D14I, K: vB_PaeS-D14K, L: vB_PaeS-D14L, O: vB_PaeS-D14O, P: vB_PaeS-D14P, Q: vB_PaeS-D14Q, S: vB_PaeP-D14S. Adaptation from reference (27).

[b]P/T, piperacillin/tazobactam; C/T, ceftolozane/tazobactam; CAZ, ceftazidime; FEP, cefepime; ATM, aztreonam; IMI, imipenem; MER, meropenem; CIP, ciprofloxacin; GM, gentamicin; NN, tobramycin; AK, amikacin; COL, colistin; FOS, Fosfomycin; TGC, tigecycline; S, susceptible; I, susceptible, increased exposure; R, resistant by EUCAST 2020 criteria.

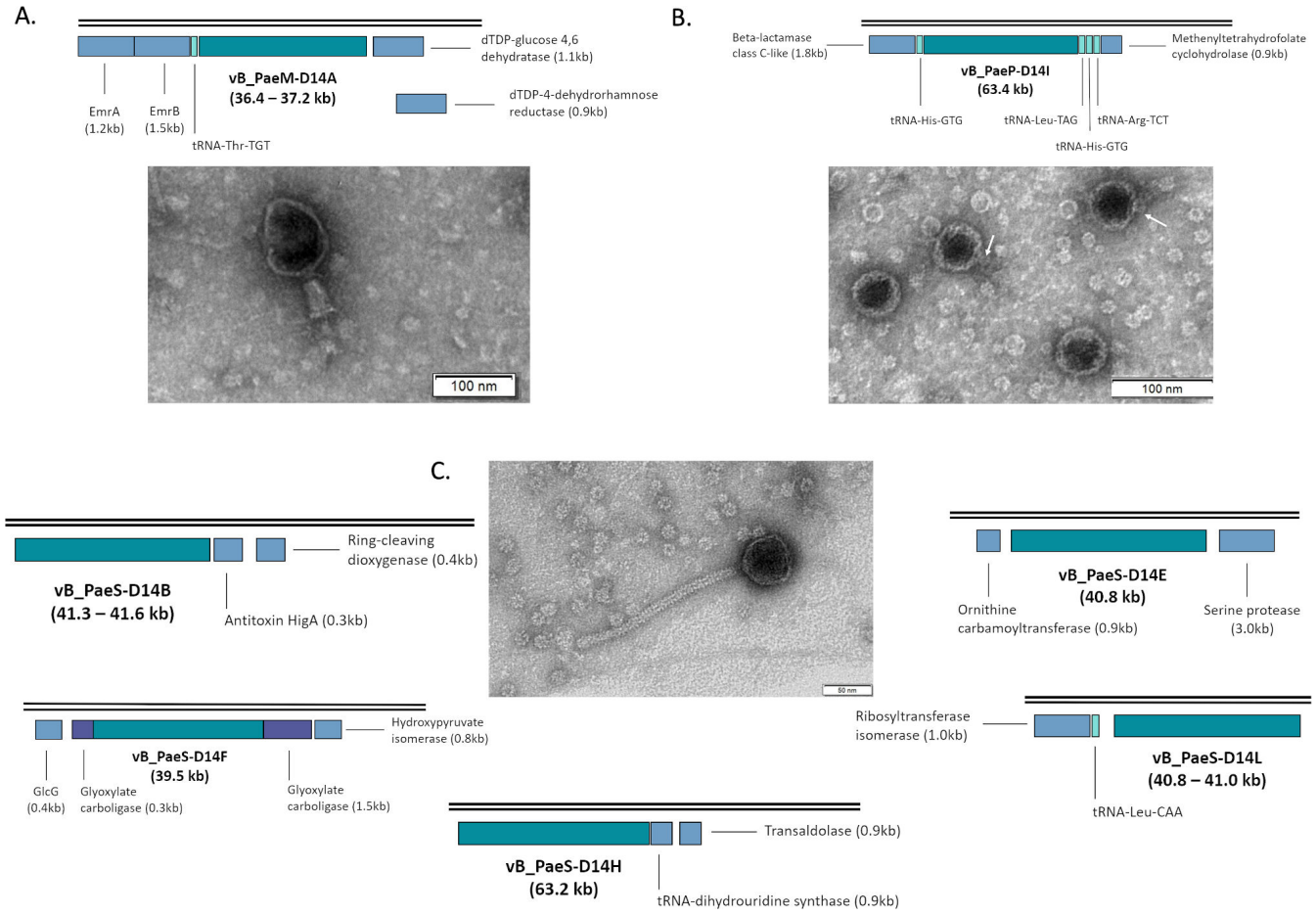

FIG 4 Transmission electron microscopy (TEM) images of the three different phage families belonging to the *Caudoviricetes* class found on this study and representation of their arrangement in the bacterial chromosome. (A) Bacteriophage of the myovirus tail morphology group (vB_PaeM-D14A); (B) bacteriophage of the podovirus group (vB_PaeP-D14I); and (C) bacteriophage of the siphovirus (vB_PaeS-D14B, vB_PaeS-D14E, vB_PaeS-D14F, vB_PaeS-D14H, and vB_PaeS-D14L). White arrows point at viral tails. Sequence segment corresponding to the prophage is not scaled to facilitate visualization.

selected (Fig. 4B); and for the siphovirus representative (vB_PaeS-D14H/vB_PaeS-D14L), the *P. aeruginosa* strain 8–24 was selected (Fig. 4C).

Conclusions

This study encompasses the search an analysis of prophages within a set of 53 invasive *P. aeruginosa* clinical strains isolated from critical care patients in different Portuguese and Spanish hospitals. With our findings, we show that these viral entities are present in the majority of circulating strains. Many of the prophages were found in more than one circulating strain simultaneously, following a similar clonal distribution pattern. In only 13.2% of the strains (7/53) no intact prophages—as given by Phaster—were found, showing that prophage harboring is a very frequent trait among circulating *P. aeruginosa* strains in critical care units in Portugal and Spain.

One limitation of our study is that *P. aeruginosa* isolates were sequenced only by short-read bridge amplification (Illumina, Oxford Genomics Centre, Oxford, UK), generating 150 bp fragments which, after assembly, led to 206–3,252 contigs per genome (average of 1,602 contigs/genome). The more fragmented genomes are, the more difficult it is to identify intact prophages, meaning that our search could have missed some of them when split into several contigs. Besides, in 6/13 prophages the viral sequence comprised a whole contig, denoting that the real length could be larger and some ORF could be missing. To circumvent this issue, a combination of both short

and long-read sequencing could be performed to obtain high-quality complete bacterial genomes.

Another point of concern is the relatively high proportion of ORF without a known function, being in 3/13 prophages greater than 50%. These findings are aligned with previous studies, which remark not only the vast number of unknown phages sequenced amidst metagenomic data—referred to as viral dark matter—but also the abundance of putative proteins whose function we ignore (72–75). In this regard, further studies concerning prophage identification, regulatory pathways, interaction with their host, and protein function should be made.

Although a great sum of viral ORFs is yet to be assigned a function, a number of proteins with interesting roles in altering the host's regulatory pathways were found within those prophages, supporting the idea that they might influence bacterial pathogenesis. Our study shows the presence of QS-related enzymes (LuxR family proteins and BCI), pyocin synthesis activating proteins (PrtN), and transcriptional regulators such as TraR homologs in almost every prophage under study (12/13), being phage vB_PaeS-D14Q the only exception.

Furthermore, in our work we found putative Acr proteins in every prophage under study, proven Acr proteins in 7/13 prophages and DNA methylation enzymes in 13/13. This highlights the importance of prophage-borne counter-defense mechanisms, which not only protect the prophage against their bacterial host's immune system but also the host against infection by other phages, enabling its survival and transmission to the bacterial progeny (76, 77). The functions of these proteins and the putative YacG-like DNA gyrase inhibitor should be confirmed experimentally with additional studies.

To continue with, in high-risk clones such as CC235 and CC175, up to four prophages were identified per isolate. These clonal complexes are known for their ability to acquire mobile genetic elements, their elevated antimicrobial resistance rates and their global distribution (78, 79). In particular, CC235, the most prevalent clone among MDR *P. aeruginosa* clinical isolates, has been shown to lack a functional CRISPR-Cas system, thus explaining its ability to acquire exogenous genetic elements such as bacteriophages (80).

Finally, the abundance of lytic cycle regulatory genes, Acr proteins and TA systems within prophage genomes detected in this study evidences the importance of characterizing the most frequent prophages in circulating clinical strains and in high-risk clones if phage therapy is to be used. This way, treatment failure upon the administration of phage therapy related to prophage-borne anti-phage mechanisms could be minimized. Since bacterial isolation and characterization are required prior to the elaboration of a phage cocktail, we propose to include prophage analysis as an additional step. We hope that further studies analyzing prophage profiles in the different circulating clinical strains will shed some light into this issue.

ACKNOWLEDGMENTS

This study has been funded by Instituto de Salud Carlos III (ISCIII) through the projects PI19/00878 and PI22/00323 and co-funded by the European Union, by Personalized and precision medicine grant from the Instituto de Salud Carlos III (MePRAM Project, PMP22/00092) and by the Study Group on Mechanisms of Action and Resistance to Antimicrobials, GEMARA (SEIMC, http://www.seimc.org/). M. González de Aledo was financially supported by the Rio Hortega program (ISCIII, CM22/00159). M. Tomás was financially supported by the Miguel Servet research program (SERGAS and ISCIII). I. Bleriot was financially supported by the pFIS program (ISCIII, FI20/00302). O. Pacios and M. López were financially supported by grants IN606A-2020/035 and IN606C-2022/002, respectively (GAIN, Xunta de Galicia).

M.G.D.A. developed the experiments, analyzed the results, and wrote the original manuscript. L.B., M.L., C.O-C., I.B., O.P., and M.H.G. visualized the results and manuscript. R.C. and M.T. re-wrote the manuscript, financed, and directed the experiments and supervised the writing of the original manuscript.

The authors declare that there are no conflicts of interest.

AUTHOR AFFILIATIONS

[1]Servicio de Microbiología, Hospital Universitario Ramón y Cajal and Instituto Ramón y Cajal de Investigación Sanitaria (IRYCIS); CIBER de Enfermedades Infecciosas (CIBERINFEC), Instituto de Salud Carlos III, Madrid, Spain
[2]Microbiología Traslacional y Multidisciplinar (MicroTM)-Instituto de Investigación Biomédica (INIBIC); Servicio de Microbiología, Hospital A Coruña (CHUAC); Universidad de A Coruña (UDC), A Coruña, Spain
[3]Study Group on Mechanisms of Action and Resistance to Antimicrobials (GEMARA) on behalf of the Spanish Society of Infectious Diseases and Clinical Microbiology (SEIMC), Madrid, Spain

AUTHOR ORCIDs

Manuel González de Aledo http://orcid.org/0000-0001-7222-4941
Lucia Blasco http://orcid.org/0000-0002-4039-4142
Maria Lopez http://orcid.org/0000-0003-4217-3295
Concha Ortiz-Cartagena http://orcid.org/0000-0001-6632-1454
Inés Bleriot http://orcid.org/0000-0002-1846-4693
Olga Pacios http://orcid.org/0000-0002-4476-856X
Marta Hernández-García http://orcid.org/0000-0003-2857-2572
Maria Tomas http://orcid.org/0000-0003-4501-0387

FUNDING

Funder	Grant(s)	Author(s)
MEC | Instituto de Salud Carlos III (ISCIII)	PI22/00323	Maria Tomas

AUTHOR CONTRIBUTIONS

Manuel González de Aledo, Investigation, Methodology, Writing – original draft | Lucia Blasco, Investigation, Supervision, Writing – review and editing | Maria Lopez, Visualization, Writing – review and editing | Concha Ortiz-Cartagena, Visualization, Writing – review and editing | Inés Bleriot, Visualization | Olga Pacios, Visualization | Marta Hernández-García, Investigation, Visualization, Writing – review and editing | Rafael Cantón, Methodology, Supervision, Validation, Visualization, Writing – review and editing | Maria Tomas, Methodology, Supervision, Writing – review and editing, Funding acquisition

DATA AVAILABILITY

All data generated or analyzed during this study are included in this published article (and its supplementary information files).

ADDITIONAL FILES

The following material is available online.

Supplemental Material

TABLE S1 (mSphere00128-23-S0001.pdf). Putative ACR proteins detected.

REFERENCES

1. Welp AL, Bomberger JM. 2020. Bacterial community interactions during chronic respiratory disease. Front Cell Infect Microbiol 10:213. https://doi.org/10.3389/fcimb.2020.00213
2. Pang Z, Raudonis R, Glick BR, Lin T-J, Cheng Z. 2019. Antibiotic resistance in *Pseudomonas aeruginosa*: mechanisms and alternative therapeutic strategies. Biotechnol Adv 37:177–192. https://doi.org/10.1016/j.biotechadv.2018.11.013
3. Rice LB. 2008. Federal funding for the study of antimicrobial resistance in nosocomial pathogens: no ESKAPE. J Infect Dis 197:1079–1081. https://doi.org/10.1086/533452

4. Jurado-Martín I, Sainz-Mejías M, McClean S. 2021. *Pseudomonas aeruginosa*: an audacious pathogen with an adaptable arsenal of virulence factors. Int J Mol Sci 22:3128. https://doi.org/10.3390/ijms22063128
5. Furfaro LL, Payne MS, Chang BJ. 2018. Bacteriophage therapy: clinical trials and regulatory hurdles. Front Cell Infect Microbiol 8:376. https://doi.org/10.3389/fcimb.2018.00376
6. Cieślik M, Bagińska N, Jończyk-Matysiak E, Węgrzyn A, Węgrzyn G, Górski A. 2021. Temperate bacteriophages-the powerful indirect Modulators of Eukaryotic cells and immune functions. Viruses 13:1013. https://doi.org/10.3390/v13061013
7. Labrie SJ, Samson JE, Moineau S. 2010. Bacteriophage resistance mechanisms. Nat Rev Microbiol 8:317–327. https://doi.org/10.1038/nrmicro2315
8. Ambroa A, Blasco L, López M, Pacios O, Bleriot I, Fernández-García L, González de Aledo M, Ortiz-Cartagena C, Millard A, Tomás M. 2021. Genomic analysis of molecular bacterial mechanisms of resistance to phage infection. Front Microbiol 12:784949. https://doi.org/10.3389/fmicb.2021.784949
9. LeRoux M, Laub MT. 2022. Toxin-antitoxin systems as phage defense elements. Annu Rev Microbiol 76:21–43. https://doi.org/10.1146/annurev-micro-020722-013730
10. Bleriot I, Blasco L, Pacios O, Fernández-García L, Ambroa A, López M, Ortiz-Cartagena C, Cuenca FF, Oteo-Iglesias J, Pascual Á, Martínez-Martínez L, Domingo-Calap P, Wood TK, Tomás M. 2022. The role of PemIK (PemK/PemI) type II TA system from *Klebsiella pneumoniae* clinical strains in lytic phage infection. Sci Rep 12:4488. https://doi.org/10.1038/s41598-022-08111-5
11. Cohen D, Melamed S, Millman A, Shulman G, Oppenheimer-Shaanan Y, Kacen A, Doron S, Amitai G, Sorek R. 2019. Cyclic GMP-AMP signalling protects bacteria against viral infection. Nature 574:691–695. https://doi.org/10.1038/s41586-019-1605-5
12. Tal N, Morehouse BR, Millman A, Stokar-Avihail A, Avraham C, Fedorenko T, Yirmiya E, Herbst E, Brandis A, Mehlman T, Oppenheimer-Shaanan Y, Keszei AFA, Shao S, Amitai G, Kranzusch PJ, Sorek R. 2021. Cyclic CMP and cyclic UMP mediate bacterial immunity against phages. Cell 184:5728–5739. https://doi.org/10.1016/j.cell.2021.09.031
13. Duncan-Lowey B, Tal N, Johnson AG, Rawson S, Mayer ML, Doron S, Millman A, Melamed S, Fedorenko T, Kacen A, Brandis A, Mehlman T, Amitai G, Sorek R, Kranzusch PJ. 2023. Cryo-EM structure of the RADAR supramolecular anti-phage defense complex. Cell 186:987–998. https://doi.org/10.1016/j.cell.2023.01.012
14. Garb J, Lopatina A, Bernheim A, Zaremba M, Siksnys V, Melamed S, Leavitt A, Millman A, Amitai G, Sorek R. 2022. Multiple phage resistance systems inhibit infection via SIR2-dependent NAD+ depletion. Nat Microbiol 7:1849–1856. https://doi.org/10.1038/s41564-022-01207-8
15. Tal N, Sorek R. 2022. Snapshot: bacterial immunity. Cell 185:578–578. https://doi.org/10.1016/j.cell.2021.12.029
16. Simmons EL, Drescher K, Nadell CD, Bucci V. 2018. Phage mobility is a core determinant of phage-bacteria coexistence in biofilms. ISME J 12:531–543. https://doi.org/10.1038/ismej.2017.190
17. Høyland-Kroghsbo NM, Maerkedahl RB, Svenningsen SL. 2013. A quorum-sensing-induced bacteriophage defense mechanism. mBio 4:e00362–12. https://doi.org/10.1128/mBio.00362-12
18. Høyland-Kroghsbo NM, Paczkowski J, Mukherjee S, Broniewski J, Westra E, Bondy-Denomy J, Bassler BL. 2017. Quorum sensing controls the *Pseudomonas aeruginosa* CRISPR-Cas adaptive immune system. Proc Natl Acad Sci USA 114:131–135. https://doi.org/10.1073/pnas.1617415113
19. Ding Y, Zhang D, Zhao X, Tan W, Zheng X, Zhang Q, Ji X, Wei Y. 2021. Autoinducer-2-mediated quorum-sensing system resists T4 phage infection in *Escherichia coli*. J Basic Microbiol 61:1113–1123. https://doi.org/10.1002/jobm.202100344
20. Manning AJ, Kuehn MJ. 2011. Contribution of bacterial outer membrane vesicles to innate bacterial defense. BMC Microbiol 11:258. https://doi.org/10.1186/1471-2180-11-258
21. Reyes-Robles T, Dillard RS, Cairns LS, Silva-Valenzuela CA, Housman M, Ali A, Wright ER, Camilli A. 2018. *Vibrio Cholerae* outer membrane vesicles inhibit bacteriophage infection. J Bacteriol 200:e00792-17. https://doi.org/10.1128/JB.00792-17
22. Vidakovic L, Singh PK, Hartmann R, Nadell CD, Drescher K. 2018. Dynamic biofilm architecture confers individual and collective mechanisms of viral protection. Nat Microbiol 3:26–31. https://doi.org/10.1038/s41564-017-0050-1
23. Hardy A, Kever L, Frunzke J. 2023. Antiphage small molecules produced by bacteria - beyond protein-mediated defenses. Trends Microbiol 31:92–106. https://doi.org/10.1016/j.tim.2022.08.001
24. Bondy-Denomy J, Pawluk A, Maxwell KL, Davidson AR. 2013. Bacteriophage genes that inactivate the CRISPR/Cas bacterial immune system. Nature 493:429–432. https://doi.org/10.1038/nature11723
25. Pawluk A, Davidson AR, Maxwell KL. 2018. Anti-CRISPR: discovery, mechanism and function. Nat Rev Microbiol 16:12–17. https://doi.org/10.1038/nrmicro.2017.120
26. Murphy J, Mahony J, Ainsworth S, Nauta A, van Sinderen D. 2013. Bacteriophage orphan DNA methyltransferases: insights from their bacterial origin, function, and occurrence. Appl Environ Microbiol 79:7547–7555. https://doi.org/10.1128/AEM.02229-13
27. Hernández-García M, García-Castillo M, García-Fernández S, Melo-Cristino J, Pinto MF, Gonçalves E, Alves V, Vieira AR, Ramalheira E, Sancho L, Diogo J, Ferreira R, Silva T, Chaves C, Bou G, Cercenado E, Delgado-Valverde M, Oliver A, Pitart C, Rodríguez-Lozano J, Tormo N, Romano J, Pássaro L, Paixão L, López-Mendoza D, Díaz-Regañón J, Cantón R, STEP and SUPERIOR study groups. 2021. Distinct epidemiology and resistance mechanisms affecting ceftolozane/tazobactam in *Pseudomonas aeruginosa* isolates recovered from ICU patients in Spain and Portugal depicted by WGS. J Antimicrob Chemother 76:370–379. https://doi.org/10.1093/jac/dkaa430
28. García-Fernández S, García-Castillo M, Bou G, Calvo J, Cercenado E, Delgado M, Pitart C, Mulet X, Tormo N, Mendoza DL, Díaz-Regañón J, Cantón R, SUPERIOR Study Group. 2019. Activity of ceftolozane/tazobactam against *Pseudomonas aeruginosa* and *Enterobacterales* isolates recovered from intensive care unit patients in Spain: the SUPERIOR multicentre study. Int J Antimicrob Agents 53:682–688. https://doi.org/10.1016/j.ijantimicag.2019.02.004
29. Hernández-García M, García-Fernández S, García-Castillo M, Pássaro L, Cantón R, STEP study group. 2021. *In vitro* characterization of *Pseudomonas aeruginosa* recovered in Portugal from low respiratory tract infections in ICU patients (STEP study). FEMS Microbiol Lett 368:fnab099. https://doi.org/10.1093/femsle/fnab099
30. Davis JJ, Wattam AR, Aziz RK, Brettin T, Butler R, Butler RM, Chlenski P, Conrad N, Dickerman A, Dietrich EM, Gabbard JL, Gerdes S, Guard A, Kenyon RW, Machi D, Mao C, Murphy-Olson D, Nguyen M, Nordberg EK, Olsen GJ, Olson RD, Overbeek JC, Overbeek R, Parrello B, Pusch GD, Shukla M, Thomas C, VanOeffelen M, Vonstein V, Warren AS, Xia F, Xie D, Yoo H, Stevens R. 2020. The PATRIC bioinformatics resource center: expanding data and analysis capabilities. Nucleic Acids Res 48:D606–D612. https://doi.org/10.1093/nar/gkz943
31. Arndt D, Grant JR, Marcu A, Sajed T, Pon A, Liang Y, Wishart DS. 2016. PHASTER: a better, faster version of the PHAST phage search tool. Nucleic Acids Res 44:W16–W21. https://doi.org/10.1093/nar/gkw387
32. Zimmermann L, Stephens A, Nam SZ, Rau D, Kübler J, Lozajic M, Gabler F, Söding J, Lupas AN, Alva V. 2018. A completely reimplemented MPI bioinformatics toolkit with a new HHpred server at its core. J Mol Biol 430:2237–2243. https://doi.org/10.1016/j.jmb.2017.12.007
33. Mihara T, Nishimura Y, Shimizu Y, Nishiyama H, Yoshikawa G, Uehara H, Hingamp P, Goto S, Ogata H. 2016. Linking virus genomes with host taxonomy. Viruses 8:66. https://doi.org/10.3390/v8030066
34. Katoh K, Misawa K, Kuma K, Miyata T. 2002. MAFFT: a novel method for rapid multiple sequence alignment based on fast Fourier transform. Nucleic Acids Res 30:3059–3066. https://doi.org/10.1093/nar/gkf436
35. Stamatakis A. 2014. RAxML version 8: a tool for phylogenetic analysis and post-analysis of large phylogenies. Bioinformatics 30:1312–1313. https://doi.org/10.1093/bioinformatics/btu033
36. Waterhouse A, Bertoni M, Bienert S, Studer G, Tauriello G, Gumienny R, Heer FT, de Beer TAP, Rempfer C, Bordoli L, Lepore R, Schwede T. 2018. SWISS-MODEL: homology modelling of protein structures and complexes. Nucleic Acids Res 46:W296–W303. https://doi.org/10.1093/nar/gky427
37. López M, Rueda A, Florido JP, Blasco L, Fernández-García L, Trastoy R, Fernández-Cuenca F, Martínez-Martínez L, Vila J, Pascual A, Bou G, Tomas M. 2018. Evolution of the Quorum network and the mobilome (plasmids and bacteriophages) in clinical strains of *Acinetobacter baumannii* during a decade. Sci Rep 8:2523. https://doi.org/10.1038/s41598-018-20847-7

38. Klockgether J, Cramer N, Wiehlmann L, Davenport CF, Tümmler B. 2011. *Pseudomonas aeruginosa* genomic structure and diversity. Front Microbiol 2:150. https://doi.org/10.3389/fmicb.2011.00150
39. Fortier LC, Sekulovic O. 2013. Importance of prophages to evolution and virulence of bacterial pathogens. Virulence 4:354–365. https://doi.org/10.4161/viru.24498
40. Bleriot I, Trastoy R, Blasco L, Fernández-Cuenca F, Ambroa A, Fernández-García L, Pacios O, Perez-Nadales E, Torre-Cisneros J, Oteo-Iglesias J, Navarro F, Miró E, Pascual A, Bou G, Martínez-Martínez L, Tomas M. 2020. Genomic analysis of 40 prophages located in the genomes of 16 carbapenemase-producing clinical strains of *Klebsiella pneumoniae*. Microb Genom 6:e000369. https://doi.org/10.1099/mgen.0.000369
41. Uribe RV, van der Helm E, Misiakou M-A, Lee S-W, Kol S, Sommer MOA. 2019. Discovery and characterization of Cas9 inhibitors disseminated across seven bacterial phyla. Cell Host Microbe 26:702. https://doi.org/10.1016/j.chom.2019.09.005
42. Stone NP, Hilbert BJ, Hidalgo D, Halloran KT, Lee J, Sontheimer EJ, Kelch BA. 2018. A hyperthermophilic phage decoration protein suggests common evolutionary origin with herpesvirus triplex proteins and an anti-CRISPR protein. Structure 26:936–947. https://doi.org/10.1016/j.str.2018.04.008
43. Wang J, Dai W, Li J, Xie R, Dunstan RA, Stubenrauch C, Zhang Y, Lithgow T. 2020. PaCRISPR: a server for predicting and visualizing anti-CRISPR proteins. Nucleic Acids Res 48:W348–W357. https://doi.org/10.1093/nar/gkaa432
44. Liu Q, Zhang H, Huang X. 2020. Anti-CRISPR proteins targeting the CRISPR-Cas system enrich the toolkit for genetic engineering. FEBS J 287:626–644. https://doi.org/10.1111/febs.15139
45. Burke EJ, Rodda SS, Lund SR, Sun Z, Zeroka MR, O'Toole KH, Parker MJ, Doshi DS, Guan C, Lee Y-J, Dai N, Hough DM, Shnider DA, Corrêa IR, Weigele PR, Saleh L. 2021. Phage-encoded ten-eleven translocation dioxygenase (TET) is active in C5-cytosine hypermodification in DNA. Proc Natl Acad Sci U S A 118:e2026742118. https://doi.org/10.1073/pnas.2026742118
46. Loenen WAM, Raleigh EA. 2014. The other face of restriction: modification-dependent enzymes. Nucleic Acids Res 42:56–69. https://doi.org/10.1093/nar/gkt747
47. Toothman P. 1981. Restriction alleviation by bacteriophages lambda and lambda reverse. J Virol 38:621–631. https://doi.org/10.1128/JVI.38.2.621-631.1981
48. Loenen WAM, Murray NE. 1986. Modification enhancement by the restriction alleviation protein (Ral) of bacteriophage Λ. J Mol Biol 190:11–22. https://doi.org/10.1016/0022-2836(86)90071-9
49. Markine-Goriaynoff N, Gillet L, Van Etten JL, Korres H, Verma N, Vanderplasschen A. 2004. Glycosyltransferases encoded by viruses. J Gen Virol 85:2741–2754. https://doi.org/10.1099/vir.0.80320-0
50. Heaton BE, Herrou J, Blackwell AE, Wysocki VH, Crosson S. 2012. Molecular structure and function of the novel BrnT/BrnA toxin-antitoxin system of Brucella abortus. J Biol Chem 287:12098–12110. https://doi.org/10.1074/jbc.M111.332163
51. Ma D, Gu H, Shi Y, Huang H, Sun D, Hu Y. 2021. *Edwardsiella piscicida* YefM-YoeB: a type II toxin-antitoxin system that is related to antibiotic resistance, biofilm formation, serum survival, and host infection. Front Microbiol 12:646299. https://doi.org/10.3389/fmicb.2021.646299
52. Jobling MG. 2018. Ectopic expression of the *ydaS* and *ydaT* genes of the cryptic prophage Rac of *Escherichia Coli* K-12 may be toxic but do they really encode toxins?: A case for using genetic context to understand function. mSphere 3:e00163-18. https://doi.org/10.1128/mSphere.00163-18
53. Zhang Y, Yamaguchi Y, Inouye M. 2009. Characterization of YafO, an *Escherichia coli* toxin. J Biol Chem 284:25522–25531. https://doi.org/10.1074/jbc.M109.036624
54. Hampton HG, Jackson SA, Fagerlund RD, Vogel AIM, Dy RL, Blower TR, Fineran PC. 2018. Abiei binds cooperatively to the type IV abiE toxin-antitoxin operator via a positively-charged surface and causes DNA bending and negative autoregulation. J Mol Biol 430:1141–1156. https://doi.org/10.1016/j.jmb.2018.02.022
55. Wyatt HDM, West SC. 2014. Holliday junction resolvases. Cold Spring Harb Perspect Biol 6:a023192. https://doi.org/10.1101/cshperspect.a023192
56. Sengupta S, Nagaraja V. 2008. YacG from *Escherichia coli* is a specific endogenous inhibitor of DNA gyrase. Nucleic Acids Res 36:4310–4316. https://doi.org/10.1093/nar/gkn355
57. De Smet J, Wagemans J, Boon M, Ceyssens P-J, Voet M, Noben J-P, Andreeva J, Ghilarov D, Severinov K, Lavigne R. 2021. The bacteriophage LUZ24 "lgy" peptide inhibits the *Pseudomonas* DNA gyrase. Cell Rep 36:109567. https://doi.org/10.1016/j.celrep.2021.109567
58. Fuqua WC, Winans SC, Greenberg EP. 1994. Quorum sensing in bacteria: the LuxR-LuxI family of cell density- responsive transcriptional regulators. J Bacteriol 176:269–275. https://doi.org/10.1128/jb.176.2.269-275.1994
59. Subramoni S, Venturi V. 2009. LuxR-family "solos": bachelor sensors/regulators of signalling molecules. Microbiology (Reading) 155:1377–1385. https://doi.org/10.1099/mic.0.026849-0
60. Bez C, Covaceuszach S, Bertani I, Choudhary KS, Venturi V. 2021. LuxR solos from environmental fluorescent pseudomonads mSphere 6:e0085321. https://doi.org/10.1128/mSphere.00853-21
61. Silpe JE, Bassler BL. 2019. Phage-encoded LuxR-type receptors responsive to host-produced bacterial quorum-sensing autoinducers. mBio 10:e00638-19. https://doi.org/10.1128/mBio.00638-19
62. Vannini A, Volpari C, Gargioli C, Muraglia E, Cortese R, De Francesco R, Neddermann P, Marco SD. 2002. The crystal structure of the quorum sensing protein TraR bound to its autoinducer and target DNA. EMBO J 21:4393–4401. https://doi.org/10.1093/emboj/cdf459
63. Gopalkrishnan S, Ross W, Akbari MS, Li X, Haycocks JRJ, Grainger DC, Court DL, Gourse RL. 2022. Homologs of the *Escherichia coli* F element protein TraR, including phage lambda Orf73, directly reprogram host transcription. mBio 13:e0095222. https://doi.org/10.1128/mbio.00952-22
64. Oppenheim AB, Kobiler O, Stavans J, Court DL, Adhya S. 2005. Switches in bacteriophage lambda development. Annu Rev Genet 39:409–429. https://doi.org/10.1146/annurev.genet.39.073003.113656
65. Matsui H, Sano Y, Ishihara H, Shinomiya T. 1993. Regulation of Pyocin genes in *Pseudomonas aeruginosa* by positive (prtN) and negative (prtR) regulatory genes. J Bacteriol 175:1257–1263. https://doi.org/10.1128/jb.175.5.1257-1263.1993
66. Michel-Briand Y, Baysse C. 2002. The Pyocins of *Pseudomonas aeruginosa*. Biochimie 84:499–510. https://doi.org/10.1016/s0300-9084(02)01422-0
67. Ambroa A, Blasco L, López-Causapé C, Trastoy R, Fernandez-García L, Bleriot I, Ponce-Alonso M, Pacios O, López M, Cantón R, Kidd TJ, Bou G, Oliver A, Tomás M. 2020. Temperate bacteriophages (prophages) in *Pseudomonas aeruginosa* isolates belonging to the International cystic fibrosis clone (CC274). Front Microbiol 11:556706. https://doi.org/10.3389/fmicb.2020.556706
68. Campbell A. 2003. Prophage insertion sites. Res Microbiol 154:277–282. https://doi.org/10.1016/S0923-2508(03)00071-8
69. Wood TL, Wood TK. 2016. The HigB/HigA toxin/antitoxin system of *Pseudomonas aeruginosa* influences the virulence factors pyochelin, pyocyanin, and biofilm formation. Microbiologyopen 5:499–511. https://doi.org/10.1002/mbo3.346
70. Krell T, Molina-Henares AJ, Ramos JL. 2006. The IclR family of transcriptional activators and repressors can be defined by a single profile. Protein Sci 15:1207–1213. https://doi.org/10.1110/ps.051857206
71. Meylan S, Porter CBM, Yang JH, Belenky P, Gutierrez A, Lobritz MA, Park J, Kim SH, Moskowitz SM, Collins JJ. 2017. Carbon sources tune antibiotic susceptibility in *Pseudomonas aeruginosa* via tricarboxylic acid cycle control. Cell Chem Biol 24:195–206. https://doi.org/10.1016/j.chembiol.2016.12.015
72. Hurwitz BL, U'Ren JM, Youens-Clark K. 2016. Computational prospecting the great viral unknown. FEMS Microbiol Lett 363:fnw077. https://doi.org/10.1093/femsle/fnw077
73. Dutilh BE. 2014. Metagenomic ventures into outer sequence space. Bacteriophage 4:e979664. https://doi.org/10.4161/21597081.2014.979664
74. Yutin N, Makarova KS, Gussow AB, Krupovic M, Segall A, Edwards RA, Koonin EV. 2018. Discovery of an expansive bacteriophage family that includes the mostabundant viruses from the human gut. Nat Microbiol 3:38–46. https://doi.org/10.1038/s41564-017-0053-y
75. Fremin BJ, Bhatt AS, Kyrpides NC, Sengupta A, Sczyrba A, Maria da Silva A, Buchan A, Gaudin A, Brune A, Hirsch AM, Neumann A, Shade A, Visel A, Campbell B, Baker B, Hedlund BP, Crump BC, Currie C, Kelly C, Craft C,

Hazard C, Francis C, Schadt CW, Averill C, Mobilian C, Buckley D, Hunt D, Noguera D, Beck D, Valentine DL, Walsh D, Sumner D, Lymperopoulou D, Bhaya D, Bryant DA, Morrison E, Brodie E, Young E, Lilleskov E, Högfors-Rönnholm E, Chen F, Stewart F, Nicol GW, Teeling H, Beller HR, Dionisi H, Liao H-L, Beman JM, Stegen J, Tiedje J, Jansson J, VanderGheynst J, Norton J, Dangl J, Blanchard J, Bowen J, Macalady J, Pett-Ridge J, Rich J, Payet JP, Gladden JD, Raff JD, Klassen JL, Tarn J, Neufeld J, Gravuer K, Hofmockel K, Chen K-H, Konstantinidis K, DeAngelis KM, Partida-Martinez LP, Meredith L, Chistoserdova L, Moran MA, Scarborough M, Schrenk M, Sullivan M, David M, O'Malley MA, Medina M, Habteselassie M, Ward ND, Pietrasiak N, Mason OU, Sorensen POEstrada de los SantosPP, Baldrian P, McKay RM, Simister R, Stepanauskas R, Neumann R, Malmstrom R, Cavicchioli R, Kelly R, Hatzenpichler R, Stocker R, Cattolico RA, Ziels R, Vilgalys R, Blumer-Schuette S, Crowe S, Roux S, Hallam S, Lindow S, Brawley SH, Tringe S, Woyke T, Whitman T, Bianchi T, Mock T, Donohue T, James TY, Kalluri UC, Karaoz U, Denef V, Liu W-T, Whitman W, Ouyang Y. 2022. Thousands of small, novel genes predicted in global phage genomes. Cell Rep 39:110984. https://doi.org/10.1016/j.celrep.2022.110984

76. Pfeifer E, Sousa JM, Touchon M, Rocha EP. 2022. When bacteria are phage playgrounds: interactions between viruses, cells, and mobile genetic elements. Curr Opin Microbiol 70:102230. https://doi.org/10.1016/j.mib.2022.102230
77. Rocha EPC, Bikard D. 2022. Microbial defenses against mobile genetic elements and viruses: who DEFENDS whom from what? PLoS Biol 20:e3001514. https://doi.org/10.1371/journal.pbio.3001514
78. Treepong P, Kos VN, Guyeux C, Blanc DS, Bertrand X, Valot B, Hocquet D. 2018. Global emergence of the widespread *Pseudomonas aeruginosa* ST235 clone. Clin Microbiol Infect 24:258–266. https://doi.org/10.1016/j.cmi.2017.06.018
79. Del Barrio-Tofiño E, López-Causapé C, Oliver A. 2020. *Pseudomonas aeruginosa* epidemic high-risk clones and their association with horizontally-acquired β-lactamases: 2020 update. Int J Antimicrob Agents 56:106196. https://doi.org/10.1016/j.ijantimicag.2020.106196
80. Miyoshi-Akiyama T, Tada T, Ohmagari N, Viet Hung N, Tharavichitkul P, Pokhrel BM, Gniadkowski M, Shimojima M, Kirikae T. 2017. Emergence and spread of epidemic multidrug-resistant *Pseudomonas aeruginosa*. Genome Biol Evol 9:3238–3245. https://doi.org/10.1093/gbe/evx243

Study 2: Hernández-García, Marta*; **González de Aledo, Manuel***; et al. (2024). Simultaneous clonal spread of NDM-1-producing *Pseudomonas aeruginosa* ST773 from Ukrainian patients in The Netherlands and Spain. IJID Reg., 100415. doi: 10.1016/J.IJREGI.2024.100415.

SUMMARY: The NDM-1 producing *Pseudomonas aeruginosa* ST773 clone constitutes an emerging high-risk clone which has been recently detected for the first time in Western Europe. In this work, we analyzed nine isolates recovered from patients evacuated to two Spanish (n = 3) and five Dutch (n = 6) hospitals between March and December 2022 as a consequence of the war in Ukraine. Antimicrobial susceptibility was studied (Sensititre, Microscan, EUCAST-2023), and whole genome sequencing (Illumina, Oxford-Nanopore) was used to analyze the genetic relatedness, the resistome, and the prophage content. All NDM-1–producing *P. aeruginosa* ST773 isolates exhibited resistance to all tested antimicrobials except colistin, aztreonam, and cefiderocol. Genomic analysis revealed that all isolates had an identical resistome and a chromosomally encoded integrative conjugative element carrying the *blaNDM-1* gene. The core genome multilocus sequence typing and core genome single nucleotide polymorphisms analysis showed highly related isolates, irrespective of country of isolation, distant from other NDM-1-ST773 *P. aeruginosa* not collected in Ukraine. Both analyses revealed two closely related clusters, spanning the Spanish and Dutch isolates. In addition, a high content of prophages was identified in all strains, most of them in more than one isolate simultaneously, regardless of their origin country. Moreover, an identical phage tail-like bacteriocin cluster was identified in all NDM-1-ST773. To conclude with, we report a clonal dissemination of NDM-producing *P. aeruginosa* ST773 to the Netherlands and Spain associated with patients from Ukraine.

IMPORTANCE: In March 2022, in the context of the Ukraine war, the European Centre for Disease Prevention and Control (ECDC) issued a document recommending the screening for carriage of MDR organisms in patients transferred from Ukrainian hospitals or with a history of hospital admission in Ukraine in the previous 12 months, due to the reported higher rates of MDR organisms in that region. Despite the preventive measures taken, the NDM-1 producing *P. aeruginosa* clone ST773 was firstly reported in Western Europe in patients transferred to The Netherlands and Spain as a consequence of the war. This study investigates the genomic characteristics of the *P. aeruginosa* isolates recovered from these patients, with particular regard to their virulence, AMR, pyocin production and prophage harboring. Our work highlights the importance of genomic surveillance and to understand the dynamics of resistance in multidrug-resistant bacteria after the transfer of patients from conflict zones, highlighting the importance of international collaboration to address global AMR.

IJID Regions 12 (2024) 100415

Contents lists available at ScienceDirect

IJID Regions

journal homepage: www.elsevier.com/locate/ijregi

Simultaneous clonal spread of NDM-1–producing *Pseudomonas aeruginosa* ST773 from Ukrainian patients in the Netherlands and Spain

Marta Hernández-García[1,2,†], Manuel González de Aledo[1,2,†], Manuel Ponce-Alonso[1,2], Beatriz González-Blanco[3], Esther Viedma[3], Jennifer Villa[3], María Tomás[4], Antoni P.A. Hendrickx[5], Patricia Ruiz-Garbajosa[1,2,*], Rafael Cantón[1,2]

[1] *Servicio de Microbiología, Hospital Universitario Ramón y Cajal and Instituto Ramón y Cajal de Investigación Sanitaria (IRYCIS), Madrid, Spain*
[2] *CIBER de Enfermedades Infecciosas (CIBERINFEC), Instituto de Salud Carlos III, Madrid, Spain*
[3] *Servicio de Microbiología, Hospital 12 de Octubre, Madrid, Spain and Instituto de Investigación Hospital 12 de Octubre (imas12), Madrid, Spain*
[4] *Grupo de Microbiología Traslacional y Multidisciplinar (MicroTM)-Servicio de Microbiología Instituto de Investigación Biomédica A Coruña (INIBIC), Hospital A Coruña (CHUAC), A Coruña, Spain*
[5] *Centre for infectious disease control (Cib), National Institute for Public Health and the Environment (RIVM), Bilthoven, The Netherlands*

ARTICLE INFO

Keywords:
NDM-1-ST773 *P. aeruginosa*
Ukrainian patients
Clonal dissemination
Spain
The Netherlands
Bacteriophages

ABSTRACT

Objectives: We describe the clonal spread of New Delhi metallo-β-lactamase (NDM) 1–producing *Pseudomonas aeruginosa* isolates belonging to the ST773 clone in Spain and the Netherlands, associated with the transfer of Ukrainian patients during the war.

Methods: Between March and December 2022, nine NDM-1–producing *P. aeruginosa* ST773 isolates were recovered from nine Ukrainian patients evacuated to two Spanish ($n = 3$) and five Dutch ($n = 6$) hospitals. Antimicrobial susceptibility testing was studied (Sensititre, Microscan, EUCAST-2023). Whole genome sequencing (Illumina, Oxford-Nanopore) was used to analyze the genetic relatedness, the resistome, and the prophage content.

Results: All NDM-1–producing *P. aeruginosa* ST773 isolates exhibited resistance to all tested antimicrobials except colistin, aztreonam, and cefiderocol. Genomic analysis revealed that all isolates had an identical resistome and a chromosomally encoded integrative conjugative element carrying the bla_{NDM-1} gene. The core genome multilocus sequence typing and core genome single nucleotide polymorphisms analysis showed highly related isolates, irrespective of country of isolation, distant from other NDM-1-ST773 *P. aeruginosa* not collected in Ukraine. Both analysis revealed two closely related clusters, spanning the Spanish and Dutch isolates. In addition, a high content of prophages was identified in all strains, most of them in more than one isolate simultaneously, regardless of their origin country. Moreover, an identical phage tail-like bacteriocin cluster was identified in all NDM-1-ST773 *P. aeruginosa*.

Conclusions: We report a clonal dissemination of NDM-producing *P. aeruginosa* ST773 to the Netherlands and Spain associated with patients from Ukraine. Our work highlights the importance of genomic surveillance and to understand the dynamics of resistance in multidrug-resistant bacteria after the transfer of patients from conflict zones. International collaboration is crucial to address global antimicrobial resistance.

Introduction

Between 2014 and 2021, Ukraine reported higher rates of antimicrobial resistance in regional and military hospitals compared to other European Union/European Economic Area countries, particularly, concerning gram-negative bacteria [1–3]. Given the ongoing conflict in Ukraine and the anticipated movement of migrants, the European Centre for Disease Prevention and Control issued a guideline in March 2022, recommending the screening for carriage of multidrug-resistant organisms and pre-emptive isolation of patients displaced and injured, transferred from hospitals in Ukraine, or with a history of hospital admission in Ukraine in the last 12 months [4]. Despite these proactive measures, some countries have notified cases of infection/colonization attributed to certain multidrug-resistant clones of *Acinetobacter baumannii, Enterobacterales*, and *Pseudomonas aeruginosa,* which are typically associated with health care settings in Ukraine [5–8].

P. aeruginosa is an opportunistic pathogen that causes severe infections, particularly, in the hospital setting and in immunocompromised

* Corresponding author.
E-mail address: pruizg@salud.madrid.org (P. Ruiz-Garbajosa).
† Marta Hernández-García and Manuel González de Aledo contributed equally to this manuscript.

https://doi.org/10.1016/j.ijregi.2024.100415
Received 15 April 2024; Accepted 27 July 2024

patients. *P. aeruginosa* high-risk clones are disseminated worldwide and often harbor acquired resistance genes that confer them a multidrug or extensively drug-resistant (MDR/XDR) profile, which facilitates their spread in the hospital setting and gives them the opportunity to obtain more resistance determinants from other gram-negative pathogens [9,10]. In addition, *P. aeruginosa* has shown a great ability to integrate other genetic structures such as temperate bacteriophages, named prophages, that can confer the parasitized bacterium or lysogen evolutionary advantages [11].

The Netherlands and Spain were the first countries to report cases of New Delhi metallo-β-lactamase (NDM) 1–producing *P. aeruginosa* isolates belonging to the ST773 clone imported from Ukraine during 2022 after the initiation of the war [6,8]. In this work, we characterized by whole genome sequencing (WGS) a collection of NDM-1-ST773 *P. aeruginosa* isolates recovered in these two countries in 2022, focusing on their genetic relationship, the characterization of mobile genetic elements involved in the dissemination of bla_{NDM}, and the prophage content.

Methods

Bacterial isolates and patient's background

Between March and December 2022, nine *P. aeruginosa* isolates compatible with the production of a metallo-β-lactamase were isolated in clinical or surveillance samples from nine Ukrainian patients transferred to general hospitals in Madrid, Spain (Hospital Universitario 12 de Octubre y Hospital Universitario Ramón y Cajal) and in five provinces at the Netherlands (Overijssel, Utrecht, Gelderland, Noord-Holland, and Limburg) (Table 1). In Spain, phenotypic characterization and WGS was performed at each of the hospitals where the isolates were recovered. The Dutch samples were phenotypically characterized in each of the centers, and then were sent to the National Institute for Public Health and the Environment for WGS. Clinical, epidemiologic, and demographic data were retrospectively reviewed. All sequences were sent to the Hospital Universitario Ramón y Cajal (Madrid, Spain) for the subsequent genomic characterization. The study was approved by the ethical committee (Ref. 104/23).

Phenotypic characterization

In the isolates detected in Spain, antimicrobial susceptibility was determined by broth microdilution using a semiautomated microdilution system (MicroScan, Beckman Coulter Diagnostics, USA) and the SENSITITRE EUMDROXF panel (ThermoFisher, USA). Minimum inhibitory concentrations (MICs) were interpreted using EUCAST-2023 clinical break points (http://www.eucast.org/clinical_breakpoints/). Cefiderocol susceptibility was assessed by gradient strips and disk diffusion (Liofilchem, Roseto degli Abruzzi, Italy). In the isolates collected in the Netherlands, meropenem susceptibility was determined using gradient strips (Liofilchem). Carbapenemase production was confirmed using the KPC/MBL/OXA-48 Confirm Kit (Rosco Diagnostica, Taastrup, Denmark), the immunochromatography test O.K.N.V.I. RESIST 5 (CORIS BioConcept, Gembloux, Belgium), the eazyplex Superbug CRE system (Amplex-Biosystems, Delaware), the NG-Test CARBA 5 (NG-Biotech, France), the Allplex Entero-DR Assay kit (Seegene Inc., Bogotá, Colombia), or the carbapenem inactivation method [12].

WGS and bioinformatic analysis

Short-read sequencing was performed using the Illumina NovaSeq 6000 platform (OGC, Oxford, UK) (Spain) and Illumina NextSeq550 (the Netherlands), with 2- × 150-bp paired-end reads. Nanopore long-read technology was also carried out using a MinION flow cell (R9.4.1) in accordance with SQK-LSK110 sequencing procedures. The Unicycler tool (v0.4.8) was used to obtain the complete hybrid genome assemblies from the combination of short- and long-reads, as previously reported [8]. All consensus assemblies were annotated using RAST Server (v2.0) (https://rast.nmpdr.org/). Assemblies were deposited at DDBJ/ENA/GenBank under the project number PRJNA949836.

Molecular characterization and resistome analysis

Antimicrobial resistance genes were screened using ABRicate (v1.0.1) (ResFinder and CARD databases, threshold, 90% coverage; 98% identity). *In silico* multilocus sequence typing (MLST) assignment was carried out using MLST (v2.16.1) (https://github.com/tseemann/mlst). Variant calling was also performed for the analysis of chromosomal determinants involved in antibiotic resistance, as described previously [13]. Core genome single nucleotide polymorphisms (cgSNPs) maximum likelihood phylogenetic trees were reconstructed and visualized using IQ-TREE (v2.0.7) software and iTOL, respectively. The core genome MLST (cgMLST) of all genomes was also created and validated using the pipeline chewBBACA [14]. In all these analysis, *P. aeruginosa* PAO1 (GenBank accession no. NC_002516.2) was used as the reference genome.

Mobile genetic elements

The complete genomes and the mobile genetic elements implicated in the dissemination of β-lactamase genes were characterized, reconstructed, and visualized using ICEfinder (https://bioinfo-mml.sjtu.edu.cn/ICEfinder/ICEfinder.html), Blast webtool (blast.ncbi.nlm.gov), Kablammo (http://kablammo.wasmuthlab.org), and Proksee (https://proksee.ca/).

Bacteriophages and pyocins

Prophage analysis was performed using the command line software VIBRANT and Blast [15]. Phage taxonomy was stablished by creating a phage proteomic tree using ViPTree version 3.7 with these prophages and phages on the virus-host database (https://www.genome.jp/viptree/) [16]. Phages clustered together were analyzed to be of the same genus using VIRIDIC (https://rhea.icbm.uni-oldenburg.de/viridic/). These results were confirmed by BLAST analysis of the terminase large subunit, whenever this gene was present in the genomes, accepting query cover and identity values above 95% as the same species. Pyocin clusters were classified by BLASTp analysis of the tail fiber proteins against the NCBI database, considering query cover and identity values above 90% as the same pyocin subtype [17].

Prophage and pyocins were annotated by RAST and Pharokka [18]. Unassigned Open Reading Frames (ORFs) were manually annotated by HMMER (http://hmmer.org/) and HHPRED, as previously described [17]. Anti-CRISPR proteins were analyzed by BLASTp against the Anti-CRISPRdb database [19]. Regions encoding prophages and pyocins were visualized using Proksee.

Results

Bacterial isolates and clinical data

Nine unrelated patients of Ukrainian origin (median age, 42 years [range: 23-74 years]; seven of nine male patients) colonized (two of nine) or infected (seven of nine) by NDM-producing *P. aeruginosa* isolates were detected in two Spanish (three patients) and five Dutch (six patients) hospitals between March and December 2022. All patients were transferred or evacuated from Ukraine as a direct consequence of the war. Previous hospital admission in Ukraine in the previous 12 months was documented in at least six patients (five injured soldiers and one older woman undergoing heart surgery). In addition, colonization or infection by other carbapenemase-producing *Enterobacterales* was also detected in seven patients (Table 1).

Table 1
Epidemiological data of Ukrainian patients infected/colonized by NDM-1-ST773 *P. aeruginosa* isolates evacuated to Spain and the Netherlands during 2022. Antimicrobial susceptibility data are also included.

Isolate	Gender	Admission diagnosis	Source of infection (+) NDM-Pa	Month (2022)	Week (2022)	Province (Country)	Remarks	Other microorganisms detected during the admission	Resistance profile[a,b]
Isolate_ESP_1	M	Septic pseudoarthritis in left femur	Abscess (Wound)	March	13	Madrid (Spain)	Previous admission to a Kyiv hospital (left femur septic pseudoarthritis)	OXA-48+NDM-1 *K. pneumoniae*	P/T4, FEP, CZA, C/T, IMI, IMI/REL, MER, MEV, TOB, AMK
Isolate_ESP_2	F	Mediastinitis	Bone sample (surgical site)	May	20	Madrid (Spain)	Refugee with previous heart surgery in November 2021 in Ukraine.	VIM-1 *K. oxytoca, Aspergillus fumigatus*, extended spectrum beta-lactamase-*Escherichia coli* and *Corynebacterium* sp.	P/T4, FEP, CZA, C/T, IMI, IMI/REL, MER, MEV, TOB, AMK
Isolate_ESP_3	M	Surgical infection in the right jaw	Abscess (Wound)	June	26	Madrid (Spain)	Ukrainian soldier with shotgun in the jaw (previous admissions to military hospitals in Ukraine, in Dnipro and Vynnitsya)	OXA-48+NDM-1 *K. pneumoniae,* OXA-48 *K. pneumoniae*	P/T4, FEP, CZA, C/T, IMI, IMI/REL, MER, MEV, TOB, AMK
Isolate_NLD_1	M	Unknown	Tissue	July	28	Overijssel (The Netherlands)	Ukrainian person	Not recovered	MER
Isolate_NLD_2	F	SSTI	Wound	August	31	Utrecht (The Netherlands)	Ukrainian person	NDM-1 *K. pneumoniae*, OXA-23-*Acinetobacter baumannii*, OXA-66-*A. baumannii*	MER
Isolate_NLD_3	M	SSTI	Wound	August	33	Overijssel (The Netherlands)	Ukrainian soldier	OXA-72-*A. baumannii*, NDM-1 *K. pneumoniae*, OXA-48 *K. pneumoniae*	MER
Isolate_NLD_4	M	Carrier screening	Rectal swab	August	34	Gelderland (The Netherlands)	Ukrainian soldier with shot wound direct transfer from military hospital in Poland	Not recovered	MER
Isolate_NLD_5	M	SSTI	Tissue biopsy	September	39	Noord-Holland (The Netherlands)	Soldier with trauma from Ukraine	NDM-1-*Proteus stuartii*	MER
Isolate_NLD_6	M	Carrier screening	Rectal swab	December	51	Limburg (The Netherlands)	Ukrainian person	NDM-5-*E. coli*, KPC-3-*E. coli*, KPC-2 *K. pneumoniae*, NDM-1 *K. pneumoniae*, OXA-48 *K. pneumoniae*	MER

AMK, amikacin; CZA, ceftazidime-avibactam; C/T, ceftolozane-tazobactam; F, female; FEP, cefepime; IMI, imipenem; IMI/REL, imipenem-relebactam; M, male; MER, meropenem; MEV, meropenem-vaborbactam; P/T4, piperacillin-tazobactam; SSTI, skin and soft tissue infection; TOB, tobramycin.

[a] Antimicrobials for which NDM-1-S773-*P. aeruginosa* isolates showed resistant minimum inhibitory concentration values (according to EUCAST).

[b] In isolates recovered in The Netherlands, only meropenem susceptibility was reported.

All NDM-producing *P. aeruginosa* isolates recovered in Spain were resistant to all tested antimicrobials, except for colistin (MIC ≤2 mg/L), aztreonam (MIC: 8-12 mg/L), and cefiderocol (MIC range 0.75-2 mg/L; disk diffusion method: 20-23 mm).

Resistance gene content and mutational resistome

Screening for antibiotic resistance genes revealed that all isolates carried an identical content of resistance genes affecting different antimicrobial groups: aminoglycosides [*aac(3), aadA11, aph(3')-IIb, rmtB4*], β-lactams (bla_{NDM-1}, $bla_{OXA-395}$, bla_{PDC-16}), chloramphenicol (*catB7*), fosfomycin (*fosA*), sulphonamides (two copies of *sul1*), and tetracyclines (*tetG*). One antiseptic-resistant gene (*qacE*) and one gene affecting the quaternary ammonium compound efflux SMR transporter (*qnrVC1*) were also found in all strains. One Dutch isolate (Isolate_NLD_2) carried two copies of the bla_{NDM-1} gene (Table 2).

The variant calling analysis of chromosomal genes also showed an identical mutational resistome, except for four genes, in which exclusive mutations were found (Table S1). These genes were involved in the transcriptional activation of *P. aeruginosa* virulence genes (*lasR*), the regulation of MexXY (*mexY*) and MexAB-OprM (*nalC*) effux pumps, and the lipid A modification (*pagL*). T543A-*mexY* (eight of nine) and G71E-*nalC* (eight of nine) mutations were encountered in several of the strains (Table S1).

Molecular typing and mobile genetic elements

All NDM-producing *P. aeruginosa* isolates belonged to the same clone (ST773) and shared a high percentage of coverage (98-99%) and identity (99.96-100%). All ST773 *P. aeruginosa* isolates carried a chromosomally encoded bla_{NDM-1} gene along with a bleomycin resistance gene between two IS*91* (IS*91*-bla_{NDM-1}-*bleMBL*-IS*91*), contained on an identical ~117 Kb integrative conjugative element (ICE) flanked by 23-pb *attL* and *attR* sequences (gtctcgtttcccgctccaaacat) (Figure S1, Table 2). The Dutch isolate (Isolate_NLD_2) that carried two copies of the bla_{NDM-1} gene (IS*91*-*bleMBL*-bla_{NDM-1}-*bleMBL*-bla_{NDM-1}-IS*91*) had a larger ICE (120.224 bp) that was located inverted in the chromosome but with identical *attR* and *attL* regions (Figure S2). *xerD* and *parA* genes, involved in the mobilization and integration of pathogenicity genomic islands structures in *P. aeruginosa*, were identified flanking all bla_{NDM-1}-ICEs. Other common regions involved in mobilization and maintenance of the pathogenicity genomic islands such as the *pil operon* were also found. In all isolates, the bla_{NDM-1}-ICE contained five additional resistance genes affecting other antimicrobial groups: sulfonamides (*sul1*), aminoglycosides (*acc*[3] and *rmtB4*), chloramphenicol (*floR*), and tetracyclines [*tet*(G)] (Figure S1).

Plasmid reconstruction showed that two Spanish (ESP_1 and ESP_2, each from one center) and one Dutch (NDL_3) NDM-1-ST773 *P. aeruginosa* isolates contained a closely related plasmid (~47-51

Table 2
Results of the genomic characterization of all NDM-1–producing *P. aeruginosa* isolates recovered from Ukrainian patients in Spain and the Netherlands during 2022.

Isolate	ST	Cluster[a]	Chromosome[b] (pb)	*bla*NDM-1-ICE size(pb)	Plasmid[c] (pb)	Antibiotic-resistant genes content	Accession number
Isolate_ESP_1	773	I	6,852,907	116,999	pH12O (46,720)	*aac(3), aadA11, aph(3′)-IIb, bla_{NDM-1}, $bla_{OXA-395}$, bla_{PDC-16}, catB7, fosA, qacE, qnrVC1, rmtB4, sul1, sul1, tet(G)*	CP142443[b], CP142444[c]
Isolate_ESP_2	773	I	6,922,344	116,997	pB81 (51,081)	*aac(3), aadA11, aph(3′)-IIb, bla_{NDM-1}, $bla_{OXA-395}$, bla_{PDC-16}, catB7, fosA, qacE, qnrVC1, rmtB4, sul1, sul1, tet(G)*	CP142449[b], CP142450[c]
Isolate_ESP_3	773	II	6,850,251	116,998	-	*aac(3), aadA11, aph(3′)-IIb, bla_{NDM-1}, $bla_{OXA-395}$, bla_{PDC-16}, catB7, fosA, qacE, qnrVC1, rmtB4, sul1, sul1, tet(G)*	CP142448[b]
Isolate_NLD_1	773	II	6,836,351	116,995	-	*aac(3), aadA11, aph(3′)-IIb, bla_{NDM-1}, $bla_{OXA-395}$, bla_{PDC-16}, catB7, fosA, qacE, qnrVC1, rmtB4, sul1, sul1, tet(G)*	JBAWKG000000000[b]
Isolate_NLD_2	773	I	6,862,835	120,224[d]	-	*aac(3), aadA11, aph(3′)-IIb, bla_{NDM-1}, bla_{NDM-1}, $bla_{OXA-395}$, bla_{PDC-16}, catB7, fosA, qacE, qnrVC1, rmtB4, sul1, sul1, tet(G)*	JBAWKH000000000[b]
Isolate_NLD_3	773	I	6,921,153	116,989	pS75 (50,326)	*aac(3), aadA11, aph(3′)-IIb, bla_{NDM-1}, $bla_{OXA-395}$, bla_{PDC-16}, catB7, fosA, qacE, qnrVC1, rmtB4, sul1, sul1, tet(G)*	JBAWKF000000000[b]
Isolate_NLD_4	773	II	6,908,226	116,997	-	*aac(3), aadA11, aph(3′)-IIb, bla_{NDM-1}, $bla_{OXA-395}$, bla_{PDC-16}, catB7, fosA, qacE, qnrVC1, rmtB4, sul1, sul1, tet(G)*	CP142447[b]
Isolate_NLD_5	773	I	6,911,612	116,993	-	*aac(3), aadA11, aph(3′)-IIb, bla_{NDM-1}, $bla_{OXA-395}$, bla_{PDC-16}, catB7, fosA, qacE, qnrVC1, rmtB4, sul1, sul1, tet(G)*	CP142446[b]
Isolate_NLD_6	773	I	6,853,133	116,997	-	*aac(3), aadA11, aph(3′)-IIb, bla_{NDM-1}, $bla_{OXA-395}$, bla_{PDC-16}, catB7, fosA, qacE, qnrVC1, rmtB4, sul1, sul1, tet(G)*	CP142445[b]

[a] Clusters detected with the cgMLST and cgSNPs analysis using *P. aeruginosa* PAO1 (NC_002516.2) as reference genome.
[b] Accession number of chromosomes of NDM-1–producing *P. aeruginosa* isolates.
[c] Accession number of plasmids detected in NDM-1–producing *P. aeruginosa* isolates.
[d] Two copies of bla_{NDM-1} in the ICE, that is flanked by attL and attR (gtctcgtttcccgctccaaacat) but inverted in the chromosome with respect to the other isolates.

Kb) without any resistance genes. Genes encoding membrane proteins belonged to the secretion system type IV transport proteins (VirB1, VirB4, VirB6, VirB8, VirB9, VirB10, VirB11, and VirD4) were detected, along with genes encoding an RNA metabolism protein (retron-type RNA-directed DNA polymerase) and proteins involved in regulation and cell signaling (HigA toxin and HigB antitoxin) (Table 2, Figure S3).

cgMLST and cgSNP analysis

A cgMLST phylogenetic tree of the Spanish and Dutch isolates in context of ten related ST773-*P. aeruginosa* isolates downloaded from Pathogenwatch (https://pathogen.watch) was constructed. Of a total of 5,694 loci searched, 5,250 loci were present in the genome of all isolates. This analysis showed that NDM-1-ST773-*P. aeruginosa* from patients of Ukrainian origin were grouped in the same cluster and more distant from the strains collected in other countries and in other years. Overall, NDM-1-ST773-*P. aeruginosa* strains diverged in distance from 4 to 17 loci and from 4 to 96 loci from strains collected in other geographical regions (Figure 1). Using *P. aeruginosa* PAO1 as reference genome, the core genome of all NDM-1-ST773 *P. aeruginosa* ranged between 5.882.658 and 5.887.317 bp, with an evolutionary distance of 54.168-54.576 SNPs (9.2-9.3 SNPs/Mb). The maximum likelihood phylogenetic tree based on the cgSNP analysis of all genomes gave highly similar results that the neighbor Joining tree from the cgMLST schema (Figure 2). Both methods clustered all Ukrainian ST773 *P. aeruginosa* strains in two clusters: cluster I, including two Spanish isolates (ESP_1 and ESP_2), and four Dutch strains (NLD_2, NLD_3, NLD_5, and NLD_6), all of them from different centers and recovered between March and December, and cluster II, formed by one Spanish (ESP_3) and two Dutch isolates (NLD_1 and NLD_4), also from different centers and from different months (June, July, and August, respectively) (Figures 1 and 2).

Prophages and pyocins analysis

A total of 11 different prophages were identified in all *P. aeruginosa* strains, and 10 of them were present in more than one strain simultaneously. A phage tail-like bacteriocin (PTLB) cluster was also identified in all isolates, at first misidentified as a prophage (Figure 3, Table S2). The prophage and PTLB cluster characteristics are summarized in Table 3.

The PTLB cluster presented a conserved structure: a PrtN/PrtR activator/repressor tandem, a zinc finger transcription factor, a phage antitermination Q-like protein, an R5-type (Rigid, with a structure similar to a Myovirus tail) pyocin, a lytic cassette, and an F-type (Flexible, analog to a Siphovirus tail) pyocin (Figure S4).

Prophage length ranged from 10.5 Kb (vB_Pae_U10) to 57.8 Kb (vB_Pae_U7), with a GC content ranging from 58.9 % (vB_Pae_U7) to 64.4 % (vB_Pae_U4). The number of ORF was also very variable, with 13 ORF the shortest (vB_Pae_U10) and 103 the longest (vB_Pae_U7). The ORF function of each prophage genome is summarized in Figure S5. A considerable number of ORF remained with an unknown function after annotation, ranging from 38.5% of hypothetical proteins (vB_Pae_U10) to 84.8% (vB_Pae_U6). The PTLB cluster had 21.1% of hypothetical proteins. Prophage vB_Pae_U4 was also found to code for an anti-CRISPR (Clustered Regularly Interspaced Short Palindromic Repeats) proteins with homology with AcrIF3 (score $8.85 \times 10\text{-}10^4$).

Regarding insertion sites, the PTLB cluster was localized within the tryptophan operon, between the anthranilate synthase components I (*trpE*) and II (*trpG*). Half of the prophages (6/12) were inserted next to transfer RNA coding genes. Prophages vB_Pae_U2, vB_Pae_U4 (in strain ESP_2) and vB_Pae_U10 were inserted inside other genes, truncating them and possibly resulting in impaired gene expression. Prophage vB_Pae_U2 was inserted inside the *lapE* gene in all strains, which codes for an outer membrane pore forming protein as a component of the type I secretion system. In ESP_2, prophage vB_Pae_U4 was inserted inside a class III aminotransferase gene and inside an ABC-type bacteriocin/lantibiotic exporter. This strain was found to have three copies

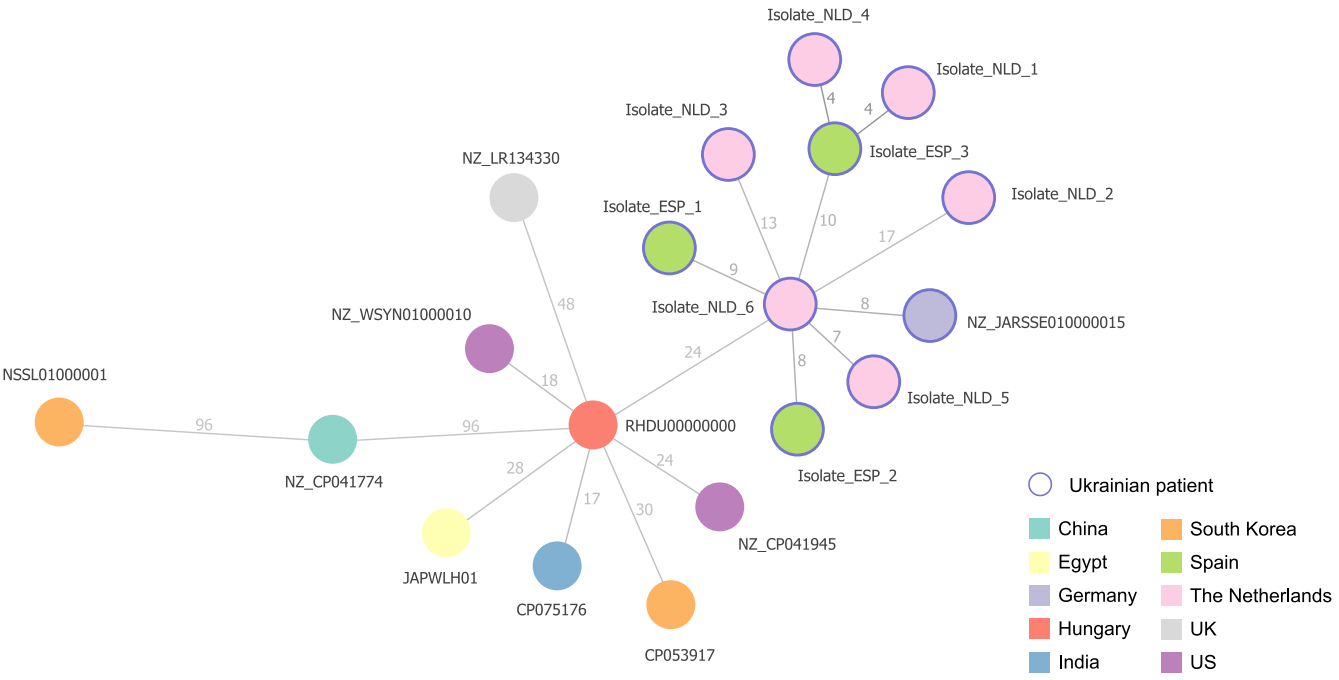

Figure 1. cgMLST based phylogenetic tree constructed with all NDM-1-ST773-*P. aeruginosa* isolates recovered in this study (purple surrounding circle; ESP: Spain; NLD: the Netherlands) and ten closely related ST773-*P. aeruginosa* isolates from other locations. *P. aeruginosa* PAO1 was used as reference genome (NC_002516.2). cgMLST is a minimum spanning tree based on the cgMLST allelic profile of *P. aeruginosa* PAO1, determined by the pipeline chewBACCA and visualized using Phyloviz Online tool.

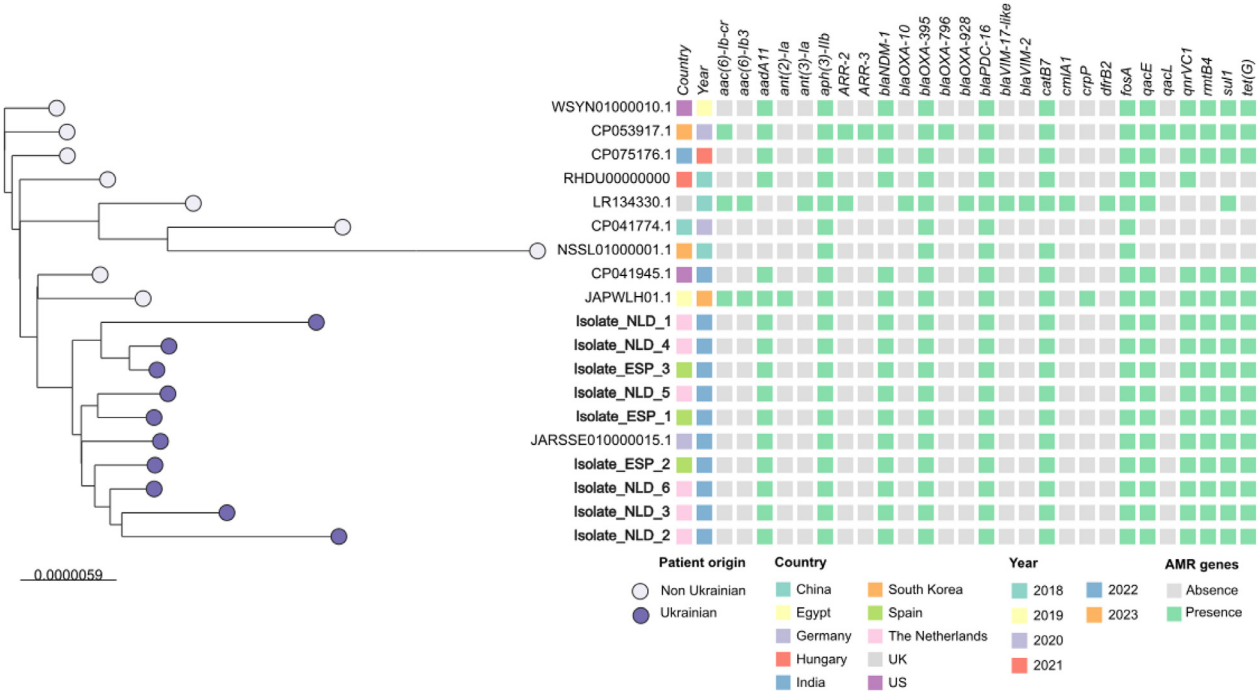

Figure 2. cgSNP based phylogenetic tree constructed with all NDM-1-ST773 *P. aeruginosa* isolates (bold letters) recovered in this study and 10 closely related ST773 *P. aeruginosa* isolates from other locations. Patient origin (Ukrainian, purple; non-Ukrainian, grey), country, year of collection, and presence (green) or absence (grey) of antimicrobial resistance genes detected using Resfinder database are indicated. cgSNP is a maximum likelihood tree based on core genome SNP analysis, reconstructed and visualized using IQ-TREE (v2.0.7) and iTOL, respectively.
AMR, antimicrobial resistance.

Table 3
Characteristics of the eleven prophages and the phage tail-like bacteriocin cluster (pyocin cluster) identified in the NDM-1-ST773 *P. aeruginosa* strains from Ukrainian patients.

Prophage /phage tail-like bacteriocin cluster name	Family /Pyocin subtype	Length (Kb)	GC content (%)	ORF (n[a])	Gene density (gene/Kb)	Host strains	Hypothetical proteins (%)	Upstream gene	Downstream gene	Accession number
vB_Pae_U1	Unclassified *Caudoviricetes*	16.2	59.3	26	1.60	9/9	65.4	Quinolinatephosphoribosyltransferase (EC 2.4.2.19)	tRNA-Thr-CGT	PP003913
vB_Pae_U2	Unclassified *Caudoviricetes* (Siphovirus tail morphology group)	45.1	61.3	67	1.49	9/9	58.8	tRNA-Pseudo-GAG	Antitoxin HigA	PP003914
vB_Pae_U3	Unclassified *Caudoviricetes* (Siphovirus tail morphology group)	38.6	62.1	53	1.37	9/9	50.9	Type I secretion system, outer membrane component LapE[b]		PP003915
vB_Pae_U4a	*Casadabanvirus*	36.4	64.4	53	1.46	3/9	39.6	FAD-dependent monooxygenase PhzS Aminotransferase, class III[b] Bacteriocin/lantibiotic efflux ABC transporter, permease/ATP-binding protein[b]	Pyridoxamine 5′-phosphate oxidase PhzG (EC 1.4.3.5)	PP003916
vB_Pae_U5	Unclassified *Caudoviricetes*	40.4	63.3	52	1.29	8/9	60.4	hypothetical protein	tRNA-Leu-CAA tRNA-Gly-CCC	PP003917
vB_Pae_U6	Unclassified *Caudoviricetes*	43.6	62.2	66	1.51	2/9	84.8	Rossmann fold nucleotide-binding protein Smf possibly involved in DNA uptake	tRNA-Gly-CCC	PP003918
vB_Pae_U7a	*Detrevirus*	57.8	58.9	103	1.78	6/9	64.1	Bis-ABC ATPase YbiT	Probable 5-carboxymethyl-2-hydroxymuconate delta isomerase	PP003919
vB_Pae_U8	Unclassified *Caudoviricetes*	41.1	62.6	60	1.46	4/9	61.7	Rossmann fold nucleotide-binding protein Smf possibly involved in DNA uptake	tRNA-Leu-CAA	PP003920
vB_Pae_U9	Unclassified *Caudoviricetes*	49.7	59.4	85	1.71	4/9	72.1	Probable 5-carboxymethyl-2-hydroxymuconate delta isomerase	Bis-ABC ATPaseYbiT	PP003921
vB_Pae_U10	Unclassified *Caudoviricetes*	10.5	60.8	13	1.24	2/9	38.5	Glycosyltransferase[b]		PP003922
vB_Pae_U11	*Beetrevirus*	39.0	63.1	56	1.44	1/9	51.8	tRNA-dihydrouridine(20/20a) synthase (EC 1.3.1.91)	hypotheticalprotein	PP003923
Pyocin_U1	R5-F cluster	28.8	64.5	38	1.32	9/9	21.1	Anthranilate synthase, amidotransferase component (EC 4.1.3.27)	Anthranilate synthase, aminase component (EC 4.1.3.27)	PP003924

[a]Three copies of vB_Pae_U4 and two copies of vB_Pae_U7 were detected in isolates ESP_2 and NLD_4, respectively.
[b] ORF truncated by the insertion of the prophage.

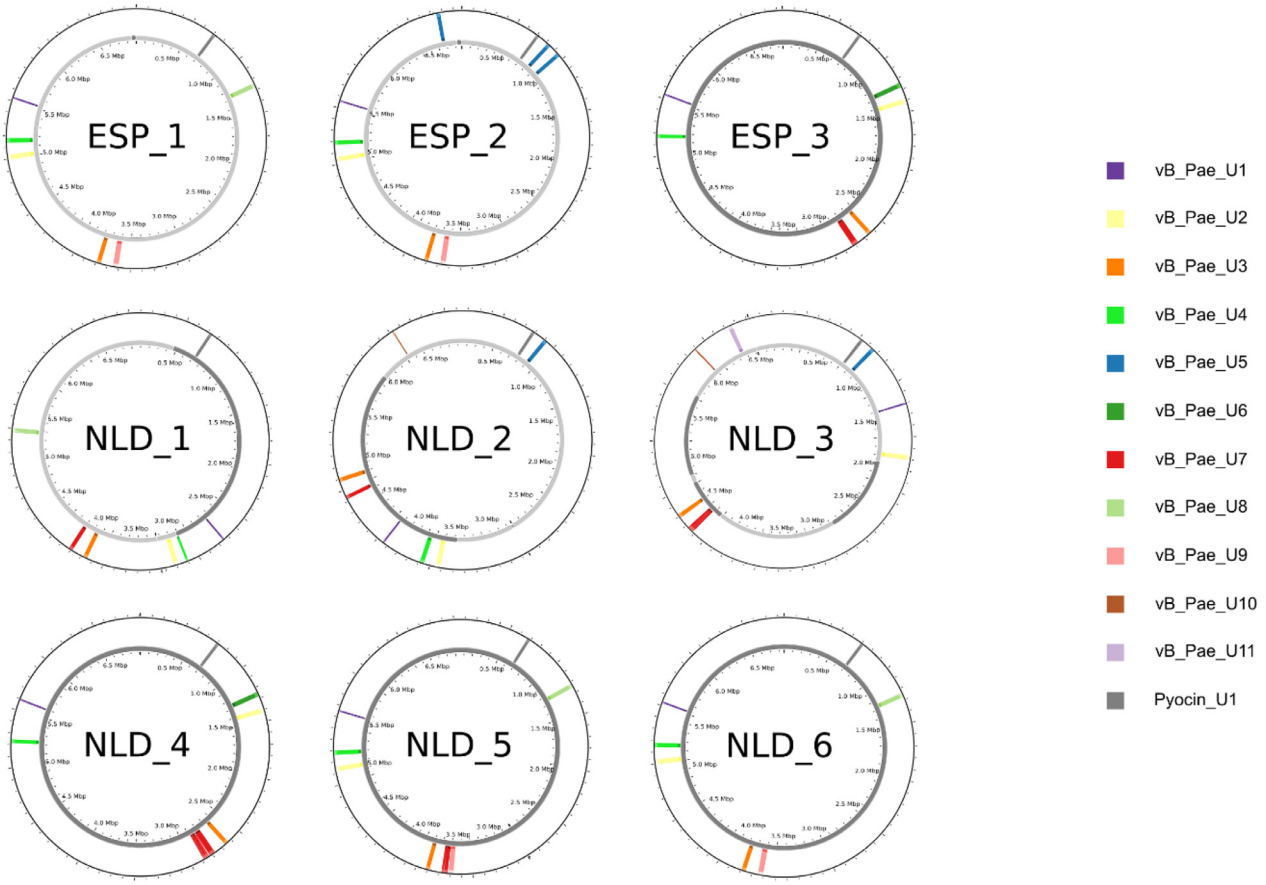

Figure 3. Map of all NDM-1-ST773 *P. aeruginosa* strains and the relative position of prophages and phage tail-like bacteriocin clusters detected within them. ESP, Spain; NLD, the Netherlands.

of the same phage, the third one being between an flavin adenine dinucleotide–dependent mooxygenase (*phzS*) and a pyridoxamine 5'-phosphate oxidase (*phzG*), as in two Dutch strains (NLD_2 and NLD_3). Finally, prophage vB_Pae_U10 was found integrated into the glycosyltransferase gene (Table 3).

Discussion

In this work, we report the clonal spread in 2022 of NDM-1 *P. aeruginosa* isolates belonging to clone ST773 in two European countries (Spain and the Netherlands) due to the transfer of Ukrainian patients because of the war.

In *P. aeruginosa*, resistance to carbapenems is usually due to mutations in chromosomal genes and, to a lesser extent, to horizontal acquisition of carbapenemase-encoding genes [9,10,20]. In Europe, *P. aeruginosa* is usually associated with the production of Verona integron-encoded MBL enzymes, and the report of NDM carbapenemases is limited to nosocomial outbreaks or imported cases from endemic areas [13,21–23]. NDM enzymes can hydrolyze all β-lactams, except for monobactams, conferring an almost pan-β-lactam-resistant phenotype that usually leaves few treatment options [24]. In our collection, all NDM-1-ST773 *P. aeruginosa* isolates were resistant to all tested antimicrobials, except for colistin, aztreonam, and cefiderocol. This high-level of resistance coincides with the alarming rates previously reported in Ukrainian health care settings [2,3].

The ST773 *P. aeruginosa* clone has been previously described associated with the production of NDM-1 in some countries such as the United States, Nepal, and South Korea [23,25,26]. However, the NDM-1-ST773 *P. aeruginosa* clone had not been described in Europe before until the arrival of Ukrainian patients [6–8]. Our analysis showed that isolates of Ukrainian origin were more genetically related to each other than to other NDM-1-ST773 *P. aeruginosa* strains recovered from other locations. Note that one NDM-1-ST773 *P. aeruginosa* recovered from a Ukrainian soldier admitted to a US military hospital in Germany in 2022 was found to be part of the same cluster as the Spanish and Dutch strains, suggesting clonal spread to Germany [7]. The cgMLST and cgSNP analysis also revealed the clustering of our strains into distinct but close subgroups, spanning the Spanish and Dutch isolates, indicating that the strains were closely related despite belonging to patients who had been transferred to different countries. The introduction of these isolates in European countries poses a risk of potential local transmission events within and between health care facilities in the country of detection.

In addition, the *bla*NDM-1 genetic environment in our isolates ($bla_{\text{NDM-1}}$-ICE) was closely related to that found in other ST773 *P. aeruginosa* isolates [23,25,26]. The identical resistome and shared genetic elements also suggest a clonal expansion of the NDM-1-ST773 *P. aeruginosa* clone. The presence of additional resistance genes within the ICE underscores the potential for further acquisition of resistance determinants, posing a continual threat to antimicrobial efficacy. Furthermore, the closely related plasmid identified in Spanish and Dutch isolates, devoid of resistance genes, suggests that plasmids could also be a potential vehicle for gene exchange in *P. aeruginosa*. Understanding the genetic platforms that facilitates the spread of virulence and resistance genes is crucial for developing targeted intervention strategies.

Recent articles have shown that lysogeny is a common trait among *P. aeruginosa* clinical isolates and that prophage role and characteristics remain understudied when compared to lytic phages [27]. In our NDM-1-ST773 *P. aeruginosa* strains, we found a high content of prophages than in other studies [27]. Most of them were found in more than one strain simultaneously, irrespective of the origin country. Moreover, an

identical pyocin (PTLB) cluster was also found in all strains, again showing a high genetic relatedness among the isolates. The pyocin cluster showed a similar pattern as R-F-type bacteriocins previously described in *P. aeruginosa* [28]. In our isolates, differences were only found in those regions of the ST773 genome where prophages were inserted, suggesting a dynamic interaction between the bacteriophage and the host bacterium. Consistent with other studies, up to three of these prophages were located truncating other genes and presumably resulting in non-functional proteins [29,30]. Prophages inserted within essential genes further emphasize their potential impact on bacterial physiology, most likely influencing virulence and antibiotic resistance.

On the other hand, it should be noted that in at least seven of these patients other MDR bacteria were isolated in addition to the NDM-1-ST773 *P. aeruginosa*. Among others, NDM-producing Enterobacterales isolates were detected, including ST147 *K. pneumoniae* producing OXA-48 or co-producing OXA-48+NDM-1 [8]. The ST147 K. *pneumoniae* clone has already been linked to the movement of Ukrainian patients to other central European countries in 2022 [5]. Co-colonization or co-infection with other MDR also carrying carbapenemases and/or extended-spectrum β-lactamases genes, such as ST78-OXA-23 *Acinetobacter baumannii,* ST395-OXA-48+NDM-1 *K. pneumoniae*, ST1047-IMP-1 *P. aeruginosa,* and ST357-VEB-9 *P. aeruginosa,* has also been reported in Ukrainian patients in Germany [7].

The timeline of cases after the conflict and the association with patients who had previous hospitalization in Ukraine suggests a direct link to the conflict-driven migration. This underlines the importance of collaborative efforts in surveillance, early detection, and the establishment of protocols for managing patients with a history of health care exposure in conflict zones. The combination of WGS and epidemiologic data allows a better understanding of the evolution of resistance mechanisms and the transmission dynamics, which helps to apply adapted infection control measures.

In conclusion, our study provides a comprehensive genomic perspective on the emergence and dissemination of NDM-1–producing *P. aeruginosa* ST773 clone in Europe after the conflict in Ukraine. The interconnectedness of health care systems and the adaptability of these strains underscore the need for international collaboration in combating the global challenge of antimicrobial resistance. Continued genomic surveillance, along with the reinforcement of infection control measures, is imperative to mitigate the impact of these highly resistant clones on public health.

Declarations of competing interest

The authors have no competing interests to declare.

Funding

This study was supported by Plan Nacional de I + D + i 2013–2016 and Instituto de Salud Carlos III, Subdirección General de Redes y Centros de Investigación Cooperativa, Ministerio de Economía, Industria y Competitividad, Spanish Network for Research in Infectious Diseases (REIPI RD16/0016/0011), co-financed by the European Development Regional Fund 'A way to achieve Europe' (ERDF), Operative program Intelligent Growth 2014–2020, research grant (PI22/01283), (PI19/00571) and CIBER de Enfermedades Infecciosas (CIBERINFEC) (CB21/13/00084), Instituto de Salud Carlos III, Madrid, Spain. MH-G is supported by a postdoctoral contract by CIBERINFEC (CB21/13/00084). MGA is supported by the Río Hortega program (CM22/00159, ISCIII).

Ethical approval

This study was approved by the Ramón y Cajal University Hospital Ethics Committee (Reference 104/23).

Author contributions

All authors have made substantial contributions to this work. MHG and MGA were involved in the design of the study, acquisition, analysis and interpretation of data, as well as in the drafting and revising the manuscript. MPC, BGB, EV, JV, MT, APAH have contributed to the acquisition/ data analysis and revising the manuscript. PRG and RC are responsible for the conception, design and supervision of the study, as well as drafting and revising the article critically for important intellectual content. All authors have reviewed and given their approval for the publication of the final manuscript.

Supplementary materials

Supplementary material associated with this article can be found, in the online version, at doi:10.1016/j.ijregi.2024.100415.

References

[1] European Centre for Disease Prevention and Control *Antimicrobial resistance surveillance in Europe, 2022–2020 data*. Boulevard: European Centre for Disease Prevention and Control; 2022.
[2] Kondratiuk V, Jones BT, Kovalchuk V, Kovalenko I, Ganiuk V, Kondratiuk O, et al. Phenotypic and genotypic characterization of antibiotic resistance in military hospital-associated bacteria from war injuries in the Eastern Ukraine conflict between 2014 and 2020. *J Hosp Infect* 2021;**112**:69–76. doi:10.1016/j.jhin.2021.03.020.
[3] Salmanov A, Shchehlov D, Svyrydiuk O, Bortnik I, Mamonova M, Korniyenko S, et al. Epidemiology of healthcare-associated infections and mechanisms of antimicrobial resistance of responsible pathogens in Ukraine: a multicentre study. *J Hosp Infect* 2023;**131**:129–38. doi:10.1016/j.jhin.2022.10.007.
[4] European Centre for Disease Prevention and Control *Operational considerations for the prevention and control of infectious diseases - Russia's aggression towards Ukraine*. Boulevard: European Centre for Disease Prevention and Control; 2022.
[5] Sandfort M, Hans JB, Fischer MA, Reichert F, Cremanns M, Eisfeld J, et al. Increase in NDM-1 and NDM-1/OXA-48-producing *Klebsiella pneumoniae* in Germany associated with the war in Ukraine, 2022. *Euro Surveill* 2022;**27**:2200926. doi:10.2807/1560-7917.ES.2022.27.50.2200926.
[6] Zwittink RD, Wielders CCH, Notermans DW, Verkaik NJ, Schoffelen AF, Witteveen S, et al. Multidrug-resistant organisms in patients from Ukraine in the Netherlands, March to August 2022. *Euro Surveill* 2022;**27**:2200896. doi:10.2807/1560-7917.ES.2022.27.50.2200896.
[7] Mc Gann PT, Lebreton F, Jones BT, Dao HD, Nelson MJ, Luo T, Wyatt AC, et al. Six extensively drug- resistant bacteria in an injured soldier, Ukraine. *Emerginf Infect Dis* 2013;**8**:1692–5. doi:10.1007/s00268.
[8] Hernández-García M, Cabello M, Ponce-Alonso M, Herrador-Gómez PM, Gioia F, Cobo J, et al. First detection in Spain of NDM-1-producing *Pseudomonas aeruginosa* in two patients transferred from Ukraine to a university hospital. *J Glob Antimicrob Resist* 2024;**36**:105–11. doi:10.1016/j.jgar.2023.12.022.
[9] Del Barrio-Tofiño E, López-Causapé C, Oliver A. *Pseudomonas aeruginosa* epidemic high-risk clones and their association with horizontally-acquired β-lactamases: 2020 update. *Int J Antimicrob Agents* 2020;**56**:106196. doi:10.1016/j.ijantimicag.2020.106196.
[10] Horcajada JP, Montero M, Oliver A, Sorlí L, Luque S, Gómez-Zorrilla S, et al. Epidemiology and treatment of multidrug-resistant and extensively drug-resistant *Pseudomonas aeruginosa* infections. *Clin Microbiol Rev* 2019;**32**:1–52. doi:10.1128/CMR.00031-19.
[11] Johnson G, Banerjee S, Putonti C. Diversity of *Pseudomonas aeruginosa* temperate phages. *mSphere* 2022;**1**:e0101521. doi:10.5281/msphere.5072377.
[12] Van Der Zwaluw K, De Haan A, Pluister GN, Bootsma HJ, De Neeling AJ, Schouls LM. The Carbapenem Inactivation Method (CIM), a simple and low-cost alternative for the carba NP test to assess phenotypic carbapenemase activity in Gram-negative rods. *PLoS One* 2015;**10**:e0123690. doi:10.1371/journal.pone.0123690.
[13] Hernández-García M, García-Castillo M, García-Fernández S, Melo-Cristino J, Pinto MF, Goncalves E, et al. Distinct epidemiology and resistance mechanisms affecting ceftolozane /tazobactam in *Pseudomonas aeruginosa* isolates recovered from ICU patients in Spain and Portugal depicted by WGS. *J Antimicrob Chemother* 2021;**76**:370–9. doi:10.1093/jac/dkaa430.
[14] Silva M, Machado MP, Silva DN, Rossi M, Moran-Gilad J, Santos S, et al. chewBBACA: a complete suite for gene-by-gene schema creation and strain identification. *Microb Genom* 2018;**4**. doi:10.1099/mgen.0.000166.
[15] Kieft K, Zhou Z, Anantharaman K. VIBRANT: automated recovery, annotation and curation of microbial viruses, and evaluation of viral community function from genomic sequences. *Microbiome* 2020;**8**:90. doi:10.1186/s40168-020-00867-0.
[16] Mihara T, Nishimura Y, Shimizu Y, Nishiyama H, Yoshikawa G, Uehara H, et al. Linking virus genomes with host taxonomy. *Viruses* 2016;**8**:66. doi:10.3390/v8030066.
[17] Blasco L, de Aledo MG, Ortiz-Cartagena C, Blériot I, Pacios O, López M, et al. Study of 32 new phage tail-like bacteriocins (pyocins) from a clinical collection of *Pseudomonas aeruginosa* and of their potential use as typing markers and antimicrobial agents. *Sci Rep* 2023;**13**:117. doi:10.1038/s41598-022-27341-1.

[18] Bouras G, Nepal R, Houtak G, Psaltis AJ, Wormald PJ, Vreugde S. Pharokka: a fast scalable bacteriophage annotation tool. *Bioinformatics* 2023;**39**:btac776. doi:10.1093/bioinformatics/btac776.

[19] Dong C, Hao GF, Hua HL, Liu S, Labena AA, Chai G, et al. Anti-CRISPRdb: a comprehensive online resource for anti-CRISPR proteins. *Nucleic Acids Res* 2018;**46**:D393–8. doi:10.1093/nar/gkx835.

[20] Tenover FC, Nicolau DP, Gill CM. Carbapenemase-producing *Pseudomonas aeruginosa* –an emerging challenge. *Emerg Microbes Infect* 2022;**11**:811–14. doi:10.1080/22221751.2022.2048972.

[21] Wendel AF, Malecki M, Mattner F, Xanthopoulou K, Wille J, Seifert H, et al. Genomic-based transmission analysis of carbapenem-resistant *Pseudomonas aeruginosa* at a tertiary care centre in Cologne (Germany) from 2015 to 2020. *JAC Antimicrob Resist* 2022;**4**:dlac057. doi:10.1093/jacamr/dlac057.

[22] Hammoudi Halat D, Ayoub Moubareck C. The intriguing carbapenemases of *Pseudomonas aeruginosa*: current status, genetic profile, and global epidemiology. *Yale J Biol Med* 2022;**95**:507–15.

[23] Khan A, Shropshire WC, Hanson B, Dinh AQ, Wanger A, Ostrosky-Zeichner L, et al. Simultaneous infection with Enterobacteriaceae and *Pseudomonas aeruginosa* harboring multiple carbapenemases in a returning traveler colonized with *Candida auris*. *Antimicrob Agents Chemother* 2020;**64**. doi:10.1128/AAC.01466-19.

[24] Kumarasamy KK, Toleman MA, Walsh TR, Bagaria J, Butt F, Balakrishnan R, et al. Emergence of a new antibiotic resistance mechanism in India, Pakistan, and the UK: a molecular, biological, and epidemiological study. *Lancet Infect Dis* 2010;**10**:597–602. doi:10.1016/S1473-3099(10)70143-2.

[25] Choi YJ, Kim YA, Junglim K, Jeong SH, Shin JH, Shin KS, et al. Emergence of NDM-1-producing *Pseudomonas aeruginosa* sequence Type 773 clone: shift of carbapenemase molecular epidemiology and spread of 16S rRNA methylase genes in Korea. *Ann Lab Med* 2023;**43**:196–9. doi:10.3343/alm.2023.43.2.196.

[26] Takahashi T, Tada T, Shrestha S, Hishinuma T, Sherchan JB, Tohya M, et al. Molecular characterisation of carbapenem-resistant *Pseudomonas aeruginosa* clinical isolates in Nepal. *J Glob Antimicrob Resist* 2021;**26**:279–84. doi:10.1016/j.jgar.2021.07.003.

[27] González de Aledo M, Blasco L, Lopez M, Ortiz-Cartagena C, Bleriot I, Pacios O, et al. Prophage identification and molecular analysis in the genomes of *Pseudomonas aeruginosa* strains isolated from critical care patients. *mSphere* 2023;**8**:e0012823. doi:10.1128/msphere.00128-23.

[28] Saha S, Ojobor CD, Li ASC, Mackinnon E, North OI, Bondy-Denomy J, et al. F-type pyocins are diverse noncontractile phage tail-like weapons for killing *Pseudomonas aeruginosa*. *J Bacteriol* 2023;**205**:e0002923. doi:10.1128/jb.00029-23.

[29] Smith TJ, Sondermann H, O'Toole GA. Type 1 does the two-step: Type 1 secretion substrates with a functional periplasmic intermediate. *J Bacteriol* 2018;**200**:e00168 e00118. doi:10.1128/JB.00168-18.

[30] Campbell A. Prophage insertion sites. *Res Microbiol* 2003;**154**:277–82. doi:10.1016/S0923-2508(03)00071-8.

Study 3: Blasco, Lucía*; **González de Aledo, Manuel***; et al. "Study of 32 new phage tail-like bacteriocins (pyocins) from a clinical collection of *Pseudomonas aeruginosa* and of their potential use as typing markers and antimicrobial agents." Scientific reports vol. 13,1 117. 3 Jan. 2023, doi:10.1038/s41598-022-27341-1

SUMMARY: Phage tail-like bacteriocins (PTLBs) are large proteomic structures similar to phage tails. These structures contribute to bacterial competition by making pores in the membrane of their competitors, disrupting proton gradients. The PTLBs identified in *P. aeruginosa* are classified as R- and F-type pyocins, which have a narrow spectrum of action. Their specificity is determined by the tail fiber and is closely related to the lipopolysaccharide type of the target competitor strain. In this study, the genome sequences of 32 *P. aeruginosa* clinical isolates were analyzed to investigate the presence of R-type and F-type pyocins, and one was detected in all strains tested. BLAST and Vector NTI Advance softwares were used to identify pyocins within contigs, flanked by the *trpD* and *trpE*. Other bioinformatic tools such as RAST, HMMER and HHPRED were use for ORF annotation. Pyocin killing spectrum assays were perfomed to determine their host range, and for that purpose pyocins were produced in liquid culture upon mitomycin induction and purified through centrifugation, filtration and precipitation. The purified pyocin extracts were visualized by transmission electron microscopy using a JEOL JEM-1011 electron microscope. The pyocins were classified into 4 groups on the basis of the tail fiber and also the homology, phylogeny and structure of the cluster components. A relationship was established between these groups and the sequence type and serotype of the strain of origin and finally the killing spectrum of the representative pyocins was determined showing a variable range of activity between 0 and 37.5%. The findings showed that these pyocins could potentially be used for typing of *P. aeruginosa* clinical isolates, on the basis of their genomic sequence and cluster structure, and also as antimicrobial agents.

IMPORTANCE: To our understanding, there is little information on phage tail-like bacteriocins, more specifically in the ones produced by *P. aeruginosa* (pyocins). In this work we analyzed pyocin production in a collection of *P. aeruginosa* strains of clinical origin while exploring their potential use as an alternative treatment to traditional antimicrobials and as typing tools.

scientific reports

Check for updates

OPEN

Study of 32 new phage tail-like bacteriocins (pyocins) from a clinical collection of *Pseudomonas aeruginosa* and of their potential use as typing markers and antimicrobial agents

Lucía Blasco[1,2,4], Manuel González de Aledo[1,2,4], Concha Ortiz-Cartagena[1,2], Inés Blériot[1,2], Olga Pacios[1,2], María López[1,2], Laura Fernández-García[1,2], Antonio Barrio-Pujante[1,2], Marta Hernández-Garcia[2,3], Rafael Cantón[2,3,4] & María Tomás[1,2,4]✉

Phage tail-like bacteriocins (PTLBs) are large proteomic structures similar to the tail phages. These structures function in bacterial competition by making pores in the membrane of their competitors. The PTLBs identified in *Pseudomonas aeruginosa* are known as R-type and F-type pyocins, which have a narrow spectrum of action. Their specificity is determined by the tail fiber and is closely related to the lipopolysaccharide type of the target competitor strain. In this study, the genome sequences of 32 clinical of *P. aeruginosa* clinical isolates were analysed to investigate the presence of R-type and F-type pyocins, and one was detected in all strains tested. The pyocins were classified into 4 groups on the basis of the tail fiber and also the homology, phylogeny and structure of the cluster components. A relationship was established between these groups and the sequence type and serotype of the strain of origin and finally the killing spectrum of the representative pyocins was determined showing a variable range of activity between 0 and 37.5%. The findings showed that these pyocins could potentially be used for typing of *P. aeruginosa* clinical isolates, on the basis of their genomic sequence and cluster structure, and also as antimicrobial agents.

Pseudomonas aeruginosa is a Gram-negative opportunistic pathogen, responsible for nosocomial infections, including bloodstream infections, pneumonia, urinary tract infections and surgical site infections[1]. This pathogen represents a serious problem in health care systems because of its capacity to acquire antibiotic resistance and its ability to produce biofilms and persist on surfaces, thereby contributing to its spread and causing outbreaks[2]. *P. aeruginosa* contains many intrinsic antibiotic resistance mechanisms that make this species a difficult to treat multidrug resistant bacteria[3]. In addition, due to the outbreaks, it is necessary to type the causative bacterial pathogen. The traditional typing methods, Pulse Field Gel Electrophoresis (PFGE) and the Multilocus Sequencing Typing (MLST), are the primary election in many clinical laboratories, but although they are very effective it should be necessary to improve the discrimination inside each Sequence Type (ST)[4]. So, new antimicrobial agents as well as new typing methods are therefore required.

Bacteria utilize phage tail-like bacteriocins (PTLBs) to enable them to compete with other strains of the same species or with different species[5] and could therefore be good candidates for use as antimicrobial agents. PTLBs are large, ribosomally synthetized[6] protein structures (2×10^6–1×10^7 KDa) encoded in the bacterial genome and

[1]Microbiología Traslacional y Multidisciplinar (MicroTM)-Instituto de Investigación Biomédica (INIBIC), Servicio de Microbiología, Hospital A Coruña (CHUAC), Universidad de A Coruña (UDC), A Coruña, Spain. [2]Study Group on Mechanisms of Action and Resistance to Antimicrobials (GEMARA) the Behalf of the Spanish Society of Infectious Diseases and Clinical Microbiology (SEIMC), Madrid, Spain. [3]Servicio de Microbiología, Hospital Universitario Ramón y Cajal, Instituto Ramón y Cajal de Investigación Sanitaria (IRYCIS), CIBER de Enfermedades Infecciosas (CIBERINFEC), Instituto de Salud Carlos III, Madrid, Spain. [4]These authors contributed equally: Lucía Blasco, Manuel González de Aledo, Rafael Cantón and María Tomás. ✉email: MA.del.Mar.Tomas.Carmona@sergas.es

structured in genetic clusters similar to the phage tail structure models, always encoding structural and assembly tail proteins, a lysis cassette and preceded by the transcription regulatory proteins[5].

P. aeruginosa produces PTLBs called pyocins, traditionally named after the species of origin, in this case *P. aeruginosa* also known as *P. pyocyanea*[5]. The PTBLs from *P. aeruginosa* are some of the most widely studied PTLBs and are used as PTLBs models[5]. The *P. aeruginosa* pyocins are grouped into three types: S-type pyocins, R-type pyocins and F-type pyocins. The S-type pyocins, not considered PTLBs, are colicin-like proteins composed by large multi domain polypeptides with DNase activity[7]. The R-type pyocins and F-type pyocins are considered PTLBs and differ in their structure. R-type (Rigid-type) pyocins are contractile tail particles similar to the *Myoviridae* phage family and are composed by a long large tube surrounded by a sheath and ending in a baseplate where the receptor-binding protein (RBP) is located. The F-type (Flexible-type) pyocins are non-contractile particles, similar to the *Siphoviridae* phage family; they are simpler than the R-type as they do not possess a sheath, but also have an RBP[5,8]. Despite the great morphological similarity of PTBLs with phages, they cannot be considered degenerate phages but both would have a common cellular ancestry along with the type VI secretion system[5,8,9].

The killing mechanism of R-type and F-type pyocins involves the phage tail fiber possessing the RBP, which recognizes the bacterial receptor in the lipopolysaccharide (LPS). The specificity of the RBP leads to a narrow spectrum of activity and the protection of the pyocin producer strain, although the producer cell dies altruistically due to the pyocins release[5]; once the cell is bound, the R-type pyocin triggers contraction of the sheath by pulling the tail and the core through the envelope, forming a channel or pore that decouples the membrane potential thus inhibiting membrane transport and causing cell death[3,5]. The killing mechanism of the F-type also involves disruption of the membrane gradient, but as it lacks a tube or core that forms a channel, its mechanism of action is not yet well understood[5,10]. The S-type pyocins are secreted as binary protein complexes that contain an effector, which is a larger protein with killing activity including DNase activity, the second component is a smaller protein with immunity activity that protects the producer strain from the activity of the released pyocin[11,12].

To date, five subtypes of R-type pyocins have been described on the basis of their target specificity: R1, R2, R3, R4 and R5[8,12,13]. Of these, R5 has the broadest spectrum, while R2 has the narrowest spectrum and encompasses the spectra of R3 and R4, which are similar. R1 is a subset of R5 but is considered a different branch. In addition, the amino acid sequence of the tail fiber protein is similar in R2, R3 and R4, but very different in R1 and R5[5,13,14]. The F-type pyocins have been less well studied and are currently classified into three groups (F1, F2 and F3) based on their lytic spectra, although another two groups have also been identified: one in *P. aeruginosa* PA14 and other in *P. aeruginosa* M18. The former is similar to F2, identified in the reference strain *P. aeruginosa* PAO1, but with differences in 210 to 340 residues from the tail fiber protein; the M18 F-type shares 66% homology with the tail fiber protein of the F1 group[12].

PTBLs are encoded in gene clusters preceded by a group of regulatory genes and organised in blocks of lytic and structural genes. These clusters can be found encoding individual R-type or F-type pyocins but also in dual R-F pyocin clusters. It has previously been reported that all clusters in *P. aeruginosa*, i.e. both individual and the dual R-F type, are located in the genome in the intergenic region of the tryptophan operon between the *trpE* and *trpGCD* genes[5,12]. The regulatory system of both individual and dual R-type and F-type pyocins is located upstream of the cluster and is composed by an activator (*prtN*) and a repressor (*prtR*); these are related to *recA*, which is activated by DNA damage, cleaving *prtR* and producing *prtN* and thus activating expression of the pyocin cluster[5,12,15]. The production of both R-type and F-type pyocins in dual R-F pyocins relies on the shared regulatory system and also the shared lysis cassette, suggesting coordinated release of the dual pyocins[8,12].

PTLBs are characterized by a narrow host spectrum, which in *P. aeruginosa* is known to be closely related to the LPS type of the target strain that acts as a receptor for the tail fiber proteins[14]. It has also been reported that each specific type of pyocin recognizes a specific serotype strain determined by the O-polysaccharide repeating portion, which acts as an O-antigen and is linked to the virulence of the strains[14,16]. The PTLBs, and more specifically the *P. aeruginosa* pyocins, can be used as antimicrobial agents and owing to their relationship with the O-antigen they were used in typing schemes before the emergence of molecular typing methods[17–19]. The value of pyocins as antimicrobial agents is currently being considered in research studies. The R-type pyocins were used for the first time in 1969 to rescue chick embryos infected with *P. aeruginosa*[20]. In addition, several assays in murine models confirmed the efficacy of R-type pyocins in the treatment of infections with *P. aeruginosa*[13,21,22]. Due to the narrow spectrum of the PTLBs, some studies focused on generating recombinant R-type pyocins to retarget them by substituting the tail fiber protein with a phage protein in order to increase the host range in several species such as *P. aeruginosa*, *Clostridioides difficile* and *Listeria monocytogenes*[10,23–26].

In the search for new pyocins, 32 genome sequences of clinical strains of *P. aeruginosa* of different clinical origins were analysed in the present study, and at least one pyocin cluster was identified in each strain. The sequence of these pyocins was analysed and homology and phylogenetic studies were conducted. The pyocins were isolated and purified and their killing spectrum was established, and they were also related to the serotype and ST of the clinical isolates.

Results

Identification and characterization of the phage tail-like bacteriocins. Thirty-two genomic sequences of *P. aeruginosa* were analysed to search for PTLBs (Table 1). In all of the genomes analysed, at least one cluster corresponding to a pyocin was found between tryptophan operon genes, *trpE* and *trpG* (Table 2; Table 1S. Supplementary material). Thus, 21 of the strains contained a cluster that corresponded to a unique pyocin corresponding to an R-type pyocin. Dual clusters were identified in the 11 remaining strains. In the *P. aeruginosa* PAO1 reference strain[5], one of these clusters corresponded to a R-type pyocin, and the contiguous

Strain	Genbank	Origin	ST	Serotype
1-13	SAMN14776823	IAI	ST235	O11
2-29	SAMN14776826	UTI	ST235	O11
3-49	SAMN14776829	IAI	ST235	O11
4-17	SAMN14776829	UTI	ST235	O11
4-71	SAMN14776839	IAI	ST235	O11
4-79	SAMN14776840	UTI	ST235	O11
4-86	SAMN14776841	IAI	ST235	O11
4-92	SAMN14776842	UTI	ST235	O11
4-93	SAMN14776843	UTI	ST235	O11
4-94	SAMN14776844	IAI	ST235	O11
4-120	SAMN14776833	UTI	ST235	O11
4-121	SAMN14776834	UTI	ST235	O11
9-41	SAMN14776860	LRTI	ST235-1LV	O11
C11	SAMN14776862	UTI	ST175	O4
C58	SAMN14776863	UTI	ST175-2LV	O4
G6	SAMN14776870	IAI	ST175-1LV	O4
G7	SAMN14776871	IAI	ST175-2LV	O4
G26	SAMN14776868	IAI	ST175-1LV	O4
G31	SAMN14776869	IAI	ST175-1LV	O4
H18	SAMN14776872	UTI	ST175-2LV	O4
H52	SAMN14776874	UTI	ST309	O11
3-5	SAMN14776830	UTI	ST348-1LV	O11
3-38	SAMN14776827	LRTI	ST348	O12
3-41	SAMN14776828	LRTI	ST348-1LV	O12
3-58	SAMN14776831	IAI	ST348	O11
9-86	SAMN14776861	IAI	ST554	O5
5-23	SAMN14776846	LRTI	ST244	O5
6-25	SAMN14776848	LRTI	ST244-1LV	O12
8-24	SAMN14776854	UTI	ST244-1LV	O5
8-36	SAMN14776855	UTI	ST244	O5
9-25	SAMN14776858	LRTI	ST244-1LV	O12
10-58	SAMN14776820	LRTI	ST244	O12

Table 1. Characteristics of the 32 clinical isolates of *P. aeruginosa* which were obtained in previous study[30]. It is indicated each Genbank code, clinical origin, sequence type (ST) and serotype. *IAI* intra-abdominal infection, *UTI* urinary tract infection, *LRTI* lower respiratory tract infection.

cluster corresponded to an F-type pyocin, both sharing the regulatory and lytic genes, as previously described for *P. aeruginosa* PAO1[12].

In order to identify the PTLBs as R or F subtypes, homology analysis of the tail fiber was conducted. In the R-type pyocins, the tail fiber proteins were compared against the reference sequence for each R subtype (R1, R2, R3, R4 and R5); the results revealed that 21 of the proteins belonged to the R5 subtype, while 11 belonged to the R2 subtype, which corresponded to those that were followed by a F-type pyocin (Fig. 1A,B). For the F-type group, the results showed a group of 5 pyocins belonging to the F2 subtype, comprising a R2-F2 pyocin, similar to the PAO1 R2-F2 pyocin[5], and a group of 6 that were similar to the *P. aeruginosa* PA14 F-type pyocin[12], thus giving rise to a pyocin cluster R2-F(PA14) (Fig. 1A,B).

The genomic analysis of the pyocin clusters identified showed a % GC content very similar, between 63.9 and 65.4 (Table 2). Analysis of the protein sequence of the pyocins revealed some differences in the protein number between the R5-type pyocins (Table 2). Thus, these pyocins were classified in two groups, including a group of 12 pyocins (group A) constituted by an R-type cluster of 14 genes, 4 lytic genes and preceded by 5 regulator genes. The second group (group B) of 8 pyocins differed from group A in the absence of the latter protein belonging to the lytic cassette. In both groups, the cluster was preceded by the regulatory region composed by 5 genes, while in the reference *P. aeruginosa* PAO1 strain it is composed by 4 genes (Fig. 1B; Table 2)[7]. The R2-F2 pyocins (group C) were composed by 38 genes, which corresponded to an R-type cluster of 14 proteins and a F-type cluster composed by 16 genes, while in *P. aeruginosa* PAO1 the F-type cluster is formed by 17 genes. In addition, the two clusters share a regulatory region of five genes and a lytic cassette composed by four proteins (Fig. 1B). The pyocins R2-F(PA14) (group D) comprised two consecutive R and F clusters: the R-type comprised 14 proteins and the F-type comprised 13 proteins, unlike *P. aeruginosa* PAO1 and the group C pyocins, in which the last three proteins are duplicated (Fig. 1B)[7].

Pyocin name	Pyocin subtype	Genbank	Genomic lenght (pb)	% GC	ORF	Group
1-13_pyoR5	R5	BK062625	16,471	65.4	23	A
2-29_pyoR5	R5	BK062626	16,471	65.4	23	
3-49_pyoR5	R5	BK062627	16,471	65.4	23	
4-17_pyoR5	R5	BK062628	16,472	65.5	23	
4-71_pyoR5	R5	BK062629	16,471	65.4	23	
4-79_pyoR5	R5	BK062630	16,471	65.4	23	
4-86_pyoR5	R5	BK062631	16,471	65.4	23	
4-92_pyoR5	R5	BK062632	16,471	65.4	23	
4-93_pyoR5	R5	BK062633	16,471	65.4	23	
4-94_pyoR5	R5	BK062634	16,803	65.4	23	
4-120_pyoR5	R5	BK062635	16,471	65.4	23	
4-121_pyoR5	R5	BK062636	16,803	65.4	23	
9-41_pyoR5	R5	BK062645	16,803	65.3	23	
C11_pyoR5	R5	BK062637	16,455	65.1	23	B
C58_pyoR5	R5	BK062638	16,455	65.1	23	
G6_pyoR5	R5	BK062639	16,312	65	23	
G7_pyoR5	R5	BK062640	16,120	65.2	23	
G26_pyoR5	R5	BK062641	16,455	65.1	22	
G31_pyoR5	R5	BK062642	16,455	65.1	22	
H18_pyoR5	R5	BK062643	16,120	65.2	22	
H52_pyoR5	R5	BK062644	16,215	65.3	22	
3-5_pyoR2-F2	R2-F2	BK062615	30,282	63.9	39	C
3-38_pyoR2-F2	R2-F2	BK062614	30,282	63.9	39	
3-41_pyoR2-F2	R2-F2	BK062616	30,282	63.9	39	
3-58_pyoR2-F2	R2-F2	BK062617	30,283	63.9	39	
9-86_pyoR2-F2	R2-F2	BK062622	30,510	64	41	
5-23_pyoR2-F(PA14)	R2-F(PA14)	BK062618	28,526	64.2	36	D
6-25_pyoR2-F(PA14)	R2-F(PA14)	BK062619	28,805	64.2	36	
8-24_pyoR2-F(PA14)	R2-F(PA14)	BK062620	28,805	64.2	36	
8-36_pyoR2-F(PA14)	R2-F(PA14)	BK062621	28,526	64.2	36	
9-25_pyoR2-F(PA14)	R2-F(PA14)	BK062623	28,805	64.2	36	
10-58_pyoR2-F(PA14)	R2-F(PA14)	BK062624	28,526	64.2	36	

Table 2. Genomic characteristics and subtype of the 32 pyocins (PTBLs) identified in this study. Each pyocin name corresponds to the producer strain. It is indicated the Genbank code, the genome size, % GC, number of ORF and the group to which each was assigned.

Homology and phylogenetic analysis of pyocins. The results obtained by the homology studies of the tail fiber specificity genes were confirmed by the homology and phylogenetic analysis of the complete pyocin genomes. The homology analysis showed that the R5-type pyocins were very similar and can be grouped in two blocks corresponding to the established groups A and B, sharing a query cover value of 97–98% and an identity value of 99.35%. The pyocin H52-R5 homology BRIG differed slightly from the two blocks but had similar homology values (Fig. 2). In the case of the R-F pyocin clusters, the homology results showed two blocks of homology, one corresponding to the R2-F2 pyocins (group C) and another corresponding to the R2-F(PA14) pyocin (group D) (Fig. 2). Despite the presence of two groups, the pyocin clusters represented by them were also similar, with a query cover value between 88 and 89% and an identity value of 98%.

The phylogenetic study of all the pyocin clusters revealed, as previously observed, that the pyocins identified are divided into four phylogenetic groups. Two closely related clades of the phylogenetic tree were represented by two blocks, one corresponding to the R5-type pyocins included in group A and another also corresponding to an R5-type pyocin grouped in B. Another two closely related clades included one corresponding to group C, which was constituted by the R2-F2 pyocin and group D, constituted by the R2-F(PA14) (Fig. 3).

Identification of pyocins by transmission electron microscopy (TEM). The purified pyocins were examined by TEM, and the images obtained (Fig. 4) revealed the presence of two different type of pyocins. One type had a structure similar to a tail of the viral family Myoviridae, corresponding to the R-type pyocins, observed in three conformations: a complete form, a contracted form and an empty sheath[27]. The other type was the F-type, observed as a flexible structure similar to a phage tail of the viral family Syphoviridae.

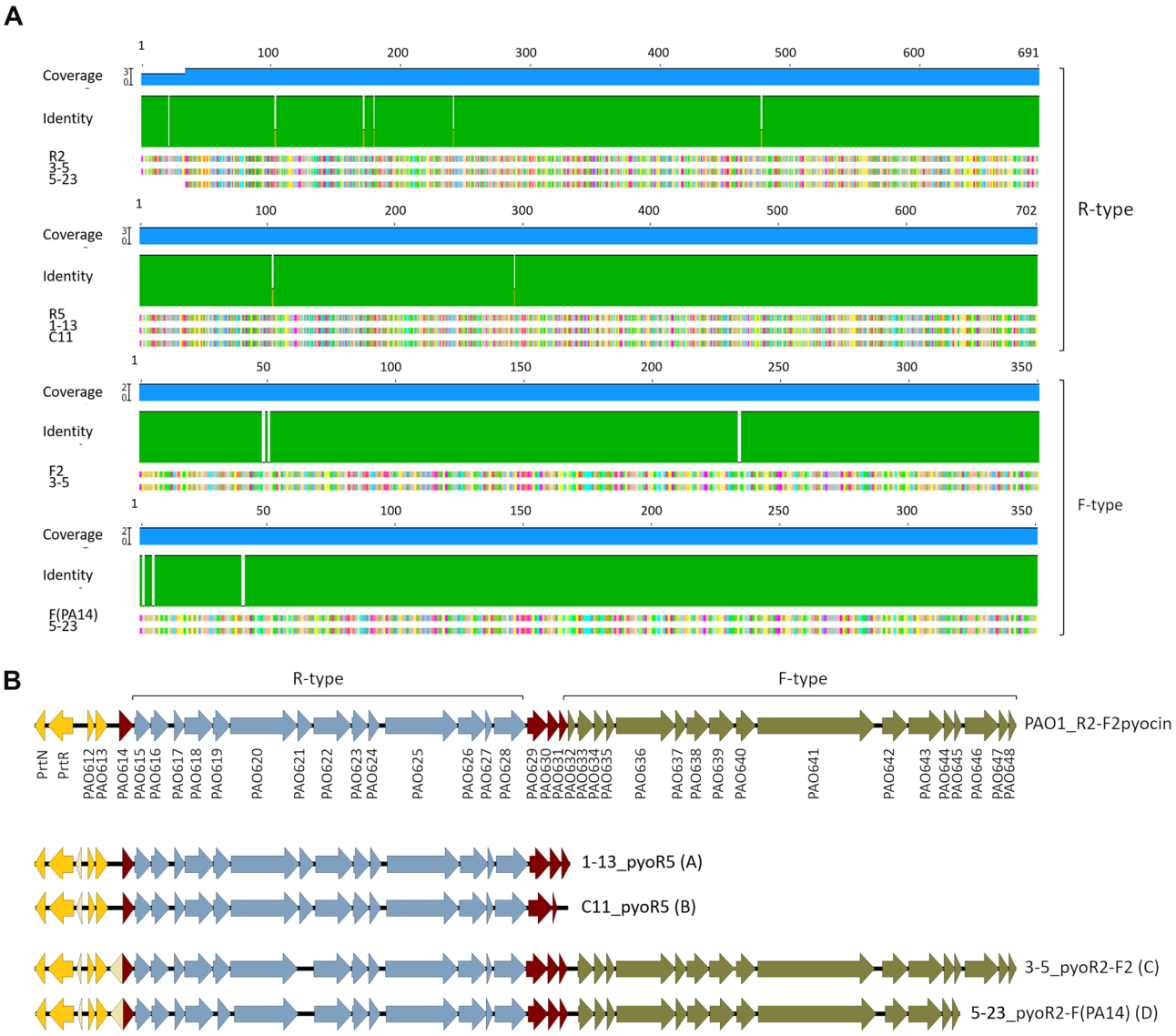

Figure 1. Identification of the pyocin subgroup. (**A**) Homology comparison of the tail fiber protein model sequence of R2, R5, F2 and F(PA14) with one representative of each pyocin type identified in this study. (**B**) Structure of the pyocin cluster of one representative of each group (A, B, C and D), and comparison with the reference pyocin R2-F2 from *P. aeruginosa* PAO1. Yellow: regulatory genes; red: lysis cassette; blue: R-type pyocin cluster genes, brown: F-type pyocin cluster genes. The representative sequences were selected by numerical order due to the high intragroup similarity.

Relationship between the pyocin type and the source *P. aeruginosa* strain serotype, sequence type and clinical origin. In this analysis, the relationship between the serotype, the sequence type (ST) and the clinical origin of the source strains and the pyocin type was determined (Table 1). The R5-type pyocin in group A was almost always present in ST235 and serotype O11 clinical isolates. However, pyocin H52_pyoR5 was quite different in the homology and phylogenetic analysis, as it was present in the H52 clinical isolate belonging to the ST309 but like the rest of group A had the O11 serotype. The R5-type pyocins from group B were associated with clinical isolates belonging to the ST175 with serotype O4. On the other hand, the group C of R2-F2 pyocins was the most variable, with isolates belonging to the ST348 and ST554 and serotype O5, O11 and O12. Finally, group D, constituted by R2-F(PA14) pyocins, was represented by isolates belonging to ST244 and serotypes O5 and O12. Finally, no relationship between the clinical origin of the isolate and each pyocin was observed.

Killing spectrum of the pyocins. The target range of the pyocins was studied by the spot test technique (Fig. 5). The pyocins included in this analysis were selected by according to ST and serotype of the strain from which they were isolated. The results revealed a great variability in the susceptibility of the strains to the pyocins of the same subtype. In addition, no spots occurred when the target strain belonged to the same ST and serotype as the source strain of the pyocin, except for pyocin 10-58_R2-F(PA14), which produced a spot in strain 3–5,

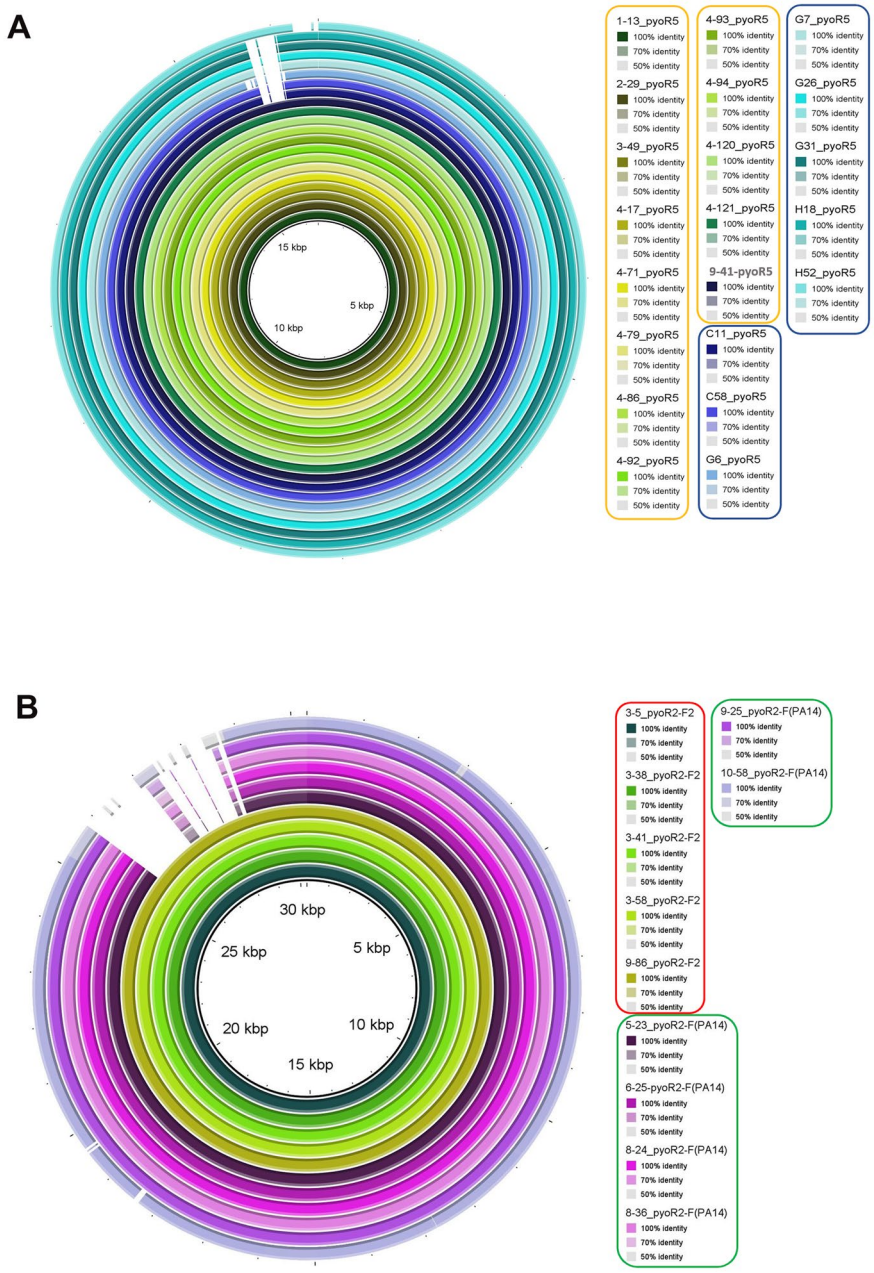

Figure 2. Homology of the pyocin clusters determined by BRIG 0.95. (**A**) R-type pyocin clusters. The clusters corresponding to group A are rounded in yellow and to group B in blue. (**B**) R-F type clusters. The cluster corresponding to group C are rounded in red and to group D in green.

which belongs to a different ST but has the same serotype (O11). Furthermore, a variable percentage of target range was observed for all of the pyocins tested, with 9-86_pyoR2F2 showing the highest value and being able to lyse 37.5% of the strains tested.

Discussion

Pyocins are PTLBs produced by *P. aeruginosa*. Like all PTBLs they are protein complexes with the same structure as phage tails. Like other phage tail particles, such as the type VI secretion systems (T6SS), they also play a role in defence and in interbacterial competition[28]. The genetic and structural similarities between the phage tails and PTBLs initially suggested that the PTBLs evolved as defective phages; however, structural comparison between the T6SS, R-type pyocins and the contractile tail phages suggests evolution from a common ancestor[5,28].

The presence of pyocins in clinical strains of *P. aeruginosa* seems to be variable. Thus, in a study conducted by Mei et al.[3], from an analysis of 852 clinical isolates of *P. aeruginosa* they found that 448 belonged to the R-type pyocin and 300 contained genes of the F-type pyocins. From those included in the R-type pyocins 144 belonged

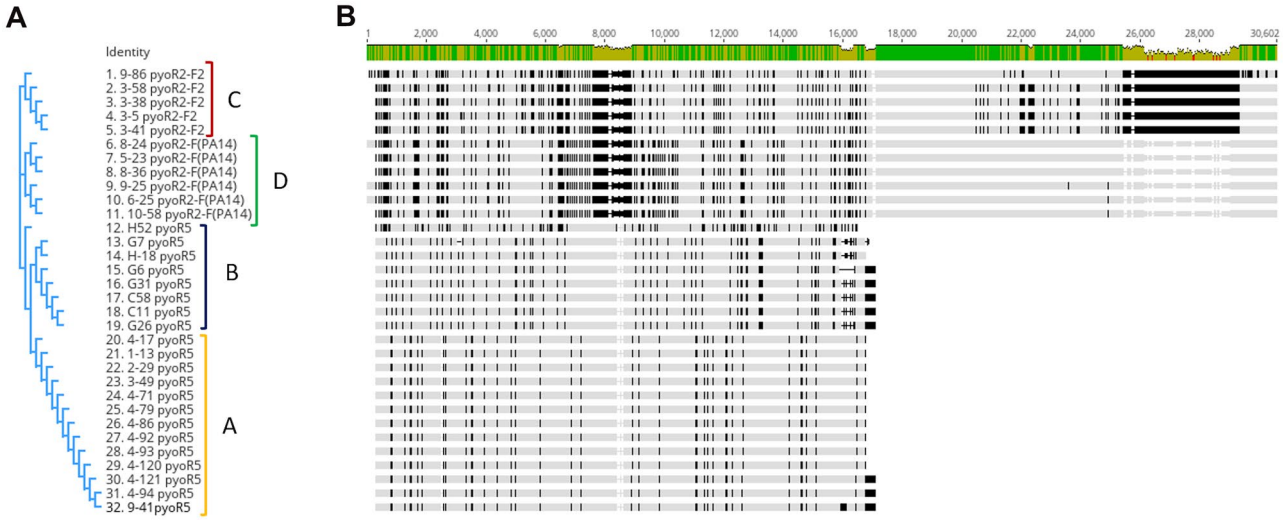

Figure 3. Similarity study of the 32 pyocin clusters identified and its relation with the established groups. (**A**) Phylogenetic tree. (**B**) Alignment of the 32 pyocins clusters.

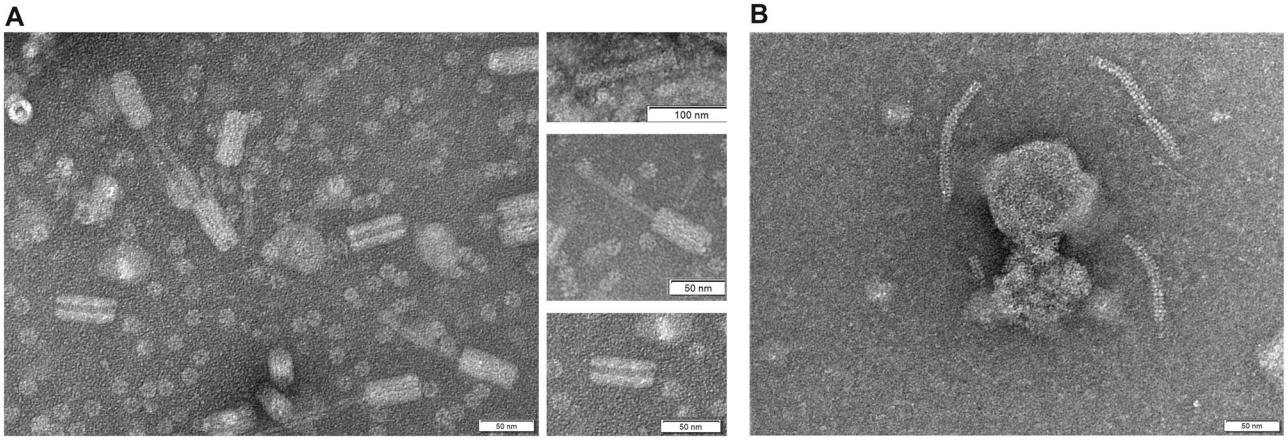

Figure 4. TEM images of pyocins. (**A**) R-type pyocin with a similar structure to a myovirus, in three conformations. Top: complete form; middle: contracted form; bottom: empty sheath of the pyocin. (**B**) F-type pyocin with a similar structure to a syphovirus.

to the R1 subtype, 76 to the R2 subtype, 43 to the R5 subtype and the remaining strains were untypeables. Köhler et al.[14] analysed the tracheal aspirates of 61 patients, in search of R-type pyocins, detecting different R subtype pyocins in 77% of the isolates. In another study of 24 isolates from the lungs of CF patients, all isolates were found to contain R-type pyocins, also mainly of the R1 subtype, and it was concluded that this subtype confers a competitive advantage in biofilms, explaining why certain strains displace others in the CF lungs[6]. In the present study, the genome of 32 clinical isolates of *P. aeruginosa* from several origins, including urinary tract infections, lower respiratory tract infections and intra-abdominal infections, were analysed in search of pyocins, and at least one cluster was found in all isolates. In contrast to the previously mentioned studies, both R-type clusters and F-type clusters were found, resulting in R pyocins and dual R-F pyocins. Analysis of the tail fibers, which determines the specificity (Fig. 1), showed that only R2, R5, F2 and F(PA14) were present in these isolates, with an equal representation of the R5 and R2 subtypes, and a lower representation of F2 than F(PA14) (Fig. 2). In other studies of CF isolates, the R1 subtype was the most commonly identified and in contrast to the results of the present study, R5 was the least well represented subtype[3,6]. In a study conducted by Köhler et al.[14], pyocins from R1, R2 and R5 were found in the same proportions.

Homology modelling and phylogenetic studies of the pyocins identified in these clinical isolates confirmed the grouping of the pyocins and also revealed the great similarity between them. The main difference observed between the R2-type and the R5-type pyocins was in the genomic region corresponding to the tail fiber, and the same was observed between the F2-type and the F(PA14)-type pyocins (Fig. 3). The tail fiber region has been described as being responsible for the specificity of the pyocins, as it acts as an RBP recognizing the target in the LPS of the target bacteria[5,8].

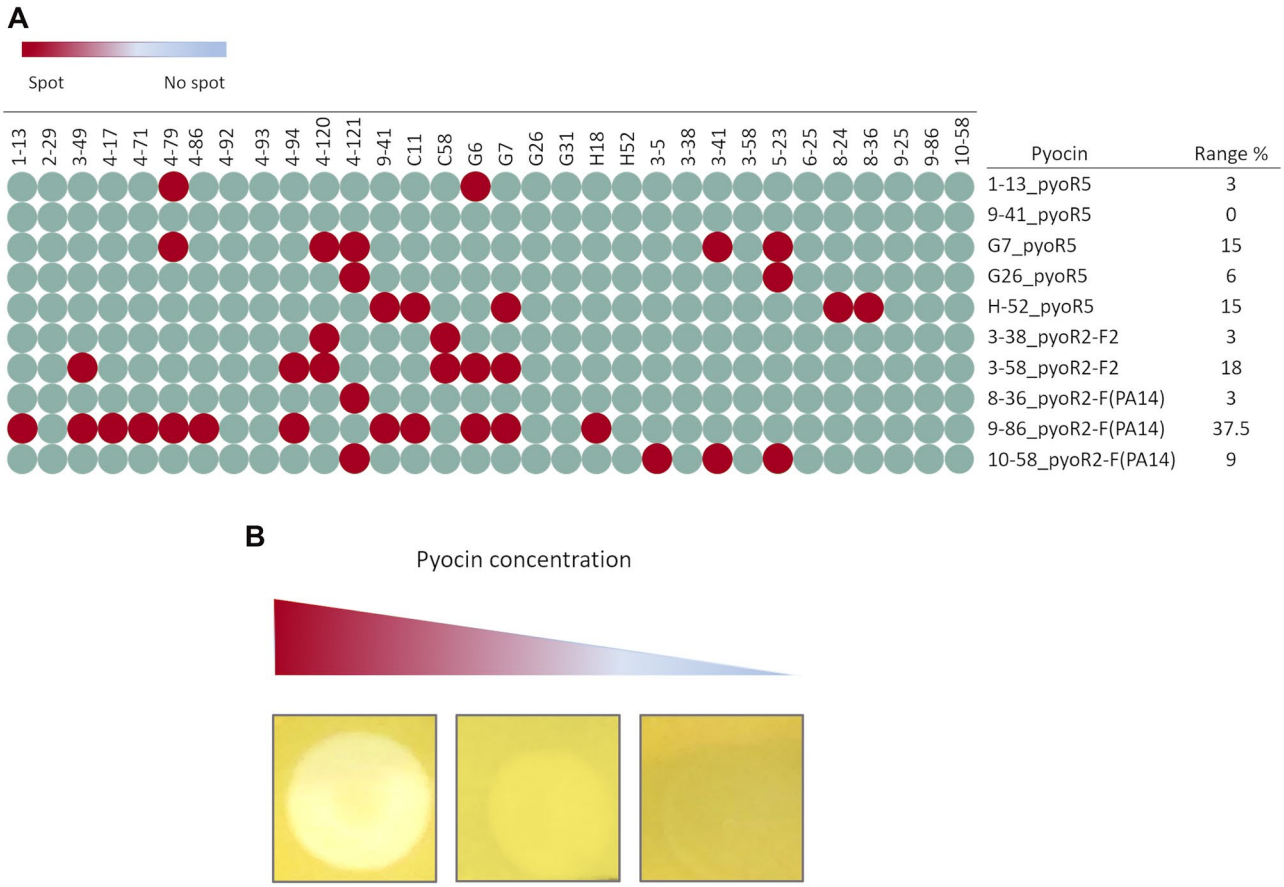

Figure 5. Target range of the pyocins. (**A**) Spot test of the pyocins originating from strains with different ST and serotype. (**B**) Spot production dependent of the pyocin concentration.

Analysis of the pyocins identified in the genomic sequence of the *P. aeruginosa* clinical isolates and the clinical ST, serotype and clinical origin established a relationship between the pyocin type and the ST and serotype, but not the clinical origin of the isolate. Although a relationship with both ST and serotype was identified, it seems that there is more variability between the serotype and the presence of pyocins than with the ST. Thus, the association between the pyocin subtype and the ST and serotype can be extended to the groups established in this work beyond the pyocin subtype, as the A and B groups, which both correspond to an R5-type pyocin, were associated with a different ST and serotype. Although the association between serotype and pyocin subtype has long been recognised[14], to our knowledge the present is the first report of the relationship with ST. The relationship between the serotype and the pyocin subtype[14] has always been established with the R-type cluster, but in the present study a relationship between the serotype and the F-type pyocin was demonstrated, as the group C and D pyocins only differ in the F-type cluster. Both groups were related to two different serotypes, but both share O12 and differ in O5 and O11, possibly as a consequence of the presence of the R-pyocin and the F-pyocin, which in this case would confer a competitive advantage to the strain as they are protected by different pyocins[28]. The observed relationship between the serotype, ST and pyocin from the clinical isolates of *P. aeruginosa* tested in this study suggests that the pyocins could potentially be used via analysis of the cluster genomic sequences. The pyocin-serotype association has been used for bacterial typing, but unlike in the present study, the typing was based on the killing activity of a pyocin from an unknown isolate over a collection of indicator strains; this method was abandoned, as it is slow and laborious, and was substituted by molecular methods[17–19]. Currently, thanks to the genome analysis, the study of the PTBLs can complement the traditional typing methods employed in the clinical laboratories.

The serotype in *P. aeruginosa* is determined by the O-antigen, which is a B-band repeating unit of LPS considered a virulence factor[14]. It is known that the pyocin tail fiber proteins recognize the LPS of the competitor strains but do not recognize their own LPS as a target, so they cannot lyse those strains with the same serotype. In a study carried out in 2010, Köhler et al.[14] deleted different genes responsible for the synthesis of the O-antigen and determined which LPS residues act as receptors for R1-type, R2-type and R5-type pyocins. When the 32 clinical isolates were tested against the 32 isolated pyocins, none were able to lyse the source strain or those strains with the same serotype or ST. As previously described, variability in the susceptibility to the pyocins was observed between those isolates that shared ST and/or serotype and the same type of pyocin, probably due to the frequently observed mutations in the LPS genes in CF, affecting recognition by the RBP[3,29,30]. Pyocins have

been considered potential alternatives to antibiotics, and several studies have demonstrated antimicrobial activity of pyocins alone or in combination with other antimicrobials and those sharing the LPS as target[13,22,23,31,32].

In this study, 32 pyocins belonging to the R5-type, R2-F2 type and R2-F(PA14) type were identified. Homology and phylogenetic analysis established four groups of pyocins (A, B, C and D), each of which was found to be related to the serotype and ST of the source strain. Pyocins are therefore good candidate markers for typing strains of *P. aeruginosa* by analysis of the tail fiber protein of the pyocin. We also observed that they could be used to type R5-type pyocins, by the number and distribution of the genes comprising the pyocin cluster. These pyocins also displayed potential antimicrobial activity as they were able to lyse some of the clinical isolates tested, particularly the 9-86_pyoR2-F(PA14) pyocin, which exhibited the highest range of activity.

Material and methods

Strains and culture conditions. Thirty-two clinical strains of *P. aeruginosa* isolated in Portuguese and Spanish hospitals within the framework of two multicentre studies, STEP in Portugal and SUPERIOR in Spain[33], were used in the study. The software mlst (v2.16.1) (https://github.com/tseemann/mlst) was used for the in silico MLST assignment[33]. Serogroups based on the O-specific antigen (OSA) gene cluster sequences were determined using Blastn tool (v2.9.0+) (http://blast.ncbi.nlm.nih.gov/Blast.cgi) and the OSA database[33]. The origin, ST and serotype of the isolates are shown in Table 1. All strains were grown in Luria–Bertani broth (LB) medium (0.5% NaCl, 0.5% yeast extract, 1% tryptone) at 37 °C and 180 rpm. LB was supplemented with agar (1.5%) when necessary.

Identification of pyocin clusters in silico. The genomes of 32 clinical isolates *P. aeruginosa* (NCBI BioProject: PRJNA629475) were analysed to search for pyocins. For this purpose, the anthranilate flanking genes, *trpD* and *trpE*, were identified in the search for the genes that typically compose the pyocin clusters, which have been reported to be included between these genes[5].

When the pyocin cluster sequences were distributed in several contigs, they were then compared by homology and assembled using BLASTn and Vector NTI Advance™ 11 (Invitrogen) programs. The complete sequences of the pyocin clusters were annotated by RAST[34], HMMER (http://hmmer.org) and HHPRED[35]. The pyocin cluster R2-F2 of *P. aeruginosa* PAO1 was used as a reference sequence, which corresponds to the region between the genes PAO610-PAO648 (Genbank: AE004091.2-AE004091.2) from the *Pseudomonas aeruginosa* database[36].

All the nucleotide sequence data reported are available in the Third Party Annotation Section of the DDBJ/ENA/GenBank databases under the accession numbers TPA: BK062614–BK062645 (Table 2).

Pyocin cluster type identification. The pyocin cluster types were assigned by homology with the tail fiber corresponding to the protein of the reference strain *P. aeruginosa* PAO1: PAO620 for the R-type pyocins and by PAO646 for the F-type pyocins[12].

These strains were compared by BLASTp against the corresponding protein of the different pyocin types: R1 (ARI05994.1), R2 (AAG04009.1), R3 (ABP93392.1), R4 (ABP93394.1), R5 (ABP93396.1), F2 (AAG04035.1) and F(PA14) (ABJ15607.1). The pyocin clusters were considered to belong to a subtype when the homology value was higher than 90%.

Homology and phylogenetic analysis. The sequences obtained for the different pyocin clusters were analysed in order to study their homology. The studies were carried out using the Easyfig 2.2.5[37] and BRIG 0.95[38] tools with the tBLASTx option. The Query Cover and Identity values were analysed with BLASTn.

The sequences were aligned and a phylogenetic tree was constructed with the bioinformatic software Geneious Prime (Dotmatics).

Extraction and concentration of phage tail-like bacteriocins. The selected strains used as sources of pyocins were cultured overnight in LB broth at 37 °C. The culture was then diluted 1:100 in LB and incubated at 37 °C and 180 rpm. Once the optical density measured at a wavelength of 600 nm (OD_{600nm}) of 0.4 was reached, 10 µg/ml of mitomycin C (Sigma-Aldrich) was added and the culture was incubated until it turned clear. The lysed cultures were centrifuged at 4000 rpm for 10 min, and the supernatant with the pyocins was recovered and incubated with 1% chloroform for 30 min. Finally, the supernatant with the pyocins was filtered through a 45 µm filter (FILTER-LAB®PES Syringe filter).

For concentration, the pyocins were precipitated with polyethylene glycol (PEG). The pyocin solution was precipitated overnight at 4 °C with 10% PEG and 0.5 M NaCl. The pyocins were collected by centrifugation for 15 min at 11,000 rpm and 4 °C. The supernatant was discarded and the pellet suspended in SM buffer (0.1 M NaCl, 1 mM MgSO4, 0.2 M Tris–HCl, pH 7.5), to obtain a tenfold concentration. Finally, a 1:1 volume of chloroform was added and incubated with gentle shaking for 20 min, and the phases were then separated by centrifugation for 10 min at 4000 rpm. The aqueous phase with the pyocin suspension was recovered and stored at 4 °C until use.

Pyocin transmission electron microscopy (TEM). The pyocin solutions were fixed in a grid and negatively stained in 1% aqueous uranil acetate for 5 min and examined in a transmission electron microscope JEOL JEM-1011.

Pyocin killing spectrum. In order to determine the target range of each isolated pyocin, each was tested against the 32 strains from which they were isolated (Table 1). The killing activity was assayed by spot test[39].

Briefly, double agar layer plates were prepared with the putative host strain mixed with the soft upper agar layer (0.4% agar). Once solidified, a drop (10 µl) of the pyocin solution was deposited on top of the agar layer, and the plates were incubated at 37 °C for 20 h.

To differentiate the R-type and F-type pyocins from the S-type pyocins, proteinase K was added to the plates, as R and F-type pyocins are protease resistant and S-type is protease sensitive[12]. In order to differentiate the pyocins from prophages induced with mitomycin C, serial dilutions were spotted on agar plates. When no individual plaques were observed at the higher dilutions, the presence of a spot was considered to be the result of the killing activity of the pyocin.

Data availability

All data generated or analysed during this study are included in this published article [and its supplementary information files].

Received: 23 September 2022; Accepted: 30 December 2022
Published online: 03 January 2023

References

1. Pires, D. P., Vilas Boas, D., Sillankorva, S. & Azeredo, J. Phage therapy: A step forward in the treatment of *Pseudomonas aeruginosa* infections. *J. Virol.* **89**, 7449–7456. https://doi.org/10.1128/JVI.00385-15 (2015).
2. de Sales, R. O., Migliorini, L. B., Puga, R., Kocsis, B. & Severino, P. A core genome multilocus sequence typing scheme for *Pseudomonas aeruginosa*. *Front. Microbiol.* **11**, 1049. https://doi.org/10.3389/fmicb.2020.01049 (2020).
3. Mei, M., Thomas, J. & Diggle, S. P. Heterogenous susceptibility to R-Pyocins in populations of *Pseudomonas aeruginosa* sourced from cystic fibrosis lungs. *MBio* https://doi.org/10.1128/mBio.00458-21 (2021).
4. Simar, S. R., Hanson, B. M. & Arias, C. A. Techniques in bacterial strain typing: Past, present, and future. *Curr. Opin. Infect. Dis.* **34**, 339–345. https://doi.org/10.1097/QCO.0000000000000743 (2021).
5. Scholl, D. Phage tail-like bacteriocins. *Annu. Rev. Virol.* **4**, 453–467. https://doi.org/10.1146/annurev-virology-101416-041632 (2017).
6. Oluyombo, O., Penfold, C. N. & Diggle, S. P. Competition in biofilms between cystic fibrosis isolates of *Pseudomonas aeruginosa* is shaped by R-Pyocins. *MBio* https://doi.org/10.1128/mBio.01828-18 (2019).
7. Nakayama, K. *et al.* The R-type pyocin of *Pseudomonas aeruginosa* is related to P2 phage, and the F-type is related to lambda phage. *Mol. Microbiol.* **38**, 213–231. https://doi.org/10.1046/j.1365-2958.2000.02135.x (2000).
8. Ghequire, M. G. K. & De Mot, R. The tailocin tale: Peeling off phage tails. *Trends Microbiol.* **23**, 587–590. https://doi.org/10.1016/j.tim.2015.07.011 (2015).
9. Vacheron, J., Heiman, C. M. & Keel, C. Live cell dynamics of production, explosive release and killing activity of phage tail-like weapons for *Pseudomonas* kin exclusion. *Commun. Biol.* **4**, 87. https://doi.org/10.1038/s42003-020-01581-1 (2021).
10. Lee, G. *et al.* F-type bacteriocins of Listeria monocytogenes: A new class of phage tail-like structures reveals broad parallel coevolution between tailed bacteriophages and high-molecular-weight bacteriocins. *J. Bacteriol.* **198**, 2784–2793. https://doi.org/10.1128/JB.00489-16 (2016).
11. Ling, H., Saeidi, N., Rasouliha, B. H. & Chang, M. W. A predicted S-type pyocin shows a bactericidal activity against clinical *Pseudomonas aeruginosa* isolates through membrane damage. *FEBS Lett.* **584**, 3354–3358. https://doi.org/10.1016/j.febslet.2010.06.021 (2010).
12. Ghequire, M. G. & De Mot, R. Ribosomally encoded antibacterial proteins and peptides from *Pseudomonas*. *FEMS Microbiol. Rev.* **38**, 523–568. https://doi.org/10.1111/1574-6976.12079 (2014).
13. Scholl, D. & Martin, D. W. Antibacterial efficacy of R-type pyocins towards *Pseudomonas aeruginosa* in a murine peritonitis model. *Antimicrob. Agents Chemother.* **52**, 1647–1652. https://doi.org/10.1128/AAC.01479-07 (2008).
14. Kohler, T., Donner, V. & van Delden, C. Lipopolysaccharide as shield and receptor for R-pyocin-mediated killing in *Pseudomonas aeruginosa*. *J. Bacteriol.* **192**, 1921–1928. https://doi.org/10.1128/JB.01459-09 (2010).
15. Matsui, H., Sano, Y., Ishihara, H. & Shinomiya, T. Regulation of pyocin genes in *Pseudomonas aeruginosa* by positive (prtN) and negative (prtR) regulatory genes. *J. Bacteriol.* **175**, 1257–1263. https://doi.org/10.1128/jb.175.5.1257-1263.1993 (1993).
16. Lu, Q. *et al. Pseudomonas aeruginosa* serotypes in nosocomial pneumonia: Prevalence and clinical outcomes. *Crit. Care* **18**, R17. https://doi.org/10.1186/cc13697 (2014).
17. Farmer, J. J. 3rd. & Herman, L. G. Epidemiological fingerprinting of *Pseudomonas aeruginosa* by the production of and sensitivity of pyocin and bacteriophage. *Appl. Microbiol.* **18**, 760–765. https://doi.org/10.1128/am.18.5.760-765.1969 (1969).
18. Rampling, A., Whitby, J. L. & Wildy, P. Pyocin-sensitivity testing as a method of typing *Pseudomonas aeruginosa*: Use of "phage-free" preparations of pyocin. *J. Med. Microbiol.* **8**, 531–541. https://doi.org/10.1099/00222615-8-4-531 (1975).
19. Fyfe, J. A., Harris, G. & Govan, J. R. Revised pyocin typing method for *Pseudomonas aeruginosa*. *J. Clin. Microbiol.* **20**, 47–50. https://doi.org/10.1128/jcm.20.1.47-50.1984 (1984).
20. Bird, T. J. & Grieble, H. G. Pyocin antibiosis in chick embryos. *Antimicrob. Agents Chemother. (Bethesda)* **9**, 495–498 (1969).
21. Haas, H., Sacks, T. & Saltz, N. Protective effect of pyocin against lethal *Pseudomonas aeruginosa* infections in mice. *J. Infect. Dis.* **129**, 470–472. https://doi.org/10.1093/infdis/129.4.470 (1974).
22. Six, A. *et al.* Pyocin efficacy in a murine model of *Pseudomonas aeruginosa* sepsis. *J. Antimicrob. Chemother.* **76**, 2317–2324. https://doi.org/10.1093/jac/dkab199 (2021).
23. Williams, S. R., Gebhart, D., Martin, D. W. & Scholl, D. Retargeting R-type pyocins to generate novel bactericidal protein complexes. *Appl. Environ. Microbiol.* **74**, 3868–3876. https://doi.org/10.1128/AEM.00141-08 (2008).
24. Gebhart, D. *et al.* A modified R-type bacteriocin specifically targeting *Clostridium difficile* prevents colonization of mice without affecting gut microbiota diversity. *MBio* https://doi.org/10.1128/mBio.02368-14 (2015).
25. Gebhart, D. *et al.* Novel high-molecular-weight, R-type bacteriocins of *Clostridium difficile*. *J. Bacteriol.* **194**, 6240–6247. https://doi.org/10.1128/JB.01272-12 (2012).
26. Alqahtani, A. *et al.* Recombinant R2-pyocin cream is effective in treating *Pseudomonas aeruginosa*-infected wounds. *Can. J. Microbiol.* **67**, 919–932. https://doi.org/10.1139/cjm-2021-0207 (2021).
27. Liu, J., Chen, P., Zheng, C. & Huang, Y. P. Characterization of maltocin P28, a novel phage tail-like bacteriocin from *Stenotrophomonas maltophilia*. *Appl. Environ. Microbiol.* **79**, 5593–5600. https://doi.org/10.1128/AEM.01648-13 (2013).
28. Patz, S. *et al.* Phage tail-like particles are versatile bacterial nanomachines—A mini-review. *J. Adv. Res.* **19**, 75–84. https://doi.org/10.1016/j.jare.2019.04.003 (2019).
29. Penterman, J. *et al.* Rapid evolution of culture-impaired bacteria during adaptation to biofilm growth. *Cell Rep.* **6**, 293–300. https://doi.org/10.1016/j.celrep.2013.12.019 (2014).

30. Davis, M. R. Jr. *et al.* Identification of the mutation responsible for the temperature-sensitive lipopolysaccharide O-antigen defect in the *Pseudomonas aeruginosa* cystic fibrosis isolate 2192. *J. Bacteriol.* **195**, 1504–1514. https://doi.org/10.1128/JB.01999-12 (2013).
31. Redero, M., Aznar, J. & Prieto, A. I. Antibacterial efficacy of R-type pyocins against *Pseudomonas aeruginosa* on biofilms and in a murine model of acute lung infection. *J. Antimicrob. Chemother.* https://doi.org/10.1093/jac/dkaa121 (2020).
32. Redero, M. *et al.* Susceptibility to R-pyocins of *Pseudomonas aeruginosa* clinical isolates from cystic fibrosis patients. *J. Antimicrob. Chemother.* **73**, 2770–2776. https://doi.org/10.1093/jac/dky261 (2018).
33. Hernandez-Garcia, M. *et al.* Distinct epidemiology and resistance mechanisms affecting ceftolozane/tazobactam in *Pseudomonas aeruginosa* isolates recovered from ICU patients in Spain and Portugal depicted by WGS. *J. Antimicrob. Chemother.* **76**, 370–379. https://doi.org/10.1093/jac/dkaa430 (2021).
34. Overbeek, R. *et al.* The SEED and the Rapid Annotation of microbial genomes using Subsystems Technology (RAST). *Nucleic Acids Res.* **42**, D206-214. https://doi.org/10.1093/nar/gkt1226 (2014).
35. Gabler, F. *et al.* Protein sequence analysis using the MPI bioinformatics toolkit. *Curr. Protoc. Bioinform.* **72**, e108. https://doi.org/10.1002/cpbi.108 (2020).
36. Winsor, G. L. *et al.* Enhanced annotations and features for comparing thousands of *Pseudomonas* genomes in the *Pseudomonas* genome database. *Nucleic Acids Res.* **44**, D646-653. https://doi.org/10.1093/nar/gkv1227 (2016).
37. Sullivan, M. J., Petty, N. K. & Beatson, S. A. Easyfig: A genome comparison visualizer. *Bioinformatics* **27**, 1009–1010. https://doi.org/10.1093/bioinformatics/btr039 (2011).
38. Alikhan, N. F., Petty, N. K., Ben Zakour, N. L. & Beatson, S. A. BLAST ring image generator (BRIG): Simple prokaryote genome comparisons. *BMC Genomics* **12**, 402. https://doi.org/10.1186/1471-2164-12-402 (2011).
39. Raya, R. R. & H'Bert, E. M. Isolation of phage via induction of lysogens. *Methods Mol. Biol.* **501**, 23–32. https://doi.org/10.1007/978-1-60327-164-6_3 (2009).

Acknowledgements

This study was financed by grant PI19/00878 and PI22/00323 awarded to M. Tomás within the State Plan for R+D+I 2013-2016 (National Plan for Scientific Research, Technological Development and Innovation 2008-2011) and co-financed by the ISCIII-Deputy General Directorate for Evaluation and Promotion of Research—European Regional Development Fund "A way of Making Europe" and Instituto de Salud Carlos III FEDER, Spanish Network for the Research in Infectious Diseases (REIPI, RD16/0016/0006 and CIBER CB21/13/00084), and by the Study Group on Mechanisms of Action and Resistance to Antimicrobials, GEMARA (SEIMC, http://www.seimc.org/). M. Tomás was financially supported by the Miguel Servet Research Programme (SERGAS and ISCIII). I. Bleriot was financially supported by the pFIS program (ISCIII, FI20/00302). O. Pacios and M. López were financially supported by grant IN606A-2020/035 and IN606C-2022/002, respectively (GAIN, Xunta de Galicia).

Author contributions

L.B., developed the experiments, analysed the results and wrote the original manuscript. M.G.A, C.O-C., I.B, O.P., M.L., L.F.-G., A.B.-P., M.H.G., visualization the results and manuscript. R.C.., M.T., re-written the manuscript, financed and directed the experiments and supervised the writing of the original manuscript.

Competing interests

The authors declare no competing interests.

Additional information

Supplementary Information The online version contains supplementary material available at https://doi.org/10.1038/s41598-022-27341-1.

Correspondence and requests for materials should be addressed to M.T.

Reprints and permissions information is available at www.nature.com/reprints.

Publisher's note Springer Nature remains neutral with regard to jurisdictional claims in published maps and institutional affiliations.

4. DISCUSSION

P. aeruginosa poses a significant global public health threat, primarily due to its combination of AMR and the production of virulence factors. Moreover, its highly versatile metabolism and remarkable adaptability enable this species to colonize a wide range of environments, contributing to its widespread dissemination and persistence in both biotic and abiotic settings. This capability is facilitated by its exceptional genomic plasticity, which allows for the accumulation of chromosomal mutations and the acquisition of exogenous DNA. Among the hotspots for genomic plasticity, the accessory genome- and more specifically prophages and genomic islands- contribute the most to genomic variability in *P. aeruginosa* (28).

On the other hand, when it comes to analyzing prophages in bacterial genomes through bioinformatic tools, some of them can mistakenly identify PTLBs as temperate phages due to their structural similarities. This was observed as an opportunity to study these ejective machineries, which as prophages, are often overlooked in the literature.

4.1. Prophage abundance

Regarding phages, although virulent *Pseudomonas* phages have been extensively researched for phage therapy as substitutes or adjuvants for traditional antimicrobials, their temperate counterparts remain understudied. Given the additional attributes that prophages provide to the parasitized bacterium -such as the production of toxins, antibiotic resistance, and the promotion of biofilm formation, bacterial fitness or tissue colonization- its analysis should not be missed when it comes to bacterial characterization (281).

In the first work of this thesis (Study 1) we showed that prophages are present in the majority of the *P. aeruginosa* circulating strains in nosocomial settings in Portugal and Spain. In only 7/53 (13.2%) clinical strains isolated from patients admitted to ICU in the Iberian Peninsula, no intact prophage -as given by the PHASTER tool- was detected. The actual number of strains not harboring any prophage could be even lower if we analyzed closed genomes, obtained by a combination of short- and long-read sequencing, since some prophages could be split into contigs and therefore not be detected by the prophage analyzing tools. However, for this study only short reads were used. For the lysogenized strains, 14/53 carried one prophage (26.4%), 11/53 carried two prophages (20.8%), 8/53 had 3 prophages (15.1%), 12/53 harbored 4 prophages (22.6%) and in 1/53 strain up to 5 prophages were found (1.9%). This shows how lysogenized bacteria might be often parasitized by more than one temperate phage simultaneously.

For the second work of this thesis (Study 2), a combination of both short- and long-reads was used to assemble the bacterial genomes, rendering an average of 2.2 contigs per genome. This was almost a thousand times lower than the number of contigs obtained only through short-read sequencing in Study 1 (1,601.8 contigs/genome), allowing for a better identification and characterization of prophages. For the genomes analyzed in Study 2, all *P. aeruginosa* strains harbored prophages as per the VIBRANT tool, with 3/9 strains bearing 6 prophages, 4/9 bearing 7 prophages and a single strain carrying up to 8 prophages. This number is considerably higher than the number of temperate phages found in Study 1 strains, possibly due to the more fragmented genomes used in the latter work and to the higher capacity of the *P. aeruginosa* ST773 clone from Study 2 to acquire exogenous genetic material. In a recent study published in

2022 analyzing 5,383 *P. aeruginosa* genomes of both human and environmental origins, a total of 6,852 intact prophages were detected, rendering an average of 1.3 prophages/genome (282). This supports our belief that the nosocomial strains from our studies did in fact contain a relatively higher number of prophages when compared to other studies.

Altogether, these results show how lysogeny is a common trait among *P. aeruginosa* strains, especially in those of nosocomial origin.

4.2. Prophage relatedness

Regarding the relatedness of phages, in Study 1 we could verify that different *P. aeruginosa* strains isolated in different Portuguese and Spanish hospitals sometimes had identical prophages. There was a total of 13 prophages present in more than one strain simultaneously, with all of them belonging to the class Caudoviricetes, which groups all tailed bacterial and archaeal phages with dsDNA packed into an icosahedral capsid (210). Moreover, the majority of them (10/13) were members of the siphovirus tail morphology group, having the remaining 3 a podovirus (2/13) and myovirus (1/13) tail morphology. The predominance of the siphovirus tail morphology group has already been described for prophages in *P. aeruginosa* genomes (282).

In addition, in Study 1 phages vB_PaeM-D14A, vB_PaeS-D14B, vB_PaeS-D14C, and vB_PaeS-D14F were the most abundant prophages, found in more than 10/53 *P. aeruginosa* isolates from Portuguese and Spanish hospitals. When analyzing the maximum likelihood phylogenetic tree based on each phage's terminase large subunit, it could be seen that prophages belonging to the podovirus tail morphology group (vB_PaeP-D14I and vB_PaeP-D14S) clustered together, separated from the rest of the collection (Study 1, FIGURE 1A). Attending to their geographical distribution, prophages vB_PaeS-D14O, vB_PaeS-D14P, and vB_PaeS-D14Q were found to be circumscribed to Spanish regions, being the remaining 10 prophages found mainly in Portuguese isolates. Interestingly, despite the geographical proximity to Portugal, prophages found at the A Coruña region resembled more similar to other Spanish regions (Study 1, FIGURE 1B). No common prophages were identified between Studies 1 and 2, highlighting the diverse nature of these entities.

When comparing clonal distribution, among the collection of 53 *P. aeruginosa* strains from patients admitted to ICUs in Portugal and Spain from Study 1, the most prevalent ST was found to be ST235 (n=14), followed by ST175 (n=10) and ST224 (n=7). This is consistent with the existing literature, with STs 235 and 175 being the most frequent high-risk clones in Portugal and Spain, respectively (188–190). For Study 2, all isolates belonged to the same clone, the ST773. With this information, correlation between the *P. aeruginosa* ST and their prophage content was studied. In the collection of 53 *P. aeruginosa strains*, ST235 was found to be the most prevalent (n = 14), followed by ST175 (n = 10) and ST244 (n = 7). For ST235, prophages vB_PaeM-D14A and vB_PaeS-D14C were found in 13/14 strains, prophage vB_PaeS-D14B in 12/14 and prophage vB_PaeS-D14F in 10/14. The only four pandrug-resistant strains out of the 53, all of them belonging to the ST235, were found to simultaneously harbor phages vB_PaeM-D14A, vB_PaeS-D14B, and vB_PaeS-D14C. Interestingly, the only single strain of the ST235 which did not harbor any of these prophages was also the only ST235 strain which did not carry the GES-13 β-lactamase. This isolate also presented point mutations in genes associated with AMR, such as the membrane porine oprD and the efflux pumps' genes *mexY* and *muxC* that the rest of the strains of the same

sequence type did not have. Efflux pumps and porins constitute phage receptors, and mutations on these proteins could explain the differential carriage of prophages. However, the number of isolates was not big enough to develop association analyses. In the strains belonging to the ST175 (n = 10), however, more diversity in prophage arrangement was found. Although all of the 10 strains coded for at least one of the prophages under study, the distribution of the phages (vB_PaeS-D14K, vB_PaeS-D14O, vB_PaeS-D14P, and vB_PaeS-D14Q) was uneven. The same appears to happen with ST244, in which prophages vB_PaeS-D14H, vB_PaeP-D14I, vB_PaeS-D14L, and vB_PaeP- D14S were found to be distributed without a clear association (Table 4).

On the other hand, since all of the strains analyzed in Study 2 had a same clonal origin, it is not surprising the similarities among the prophages they harbor, expecting the different isolates to carry the same prophages. However, the prophage content was in fact the only significant difference between those almost identical genomes, highlighting how these regions can be the most plastic ones in the bacterial chromosome. A total of 11 unique prophages were identified among the nine NDM-1-ST773-*P. aeruginosa* strains from Ukrainian patients, the majority of them (10/11) present in more than one bacterial isolate simultaneously. Some prophages were carried in multiple copies, as it is the case of the isolate ESP_2, which harbored three copies of vB_Pae_U4, and the isolate NDL_2, which had two copies of the vB_Pae_U7 prophage. This is a phenomenon that we did not observe in Study 1, where all prophages were carried in single copies. Chromosomal rearrangements or a simultaneous integration of several prophage copies are more feasible possibilities than a first infection followed by a second one, due to the protection to infection that a prophage confers to the lysogen, known as superinfection exclusion (245). Regarding tail morphology, no terminase large subunit was identifiable for phages vB_Pae_U1 and vB_Pae_U10, and no homology with the BLAST database was found for the terminases of phages vB_Pae_U3, vB_Pae_U5, vB_Pae_U6, vB_Pae_U8 and vB_Pae_U9. This hampered the correct identification of the species or the tail morphology group. Thus, a different approach than in Study 1 was used, combining a phylogenetic tree of these prophages and the prophages within the Virus-Host database using ViPTree 3.7. and a posterior confirmation to assess if phages clustered together were of the same genus by using VIRIDIC. This way, 5/11 prophages were classified as members of the siphovirus tail morphology group, being able to assign to three of them a genus: *Casadabanvirus* for phage vB_Pae_U4; *Detrevirus* for phage vB_Pae_U7; and *Beetrevirus* for phage vB_Pae_U11. The resting 6 prophages were grouped as unclassified Caudoviricetes.

4.3. Prophage insertion sites

While some temperate phages transpose randomly into the bacterial chromosome, others insert at given regions through site-specific recombination (283). Prophage integration into the bacterial genome can be an important event for bacterial fitness, since it can truncate key genes when it occurs in the middle of an ORF and operons when it happens between related genes. In Study 1, we were able to locate the prophage insertion sites within the bacterial chromosome in 7/13 cases (Study 1, Figure 4). Three phages (vB_PaeM-D14A, vB_PaeP-D14I, and vB_PaeS-D14L) were inserted before, between or after host tRNA coding sequences, and since all of the sequences were intact, it could be speculated that the prophage integration did not affect their integrity. This was especially relevant for phage vB_PaeM-D14A, where the attR/L sequence was identified within the tRNA-Thr-TGT gene. This suggests that the prophage carried a duplicate of

the gene, allowing its integration to replace the truncated version, a finding consistent with earlier studies (283). Similarly, in Study 2 more than half (6/11) of the prophages were inserted next to tRNA coding genes (Study 2, Table 3).

Interestingly, in some cases different phages from both studies had the same insertion sites. It is the case of prophage vB_PaeS-D14L from Study 1 and prophage vB_Pae_U5 from Study 2, which share the tRNA-Leu-CAA gene as their insertion site; prophages vB_PaeS-D14B and vB_Pae_U2 from Studies 1 and 2 respectively, which integrate next to a HigA antitoxin encoding gene; and prophages vB_Pae_U5 and vB_Pae_U6 from Study 2 which insert next to a tRNA-Gly-CC encoding gene. This supports the idea of some chromosomal regions being hotspots for prophage acquisition. Regarding the antitoxin HigA, it should also be noted that it is usually arranged downstream its cognate toxin (HigB), but in neither of the lysogens of both studies the toxin could be localized. This could indicate that prophage integration might have cleared the HigB toxin, promoting bacterial survival (284).

It is also noteworthy that some genes were in fact truncated upon the insertion of the prophage in the midst of their corresponding ORF. In Study 1, a glyoxylate carboligase encoding gene, responsible for the metabolism of glyoxylate, was interrupted by the vB_PaeS-D14F prophage; whereas in Study 2 it was the T1SS component LapE, the class III aminotransferase, a bacteriocin ABC transporter and a glycosyltransferase by prophages vB_Pae_U3, vB_Pae_U4, and vB_Pae_U10 respectively. The implications of the loss of function of these genes remain unknown.

Finally, in 5/13 prophages from Study 1 we could not identify the prophage insertion sites due to the fragmentation of the bacterial genome into hundreds or thousands of contigs. The consequence was having isolated sequences corresponding to a prophage representing a whole contig, without any identifiable flanking genes. This issue was addressed in Study 2, where all genomes were also sequenced using long reads and all of the prophage flanking genes were identified.

4.4. Prophage composition

In Study 1, prophages had a length ranging from 20.2 kb (prophage vB_PaeS-D14Q) to 63.4 kb (prophage vB_PaeP-D14I). This is comparable to Study 2, where prophages had an extension between 10.5 kb and 57.8 kb (prophages vB_Pae_U10 and vB_Pae_U7). In all of the cases, their genome length had an extension inside the limits of what is expected for dsDNA tailed bacteriophages, between 17 and 498 kb (285). No Jumbo phages (>200 kb) were found in any of the studies (286).

Regarding their GC content, in Study 1 it was found to be between 56.2% (prophage vB_PaeS_D14O) and 63.6% (vB_PaeP-D14I), very similar as in Study 2 (between 58.9% for prophage vB_Pae_U7 and 64.4% for prophage vB_Pae_U4). Such differences with their host's GC content (65 – 67% for *P. aeruginosa*) indicate an exogenous origin of the prophages and correlate with a recent acquisition. This highlights the dynamic nature of temperate phages, allowed by the characteristic genome plasticity in *P. aeruginosa* (287).

When analyzing the number of genes per prophage, it ranged from 32 ORF (prophage vB_PaeS-D14Q) to 88 ORF (vB_PaeS-D14O) in Study 1, and from 13 ORF (vB_Pae_U10) to 103 ORF

(vB_Pae_U7) in Study 2. After annotation, 3/13 prophages in Study 1 and 9/11 prophages in Study 2 had over 50% of their ORFs classified as hypothetical proteins. This percentage is remarkably high when compared to the number of unassigned ORFs in the whole bacterial chromosome, estimated to be around 10% in *E. coli* (288) and 17.6% (1,050 out of 5975) in *P. aeruginosa* PAO1, as for our annotations. These findings are consistent with previous studies, which highlight not only the large number of unknown phages sequenced within metagenomic data -often termed viral dark matter- but also the abundance of putative proteins with unknown functions (289–291). In this regard, further studies decrypting bacteriophage gene function should be made in order to unravel the mechanisms underlying viral regulation, replication and interactions with their host.

4.5. PTLBs

In the third work of this thesis, Study 3, we analyzed the genomic sequences of 32 *P. aeruginosa* strains from critical care patients in Spain and Portugal, finding a PTLB or a PTLB cluster in each of them. These strains could be grouped into 4 classes (A-D) attending to their pyocin subtype, GC content and ORF number. Interestingly, great differences were observed among strains depending on their country of origin, with Spanish isolates characterized by an R5 PTLB flanked by 3 lytic proteins (Class B). On the other hand, Portuguese strains showed more variability when it came to PTLB arrangement: Class A pyocins showed an R5 PTLB flanked by 4 lytic proteins and Classes C and D consisted on an R2-type PTLB followed by an F2 and F(PA14) PTLB, respectively (Study 3, Figure 1). This same division into classes was observed in a phylogenetic tree upon sequence alignment, with each class representing a clade (Study 3, Figure 3).

On the other hand, in 9/9 strains from Study 2 and identical PTLB cluster was found, in contrast with the prophage variability we observed among strains of the same clone. Its structure was conserved, with upstream regulatory genes, an R-type PTLB, a 4-gene lysis cassette and an F-type PTLB (Study 2, Supplementary Figure S4). The R pyocin was classified as R5 by sequence homology of the tail fiber, and the F pyocin did not share homology with any previously described F-type PTLB.

When comparing PTLBs from both studies, a clear association between the host's ST and the PTLB they produced was found. In Study 2, all R5 PTLBs belonging to class A belonged to the ST235; R5 PTLBs from class B to ST175 and ST309; R2-F2 PTLBs from class C to ST348 and ST554; and finally, R2-F(PA14) from class D to ST244. In Study 3, all strains belonged to the ST773 and produced an identical pyocin cluster. However, this relation could not be found with the host's serotype (Study 3, Table 1). This suggests that pyocin genomic analysis can be a better typing tool than the serotype itself (292).

Regarding PTLB killing spectrum, it was irrespective of the pyocin class, with PTLBs from different classes with similar host ranges and PTLBs from similar classes with diverse host ranges (Study 3, Figure 5). As expected, in Study 3 the PTLB producing strain was resistant to the killing action of its own pyocin in all cases, and for this reason no killing spectrum experiment was performed for Study 2, in which all strains produced the same PTLBs.

Finally, all of the PTLBs from Studies 2 and 3 were located into the tryptophan operon, between the *trpE* and *trpG* genes, as previously described (272).

4.6. Perspective on prophages, phage morons, and phage therapy

Phage morons are genes encoded by prophages which can be transcribed despite the quiescent state of these entities, unlike the rest of the viral genes which remain repressed (293). When lysogenic phages parasitize a bacterium, their survival becomes tightly linked to their host's. In the context of a continuous arms race between bacteria and phages, prophages -and more importantly their morons- can serve as valuable allies against strictly lytic phages. Prophages can also be crucial for bacterial fitness, with morons being able to interfere with bacterial motility and adhesion, to modify their host's metabolism, or even to enhance antibiotic resistance.

In Study 1 we were able to identify 7 novel anti-CRISPR proteins in 7 different prophages. Two of them were identified by homology with already described proteins which directly inhibit the HNH endonuclease activity of Cas9, and the remaining 5 were simultaneously detected by two different bioinformatic tools (PaCRISPR and ACRFinder). In Study 2, phage vB_Pae_U4 was found to carry an anti-CRISPR protein with homology with AcrIF3. Prophages can carry these genes to defend themselves from the host's CRISPR-Cas system, and therefore escaping the autoimmunity which would represent the bacterium targeting its own chromosome (294). Moreover, although CRISPR-Cas systems protect bacteria from invading phages, they also avoid the acquisition of other mobile genetic elements, limiting bacterial adaptation. On average, *P. aeruginosa* clinical isolates with active CRISPR-Cas systems have approximately 300kb smaller genomes (295). In addition, 8/13 prophages in Study 1 and 3/12 prophages in Study 2 coded for DNA methyltransferases, which mask viral DNA to protect it from the host's restriction enzymes. Prophage morons inactivating these two systems can promote exogenous DNA uptake and enhance bacterial fitness.

Regarding T/A systems, in Study 1 we observed that 2/13 prophages coded for complete T/A sets, 2/13 coded for the toxin alone, and other 2/13 coded for solitary antitoxins. Recent evidence supports the defensive role of these systems in phage infection, arresting bacterial growth when toxins are produced -or antitoxins degraded- and therefore preventing phage replication. In this context, it seems feasible that phages can carry complete systems to defend their host from further phage infection, toxins alone to limit cell growth and help their host transition to a chronic or persister state, or antitoxins alone to counteract the host's toxins. In Study 2, no T/A systems were detected.

Another type of morons detected in the prophages from Study 1 were QS receptors. Transcriptional regulators from the LuxR family were found in prophages vB_PaeS-D14B, vB_PaeS-D14E, and vB_PaeS-D14L, and prophages vB_PaeM-D14A, vB_PaeS-D14C, and vB_PaeS-D14O coded for transcriptional regulators from the TraR family. Although the role of these regulators is yet to be clarified, having QS receptors could mean that phages are able to listen to -but not to speak- the interspecies communication of their bacterial hosts. If phages can sense bacterial density they could also act accordingly, leaning toward the activation of the lytic cycle when their prey is abundant or favoring a lysogenic cycle when their host is scarce. This way, the phage would never completely erase a bacterial population, ensuring its own survival (296).

Finally, no AMR genes and no virulence toxins with activity against the human hosts were detected in either Studies 1 or 2. However, a potential DNA gyrase inhibitor with homology with YacG in *E. coli* was detected in prophage vB_PaeP-D14I (Study 1).

In sum, a myriad of anti-phage mechanisms can be coded by prophage morons in *P. aeruginosa* clinical strains, affecting the ability of virulent phages to infect their hosts. This can difficult the process of finding effective lytic phages for phage therapy, specially taking into account that prophages are more frequent in pathogens, which are usually polylysogens (297–299). Furthermore, many phage hunting protocols include an enrichment step in which the sample which is screened for phages is pre-incubated with the target strain (300–302). However, if the target strain harbors prophages, as it is the case of the majority of our *P. aeruginosa* clinical strains, it is highly discouraged to use it, being the main reasons: 1) the cross-contamination of the virulent phage preparations with temperate phages from the target strain; 2) the difficulty to differentiate plaques caused by prophage activation from the ones originated by the candidate virulent phages, and 3) the potential recombination events that can occur between the virulent and temperate phages (303). For those reasons, phages have to be previously isolated using surrogate hosts of the same species that do not carry prophages and then tested against the desired prophage-bearing hosts, in a time-consuming screening process.

However, it should also be noted that the carrying of prophages is not always detrimental for treatment. Subinhibitory concentrations of antibiotics, such as β-lactams or quinolones, have been shown to cause the activation of the lytic cycle of prophages, resulting in the death of the lysogen cells (304, 305). In this sense, a new innovative treatment alternative to traditional antibiotics has been proposed against MDR bacteria: prophage induction. This strategy seeks to activate the target bacterium's temperate phage lytic cycle through molecules that interact with prophage repressors -such as cI, cII, or Cro (306, 307)-. For these purposes, more efforts to study the characteristics, abundance and dynamics of prophages should be made.

4.7. Resistome

In Study 1, a collection of 28 C/T resistant and 25 susceptible *P. aeruginosa* isolates was analyzed. Among the resistant ones, 13/28 isolates produced GES-13 carbapenemases, 9/28 produced VIM carbapenemases and in 6/28 no carbapenemase-coding gene was detected. As expected, all of these isolates were resistant to antipseudomonal β-lactams, with the exception of aztreonam in the metallo-β-lactamase producers and piperacillin/tazobactam in the VIM-20 producers. Interestingly, the number of intact prophages was greater in carbapenemase-producing strains (average of 3.0 prophages/strain) than in C/T resistant non carbapenemase-producing strains (average of 1.8 prophages/strain) and even greater than in C/T susceptible strains (average of 1.4 prophages/strain). This relationship between prophages and carbapenemases could be explained by the increased genomic plasticity of certain clones, such as the high-risk clone ST235, which makes bacteria more prone to acquiring mobile genetic elements such as phages or plasmids encoding AMR genes. Moreover, the only four PDR isolates in the collection -all of them belonging to the ST235- were found to simultaneously harbor prophages vB_PaeM-D14A, vB_PaeS-D14B, and vB_PaeS-D14C. It should also be noted that out of the 53 strains of the collection, 7 of them did not carry any intact prophage as analyzed by PHASTER, belonging 6 of them to the C/T susceptible group and reinforcing the association between antibiotic resistance and prophage harboring. In Study 2, all of the strains belonged to the ST773 and had a same

clonal origin, which explains why all of them had the same antibiotic susceptibility profiles, being only susceptible to colistin, aztreonam, and cefiderocol. As seen in Study 1, the number of prophages per genome in these resistant isolates was significantly higher (6-8 intact prophages/genome).

4.8. International collaboration and stewardship

The monitoring of MDR bacteria can serve both to understand the current epidemiological situation and to take preventive measures in consequence. On the one hand, the collection of data by international organisms, such as the European Antimicrobial Resistance Surveillance Network (EARS-Net) (308), can play a crucial role in increasing awareness among policymakers, public health authorities, the scientific community, and the general public. On the other hand, understanding the genomic background of the main bacterial pathogens in the local medical setting can help in the selection of an empirical antibiotic treatment, the combination of different synergistic antimicrobials, or, given the case, the development of future antimicrobial compounds.

For these purposes, international collaboration between Microbiology laboratories worldwide is essential. The collection of bacterial strains with highly resistant phenotypes begins in clinical microbiology laboratories, and genome analysis enables the understanding of their resistance patterns and transmission dynamics. In Studies 1 and 2, the genomic data was collected from 11 hospitals in 8 Portuguese cities (Lisboa, Matosinhos, Porto, Aveiro, Amadora, Almada, Faro, and Coimbra) (309) and 8 facilities from 7 Spanish cities (Madrid, Barcelona, Seville, Santander, La Coruña, Valencia and Palma de Majorca) (310). In Study 3 we were able to trace the dissemination of NDM-producing *P. aeruginosa* strains with a common clonal origin from Ukrainian healthcare centers to Dutch and Spanish hospitals. Moreover, this same clone was detected in a German facility unrelated to this study, as seen by the cgMLST analysis. An early detection of these isolates, encouraged by ECDC recommendations on MDR screening in patients transferred from Ukraine, allowed for an adequate antibiotic treatment and the instauration of preventive measures to avoid the intrahospital transmission of this pathogen.

In conclusion, the genomic analysis of the different *P. aeruginosa* nosocomial isolates in Studies 1, 2 and 3 responds to the need to monitor the virulence and antibiotic resistance profiles of the main nosocomial pathogens worldwide. In a globalized world, being able to detect in time transmissible public health threats such as high-risk clones, understanding how to adequately treat them, and preventing future infections will be necessary to ensure the free movement of people. The three studies that compose this thesis have been possible thanks to the international collaboration between different European nations (Portugal, The Netherlands, Ukraine, and Spain) and have helped us in understanding this ubiquitous pathogen, which certainly does not know about borders.

4.9. Limitations and future directions

While this research provides valuable insights into the prophage and PTLB characteristics within the genomes of *P. aeruginosa* clinical strains, it also presents some limitations. In the first place, and as explained above, for Study 1 only short reads obtained through Illumina sequencing were used, yielding an average of 1,601.8 contigs per genome. Such fragmented genomes can pose a limitation for the detection of prophages by bioinformatic tools, given the possibility that some

prophages could be split across different contigs. This could also affect the estimated length of the analyzed prophages, as 5 out of 13 prophages identified in this study comprised the entire contig, making it impossible to identify the prophage boundaries. Therefore, it could not be ruled out that additional ORFs belonging to these prophages were missed during sequencing. Moreover, for 6 out of 13 prophages, it was not possible to localize them within the bacterial chromosome, preventing the detection of whether the insertion of the prophage had disrupted any bacterial gene, and thus making it impossible to assess its effect on bacterial fitness. In general, short read sequencing by itself can present limitations when it comes to mapping MGE such as plasmids or phages due to the presence of long repetitive regions or palindromic and GC-enriched elements (311, 312). This issue was successfully addressed in Study 2, where a combination of both short- and long-reads was used to assemble the bacterial genomes, rendering an average of 2.2 contigs per genome, allowing for a better identification and characterization of prophages.

It should also be noted that different prophage-seeking tools were used in our two studies. Whereas PHASTER was chosen for Study 1, the VIBRANT tool was employed in Study 2. This change in the methodology responds to a study carried out between both publications in which we showed how the VIBRANT tool was able to identify more prophages than PHASTER in the genomes of clinical and environmental *Serratia marcescens* strains, although after annotation some of them resulted to be incomplete prophages. This higher sensitivity postulates VIBRANT as a better tool for prophage screening as long as the obtained prophages are annotated and curated to eliminate the incomplete ones. These results were presented in the XXVI National Congress of the Spanish Society for Infectious Diseases and Clinical Microbiology (ANNEX 1). Taking these differences between bioinformatic tools into account, we used the PHASTER tool with the *P. aeruginosa* ST773 strains to confirm the higher content in prophages of these strains, obtaining similar results as with VIBRANT (ANNEX 2). This confirmed us that the differences in the number of prophages per genome between Studies 1 and 2 did not attend to the different tools used.

Another factor that could have underestimated the total number of prophages is the limitation found for the different bioinformatic tools -PHASTER and VIBRANT, indistinctively- to identify filamentous phages such as Pf1, Pf4 or Pf5 (282). Given their short genomes (7.3 – 13 kb), automatic tools for prophage identification often fail to detect them. In Study 1, the shortest prophage detected using PHASTER was 20kb long, and no filamentous phage was identified (Study1, Table 2). In Study 3, the shortest prophage found by VIBRANT had a length of 10.5kb, within the filamentous phage range, but none of these entities was found (Study 2, Table 3). However, when manually searching for characteristic genes from filamentous phages- such as the coat proteins A and B, the zonular occludens toxin family protein or the DUF2523 gene- this kind of prophages were found (ANNEX 3).

Finally, it would be very enriching to delve into the functionality of prophage morons and its impact into bacterial fitness. As commented above, after annotation 3/13 prophages in Study 1 and 9/11 prophages in Study 2 had over 50% of their ORFs classified as hypothetical proteins. Given the fact that phages tend to economize their genomes, it is unlikely that they accumulate non-functional or 'junk' DNA. Therefore, it is reasonable to assume that most, if not all, of the ORFs they contain serve some function, even if that function remains unknown at present (289–

291). More studies analyzing the mRNA expression of these genes upon incubation with QS inducers, QQ enzymes and different stressors (UV light, extreme temperatures, nutrient starvation, or antibiotic subinhibitory concentrations) could be developed to shed some light into this matter.

5. CONCLUSIONS

1. Prophages are widely distributed in *P. aeruginosa* strains, particularly in nosocomial settings. In both studies, the majority of strains harbored at least one prophage, with some carrying up to 8.

2. The use of different prophage detection tools can yield different results. VIBRANT demonstrated a higher sensitivity, detecting a higher number of prophages, especially when dealing with fragmented genomes.

3. Prophage content varies between the different *P. aeruginosa* clones, with significant variations in their distribution and abundance. The ST773 clone exhibited a higher diversity of prophages compared to the more uniform prophage content of the analized strains belonging ST235 clone.

4. Prophages frequently integrate near tRNA genes, with some prophages truncating genes upon insertion. Prophage insertion can lead to loss of function in certain genes, which might impact bacterial metabolism and virulence.

5. A significant portion of the genes within the prophages were classified as hypothetical proteins, contributing to the “dark matter” of the viral genomes. This emphasizes the need for further functional studies to better understand the roles of these unknown proteins and their potential impact on prophage biology and host interactions.

6. Genomic analysis of *P. aeruginosa* strains revealed significant diversity in PTLB arrangements, with distinct classes observed across Spanish and Portuguese isolates. PTLB classification can be useful for bacterial typing, with each ST sharing the same PTLB composition.

7. Prophage morons, including anti-CRISPR proteins, DNA methyltransferases, and Toxin-Antitoxin (T/A) systems, can enhance bacterial survival by protecting against further phage attack and modulating bacterial metabolism and antibiotic resistance. Prophages could also act according to their host’s QS signals.

8. Prophage presence correlates with antibiotic resistance in *P. aeruginosa* isolates from nosocomial origin, particularly in carbapenemase-producing strains. Isolates with a higher genomic plasticity are able to acquire exogenous genetic material that promotes survival.

9. The presence of prophages in *P. aeruginosa* clinical strains presents both challenges and opportunities for therapeutic strategies. While prophages can hinder the isolation of virulent phages for phage therapy, they also open the door to innovative treatments such as prophage

induction. Further research into prophage biology is essential to fully exploit their potential in combating multidrug-resistant infections.

10. Global monitoring of MDR bacteria in different geographic areas is essential for understanding the epidemiology, resistance profiles, and transmission dynamics of *P. aeruginosa*. Early detection and surveillance of high-risk clones with emerging resistance are key to preventing public health threats and ensuring effective treatment strategies.

6. Bibliography

1. Samaržija D, Zamberlin Š. 2022. Psychrotrophic Bacteria: *Pseudomonas spp*. Encycl Dairy Sci Third Ed 4:375–383.

2. Parte AC, Carbasse JS, Meier-Kolthoff JP, Reimer LC, Göker M. 2020. List of prokaryotic names with standing in nomenclature (LPSN) moves to the DSMZ. Int J Syst Evol Microbiol 70:5607–5612.

3. Palleroni NJ. 2010. The *Pseudomonas* story. Environ Microbiol. Environ Microbiol.

4. Peix A, Ramírez-Bahena MH, Velázquez E. 2009. Historical evolution and current status of the taxonomy of genus *Pseudomonas*. Infect Genet Evol 9:1132–1147.

5. Crone S, Vives-Flórez M, Kvich L, Saunders AM, Malone M, Nicolaisen MH, Martínez-García E, Rojas-Acosta C, Catalina Gomez-Puerto M, Calum H, Whiteley M, Kolter R, Bjarnsholt T. 2020. The environmental occurrence of *Pseudomonas aeruginosa*. APMIS 128:220–231.

6. Khan NH, Ishii Y, Kimata-Kino N, Esaki H, Nishino T, Nishimura M, Kogure K. 2007. Isolation of *Pseudomonas aeruginosa* from open ocean and comparison with freshwater, clinical, and animal isolates. Microb Ecol 53:173–186.

7. Schroth MN, Cho JJ, Green SK, Kominos SD. 2018. Epidemiology of *Pseudomonas aeruginosa* in agricultural areas. J Med Microbiol 67:1191–1201.

8. Henry DA, Speert DP. 2022. *Pseudomonas*, p. 677–691. *In* Manual of Clinical Microbiology: Tenth Edition. University of Texas Medical Branch at Galveston.

9. Bennett JE, Dolin R, Blaser MJ. 2015. 221: *Pseudomonas aeruginosa* and other Pseudomonas species, p. 2518-2531.e3. *In* Mandell, Douglas, and Bennett's Principles and Practice of Infectious Diseases, 8th ed.

10. Rice LB. 2008. Federal funding for the study of antimicrobial resistance in nosocomial pathogens: No ESKAPE. J Infect Dis. Oxford Academic.

11. WHO. 2024. WHO bacterial priority pathogens list, 2024: Bacterial pathogens of public health importance to guide research, development and strategies to prevent and control antimicrobial resistance.

12. Alam K, Islam MM, Li C, Sultana S, Zhong L, Shen Q, Yu G, Hao J, Zhang Y, Li R, Li A. 2021. Genome Mining of *Pseudomonas* Species: Diversity and Evolution of Metabolic and Biosynthetic Potential. Molecules 26.

13. Jørgensen KM, Wassermann T, Johansen HK, Christiansen LE, Molin S, Høiby N, Ciofu O. 2015. Diversity of metabolic profiles of cystic fibrosis *Pseudomonas aeruginosa* during the early stages of lung infection. Microbiology 161:1447–1462.

14. Schwermer CU, de Beer D, Stoodley P. 2022. Nitrate respiration occurs throughout the depth of mucoid and non-mucoid *Pseudomonas aeruginosa* submerged agar colony biofilms including the oxic zone. Sci Rep 12.

15. Elkins JG, Hassett DJ, Stewart PS, Schweizer HP, McDermott TR. 1999. Protective role of catalase in *Pseudomonas aeruginosa* biofilm resistance to hydrogen peroxide. Appl Environ Microbiol 65:4594–4600.

16. Kovacs N. 1956. Identification of *Pseudomonas pyocyanea* by the Oxidase Reaction. Nat 1956 1784535 178:703–703.

17. Fukumori Y, Nakayama K, Yamanaka T. 1985. Cytochrome c oxidase of *Pseudomonas* AM 1: purification, and molecular and enzymatic properties. J Biochem 98:493–499.

18. Silvestrini MC, Falcinelli S, Ciabatti I, Cutruzzolà F, Brunori M. 1994. *Pseudomonas aeruginosa* nitrite reductase (or cytochrome oxidase): an overview. Biochimie 76:641–654.

19. Daddaoua A, Krell T, Ramos JL. 2009. Regulation of Glucose Metabolism in *Pseudomonas*: THE PHOSPHORYLATIVE

BRANCH AND ENTNER-DOUDOROFF ENZYMES ARE REGULATED BY A REPRESSOR CONTAINING A SUGAR ISOMERASE DOMAIN*. J Biol Chem 284:21360.

20. Conway T. 1992. The Entner-Doudoroff pathway: history, physiology and molecular biology. FEMS Microbiol Rev 9:1–28.

21. Rojo F. 2010. Carbon catabolite repression in *Pseudomonas*: optimizing metabolic versatility and interactions with the environment. FEMS Microbiol Rev 34:658–684.

22. Wu M, Guina T, Brittnacher M, Nguyen H, Eng J, Miller SI. 2005. The *Pseudomonas aeruginosa* Proteome during Anaerobic Growth. J Bacteriol 187:8185.

23. Arai H. 2011. Regulation and function of versatile aerobic and anaerobic respiratory metabolism in *Pseudomonas aeruginosa*. Front Microbiol 2:10255.

24. Stover CK, Pham XQ, Erwin AL, Mizoguchi SD, Warrener P, Hickey MJ, Brinkman FSL, Hufnagle WO, Kowallk DJ, Lagrou M, Garber RL, Goltry L, Tolentino E, Westbrock-Wadman S, Yuan Y, Brody LL, Coulter SN, Folger KR, Kas A, Larbig K, Lim R, Smith K, Spencer D, Wong GKS, Wu Z, Paulsen IT, Relzer J, Saler MH, Hancock REW, Lory S, Olson M V. 2000. Complete genome sequence of *Pseudomonas aeruginosa* PAO1, an opportunistic pathogen. Nat 2000 4066799 406:959–964.

25. Klockgether J, Munder A, Neugebauer J, Davenport CF, Stanke F, Larbig KD, Heeb S, Schöck U, Pohl TM, Wiehlmann L, Tümmler B. 2010. Genome Diversity of *Pseudomonas aeruginosa* PAO1 Laboratory Strains. J Bacteriol 192:1113.

26. Winsor GL, Griffiths EJ, Lo R, Dhillon BK, Shay JA, Brinkman FSL. 2016. Enhanced annotations and features for comparing thousands of *Pseudomonas* genomes in the *Pseudomonas* genome database. Nucleic Acids Res 44:D646–D653.

27. de Sousa T, Hébraud M, Enes Dapkevicius MLN, Maltez L, Pereira JE, Capita R, Alonso-Calleja C, Igrejas G, Poeta P. 2021. Genomic and metabolic characteristics of the pathogenicity in *Pseudomonas aeruginosa*. Int J Mol Sci. Int J Mol Sci.

28. Silby MW, Winstanley C, Godfrey SAC, Levy SB, Jackson RW. 2011. *Pseudomonas* genomes: diverse and adaptable. FEMS Microbiol Rev 35:652–680.

29. Strateva T, Mitov I. 2011. Contribution of an arsenal of virulence factors to pathogenesis of *Pseudomonas aeruginosa* infections. Ann Microbiol 2011 614 61:717–732.

30. Bouteiller M, Dupont C, Bourigault Y, Latour X, Barbey C, Konto-ghiorghi Y, Merieau A. 2021. *Pseudomonas* Flagella: Generalities and Specificities. Int J Mol Sci 22.

31. Bucior I, Pielage JF, Engel JN. 2012. *Pseudomonas aeruginosa* Pili and Flagella Mediate Distinct Binding and Signaling Events at the Apical and Basolateral Surface of Airway Epithelium. PLoS Pathog 8:1002616.

32. Van Schaik EJ, Giltner CL, Audette GF, Keizer DW, Bautista DL, Slupsky CM, Sykes BD, Irvin RT. 2005. DNA Binding: a Novel Function of *Pseudomonas aeruginosa* Type IV Pili. J Bacteriol 187:1455.

33. Nolan LM, Turnbull L, Katrib M, Osvath SR, Losa D, Lazenby JJ, Whitchurch CB. 2020. *Pseudomonas aeruginosa* is capable of natural transformation in biofilms. Microbiology 166:995–1003.

34. Wiener-Kronish JP, Pittet JF. 2011. Therapies against virulence products of *Staphylococcus aureus* and *Pseudomonas aeruginosa*. Semin Respir Crit Care Med 32:228–235.

35. Filloux A. 2011. Protein secretion systems in *Pseudomonas aeruginosa*: An essay on diversity, evolution, and function. Front Microbiol 2:11358.

36. Delepelaire P. 2004. Type I secretion in gram-negative bacteria. Biochim Biophys Acta - Mol Cell Res 1694:149–161.

37. Durand É, Bernadac A, Ball G, Lazdunski A, Sturgis JN, Filloux A. 2003. Type II

Protein Secretion in *Pseudomonas aeruginosa*: the Pseudopilus Is a Multifibrillar and Adhesive Structure. J Bacteriol 185:2749.

38. Wu T, Zhang Z, Li T, Dong X, Wu D, Zhu L, Xu K, Zhang Y. 2024. The type III secretion system facilitates systemic infections of *Pseudomonas aeruginosa* in the clinic. Microbiol Spectr 12.

39. Van Ulsen P, Rahman S ur, Jong WSP, Daleke-Schermerhorn MH, Luirink J. 2014. Type V secretion: From biogenesis to biotechnology. Biochim Biophys Acta - Mol Cell Res 1843:1592–1611.

40. Xiong X, Wan W, Ding B, Cai M, Lu M, Liu W. 2024. Type VI secretion system drives bacterial diversity and functions in multispecies biofilms. Microbiol Res 279.

41. Cianfanelli FR, Monlezun L, Coulthurst SJ. 2016. Aim, Load, Fire: The Type VI Secretion System, a Bacterial Nanoweapon. Trends Microbiol 24:51–62.

42. Gorman A, Golovanov AP. 2022. Lipopolysaccharide Structure and the Phenomenon of Low Endotoxin Recovery. Eur J Pharm Biopharm. Elsevier.

43. Constantino-Teles P, Jouault A, Touqui L, Saliba AM. 2022. Role of Host and Bacterial Lipids in P*seudomonas aeruginosa* Respiratory Infections. Front Immunol 13.

44. Erridge C, Bennett-Guerrero E, Poxton IR. 2002. Structure and function of lipopolysaccharides. Microbes Infect 4:837–851.

45. Kocincova D, Lam JS. 2011. Structural diversity of the core oligosaccharide domain of *Pseudomonas aeruginosa* lipopolysaccharide. Biochem. Biochemistry (Mosc).

46. Huszczynski SM, Lam JS, Khursigara CM. 2019. The Role of *Pseudomonas aeruginosa* Lipopolysaccharide in Bacterial Pathogenesis and Physiology. Pathog 2020, Vol 9, Page 6 9:6.

47. Chung J, Eisha S, Park S, Morris AJ, Martin I. 2023. How Three Self-Secreted Biofilm Exopolysaccharides of *Pseudomonas aeruginosa*, Psl, Pel, and Alginate, Can Each Be Exploited for Antibiotic Adjuvant Effects in Cystic Fibrosis Lung Infection. Int J Mol Sci. Int J Mol Sci.

48. Ma LZ, Wang D, Liu Y, Zhang Z, Wozniak DJ. 2022. Regulation of Biofilm Exopolysaccharide Biosynthesis and Degradation in *Pseudomonas aeruginosa*. Annu Rev Microbiol 76:413–433.

49. Gheorghita AA, Wozniak DJ, Parsek MR, Howell PL. 2023. *Pseudomonas aeruginosa* biofilm exopolysaccharides: assembly, function, and degradation. FEMS Microbiol Rev 47.

50. Maier RM, Soberón-Chávez G. 2000. *Pseudomonas aeruginosa* rhamnolipids: Biosynthesis and potential applications. Appl Microbiol Biotechnol 54:625–633.

51. Soberón-Chávez G, Lépine F, Déziel E. 2005. Production of rhamnolipids by *Pseudomonas aeruginosa*. Appl Microbiol Biotechnol 68:718–725.

52. Aleksic I, Petkovic M, Jovanovic M, Milivojevic D, Vasiljevic B, Nikodinovic-Runic J, Senerovic L. 2017. Anti-biofilm properties of bacterial di-rhamnolipids and their semi-synthetic amide derivatives. Front Microbiol 8.

53. Calfee MW, Shelton JG, McCubrey JA, Pesci EC. 2005. Solubility and bioactivity of the *Pseudomonas* quinolone signal are increased by a *Pseudomonas aeruginosa*-produced surfactant. Infect Immun 73:878–882.

54. García-Contreras R, Loarca D, Pérez-González C, Jiménez-Cortés JG, Gonzalez-Valdez A, Soberón-Chávez G. 2020. Rhamnolipids stabilize quorum sensing mediated cooperation in *Pseudomonas aeruginosa*. FEMS Microbiol Lett 367:80.

55. Beal R, Betts WB. 2000. Role of rhamnolipid biosurfactants in the uptake and mineralization of hexadecane in *Pseudomonas aeruginosa*. J Appl Microbiol 89:158–168.

56. Bédard M, McClure CD, Schiller NL,

Francoeur C, Cantin A, Denis M. 1993. Release of interleukin-8, interleukin-6, and colony-stimulating factors by upper airway epithelial cells: implications for cystic fibrosis. Am J Respir Cell Mol Biol 9:455–462.

57. Fung DC, Somerville M, Richardson PS, Sheehan JK. 1995. Mucus glycoconjugate complexes released from feline trachea by a bacterial toxin. Am J Respir Cell Mol Biol 12:296–306.

58. Kanthakumar K, Taylor GW, Cundell DR, Dowling RB, Johnson M, Cole PJ, Wilson R. 1996. The effect of bacterial toxins on levels of intracellular adenosine nucleotides and human ciliary beat frequency. Pulm Pharmacol 9:223–230.

59. Köhler T, Guanella R, Carlet J, Van Delden C. 2010. Quorum sensing-dependent virulence during *Pseudomonas aeruginosa* colonisation and pneumonia in mechanically ventilated patients. Thorax 65:703–710.

60. Ghssein G, Ezzeddine Z. 2022. A Review of *Pseudomonas aeruginosa* Metallophores: Pyoverdine, Pyochelin and Pseudopaline. Biology (Basel) 11.

61. Crespo A, Blanco-Cabra N, Torrents E. 2018. Aerobic Vitamin B12 Biosynthesis Is Essential for *Pseudomonas aeruginosa* Class II Ribonucleotide Reductase Activity During Planktonic and Biofilm Growth. Front Microbiol 9:986.

62. Subramaniyan Y, Khan A, Fathima F, Rekha PD. 2023. Differential expression of urease genes and ureolytic activity of uropathogenic *Escherichia coli* and *Pseudomonas aeruginosa* isolates in different nutritional conditions. Arch Microbiol 205:1–16.

63. Hong DJ, Bae IK, Jang IH, Jeong SH, Kang HK, Lee K. 2015. Epidemiology and Characteristics of Metallo-β-Lactamase-Producing *Pseudomonas aeruginosa*. Infect Chemother 47:81.

64. Dumas Z, Ross-Gillespie A, Kümmerli R. 2013. Switching between apparently redundant iron-uptake mechanisms benefits bacteria in changeable environments. Proceedings Biol Sci 280.

65. Takase H, Nitanai H, Hoshino K, Otani T. 2000. Impact of siderophore production on *Pseudomonas aeruginosa* infections in immunosuppressed mice. Infect Immun 68:1834–1839.

66. Lamont IL, Beare PA, Ochsner U, Vasil AI, Vasil ML. 2002. Siderophore-mediated signaling regulates virulence factor production in *Pseudomonas aeruginosa*. Proc Natl Acad Sci U S A 99:7072–7077.

67. De Vos D, De Chial M, Cochez C, Jansen S, Tümmler B, Meyer JM, Cornelis P. 2001. Study of pyoverdine type and production by *Pseudomonas aeruginosa* isolated from cystic fibrosis patients: prevalence of type II pyoverdine isolates and accumulation of pyoverdine-negative mutations. Arch Microbiol 175:384–388.

68. Abdelaziz AA, Kamer AMA, Al-Monofy KB, Al-Madboly LA. 2023. *Pseudomonas aeruginosa*'s greenish-blue pigment pyocyanin: its production and biological activities. Microb Cell Fact 22.

69. Hall S, McDermott C, Anoopkumar-Dukie S, McFarland AJ, Forbes A, Perkins A V., Davey AK, Chess-Williams R, Kiefel MJ, Arora D, Grant GD. 2016. Cellular Effects of Pyocyanin, a Secreted Virulence Factor of *Pseudomonas aeruginosa*. Toxins (Basel) 8.

70. Das T, Kutty SK, Kumar N, Manefield M. 2013. Pyocyanin facilitates extracellular DNA binding to *Pseudomonas aeruginosa* influencing cell surface properties and aggregation. PLoS One 8.

71. Das T, Manefield M. 2012. Pyocyanin promotes extracellular DNA release in *Pseudomonas aeruginosa*. PLoS One 7.

72. Wang Y, Wilks JC, Danhorn T, Ramos I, Croal L, Newman DK. 2011. Phenazine-1-carboxylic acid promotes bacterial biofilm development via ferrous iron acquisition. J Bacteriol 193:3606–3617.

73. Hocquet D, Petitjean M, Rohmer L, Valot B, Kulasekara HD, Bedel E, Bertrand X, Plésiat P, Köhler T, Pantel A, Jacobs MA, Hoffman LR, Miller SI. 2016. Pyomelanin-producing *Pseudomonas aeruginosa* selected during chronic infections have a large chromosomal deletion which confers resistance to pyocins. Environ Microbiol 18:3482–

3493.

74. Rodríguez-Rojas A, Mena A, Martín S, Borrell N, Oliver A, Blázquez J. 2009. Inactivation of the hmgA gene of *Pseudomonas aeruginosa* leads to pyomelanin hyperproduction, stress resistance and increased persistence in chronic lung infection. Microbiology 155:1050–1057.

75. Zheng H, Chatfield CH, Liles MR, Cianciotto NP. 2013. Secreted pyomelanin of *Legionella pneumophila* promotes bacterial iron uptake and growth under iron-limiting conditions. Infect Immun 81:4182–4191.

76. Ogunnariwo J, Hamilton Miller JMT. 1975. Brown and red pigmented *Pseudomonas aeruginosa*: differentiation between melanin and pyorubrin. J Med Microbiol 8:199–203.

77. Fuqua WC, Winans SC, Greenberg EP. 1994. Quorum sensing in bacteria: the LuxR-LuxI family of cell density-responsive transcriptional regulators. J Bacteriol 176:269.

78. Liu YC, Chan KG, Chang CY. 2015. Modulation of host biology by *Pseudomonas aeruginosa* quorum sensing signal molecules: Messengers or traitors. Front Microbiol 6:168355.

79. Williams P, Cámara M. 2009. Quorum sensing and environmental adaptation in *Pseudomonas aeruginosa*: a tale of regulatory networks and multifunctional signal molecules. Curr Opin Microbiol. Curr Opin Microbiol.

80. Oh J, Li XH, Kim SK, Lee JH. 2017. Post-secretional activation of Protease IV by quorum sensing in *Pseudomonas aeruginosa*. Sci Rep 7.

81. Blus-Kadosh I, Zilka A, Yerushalmi G, Banin E. 2013. The effect of pstS and phoB on quorum sensing and swarming motility in *Pseudomonas aeruginosa*. PLoS One 8.

82. Sadikot RT, Blackwell TS, Christman JW, Prince AS. 2005. Pathogen-host interactions in *Pseudomonas aeruginosa* pneumonia. Am J Respir Crit Care Med 171:1209–1223.

83. Kaufmann GF, Sartorio R, Lee SH, Rogers CJ, Meijler MM, Moss JA, Clapham B, Brogan AP, Dickerson TJ, Janda KD. 2005. Revisiting quorum sensing: Discovery of additional chemical and biological functions for 3-oxo-N-acylhomoserine lactones. Proc Natl Acad Sci U S A 102:309–314.

84. Jeong GJ, Khan F, Khan S, Tabassum N, Mehta S, Kim YM. 2023. *Pseudomonas aeruginosa* virulence attenuation by inhibiting siderophore functions. Appl Microbiol Biotechnol 107:1019–1038.

85. Dietrich LEP, Price-Whelan A, Petersen A, Whiteley M, Newman DK. 2006. The phenazine pyocyanin is a terminal signalling factor in the quorum sensing network of *Pseudomonas aeruginosa*. Mol Microbiol 61:1308–1321.

86. Qin S, Xiao W, Zhou C, Pu Q, Deng X, Lan L, Liang H, Song X, Wu M. 2022. *Pseudomonas aeruginosa*: pathogenesis, virulence factors, antibiotic resistance, interaction with host, technology advances and emerging therapeutics. Signal Transduct Target Ther 7.

87. Vadakkan K, Ngangbam AK, Sathishkumar K, Rumjit NP, Cheruvathur MK. 2024. A review of chemical signaling pathways in the quorum sensing circuit of *Pseudomonas aeruginosa*. Int J Biol Macromol. Int J Biol Macromol.

88. O'Loughlin CT, Miller LC, Siryaporn A, Drescher K, Semmelhack MF, Bassler BL. 2013. A quorum-sensing inhibitor blocks *Pseudomonas aeruginosa* virulence and biofilm formation. Proc Natl Acad Sci U S A 110:17981–17986.

89. Pesci EC, Milbank JBJ, Pearson JP, Mcknight S, Kende AS, Greenberg EP, Iglewski BH. 1999. Quinolone signaling in the cell-to-cell communication system of *Pseudomonas aeruginosa*. Proc Natl Acad Sci U S A 96:11229–11234.

90. Häussler S, Becker T. 2008. The *Pseudomonas* quinolone signal (PQS) balances life and death in *Pseudomonas aeruginosa* populations. PLoS Pathog 4.

91. Holden MTG, Chhabra SR, De Nys R, Stead P, Bainton NJ, Hill PJ, Manefield M, Kumar N, Labatte M, England D, Rice S,

Givskov M, Salmond GPC, Stewart GSAB, Bycroft BW, Kjelleberg S, Williams P. 1999. Quorum-sensing cross talk: isolation and chemical characterization of cyclic dipeptides from *Pseudomonas aeruginosa* and other gram-negative bacteria. Mol Microbiol 33:1254–1266.

92. Campbell J, Lin Q, Geske GD, Blackwell HE. 2009. New and unexpected insights into the modulation of LuxR-type quorum sensing by cyclic dipeptides. ACS Chem Biol 4:1051–1059.

93. Wolfgang MC, Lee VT, Gilmore ME, Lory S. 2003. Coordinate regulation of bacterial virulence genes by a novel adenylate cyclase-dependent signaling pathway. Dev Cell 4:253–263.

94. Harman JG. 2001. Allosteric regulation of the cAMP receptor protein. Biochim Biophys Acta 1547:1–17.

95. Albus AM, Pesci EC, Runyen-Janecky LJ, West SEH, Iglewski BH. 1997. Vfr controls quorum sensing in *Pseudomonas aeruginosa*. J Bacteriol 179:3928–3935.

96. Dasgupta N, Ferrell EP, Kanack KJ, West SEH, Ramphal R. 2002. fleQ, the gene encoding the major flagellar regulator of *Pseudomonas aeruginosa*, is sigma70 dependent and is downregulated by Vfr, a homolog of *Escherichia coli* cyclic AMP receptor protein. J Bacteriol 184:5240–5250.

97. Lichtenberg M, Kragh KN, Fritz B, Kirkegaard JB, Tolker-Nielsen T, Bjarnsholt T. 2022. Cyclic-di-GMP signaling controls metabolic activity in *Pseudomonas aeruginosa*. Cell Rep 41.

98. Valentini M, Filloux A. 2016. Biofilms and Cyclic di-GMP (c-di-GMP) Signaling: Lessons from *Pseudomonas aeruginosa* and Other Bacteria. J Biol Chem 291:12547–12555.

99. Bense S, Witte J, Preuße M, Koska M, Pezoldt L, Dröge A, Hartmann O, Müsken M, Schulze J, Fiebig T, Bähre H, Felgner S, Pich A, Häussler S. 2022. *Pseudomonas aeruginosa* post-translational responses to elevated c-di-GMP levels. Mol Microbiol 117:1213–1226.

100. Lory S, Merighi M, Hyodo M. 2009. Multiple activities of c-di-GMP in *Pseudomonas aeruginosa*. Nucleic Acids Symp Ser (Oxf) 51–52.

101. Hall CL, Lee VT. 2018. Cyclic-di-GMP regulation of virulence in bacterial pathogens. Wiley Interdiscip Rev RNA 9.

102. Nadal Jimenez P, Koch G, Thompson JA, Xavier KB, Cool RH, Quax WJ. 2012. The Multiple Signaling Systems Regulating Virulence in *Pseudomonas aeruginosa*. Microbiol Mol Biol Rev 76:46–65.

103. Kim HY, Schlictman D, Shankar S, Xie Z, Chakrabarty AM, Kornberg A. 1998. Alginate, inorganic polyphosphate, GTP and ppGpp synthesis co-regulated in *Pseudomonas aeruginosa*: implications for stationary phase survival and synthesis of RNA/DNA precursors. Mol Microbiol 27:717–725.

104. Xu X, Yu H, Zhang D, Xiong J, Qiu J, Xin R, He X, Sheng H, Cai W, Jiang L, Zhang K, Hu X. 2016. Role of ppGpp in *Pseudomonas aeruginosa* acute pulmonary infection and virulence regulation. Microbiol Res 192:84–95.

105. Khakimova M, Ahlgren HG, Harrison JJ, English AM, Nguyen D. 2013. The stringent response controls catalases in *Pseudomonas aeruginosa* and is required for hydrogen peroxide and antibiotic tolerance. J Bacteriol 195:2011–2020.

106. Corley JM, Intile P, Yahr TL. 2022. Direct Inhibition of RetS Synthesis by RsmA Contributes to Homeostasis of the *Pseudomonas aeruginosa* Gac/Rsm Signaling System. J Bacteriol 204.

107. Brencic A, McFarland KA, McManus HR, Castang S, Mogno I, Dove SL, Lory S. 2009. The GacS/GacA signal transduction system of *Pseudomonas aeruginosa* acts exclusively through its control over the transcription of the RsmY and RsmZ regulatory small RNAs. Mol Microbiol 73:434–445.

108. Barber CE, Tang JL, Feng JX, Pan MQ, Wilson TJG, Slater H, Dow JM, Williams P, Daniels MJ. 1997. A novel regulatory system required for pathogenicity of *Xanthomonas campestris* is mediated by a small diffusible signal molecule. Mol

Microbiol 24:555–566.

109. Ryan RP, An S qi, Allan JH, McCarthy Y, Dow JM. 2015. The DSF Family of Cell-Cell Signals: An Expanding Class of Bacterial Virulence Regulators. PLoS Pathog 11.

110. Zhou L, Zhang LH, Cámara M, He YW. 2017. The DSF Family of Quorum Sensing Signals: Diversity, Biosynthesis, and Turnover. Trends Microbiol 25:293–303.

111. Rahmani-Badi A, Sepehr S, Fallahi H, Heidari-Keshel S. 2015. Dissection of the cis-2-decenoic acid signaling network in *Pseudomonas aeruginosa* using microarray technique Azadeh. Front Microbiol 6.

112. Almblad H, Harrison JJ, Rybtke M, Groizeleau J, Givskov M, Parsek MR, Tolker-Nielsen T. 2015. The Cyclic AMP-Vfr Signaling Pathway in *Pseudomonas aeruginosa* Is Inhibited by Cyclic Di-GMP. J Bacteriol 197:2190–2200.

113. Van Delden C, Comte R, Bally M. 2001. Stringent response activates quorum sensing and modulates cell density-dependent gene expression in *Pseudomonas aeruginosa*. J Bacteriol 183:5376–5384.

114. Frangipani E, Visaggio D, Heeb S, Kaever V, Cámara M, Visca P, Imperi F. 2014. The Gac/Rsm and cyclic-di-GMP signalling networks coordinately regulate iron uptake in *Pseudomonas aeruginosa*. Environ Microbiol 16:676–688.

115. Qazi S, Middleton B, Muharram SH, Cockayne A, Hill P, O'Shea P, Chhabra SR, Cámara M, Williams P. 2006. N-acylhomoserine lactones antagonize virulence gene expression and quorum sensing in *Staphylococcus aureus*. Infect Immun 74:910–919.

116. Hogan DA, Vik Å, Kolter R. 2004. A *Pseudomonas aeruginosa* quorum-sensing molecule influences Candida albicans morphology. Mol Microbiol 54:1212–1223.

117. Grainha T, Jorge P, Alves D, Lopes SP, Pereira MO. 2020. Unraveling *Pseudomonas aeruginosa* and Candida albicans Communication in Coinfection Scenarios: Insights Through Network Analysis. Front Cell Infect Microbiol 10.

118. Hooi DSW, Bycroft BW, Chhabra SR, Williams P, Pritchard DI. 2004. Differential immune modulatory activity of *Pseudomonas aeruginosa* quorum-sensing signal molecules. Infect Immun 72:6463–6470.

119. Glucksam-Galnoy Y, Sananes R, Silberstein N, Krief P, Kravchenko V V., Meijler MM, Zor T. 2013. The bacterial quorum-sensing signal molecule N-3-oxo-dodecanoyl-L-homoserine lactone reciprocally modulates pro- and anti-inflammatory cytokines in activated macrophages. J Immunol 191:337–344.

120. Tateda K, Ishii Y, Horikawa M, Matsumoto T, Miyairi S, Pechere JC, Standiford TJ, Ishiguro M, Yamaguchi K. 2003. The *Pseudomonas aeruginosa* autoinducer N-3-oxododecanoyl homoserine lactone accelerates apoptosis in macrophages and neutrophils. Infect Immun 71:5785–5793.

121. Shiner EK, Terentyev D, Bryan A, Sennoune S, Martinez-zaguilan R, Li G, Gyorke S, Williams SC, Rumbaugh KP. 2006. *Pseudomonas aeruginosa* autoinducer modulates host cell responses through calcium signalling. Cell Microbiol 8:1601–1610.

122. Schwarzer C, Wong S, Shi J, Matthes E, Illek B, Ianowski JP, Arant RJ, Isacoff E, Vais H, Foskett JK, Maiellaro I, Hofer AM, Machen TE. 2010. *Pseudomonas aeruginosa* Homoserine lactone activates store-operated cAMP and cystic fibrosis transmembrane regulator-dependent Cl- secretion by human airway epithelia. J Biol Chem 285:34850–34863.

123. Vikström E, Bui L, Konradsson P, Magnusson KE. 2010. Role of calcium signalling and phosphorylations in disruption of the epithelial junctions by *Pseudomonas aeruginosa* quorum sensing molecule. Eur J Cell Biol 89:584–597.

124. Vikström E, Bui L, Konradsson P, Magnusson KE. 2009. The junctional

integrity of epithelial cells is modulated by *Pseudomonas aeruginosa* quorum sensing molecule through phosphorylation-dependent mechanisms. Exp Cell Res 315:313–326.

125. Zhou L, Zhang Y, Ge Y, Zhu X, Pan J. 2020. Regulatory Mechanisms and Promising Applications of Quorum Sensing-Inhibiting Agents in Control of Bacterial Biofilm Formation. Front Microbiol 11.

126. Rather MA, Saha D, Bhuyan S, Jha AN, Mandal M. 2022. Quorum Quenching: A Drug Discovery Approach Against *Pseudomonas aeruginosa*. Microbiol Res 264.

127. Magiorakos AP, Srinivasan A, Carey RB, Carmeli Y, Falagas ME, Giske CG, Harbarth S, Hindler JF, Kahlmeter G, Olsson-Liljequist B, Paterson DL, Rice LB, Stelling J, Struelens MJ, Vatopoulos A, Weber JT, Monnet DL. 2012. Multidrug-resistant, extensively drug-resistant and pandrug-resistant bacteria: an international expert proposal for interim standard definitions for acquired resistance. Clin Microbiol Infect 18:268–281.

128. Kadri SS, Adjemian J, Lai YL, Spaulding AB, Ricotta E, Rebecca Prevots D, Palmore TN, Rhee C, Klompas M, Dekker JP, Powers JH, Suffredini AF, Hooper DC, Fridkin S, Danner RL. 2018. Difficult-to-treat resistance in gram-negative bacteremia at 173 US hospitals: Retrospective cohort analysis of prevalence, predictors, and outcome of resistance to all first-line agents. Clin Infect Dis 67:1803–1814.

129. Walkty A, Karlowsky JA, Lagacé-Wiens PRS, Baxter MR, Adam HJ, Bay DC, Zhanel GG. 2024. Moving towards a standardized definition of antimicrobial resistance: a comparison of the antimicrobial susceptibility profile of difficult-to-treat resistance (DTR) versus multidrug-resistant (MDR) *Pseudomonas aeruginosa* clinical isolates (CANWARD, 2016-2021). Diagn Microbiol Infect Dis 108.

130. Pang Z, Raudonis R, Glick BR, Lin TJ, Cheng Z. 2019. Antibiotic resistance in *Pseudomonas aeruginosa*: mechanisms and alternative therapeutic strategies. Biotechnol Adv 37:177–192.

131. Yoshimura F, Nikaido H. 1982. Permeability of *Pseudomonas aeruginosa* outer membrane to hydrophilic solutes. J Bacteriol 152:636–642.

132. Benz R, Hancock REW. 1981. Properties of the large ion-permeable pores formed from protein F of *Pseudomonas aeruginosa* in lipid bilayer membranes. Biochim Biophys Acta 646:298–308.

133. Nakae T. 1995. Role of Membrane Permeability in Determining Antibiotic Resistance in *Pseudomonas aeruginosa*. Microbiol Immunol 39:221–229.

134. Hancock REW, Brinkman FSL. 2002. Function of *Pseudomonas* porins in uptake and efflux. Annu Rev Microbiol 56:17–38.

135. Oliveira WK, Ferrarini M, Morello LG, Faoro H. 2020. Resistome analysis of bloodstream infection bacterial genomes reveals a specific set of proteins involved in antibiotic resistance and drug efflux. NAR Genomics Bioinforma 2.

136. Schneider E, Hunke S. 1998. ATP-binding-cassette (ABC) transport systems: functional and structural aspects of the ATP-hydrolyzing subunits/domains. FEMS Microbiol Rev 22:1–20.

137. He GX, Kuroda T, Mima T, Morita Y, Mizushima T, Tsuchiya T. 2004. An H+-Coupled Multidrug Efflux Pump, PmpM, a Member of the MATE Family of Transporters, from *Pseudomonas aeruginosa*. J Bacteriol 186:262.

138. Dulyayangkul P, Satapoomin N, Avison MB, Charoenlap N, Vattanaviboon P, Mongkolsuk S. 2021. Over-Expression of Hypochlorite Inducible Major Facilitator Superfamily (MFS) Pumps Reduces Antimicrobial Drug Susceptibility by Increasing the Production of MexXY Mediated by ArmZ in *Pseudomonas aeruginosa*. Front Microbiol 11.

139. Zhao J, Hellwig N, Djahanschiri B, Khera R, Morgner N, Ebersberger I, Wang J, Michel H. 2022. Assembly and Functional Role of PACE Transporter

PA2880 from *Pseudomonas aeruginosa*. Microbiol Spectr 10.

140. Puzari M, Chetia P. 2017. RND efflux pump mediated antibiotic resistance in Gram-negative bacteria Escherichia coli and *Pseudomonas aeruginosa*: a major issue worldwide. World J Microbiol Biotechnol 33.

141. Sun J, Deng Z, Yan A. 2014. Bacterial multidrug efflux pumps: mechanisms, physiology and pharmacological exploitations. Biochem Biophys Res Commun 453:254–267.

142. Lorusso AB, Carrara JA, Barroso CDN, Tuon FF, Faoro H. 2022. Role of Efflux Pumps on Antimicrobial Resistance in *Pseudomonas aeruginosa*. Int J Mol Sci 23.

143. Höltje J-V. 1998. Growth of the Stress-Bearing and Shape-Maintaining Murein Sacculus of *Escherichia coli*. Microbiol Mol Biol Rev 62:181–203.

144. Jacobs C, Frère JM, Normark S. 1997. Cytosolic intermediates for cell wall biosynthesis and degradation control inducible beta-lactam resistance in gram-negative bacteria. Cell 88:823–832.

145. Breidenstein EBM, de la Fuente-Núñez C, Hancock REW. 2011. *Pseudomonas aeruginosa*: All roads lead to resistance. Trends Microbiol. Elsevier Current Trends.

146. Torrens G, Hernández SB, Ayala JA, Moya B, Juan C, Cava F, Oliver A. 2019. Regulation of AmpC-Driven β-Lactam Resistance in *Pseudomonas aeruginosa*: Different Pathways, Different Signaling. mSystems 4.

147. Fernández L, Gooderham WJ, Bains M, McPhee JB, Wiegand I, Hancock REW. 2010. Adaptive resistance to the "last hope" antibiotics polymyxin B and colistin in *Pseudomonas aeruginosa* is mediated by the novel two-component regulatory system ParR-ParS. Antimicrob Agents Chemother 54:3372–3382.

148. Hocquet D, Vogne C, El Garch F, Vejux A, Gotoh N, Lee A, Lomovskaya O, Plésiat P. 2003. MexXy-OprM efflux pump is necessary for adaptive resistance of *Pseudomonas aeruginosa* to aminoglycosides. Antimicrob Agents Chemother 47:1371–1375.

149. Gupta S, Laskar N, Kadouri DE. 2016. Evaluating the Effect of Oxygen Concentrations on Antibiotic Sensitivity, Growth, and Biofilm Formation of Human Pathogens. Microbiol insights 9:MBI.S40767.

150. Lister PD, Wolter DJ, Hanson ND. 2009. Antibacterial-resistant *Pseudomonas aeruginosa*: Clinical impact and complex regulation of chromosomally encoded resistance mechanisms. Clin Microbiol Rev. Clin Microbiol Rev.

151. Ropy A, Cabot G, Sánchez-Diener I, Aguilera C, Moya B, Ayala JA, Oliver A. 2015. Role of *Pseudomonas aeruginosa* low-molecular-mass penicillin-binding proteins in AmpC expression, β-lactam resistance, and peptidoglycan structure. Antimicrob Agents Chemother 59:3925–3934.

152. Pirnay JP, De Vos D, Mossialos D, Vanderkelen A, Cornelis P, Zizi M. 2002. Analysis of the *Pseudomonas aeruginosa* oprD gene from clinical and environmental isolates. Environ Microbiol 4:872–882.

153. Ocampo-Sosa AA, Cabot G, Rodríguez C, Roman E, Tubau F, Macia MD, Moya B, Zamorano L, Suárez C, Peña C, Domínguez MA, Moncalián G, Oliver A, Martínez-Martínez L. 2012. Alterations of OprD in carbapenem-intermediate and -susceptible strains of *Pseudomonas aeruginosa* isolated from patients with bacteremia in a Spanish multicenter study. Antimicrob Agents Chemother 56:1703–1713.

154. Stanisich V, Holloway BW. 1969. Conjugation in *Pseudomonas aeruginosa*. Genetics 61:327–339.

155. Holloway BW, Monk M. 1959. Transduction in *Pseudomonas aeruginosa*. Nature 184(Suppl 18):1426–1427.

156. Tenover FC, Nicolau DP, Gill CM. 2022. Carbapenemase-producing *Pseudomonas aeruginosa* –an emerging challenge. Emerg Microbes Infect.

Emerg Microbes Infect.

157. Sawa T, Kooguchi K, Moriyama K. 2020. Molecular diversity of extended-spectrum β-lactamases and carbapenemases, and antimicrobial resistance. J Intensive Care 8:1–13.

158. Queenan AM, Bush K. 2007. Carbapenemases: the versatile beta-lactamases. Clin Microbiol Rev 20:440–458.

159. Nordmann P. 2014. Carbapenemase-producing Enterobacteriaceae: overview of a major public health challenge. Med Mal Infect 44:51–56.

160. Halat DH, Moubareck CA. 2022. Focus: Antimicrobial Resistance: The Intriguing Carbapenemases of *Pseudomonas aeruginosa*: CurrentStatus, Genetic Profile, and Global Epidemiology. Yale J Biol Med 95:507.

161. Reyes J, Komarow L, Chen L, Ge L, Hanson BM, Cober E, Herc E, Alenazi T, Kaye KS, Garcia-Diaz J, Li L, Kanj SS, Liu Z, Oñate JM, Salata RA, Marimuthu K, Gao H, Zong Z, Valderrama-Beltrán SL, Yu Y, Tambyah P, Weston G, Salcedo S, Abbo LM, Xie Q, Ordoñez K, Wang M, Stryjewski ME, Munita JM, Paterson DL, Evans S, Hill C, Baum K, Bonomo RA, Kreiswirth BN, Villegas MV, Patel R, Arias CA, Chambers HF, Fowler VG, Doi Y, van Duin D, Satlin MJ, Hanson B, Kaye K, Oñate J, Salata R, Valderrama-Beltrán S, Abbo L, Stryjewski M, Munita J, Paterson D, Kreiswirth B, Virginia Villegas M, Arias C, Chambers H, Fowler V, Satlin M. 2023. Global epidemiology and clinical outcomes of carbapenem-resistant *Pseudomonas aeruginosa* and associated carbapenemases (POP): a prospective cohort study. The Lancet Microbe 4:e159.

162. Kazmierczak KM, De Jonge BLM, Stone GG, Sahm DF. 2020. Longitudinal analysis of ESBL and carbapenemase carriage among Enterobacterales and *Pseudomonas aeruginosa* isolates collected in Europe as part of the International Network for Optimal Resistance Monitoring (INFORM) global surveillance programme, 2013–17. J Antimicrob Chemother 75:1165–1173.

163. Rawat D, Nair D. 2010. Extended-spectrum β-lactamases in Gram Negative Bacteria. J Glob Infect Dis 2:263.

164. Vaziri F, Peerayeh SN, Nejad QB, Farhadian A. 2011. The prevalence of aminoglycoside-modifying enzyme genes (aac (6')-I, aac (6')-II, ant (2")-I, aph (3')-VI) in *Pseudomonas aeruginosa*. Clinics (Sao Paulo) 66:1519–1522.

165. Poole K. 2005. Aminoglycoside resistance in *Pseudomonas aeruginosa*. Antimicrob Agents Chemother 49:479–487.

166. Bryan LE, O'Hara K, Wong S. 1984. Lipopolysaccharide changes in impermeability-type aminoglycoside resistance in *Pseudomonas aeruginosa*. Antimicrob Agents Chemother 26:250–255.

167. Moffatt JH, Harper M, Boyce JD. 2019. Mechanisms of Polymyxin Resistance. Adv Exp Med Biol 1145:55–71.

168. Ojeniyi B, Høiby N. 1991. Comparison of different typing methods of *Pseudomonas aeruginosa*. Antibiot Chemother 44:13–22.

169. Speert DP. 2002. Molecular epidemiology of *Pseudomonas aeruginosa*. Front Biosci. Front Biosci.

170. Kono M, Sei S. 1977. Serotyping of *Pseudomonas aeruginosa* isolated from clinical specimens. Jpn J Exp Med 47:1–7.

171. Huber CA, Reed SJ, Paterson DL. 2021. Bacterial Sub-Species Typing Using Matrix-Assisted Laser Desorption/Ionization Time of Flight Mass Spectrometry: What Is Promising? Curr Issues Mol Biol 43:749.

172. Novais Â, Freitas AR, Rodrigues C, Peixe L. 2018. Fourier transform infrared spectroscopy: unlocking fundamentals and prospects for bacterial strain typing. Eur J Clin Microbiol Infect Dis 2018 383 38:427–448.

173. Cabrolier N, Sauget M, Bertrand X, Hocquet D. 2015. Matrix-assisted laser desorption ionization-time of flight mass spectrometry identifies *Pseudomonas*

aeruginosa high-risk clones. J Clin Microbiol 53:1395–1398.

174. Kohanteb J, Dayaghi M, Motazedian M, Ghayumi MA. 2007. Comparison of biotyping and antibiotyping of *Pseudomonas aeruginosa* isolated from patients with burn wound infection and nosocomial pneumonia in Shiraz, Iran. Pakistan J Biol Sci PJBS 10:1817–1822.

175. Sjöberg L, Lindberg AA. 1968. Phage typing of *Pseudomonas aeruginosa*. Acta Pathol Microbiol Scand 74:61–68.

176. Bernstein-Ziv R, Mushin R, Rabinowitz K. 1973. Typing of *Pseudomonas aeruginosa*: comparison of the phage procedure with the pyocine technique. J Hyg (Lond) 71:403–410.

177. Fyfe JAM, Harris G, Govan JRW. 1984. Revised pyocin typing method for *Pseudomonas aeruginosa*. J Clin Microbiol 20:47.

178. Hancock REW, Mutharia LM, Chan L, Darveau RP, Speert DP, Pier GB. 1983. *Pseudomonas aeruginosa* isolates from patients with cystic fibrosis: a class of serum-sensitive, nontypable strains deficient in lipopolysaccharide O side chains. Infect Immun 42:170–177.

179. Neoh H min, Tan XE, Sapri HF, Tan TL. 2019. Pulsed-field gel electrophoresis (PFGE): A review of the "gold standard" for bacteria typing and current alternatives. Infect Genet Evol. Infect Genet Evol.

180. Curran B, Jonas D, Grundmann H, Pitt T, Dowson CG. 2004. Development of a multilocus sequence typing scheme for the opportunistic pathogen *Pseudomonas aeruginosa*. J Clin Microbiol 42:5644–5649.

181. Pirnay JP, Bilocq F, Pot B, Cornelis P, Zizi M, Van Eldere J, Deschaght P, Vaneechoutte M, Jennes S, Pitt T, De Vos D. 2009. *Pseudomonas aeruginosa* Population Structure Revisited. PLoS One 4:e7740.

182. Pirnay JP, De Vos D, Cochez C, Bilocq F, Vanderkelen A, Zizi M, Ghysels B, Cornelis P. 2002. *Pseudomonas aeruginosa* displays an epidemic population structure. Environ Microbiol 4:898–911.

183. Jolley KA, Bray JE, Maiden MCJ. 2018. Open-access bacterial population genomics: BIGSdb software, the PubMLST.org website and their applications. Wellcome Open Res 3.

184. Woodford N, Turton JF, Livermore DM. 2011. Multiresistant Gram-negative bacteria: the role of high-risk clones in the dissemination of antibiotic resistance. FEMS Microbiol Rev 35:736–755.

185. Treepong P, Kos VN, Guyeux C, Blanc DS, Bertrand X, Valot B, Hocquet D. 2018. Global emergence of the widespread *Pseudomonas aeruginosa* ST235 clone. Clin Microbiol Infect 24:258–266.

186. Oliver A, Mulet X, López-Causapé C, Juan C. 2015. The increasing threat of *Pseudomonas aeruginosa* high-risk clones. Drug Resist Updat. Drug Resist Updat.

187. del Barrio-Tofiño E, López-Causapé C, Oliver A. 2020. *Pseudomonas aeruginosa* epidemic high-risk clones and their association with horizontally-acquired β-lactamases: 2020 update. Int J Antimicrob Agents 56.

188. Botelho J, Grosso F, Sousa C, Peixe L. 2015. Characterization of a new genetic environment associated with GES-6 carbapenemase from a *Pseudomonas aeruginosa* isolate belonging to the high-risk clone ST235. J Antimicrob Chemother 70:615–617.

189. Hernández-Garciá M, Garciá-Castillo M, Garciá-Fernández S, Melo-Cristino J, Pinto MF, Goncąlves E, Alves V, Vieira AR, Ramalheira E, Sancho L, Diogo J, Ferreira R, Silva T, Chaves C, Bou G, Cercenado E, Delgado-Valverde M, Oliver A, Pitart C, Rodríguez-Lozano J, Tormo N, Romano J, Pássaro L, Paixaõ L, López-Mendoza D, Diáz-Reganõn J, Cantón R, Melo-Cristino J, Pinto MF, Marcelo C, Peres H, Lourenço I, Peres I, Marques J, Chantre O, Pina T, Goncąlves E, Toscano C, Alves V, Ribeiro M, Costa E, Vieira AR, Ferreira S, Diaz R, Ramalheira E, Schäfer S, Tancredo L, Sancho L, Rodrigues A, Diogo J, Ferreira R, Ramos H, Silva T, Silva D, Chaves C,

Queiroz C, Nabiev A, Pássaro L, Paixao L, Romano J, Moura C. 2021. Distinct epidemiology and resistance mechanisms affecting ceftolozane/tazobactam in *Pseudomonas aeruginosa* isolates recovered from ICU patients in Spain and Portugal depicted by WGS. J Antimicrob Chemother 76:370–379.

190. Sastre-Femenia MÀ, Fernández-Muñoz A, Gomis-Font MA, Taltavull B, López-Causapé C, Arca-Suárez J, Martínez-Martínez L, Cantón R, Larrosa N, Oteo-Iglesias J, Zamorano L, Oliver A, Galán-Sánchez F, Gracia-Ahufinger I, Liébana-Martos C, Roldán C, Sánchez-Calvo JM, Clavijo E, Mora-Navas L, Aznar J, Lepe JA, Rodríguez-Villodres Á, Recacha E, Casas-Círia FJ, Martínez-Rubio C, Sempere-Alcocer MA, Martín-Hita L, Seral C, López-Calleja AI, Aspiroz C, Monforte M, Iglesia-Martínez P de la, Jimenez-Guerra G, Riera-Pérez E, Collado C, Gallegos C, Mulet X, Sastre-Femenía MÀ, Siller-Ruiz M, Calvo J, Quesada D, Wang JH, Pitart C, Marco F, Prim N, Horcajada JP, Padilla E, Del Barrio-Tofiño E, Viñado-Pérez B, Tubau F, Capilla S, Casabella A, Pérez-Moreno MO, Padilla E, Ballestero M, Rivera A, Navarro F, Gómez-Bertomeu F, Pardo-Granell S, Picó-Plana E, Guerrero D, Sarvisé-Buil C, Belles-Belles A, Fernández-Esgueva M, Ortega-Lafont M del P, García I, Arenal-Andrés N, Hernando-Real S, Ibáñez R, Martínez J, Becerra F, Aldea-Mansilla C, Alaoui-Sosse A, González JC, Guzman-Puche J, Blázquez-Andrada MÁ, Martínez-Ramírez NM, Beteta A, Gomila-Sard B, Almaraz SG, Garduño E, Juiz-González PM, Alba J, Alonso P, Rodríguez AI, Paz-Vidal MI, García-Campello M, Camacho P, Pallarés M de los Á, Pérez del Molino ML, Coira A, Barbeito G, Rincón A, Vasallo-Vidal FJ, Alonso-Acero L, Iglesias-Llorente L, Bordes-Benites A, Florén-Zabala L, Azcona JM, Alonso CA, Sáenz Y, Lamata-Subero M, Molina D, González-Torralba A, Villa J, Viedma E, Cercenado E, Alarcón T, Vargas P, Díez M, Ruiz P, Sánchez-Romero MI, Pérez-García F, Yagüe-Guirao G, Oteiza AC, Leiva J, Portillo ME, Canut-Blasco A, Vidal M, Alonso I, Zuriarrain M, Barrios-Andrés JL. 2023. *Pseudomonas aeruginosa* antibiotic susceptibility profiles, genomic epidemiology and resistance mechanisms: a nation-wide five-year time lapse analysis. Lancet Reg Heal - Eur 34:100736.

191. Choi YJ, Kim YA, Junglim K, Jeong SH, Shin JH, Shin KS, Shin JH, Kim YR, Kim HS, Uh Y, Ryoo NH. 2023. Emergence of NDM-1-producing *Pseudomonas aeruginosa* Sequence Type 773 Clone: Shift of Carbapenemase Molecular Epidemiology and Spread of 16S rRNA Methylase Genes in Korea. Ann Lab Med 43:196–199.

192. Berger O, Lurie-Weinberger MN, Tsyba E, Talisman R. 2024. ST773 *Pseudomonas aeruginosa* wound infection as a result of medical tourism to Turkey. J Travel Med 31.

193. Jung H, Pitout JDD, Matsumura Y, Strydom KA, Kingsburgh C, Ehlers MM, Kock MM. 2024. Genomic epidemiology and molecular characteristics of blaNDM-1-positive carbapenem-resistant *Pseudomonas aeruginosa* belonging to international high-risk clone ST773 in the Gauteng region, South Africa. Eur J Clin Microbiol Infect Dis 43:627–640.

194. Kim MJ, Bae IK, Jeong SH, Kim SH, Song JH, Choi JY, Yoon SS, Thamlikitkul V, Hsueh PR, Yasin RM, Lalitha MK, Lee K. 2013. Dissemination of metallo-β-lactamase-producing *Pseudomonas aeruginosa* of sequence type 235 in Asian countries. J Antimicrob Chemother 68:2820–2824.

195. Hernández-García M, Cabello M, Ponce-Alonso M, Herrador-Gómez PM, Gioia F, Cobo J, Cantón R, Ruiz-Garbajosa P. 2024. First detection in Spain of NDM-1-producing *Pseudomonas aeruginosa* in two patients transferred from Ukraine to a university hospital. J Glob Antimicrob Resist 36:105–111.

196. Kondratiuk V, Jones BT, Kovalchuk V, Kovalenko I, Ganiuk V, Kondratiuk O, Frantsishko A. 2021. Phenotypic and genotypic characterization of antibiotic resistance in military hospital-associated bacteria from war injuries in the Eastern Ukraine conflict between 2014 and 2020. J Hosp Infect 112:69–76.

197. Mc Gann PT, Lebreton F, Jones BT, Dao HD, Martin MJ, Nelson MJ, Luo T, Wyatt AC, Smedberg JR, Kettlewell JM, Cohee BM, Hawley-Molloy JS, Bennett JW. 2023. Six Extensively Drug-Resistant Bacteria in an Injured Soldier, Ukraine. Emerg Infect Dis 29:1692–1695.

198. ECDC. 2022. Operational public health considerations for the prevention and control of infectious diseases in the context of Russia ' s aggression towards Key messages.

199. Whitman WB, Coleman DC, Wiebe WJ. 1998. Prokaryotes: the unseen majority. Proc Natl Acad Sci U S A 95:6578–6583.

200. Wommack KE, Ravel J, Hill RT, Colwell RR. 1999. Hybridization analysis of chesapeake bay virioplankton. Appl Environ Microbiol 65:241–250.

201. Dennehy JJ, Abedon ST. 2020. Bacteriophage Ecology, p. 1–42. *In* Bacteriophages. Springer, Cham.

202. Williamson KE, Fuhrmann JJ, Wommack KE, Radosevich M. 2017. Viruses in Soil Ecosystems: An Unknown Quantity Within an Unexplored Territory. Annu Rev Virol 4:201–219.

203. Gregory AC, Zayed AA, Conceição-Neto N, Temperton B, Bolduc B, Alberti A, Ardyna M, Arkhipova K, Carmichael M, Cruaud C, Dimier C, Domínguez-Huerta G, Ferland J, Kandels S, Liu Y, Marec C, Pesant S, Picheral M, Pisarev S, Poulain J, Tremblay JÉ, Vik D, Acinas SG, Babin M, Bork P, Boss E, Bowler C, Cochrane G, de Vargas C, Follows M, Gorsky G, Grimsley N, Guidi L, Hingamp P, Iudicone D, Jaillon O, Kandels-Lewis S, Karp-Boss L, Karsenti E, Not F, Ogata H, Poulton N, Raes J, Sardet C, Speich S, Stemmann L, Sullivan MB, Sunagawa S, Wincker P, Culley AI, Dutilh BE, Roux S. 2019. Marine DNA Viral Macro- and Microdiversity from Pole to Pole. Cell 177:1109-1123.e14.

204. Kim MS, Park EJ, Roh SW, Bae JW. 2011. Diversity and abundance of single-stranded DNA viruses in human feces. Appl Environ Microbiol 77:8062–8070.

205. Minot S, Sinha R, Chen J, Li H, Keilbaugh SA, Wu GD, Lewis JD, Bushman FD. 2011. The human gut virome: inter-individual variation and dynamic response to diet. Genome Res 21:1616–1625.

206. Reyes A, Haynes M, Hanson N, Angly FE, Heath AC, Rohwer F, Gordon JI. 2010. Viruses in the faecal microbiota of monozygotic twins and their mothers. Nature 466:334–338.

207. Battista JR, Moya A, Pride DT, Ogilvie LA, Jones B V. 2015. The human gut virome: a multifaceted majority https://doi.org/10.3389/fmicb.2015.00918.

208. Vandamme EJ, Mortelmans K. 2019. A century of bacteriophage research and applications: impacts on biotechnology, health, ecology and the economy! J Chem Technol Biotechnol. John Wiley & Sons, Ltd.

209. Ackermann HW. 2012. Bacteriophage Electron Microscopy, p. 1–32. *In* Advances in Virus Research. Academic Press.

210. Turner D, Shkoporov AN, Lood C, Millard AD, Dutilh BE, Alfenas-Zerbini P, van Zyl LJ, Aziz RK, Oksanen HM, Poranen MM, Kropinski AM, Barylski J, Brister JR, Chanisvili N, Edwards RA, Enault F, Gillis A, Knezevic P, Krupovic M, Kurtböke I, Kushkina A, Lavigne R, Lehman S, Lobocka M, Moraru C, Moreno Switt A, Morozova V, Nakavuma J, Reyes Muñoz A, Rūmnieks J, Sarkar B, Sullivan MB, Uchiyama J, Wittmann J, Yigang T, Adriaenssens EM. 2023. Abolishment of morphology-based taxa and change to binomial species names: 2022 taxonomy update of the ICTV bacterial viruses subcommittee. Arch Virol 168:74.

211. Díaz-Muñoz SL, Koskella B. 2014. Bacteria-Phage interactions in natural environments, p. 135–183. *In* Advances in Applied Microbiology. Adv Appl Microbiol.

212. Bertozzi Silva J, Storms Z, Sauvageau D. 2016. Host receptors for bacteriophage adsorption. FEMS Microbiol Lett 363.

213. Weinbauer MG. 2004. Ecology of prokaryotic viruses. FEMS Microbiol Rev 28:127–181.

214. Molineux IJ, Panja D. 2013. Popping the cork: mechanisms of phage genome

ejection. Nat Rev Microbiol 11:194–204.

215. Rajaure M, Berry J, Kongari R, Cahill J, Young R. 2015. Membrane fusion during phage lysis. Proc Natl Acad Sci U S A 112:5497–5502.

216. Publications service. 2007. On an invisible microbe antagonistic toward dysenteric bacilli: brief note by Mr. F. D'Herelle, presented by Mr. Roux. Res Microbiol. Res Microbiol.

217. McCallin S, Drulis-Kawa Z, Ferry T, Pirnay JP, Nir-Paz R. 2023. Phages and phage-borne enzymes as new antibacterial agents. Clin Microbiol Infect https://doi.org/10.1016/J.CMI.2023.10.018.

218. Landy A. 2015. The λ Integrase Site-specific Recombination Pathway. Microbiol Spectr 3.

219. Henrot C, Petit MA. 2022. Signals triggering prophage induction in the gut microbiota. Mol Microbiol. Mol Microbiol.

220. Erez Z, Steinberger-Levy I, Shamir M, Doron S, Stokar-Avihail A, Peleg Y, Melamed S, Leavitt A, Savidor A, Albeck S, Amitai G, Sorek R. 2017. Communication between viruses guides lysis-lysogeny decisions. Nature 541:488–493.

221. Brady A, Quiles-Puchalt N, Gallego del Sol F, Zamora-Caballero S, Felipe-Ruíz A, Val-Calvo J, Meijer WJJ, Marina A, Penadés JR. 2021. The arbitrium system controls prophage induction. Curr Biol 31:5037-5045.e3.

222. Hargreaves KR, Kropinski AM, Clokie MRJ. 2014. What does the talking?: quorum sensing signalling genes discovered in a bacteriophage genome. PLoS One 9.

223. Hobbs Z, Abedon ST. 2016. Diversity of phage infection types and associated terminology: the problem with 'Lytic or lysogenic.' FEMS Microbiol Lett 363:47.

224. Olszak T, Latka A, Roszniowski B, Valvano MA, Drulis-Kawa Z. 2017. Phage Life Cycles Behind Bacterial Biodiversity. Curr Med Chem 24.

225. Tsao YF, Taylor VL, Kala S, Bondy-Denomy J, Khan AN, Bona D, Cattoir V, Lory S, Davidson AR, Maxwell KL. 2018. Phage Morons Play an Important Role in *Pseudomonas aeruginosa* Phenotypes. J Bacteriol 200.

226. Kondo K, Kawano M, Sugai M. 2021. Distribution of Antimicrobial Resistance and Virulence Genes within the Prophage-Associated Regions in Nosocomial Pathogens. mSphere 6.

227. Blanco-Picazo P, Morales-Cortes S, Ramos-Barbero MD, García-Aljaro C, Rodríguez-Rubio L, Muniesa M. 2022. Dominance of phage particles carrying antibiotic resistance genes in the viromes of retail food sources. ISME J 2022 172 17:195–203.

228. López-Leal G, Santamaria RI, Cevallos MÁ, Gonzalez V, Castillo-Ramírez S. 2020. Letter to the Editor: Prophages Encode Antibiotic Resistance Genes in *Acinetobacter baumannii*. Microb Drug Resist. Microb Drug Resist.

229. Li D, Liang W, Huang Z, Ma W, Liu Q. 2024. The spontaneously produced lysogenic prophage phi456 promotes bacterial resistance to adverse environments and enhances the colonization ability of avian pathogenic *Escherichia coli* strain DE456. Vet Res 55:37.

230. Vaca-Pacheco S, Paniagua-Contreras GL, García-González O, De La Garza M. 1999. The clinically isolated FIZ15 bacteriophage causes lysogenic conversion in *Pseudomonas aeruginosa* PAO1. Curr Microbiol 38:239–243.

231. Vaca Pacheco S, Garcıća González O, Paniagua Contreras GL. 1997. The lom gene of bacteriophage lambda is involved in *Escherichia coli* K12 adhesion to human buccal epithelial cells. FEMS Microbiol Lett 156:129–132.

232. Winstanley C, Langille MGI, Fothergill JL, Kukavica-Ibrulj I, Paradis-Bleau C, Sanschagrin F, Thomson NR, Winsor GL, Quail MA, Lennard N, Bignell A, Clarke L, Seeger K, Saunders D, Harris D, Parkhill J, Hancock REW, Brinkman FSL, Levesque RC. 2009. Newly introduced genomic prophage islands are critical determinants of in vivo competitiveness

in the Liverpool Epidemic Strain of *Pseudomonas aeruginosa*. Genome Res 19:12–23.

233. Lonati D, Schicchi A, Crevani M, Buscaglia E, Scaravaggi G, Maida F, Cirronis M, Petrolini VM, Locatelli CA. 2020. Foodborne botulism: Clinical diagnosis and medical treatment. Toxins (Basel). Toxins (Basel).

234. Montecucco C, Schiavo G, Rossetto O. 1996. The mechanism of action of tetanus and botulinum neurotoxins. Arch Toxicol Suppl 18:342–354.

235. Clemens JD, Nair GB, Ahmed T, Qadri F, Holmgren J. 2017. Cholera. Lancet. Lancet.

236. Murphy JR. 2011. Mechanism of diphtheria toxin catalytic domain delivery to the eukaryotic cell cytosol and the cellular factors that directly participate in the process. Toxins (Basel) 3:294–308.

237. Melton-Celsa AR. 2014. Shiga Toxin (Stx) Classification, Structure, and Function. Microbiol Spectr 2.

238. Lee SF, Li L, Jalal N, Halperin SA. 2021. Identification of a thiol-disulfide oxidoreductase (sdba) catalyzing disulfide bond formation in the superantigen spea in *Streptococcus pyogenes*. J Bacteriol 203.

239. Papageorgiou AC, Collins CM, Gutman DM, Kline JB, O'Brien SM, Tranter HS, Acharya KR. 1999. Structural basis for the recognition of superantigen streptococcal pyrogenic exotoxin A (SpeA1) by MHC class II molecules and T-cell receptors. EMBO J 18:9–21.

240. Chatila T, Scholl P, Spertini F, Ramesh N, Trede N, Fuleihan R, Geha RS. 1991. Toxic shock syndrome toxin-1, toxic shock, and the immune system. Curr Top Microbiol Immunol 174:63–79.

241. Magill DJ, Kucher PA, Krylov VN, Pleteneva EA, Quinn JP, Kulakov LA. 2017. Localised genetic heterogeneity provides a novel mode of evolution in dsDNA phages. Sci Rep 7.

242. Negatu SG, Arreguin MC, Jurado KA, Vazquez C. 2022. Being the Alice of academia: lessons from the Red Queen hypothesis. Pathog Dis 80.

243. Brockhurst MA, Chapman T, King KC, Mank JE, Paterson S, Hurst GDD. 2014. Running with the Red Queen: the role of biotic conflicts in evolution. Proceedings Biol Sci 281.

244. Wang Y, Fan H, Tong Y. 2023. Unveil the Secret of the Bacteria and Phage Arms Race. Int J Mol Sci 24.

245. Bondy-Denomy J, Qian J, Westra ER, Buckling A, Guttman DS, Davidson AR, Maxwell KL. 2016. Prophages mediate defense against phage infection through diverse mechanisms. ISME J 10:2854–2866.

246. Lopatina A, Tal N, Sorek R. 2020. Abortive Infection: Bacterial Suicide as an Antiviral Immune Strategy. Annu Rev Virol. Annu Rev Virol.

247. Cohen D, Melamed S, Millman A, Shulman G, Oppenheimer-Shaanan Y, Kacen A, Doron S, Amitai G, Sorek R. 2019. Cyclic GMP-AMP signalling protects bacteria against viral infection. Nature 574:691–695.

248. Durmaz E, Klaenhammer TR. 2007. Abortive phage resistance mechanism AbiZ speeds the lysis clock to cause premature lysis of phage-infected *Lactococcus lactis*. J Bacteriol 189:1417–1425.

249. Lau RK, Ye Q, Birkholz EA, Berg KR, Patel L, Mathews IT, Watrous JD, Ego K, Whiteley AT, Lowey B, Mekalanos JJ, Kranzusch PJ, Jain M, Pogliano J, Corbett KD. 2020. Structure and Mechanism of a Cyclic Trinucleotide-Activated Bacterial Endonuclease Mediating Bacteriophage Immunity. Mol Cell 77:723-733.e6.

250. Kazlauskiene M, Kostiuk G, Venclovas Č, Tamulaitis G, Siksnys V. 2017. A cyclic oligonucleotide signaling pathway in type III CRISPR-Cas systems. Science 357:605–609.

251. Levitz R, Chapman D, Amitsur M, Green R, Snyder L, Kaufmann G. 1990. The optional *E. coli* prr locus encodes a latent form of phage T4-induced anticodon nuclease. EMBO J 9:1383–1389.

252. Yu YTN, Snyder L. 1994. Translation elongation factor Tu cleaved by a phage-exclusion system. Proc Natl Acad Sci U S A 91:802–806.

253. Wang L, Zhang L. 2023. The arms race between bacteria CBASS and bacteriophages. Front Immunol 14.

254. Leroux M, Laub MT. 2022. Toxin-Antitoxin Systems as Phage Defense Elements. Annu Rev Microbiol 76:21–43.

255. Labrie SJ, Samson JE, Moineau S. 2010. Bacteriophage resistance mechanisms. Nat Rev Microbiol 8:317–327.

256. González de Aledo M, González-Bardanca M, Blasco L, Pacios O, Bleriot I, Fernández-García L, Fernández-Quejo M, López M, Bou G, Tomás M. 2021. CRISPR-Cas, a revolution in the treatment and study of eskape infections: Pre-clinical studies. Antibiotics. Antibiotics (Basel).

257. Shinedling S, Parma D, Gold L. 1987. Wild-type bacteriophage T4 is restricted by the lambda rex genes. J Virol 61:3790–3794.

258. Amitsur M, Levitz R, Kaufmann G. 1987. Bacteriophage T4 anticodon nuclease, polynucleotide kinase and RNA ligase reprocess the host lysine tRNA. EMBO J 6:2499–2503.

259. Murphy J, Mahony J, Ainsworth S, Nauta A, van Sinderen D. 2013. Bacteriophage orphan DNA methyltransferases: insights from their bacterial origin, function, and occurrence. Appl Environ Microbiol 79:7547–7555.

260. Koonin E V., Krupovic M. 2020. Phages build anti-defence barriers. Nat Microbiol 5:8–9.

261. Pawluk A, Davidson AR, Maxwell KL. 2017. Anti-CRISPR: discovery, mechanism and function. Nat Rev Microbiol 2017 161 16:12–17.

262. Fiedoruk K, Zakrzewska M, Daniluk T, Piktel E, Chmielewska S, Bucki R. 2020. Two Lineages of *Pseudomonas aeruginosa* Filamentous Phages: Structural Uniformity over Integration Preferences. Genome Biol Evol 12:1765.

263. Burgener EB, Cai P, Kratochvil MJ, Rojas-Hernandez LS, Joo NS, Gupta A, Secor PR, Heilshorn SC, Spakowitz AJ, Wine JJ, Bollyky PL, Milla CE. 2024. The lysogenic filamentous *Pseudomonas* bacteriophage phage Pf slows mucociliary transport . PNAS Nexus 3.

264. Guo Y, Tang K, Sit B, Gu J, Chen R, Shao X, Lin S, Huang Z, Nie Z, Lin J, Liu X, Wang W, Gao X, Liu T, Liu F, Luo HR, Waldor MK, Wang X. 2024. Control of lysogeny and antiphage defense by a prophage-encoded kinase-phosphatase module. Nat Commun 15.

265. Blasco L, Ibarguren-Quiles C, López-Causape C, Armán L, Barrio-Pujante A, Bleriot I, Pacios O, Fernández-García L, Ortiz-Cartagena C, Cantón R, Oliver A, Tomás M. 2025. Study of the probability of resistance to phage infection in a collection of clinical isolates of *Pseudomonas aeruginosa* in relation to the presence of Pf phages. Microbiol Spectr 13:e0301024.

266. Johnson G, Banerjee S, Putonti C. 2022. Diversity of *Pseudomonas aeruginosa* Temperate Phages. mSphere 7.

267. Ma W, Guo J, Deng C, Huang X, Sun Y, Xu L, Qin Q. 2024. Characterization of the Chromosomally Located Metallo-b-Lactamase Genes blaIMP-45 and blaVIM-2 in a Carbapenem-Resistant *Pseudomonas aeruginosa* Clinical Isolate. Microb Drug Resist https://doi.org/10.1089/MDR.2024.0059/ASSET/IMAGES/MDR.2024.0059-FIGURE5.JPG.

268. Xavier KVM, de Oliveira Luz AC, Silva-Junior JW, de Melo BST, de Aragão Batista MV, de Albuquerque Silva AM, de Queiroz Balbino V, Leal-Balbino TC. 2025. Molecular epidemiological study of *Pseudomonas aeruginosa* strains isolated from hospitals in Brazil by MLST and CRISPR/Cas system analysis. Mol Genet Genomics 300.

269. Chang TH, Pourtois JD, Haddock NL, Furukawa D, Kelly KE, Amanatullah DF, Burgener E, Milla C, Banaei N, Bollyky PL. 2025. Prophages are infrequently associated with antibiotic resistance in *Pseudomonas aeruginosa* clinical isolates. mSphere 10.

270. Kyrkou I, Bartell J, Lechuga A, Lood C, Marvig RL, Lavigne R, Molin S, Krogh Johansen H. 2025. *Pseudomonas aeruginosa* maintains an inducible array of novel and diverse prophages over lengthy persistence in cystic fibrosis lungs. FEMS Microbiol Lett 372.

271. Sugrue I, Ross RP, Hill C. 2024. Bacteriocin diversity, function, discovery and application as antimicrobials. Nat Rev Microbiol https://doi.org/10.1038/S41579-024-01045-X.

272. Ghequire MGK, De Mot R. 2014. Ribosomally encoded antibacterial proteins and peptides from *Pseudomonas*. FEMS Microbiol Rev 38:523–568.

273. Lewis BB, Pamer EG. 2017. Microbiota-Based Therapies for *Clostridium difficile* and Antibiotic-Resistant Enteric Infections. Annu Rev Microbiol 71:157–178.

274. Heilbronner S, Krismer B, Brötz-Oesterhelt H, Peschel A. 2021. The microbiome-shaping roles of bacteriocins. Nat Rev Microbiol 19:726–739.

275. Willey JM, Van Der Donk WA. 2007. Lantibiotics: Peptides of diverse structure and function. Annu Rev Microbiol. Annu Rev Microbiol.

276. Charest AM, Reed E, Bozorgzadeh S, Hernandez L, Getsey N V., Smith L, Galperina A, Beauregard HE, Charest HA, Mitchell M, Riley MA. 2024. Nisin Inhibition of Gram-Negative Bacteria. Microorganisms 12.

277. Michel-Briand Y, Baysse C. 2002. The pyocins of *Pseudomonas aeruginosa*. Biochimie. Elsevier.

278. Backman T, Latorre SM, Symeonidi E, Muszyński A, Bleak E, Eads L, Martinez-Koury PI, Som S, Hawks A, Gloss AD, Belnap DM, Manuel AM, Deutschbauer AM, Bergelson J, Azadi P, Burbano HA, Karasov TL. 2024. A phage tail-like bacteriocin suppresses competitors in metapopulations of pathogenic bacteria. Science 384.

279. Matsui H, Sano Y, Ishihara H, Shinomiya T. 1993. Regulation of pyocin genes in *Pseudomonas aeruginosa* by positive (prtN) and negative (prtR) regulatory genes. J Bacteriol 175:1257–1263.

280. Brackmann M, Nazarov S, Wang J, Basler M. 2017. Using Force to Punch Holes: Mechanics of Contractile Nanomachines. Trends Cell Biol. Trends Cell Biol.

281. Yates CR, Nguyen A, Liao J, Cheng RA. 2024. What's on a prophage: analysis of *Salmonella spp*. prophages identifies a diverse range of cargo with multiple virulence- and metabolism-associated functions. mSphere 9.

282. Johnson G, Banerjee S, Putonti C. 2022. Diversity of *Pseudomonas aeruginosa* Temperate Phages. mSphere 7.

283. Campbell A. 2003. Prophage insertion sites. Res Microbiol 154:277–282.

284. Wood TL, Wood TK. 2016. The HigB/HigA toxin/antitoxin system of *Pseudomonas aeruginosa* influences the virulence factors pyochelin, pyocyanin, and biofilm formation. Microbiologyopen 5:499.

285. Ackermann HW. 2008. Tailed Bacteriophages: The Order Caudovirales. Adv Virus Res 51:135.

286. Yuan Y, Gao M. 2017. Jumbo bacteriophages: An overview. Front Microbiol 8:226872.

287. Fortier LC, Sekulovic O. 2013. Importance of prophages to evolution and virulence of bacterial pathogens. Virulence 4:354–365.

288. Vincent AT. 2024. Bacterial hypothetical proteins may be of functional interest. Front Bacteriol 3:1334712.

289. Hurwitz BL, U'Ren JM, Youens-Clark K. 2016. Computational prospecting the great viral unknown. FEMS Microbiol Lett 363.

290. Dutilh BE. 2014. Metagenomic ventures into outer sequence space. Bacteriophage 4:e979664.

291. Fremin BJ, Bhatt AS, Kyrpides NC, Sengupta A, Sczyrba A, Maria da Silva A, Buchan A, Gaudin A, Brune A, Hirsch AM,

Neumann A, Shade A, Visel A, Campbell B, Baker B, Hedlund BP, Crump BC, Currie C, Kelly C, Craft C, Hazard C, Francis C, Schadt CW, Averill C, Mobilian C, Buckley D, Hunt D, Noguera D, Beck D, Valentine DL, Walsh D, Sumner D, Lymperopoulou D, Bhaya D, Bryant DA, Morrison E, Brodie E, Young E, Lilleskov E, Högfors-Rönnholm E, Chen F, Stewart F, Nicol GW, Teeling H, Beller HR, Dionisi H, Liao HL, Beman JM, Stegen J, Tiedje J, Jansson J, VanderGheynst J, Norton J, Dangl J, Blanchard J, Bowen J, Macalady J, Pett-Ridge J, Rich J, Payet JP, Gladden JD, Raff JD, Klassen JL, Tarn J, Neufeld J, Gravuer K, Hofmockel K, Chen KH, Konstantinidis K, DeAngelis KM, Partida-Martinez LP, Meredith L, Chistoserdova L, Moran MA, Scarborough M, Schrenk M, Sullivan M, David M, O'Malley MA, Medina M, Habteselassie M, Ward ND, Pietrasiak N, Mason OU, Sorensen PO, Estrada de los Santos P, Baldrian P, McKay RM, Simister R, Stepanauskas R, Neumann R, Malmstrom R, Cavicchioli R, Kelly R, Hatzenpichler R, Stocker R, Cattolico RA, Ziels R, Vilgalys R, Blumer-Schuette S, Crowe S, Roux S, Hallam S, Lindow S, Brawley SH, Tringe S, Woyke T, Whitman T, Bianchi T, Mock T, Donohue T, James TY, Kalluri UC, Karaoz U, Denef V, Liu WT, Whitman W, Ouyang Y. 2022. Thousands of small, novel genes predicted in global phage genomes. Cell Rep 39:110984.

292. Blasco L, González de Aledo M, Ortiz-Cartagena C, Blériot I, Pacios O, López M, Fernández-García L, Barrio-Pujante A, Hernández-Garcia M, Cantón R, Tomás M. 2023. Study of 32 new phage tail-like bacteriocins (pyocins) from a clinical collection of *Pseudomonas aeruginosa* and of their potential use as typing markers and antimicrobial agents. Sci Rep 13.

293. Getz LJ, Maxwell KL. 2024. Diverse Antiphage Defenses Are Widespread Among Prophages and Mobile Genetic Elements. Annu Rev Virol 11.

294. Bondy-Denomy J, Pawluk A, Maxwell KL, Davidson AR. 2013. Bacteriophage genes that inactivate the CRISPR/Cas bacterial immune system. Nature 493:429.

295. van Belkum A, Soriaga LB, LaFave MC, Akella S, Veyrieras JB, Barbu EM, Shortridge D, Blanc B, Hannum G, Zambardi G, Miller K, Enright MC, Mugnier N, Brami D, Schicklin S, Felderman M, Schwartz AS, Richardson TH, Peterson TC, Hubby B, Cady KC. 2015. Phylogenetic Distribution of CRISPR-Cas Systems in Antibiotic-Resistant *Pseudomonas aeruginosa*. MBio 6.

296. Silpe JE, Bassler BL. 2019. Phage-encoded LuxR-type receptors responsive to host-produced bacterial quorum-sensing autoinducers. MBio 10.

297. Górski A, Międzybrodzki R, Łobocka M, Głowacka-Rutkowska A, Bednarek A, Borysowski J, Jończyk-Matysiak E, Łusiak-Szelachowska M, Weber-Dabrowska B, Bagińska N, Letkiewicz S, Dabrowska K, Scheres J. 2018. Phage Therapy: What Have We Learned? Viruses 10.

298. Boyd EF, Brüssow H. 2002. Common themes among bacteriophage-encoded virulence factors and diversity among the bacteriophages involved. Trends Microbiol. Elsevier.

299. Touchon M, Bernheim A, Rocha EPC. 2016. Genetic and life-history traits associated with the distribution of prophages in bacteria. ISME J 10:2744.

300. Ferriol-González C, Concha-Eloko R, Bernabéu-Gimeno M, Fernández-Cuenca F, Cañada-García JE, García-Cobos S, Sanjuán R, Domingo-Calap P. 2024. Targeted phage hunting to specific *Klebsiella pneumoniae* clinical isolates is an efficient antibiotic resistance and infection control strategy. Microbiol Spectr 12:e00254-24.

301. Shamsuzzaman M, Choi YJ, Kim S, Kim J. 2025. Characterization and genome analyses of the novel phages targeting extraintestinal *Escherichia coli* clones ST131 and ST410. Int Microbiol 1–13.

302. Zhong L, Sun Y, Sun Y, Yu G, Cheng P, Zheng J, Peng D, Sun M. 2025. Characterization and genetic analysis of two sugarlandviruses: *Klebsiella variicola* lytic phages vB_PZK-KV7 and vB_PZK-KV23. Arch Virol 170:1–15.

303. Kobakhidze S, Koulouris S, Kakabadze N, Kotetishvili M. 2024. Genetic recombination-mediated evolutionary interactions between phages of potential industrial importance and prophages of their hosts within or across the domains of *Escherichia*, *Listeria*, *Salmonella*, *Campylobacter*, and *Staphylococcus*. BMC Microbiol 24:155.

304. Al-Anany AM, Fatima R, Hynes AP. 2021. Temperate phage-antibiotic synergy eradicates bacteria through depletion of lysogens. Cell Rep 35.

305. Fatima R, Hynes AP. 2025. Temperate phage-antibiotic synergy is widespread—extending to *Pseudomonas*—but varies by phage, host strain, and antibiotic pairing. MBio 16.

306. Lakshminarasimhan A. 2022. Prophage induction therapy: Activation of the lytic phase in prophages for the elimination of pathogenic bacteria. Med Hypotheses 169:110980.

307. Bleriot I, Pacios O, Blasco L, Fernández-García L, López M, Ortiz-Cartagena C, Barrio-Pujante A, García-Contreras R, Pirnay J-P, Wood TK, Tomás M. 2024. Improving phage therapy by evasion of phage resistance mechanisms. JAC-antimicrobial Resist 6.

308. European Centre for Disease Prevention and Control. European Antimicrobial Resistance Surveillance Network (EARS-Net).

309. Hernández-García M, García-Fernández S, García-Castillo M, Pássaro L, Cantón R. 2021. In vitro characterization of *Pseudomonas aeruginosa* recovered in Portugal from low respiratory tract infections in ICU patients (STEP Study). FEMS Microbiol Lett. FEMS Microbiol Lett.

310. García-Fernández S, García-Castillo M, Bou G, Calvo J, Cercenado E, Delgado M, Pitart C, Mulet X, Tormo N, Mendoza DL, Díaz-Regañón J, Cantón R, SUPERIOR Study Group. 2019. Activity of ceftolozane/tazobactam against *Pseudomonas aeruginosa* and Enterobacterales isolates recovered from intensive care unit patients in Spain: The SUPERIOR multicentre study. Int J Antimicrob Agents 53:682–688.

311. Juraschek K, Borowiak M, Tausch SH, Malorny B, Käsbohrer A, Otani S, Schwarz S, Meemken D, Deneke C, Hammerl JA. 2021. Outcome of Different Sequencing and Assembly Approaches on the Detection of Plasmids and Localization of Antimicrobial Resistance Genes in Commensal *Escherichia coli.* Microorganisms 9:598.

312. Kingsford C, Schatz MC, Pop M. 2010. Assembly complexity of prokaryotic genomes using short reads. BMC Bioinformatics 11.

7. Annexes

Annex 1. "Bioinformatic tool comparison for the search of lysogenic phages (prophages) in the genomes of carbapenemase-producing *Serratia marcescens*" SEIMC XXVI Congress – Poster communication.

Title: Comparación de herramientas bioinformáticas para la búsqueda de fagos lisogénicos (profagos) en genomas de *Serratia marcescens* productora de carbapenemasas.

Authors: Manuel González De Aledo[1], Blanca Pérez-Viso[1], Ainhize Maruri[1], Marta Hernández-García[1], Lucía Blasco[2], María Tomás[2], Rafael Cantón[1]. [1]Hospital Ramón y Cajal, Madrid, [2]Complexo Hospitalario Universitario de A Coruña, A Coruña.

ISBN: 978-84-09-50940-9

Introduction/Objective: Phages are viruses with the ability to infect bacteria, and they constitute the most abundant entity in the biosphere. Lysogenic phages can integrate into the bacterial chromosome and reproduce together with their host, indefinitely inhibiting the synthesis of lytic proteins and affecting bacterial pathogenesis (toxin production, quorum sensing system regulation, virulence factors, etc.). Nowadays there are several tools for prophage investigation in bacterial genomes, ranging from user-friendly programs to command-line software, with different approaches.

The goal of the current study was to compare the ability of three different bioinformatic tools (PHASTER, PhiSpy and VIBRANT) to detect complete lysogenic phages in the genomes of carbapenemase-producing *Serratia marcescens* clinical strains isolated in a third-level hospital between March 2016 and December 2018.

Materials & methods. Six representative isolates from a 50-strain *S. marcescens* collection were selected, each of them belonging to different clones. Whole genome sequencing was performed by Illumina-NovaSeq 6000 (OGC, Oxford, UK) and SPAdes v3.11.1.19 was used for the assembly. Prophage search was carried out by the PHASTER (https://phaster.ca), PhiSpy (https://github.com/linsalrob/PhiSpy) and VIBRANT (https://github.com/AnantharamanLab/VIBRANT) tools. Both the complete genomes and the detected prophages were annotated using RAST (https://rast.nmpdr.org/). To consider a prophage as complete, at least 4 out of the following proteins had to be detected: a lysogenic cycle regulatory protein (cI, Cro, cII, P or Q antitermination proteins), a terminase large subunit, an integrase, a tail length tape measure protein, a capsid protein or a lytic protein (holin, spanin or endolysin). Whenever this threshold could not be reached, prophages were manually

annotated through HMMER v3.3.2 (http://hmmer.org/) to improve the annotation quality. Those prophages which after HMMER annotation did not have at least 4/6 of these proteins, were considered as incomplete. To compare prophage sequences, the BLAST tool was used (https://blast.ncbi.nlm.nih.gov/Blast.cgi) as well as SnapGene for the graphical representation of the prophage sequence.

Results: In total, 36 prophages were detected, between 0 and 4 per isolate (TABLE 1). Through sequence comparison, 9 single sequences were located among the 29 complete prophages detected (FIGURES 1A and 1B).

Conclusions: Despite being of the most commonly used tools, probably due to its simplicity, the PHASTER tools could not detect 4 complete prophages which were in turn located by the other two software. Although PhiSpy and VIBRANT also detected several incomplete prophages, with the automatic RAST and the manual HMMER annotations they could be discarded. Due to the only difference between PhiSpy and VIBRANT was a single prophage discarded as incomplete, it could be concluded that the performance of both software is very similar and superior to PHASTER.

Table 1. Total number of prophages. In brackets, incomplete phages.

Strain	Carbapenemase	PHASTER	PhiSpy	VIBRANT
B77	VIM-1	0	2(0)	2(0)
E78	KPC	2(0)	3(1)	2(0)
H28	OXA-48	3(0)	3(0)	4(1)
I54	OXA-48	2(0)	3(1)	3(1)
M52	VIM-1	0	2(0)	2(0)
P60	VIM-1	0	1(1)	2(2)
Total		7(0)	14(3)	15(4)

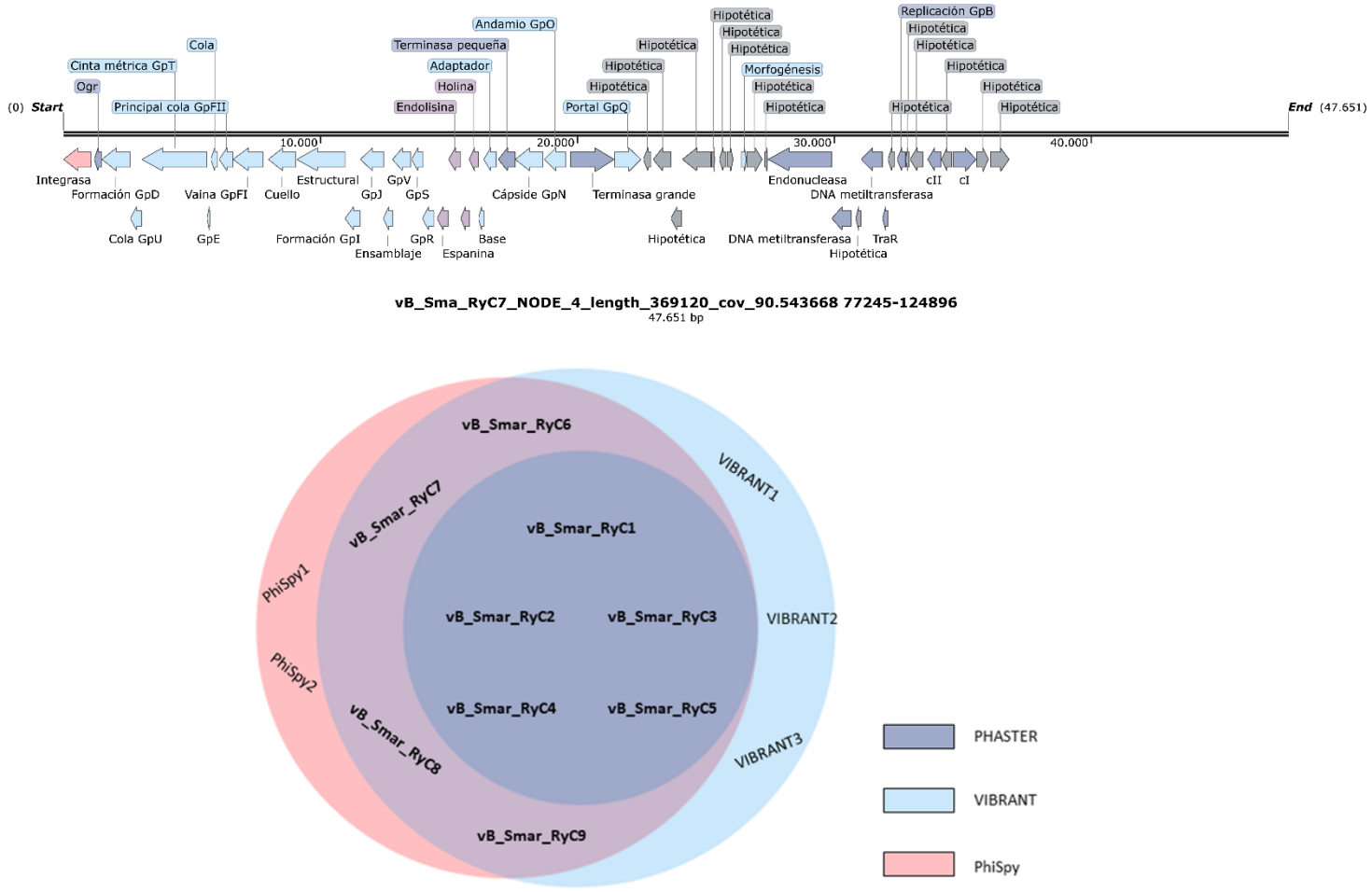

Figure 1A: Venn diagram representation of the different prophages detected by the analyzed softwares. In bold, complete prophages. Figure 1B: Genome representation of the vB_Smar_RyC7 prophage.

Annex 2. Comparison of the number of prophages identified in the *P. aeruginosa* genomes from Study 2 by PHASTER and VIBRANT

Strain	PHASTER	VIBRANT
ESP-1	8	6
ESP-2	11	9
ESP-3	8	7
NLD-1	8	8
NLD-2	8	8
NLD-3	9	8
NLD-4	9	7
NLD-5	8	7
NLD-6	8	7

Annex 3. Number of filamentous phages found in each *P. aeruginosa* strain from Studies 1 and 2.

Strain	Study	ST	Filamentous phages
1 (1-13)	1	ST235	0
2 (2-10)	1	ST499	0
3 (2-21)	1	ST309	1
4 (2-29)	1	ST235	0
5 (3-5)	1	ST348	0
6 (3-38)	1	ST348	0
7 (3-41)	1	ST348	0
8 (3-49)	1	ST235	0
9 (3-58)	1	ST348	0
10 (3-69)	1	ST554	1
11 (4-14)	1	ST313	1
12 (4-17)	1	ST235	0
13 (4-29)	1	ST179	1
14 (4-71)	1	ST235	0
15 (4-79)	1	ST235	0
16 (4-86)	1	ST235	0
17 (4-92)	1	ST235	0
18 (4-93)	1	ST235	0
19 (4-94)	1	ST235	0
20 (4-120)	1	ST235	0
21 (4-121)	1	ST235	0
22 (4-125)	1	ST253	1
23 (5-15)	1	ST235	0
24 (5-23)	1	ST244	0
25 (6-25)	1	ST244	2
26 (6-38)	1	ST253	0
27 (6-59)	1	ST179	1
28 (6-102)	1	ST446	2
29 (7-41)	1	ST3292	2
30 (8-1)	1	ST348	0

31 (8-12)	1	ST253	1
32 (8-24)	1	ST244	0
33 (8-36)	1	ST244	0
34 (8-58)	1	ST244	0
36 (9-25)	1	ST244	2
37 (9-35)	1	ST308	3
38 (9-41)	1	ST235	0
39 (9-86)	1	ST554	1
40 (10-58)	1	ST244	2
42 (10-99)	1	ST1233	1
44 (C11)	1	ST175	0
45 (C58)	1	ST175	0
46 (D4)	1	ST27	0
47 (E16)	1	ST175	0
48 (E17)	1	ST175	0
49 (F43)	1	ST175	0
50 (G6)	1	ST175	0
51 (G7)	1	ST175	0
52 (G26)	1	ST175	0
53 (G31)	1	ST175	0
54 (H18)	1	ST175	0
55 (H19)	1	ST309	1
56 (H52)	1	ST309	1
ESP-1	2	ST773	1
ESP-2	2	ST773	1
ESP-3	2	ST773	1
NLD-1	2	ST773	1
NLD-2	2	ST773	1
NLD-3	2	ST773	2
NLD-4	2	ST773	1
NLD-5	2	ST773	1
NLD-6	2	ST773	1

Barcelona 2025